Addis Ababa University

School of Graduate Studies

College of Technology and Built Environment

School of Civil and Environmental Engineering

AN INTEGRATED APPROACH TO SUSTAINABLE CONSTRUCTION THROUGH RECYCLING, CO_2 CAPTURE AND ARTIFICIAL INTELLIGENCE

Dissertation for the Degree of Doctor of Philosophy

Hintsa Gebrezgiher Gebremariam

Addis Ababa

June 2026

AN INTEGRATED APPROACH TO SUSTAINABLE CONSTRUCTION THROUGH RECYCLING, CO_2 CAPTURE AND ARTIFICIAL INTELLIGENCE

By

Hintsa Gebrezgiher Gebremariam

Advisors

Professor Dr. Shifferaw Taye

Associate Professor Dr. Abrham Gebre

A PhD dissertation submitted to the School of Graduate Studies, Addis Ababa University, for the partial fulfilment of the requirements for the degree of Doctor of Philosophy in Civil/Structural engineering

Addis Ababa

June 2026

DOCTORAL DISSERTATION APPROVAL SHEET

The undersigned have examined the dissertation and hereby certify that it is worthy of acceptance.

Name of Candidate:	Hintsa Gebrezgiher Gebremariam
Degree sought:	PhD in Civil / Structural Engineering
Institution:	Addis Ababa University College of Technology & Built Environment School of Civil & Environmental Engineering
Dissertation Title:	An Integrated Approach to Sustainable Construction through Recycling, CO_2 Capture and Artificial Intelligence.

<u>Supervisory Committee Approval</u>	<u>Signatures</u>	
Prof. Dr. Shifferaw Taye Advisor	Signature	Date
Dr. Abraham Gebre Co-Advisor	Signature	Date
Examination Committee Approval		
Dr. Woubishet Taffese External Examiner	Signature	Date
Dr. Essayas Gebreyouhannes Internal Examiner	Signature	Date
Dr. Yenesew Mengstie Chairperson	Signature	Date
Dr. Yenesew Mengstie Dean (SCEE)	Signature	Date

DEDICATION

To the memory of my father, who passed away during my PhD study. His support and the foundation he gave me in education made this achievement possible.

DECLARATION OF AUTHORSHIP

I hereby declare that this PhD dissertation is the result of my original work and has been prepared entirely during my pursuit of the PhD degree at College of Technology and Built Environment, Addis Ababa University. Furthermore, it has not been submitted, in whole or in part, for the award of a degree at any other university or institution of higher learning or research. All sources of information and materials that are not my own have been duly acknowledged and appropriately referenced. The articles listed below were produced during the study period and form part of the dissertation prepared by me and my supervisors, Professor Dr. Shifferaw Taye and Associate Professor Dr. Abrham Gebre.

1. Gebremariam, H.G., Taye, S., Tarekegn, A.G., (2024). Parent Concrete Strength Effects on the Quality of Recycled Aggregate Concrete: A Review, Heliyon, Volume 10, Issue 4, e26212, https://doi.org/10.1016/j.heliyon.2024.e26212
2. Gebremariam, H.G., Taye, S., Tarekegn, A.G., (2023). Disparity in Research Findings on Parent Concrete Strength Effects on Recycled Aggregate Quality as a Challenge in Aggregate Recycling, Case Studies in Construction Materials, Volume 19, e02342, https://doi.org/10.1016/j.cscm.2023.e02342
3. Gebremariam, H. G., Taye, S., Tarekegn, A. G., & Woldesenbet, A. (2025). Revolutionizing Sustainable Construction through Recycled Concrete Aggregate Production: A Systemic Review of Codes, Standards and Guidelines. Journal of Civil Engineering, Science and Technology, Volume 16 (1), 102–118. https://doi.org/10.33736/jcest.6847.2025
4. Gebremariam, H. G., Taye, S., Tarekegn, A. G. Carbon Smart Concrete: Recycled Aggregates as CO_2 Sinks through Natural and Accelerated Carbonation Pathways. Manuscript under review.
5. Gebremariam, H.G., Taye, S., Tarekegn, A.G. Compressive Strength Prediction of Carbonated Recycled Aggregate Concrete using Regression-based Machine Learning Models. Sci Rep 16, 5825 (2026). https://doi.org/10.1038/s41598-026-36197-8

Hintsa Gebrezgiher	______________________________	______________
Candidate	Signature	Date

TABLE OF CONTENTS

LIST OF TABLES

LIST OF FIGURES

LIST OF APPENDICES

ABRIVATIONS

ACI	American concrete institute
AN	Angularity number
ARCA	Accelerated carbonated recycled concrete aggregates
ASTEM	American society for testing and materials
C&D waste	Construction and demolition waste
C/C_a	Cement to coarse aggregate ratio
C/F_a	Cement to fine aggregate ratio,
$Ca(OH)_2$	Calcium hydroxide
$CaCO_3$	Calcium carbonate
CI	Concordance Index
CO_2	Carbon dioxide
CPU	Central processing units
CS	Compressive strength.
C-S-H	Calcium silicate hydrate
C_v	Crushing value
D_c	Degree of carbonation
DDPM	Denoising diffusion probabilistic models
ECC	Engineered cementitious composite
FTiR	Fourier transform infrared spectroscopy
GPU	Graphics processing units
IAPST	Index of aggregate particle shape and texture
IPCC	Intergovernmental panel on climate change

ITZ	Interfacial transition zone
KGE	Kling gupta efficiency
LightGBM	Light gradient boosting machine
MAE	Mean absolute error,
MAPE	Mean absolute percentage error
ML	Machine learning
MLR	Multilinear regression
MPa	Mega pascal
NA	Natural aggregates
NRCA	Naturally carbonated recycled concrete aggregates
OC	Original concrete strength
OPC	Ordinary Portland cement
PC	Parent concrete
P_{cs}	Parent concrete strength
Poly MLR	Polynomial multilinear regression
Q-Q	Quantile-quantile
RAC	Recycled aggregate concrete
RCA	Recycled concrete aggregates
RMC	Residual mortar content
RMSE	Root mean square error
R_r	Replacement ratio
SEM	Scanning electron microscopy
SHAP	Shapley additive exPlanations

SSD	Saturated surface dry
STS	Split tensile strength
TGA	Thermogravimetric analysis
W/C	water to cement ratio
W_a	water absorption
XRD	X-ray diffraction
R^2	Coefficient of determination

ACKNOWLEDGMENT

First and foremost, I am profoundly grateful to the Almighty God for his boundless care, love, and blessings throughout the course of this work. I would like to express my deepest appreciation to my advisors, **Professor Dr. Shifferaw Taye**, and **Dr. Abraham Gebre (Associate Professor),** for their invaluable academic guidance, constructive feedback, and continuous support. My sincere gratitude also extends to the faculty and staff of the **Structural Engineering Stream** for their encouragement and professional assistance. I am equally thankful to the **CTBE Material Engineering Laboratory Management and Assistants** for their technical guidance and cooperation during the laboratory investigations. I also wish to acknowledge the contributions of the former EIABC research team members, whose collaboration and insights enriched this work with valuable perspectives. I extend my heartfelt gratitude to my family, friends, and all those who supported me in various ways throughout this journey. Their unwavering encouragement has been indispensable to the successful completion of this dissertation.

ABSTRACT

The construction industry is one of the largest contributors to climate change, driven largely by carbon dioxide (CO_2) emissions from anthropogenic activities. In addition to putting tremendous strain on natural resources through aggregate extraction, the production of cement and concrete alone is responsible for over 8% of global CO_2 emissions. Concurrently, the construction sector produces enormous amounts of construction and demolition (C&D) waste, which exacerbates resource and environmental problems. Recycling this waste into recycled concrete aggregates (RCA) provides a sustainable path forward by conserving raw materials, reducing pressure on landfills, and enabling the sequestration of CO_2. However, RCAs' limited range of applications is due to their lower quality when compared to natural aggregates (NAs). While many studies have explored not only how to enhance RCA performance but also how to effectively incorporate it into construction applications, several important gaps still remain. These include, inconsistencies in results on the influence of parent concrete (PC) strength on RCAs and RAC (recycled aggregate concrete) characteristics, the interaction between carbonation treatment and aggregate characteristics, and the effect of natural preprocessing carbonation on the carbonation potential of the accelerated carbonation. In addition, predictive modelling frameworks capable of linking CO_2 uptake with the mechanical performance of concretes containing carbonated aggregates are still unexplored.

This dissertation addresses these gaps through a comprehensive experimental and data driven programs. RCAs were obtained from both laboratory produced concretes of varying strengths and demolished structures. Their physical and mechanical properties were characterized under controlled crushing, ambient carbonation, and pressurized accelerated carbonation conditions. Custom built carbonation chamber with controlled environment and 99.5% purity CO_2 gas purchased from local suppliers was used in the pressurized carbonation process. Advanced analytical techniques, including thermogravimetric analysis (TGA-DTA), X-ray diffraction (XRD), and Fourier transform infrared spectroscopy (FTiR), were employed to assess microstructural and chemical changes before and after carbonation. Concrete mixes produced with these aggregates were evaluated for compressive, split tensile, and flexural strength. Complementary regression

based machine learning models were developed using 108 datasets to predict compressive strength, explicitly incorporating aggregate quality parameters, mix proportioning parameters, carbonation degree, and percent replacement of natural aggregates by RCAs.

The results demonstrated that PC strength has an effect on the characteristics of RCAs and RAC. Higher strength PCs produced aggregates with improved abrasion resistance, impact resistance, crushing resistance, and specific gravity, alongside reduced water absorption, although mortar content increased. Carbonation treatment further enhanced performance, with natural storage achieving up to 7.5% CO_2 uptake by mortar mass and accelerated carbonation achieving up to 12% CO_2 storage in the form of calcium carbonate polymorphs. Concrete produced with carbonated aggregates exhibited strength improvements of up to 12.5% in compression, 8.6% in tension, and 3.3% in flexure. Replacing normal strength aggregates with those from high strength concretes yielded further gains of 18%, 26%, and 30% respectively. Microstructural analyses confirmed that carbonation refined pore structures and improved durability, although dense aggregates from high strength concretes limited CO_2 penetration and resulted in incomplete carbonation. The machine learning models provided robust predictive capability, with ensemble methods such as Random Forest achieving the highest accuracy within a ±13% maximum error ranges. Sensitivity analysis identified mix proportioning, carbonation degree, and aggregate performance as the most influential factors.

While the controlled laboratory environment ensured systematic testing, real world demolition waste presents greater variability due to the presence of impurities and weak segregation practices, which remains a limitation of this study for large scale application. In the Ethiopian context, both challenges and opportunities exist for mainstreaming RACs. Establishing national guidelines, improving demolition and waste segregation practices, and integrating CO_2 utilization with industrial emitters such as cement and steel plants will be critical for adoption. With the current trend in corridor development and city renewals in Addis Ababa and other cities of Ethiopia, embedding RACs into the construction sector can establish a circular economy model that reduces reliance on virgin materials, diverts waste from the demolition processes, and supports the country’s climate commitments. To establish waste materials as a sustainable building material and a pillar of low carbon development, legislators, researchers, industry, and contractors must work together.

Keywords: Recycled concrete aggregates; Sustainable construction; Carbon dioxide sequestration; Machine learning; Accelerated carbonation

CHAPTER 1

GENERAL INTRODUCTION

1.1. Background

One of the most pressing issues facing our world is climate change. This climate change is mostly caused by anthropogenic activities [1-3]. The Earth's climate system has undergone a dramatic transformation since the industrial revolution, marked by a significant and unprecedented rise in global average temperatures. In the years 2011 to 2020, the global surface temperature had already climbed by approximately 1.1 °C above the pre industrial baseline (1850-1900). This trend has since continued to accelerate [3]. This warming is a direct consequence of the massive influx of greenhouse gases into the atmosphere from industrial processes and societal consumption. This results in altering the planet's energy balance and setting a dangerous precedent for future climate instability [4].

The implications of this warming are not merely theoretical. But, they are manifesting in increasingly severe and frequent extreme weather events. Sea level rising, and disruptions to global ecosystems are some of the outcomes of the worldwide temperature change [5]. Projections from leading climate models forecast a continued and rapid ascent in temperature, with the critical 1.5 °C warming threshold likely to be breached in the near future, potentially as early as the 2030s [6]. The biggest driver of this climate change is CO_2 from human activities. Burning fossil fuels, deforestation, and industry release large amounts of CO_2 into the air [3]. This traps heat and warms the planet. The IPCC confirms that CO_2 is the main cause of recent climate change [3]. As can be seen from (Figure.1.1 a) and b)), the global cumulative and annual CO_2 emissions worldwide from fossil fuels and industry has passed 1.8 trillion and 35 billion tonnes respectively by 2023 [7].

Globally, the construction industry particularly accounts for 30-40% of total energy consumption and are responsible for about 40% of carbon dioxide emissions, both directly and indirectly [8, 9]. If current energy use and emission trends continue, the construction sector’s share of carbon emissions could rise to 50% by 2050 [8, 10]. Concrete is the most often used material in the construction industry, which is one of the most resource intensive industries in the world. This material is now the foundation of contemporary infrastructure and urban development because of its strength, affordability, and structural performance. However, excessive use of concrete is outweighed by serious environmental problems at every stage of its life cycle, from the extraction of raw materials to production, use, and disposal at the end of its service life [11].

Today, the construction sector is confronted with three key sustainability challenges. These challenges include the depletion of natural resources, the release of greenhouse gases, and the generation of construction and demolition waste [12]. Concrete's large scale use places heavy pressure on natural resources, contributes to greenhouse gas emissions, and results in significant waste at the end of its service life [4, 11-12]. Cement, which is the primary binder in concrete, is among the most environmentally intensive construction materials [13]. Its production process demands vast amounts of energy. Similarly, its heavy reliance on raw material extraction disturbs the ecosystem, and involves calcining limestone at high temperatures a process that emits substantial CO_2. In fact, cement manufacturing alone contributes a significant share of global CO_2 emissions [13-17]. At present, cement and concrete production accounts for over 8% of global carbon dioxide emissions [18, 19]. On the contrary, the report by world in data showed that the annual CO_2 emission by cement accounts for 4.5% of annual total emissions in 2023 (Figure. 1.1 c) [7]. By 2030, worldwide cement production is expected to reach 5 billion tons [18]. Consequently, CO_2 emissions from cement and concrete are anticipated to contribute more than 10% of total global emissions between 2030 and 2050 [18].

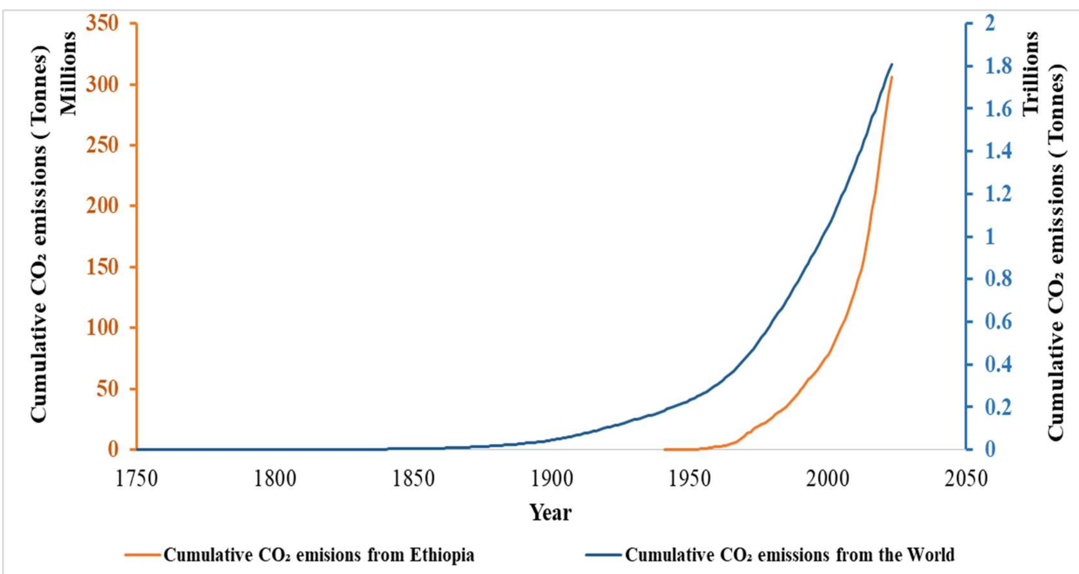

a)

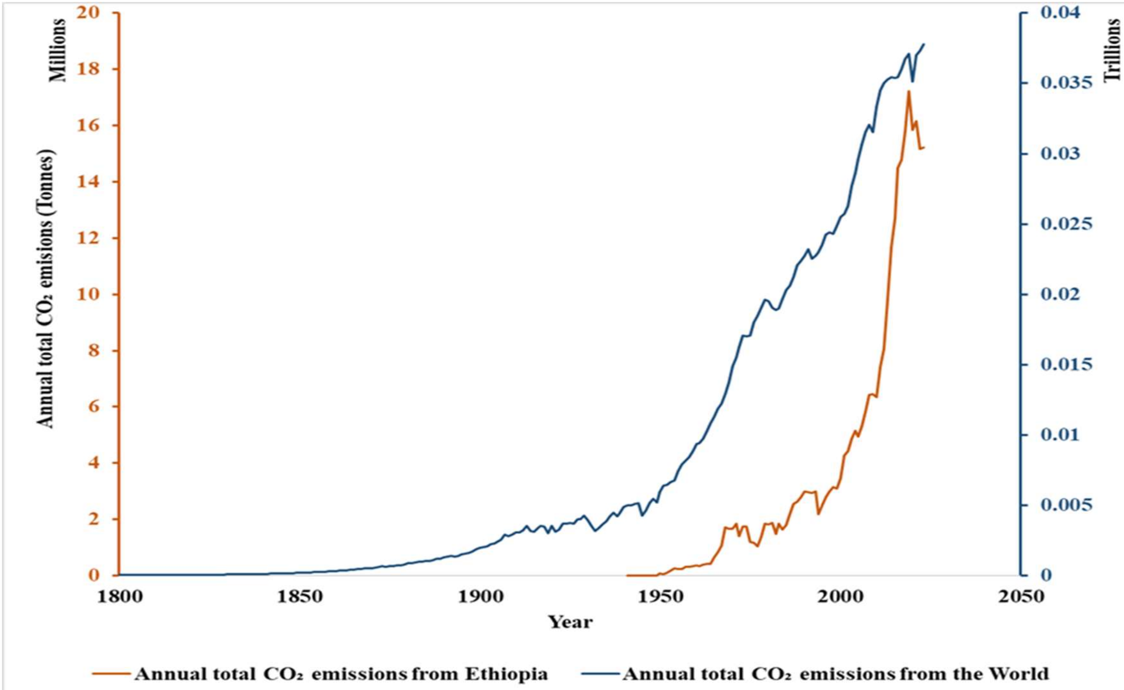

b)

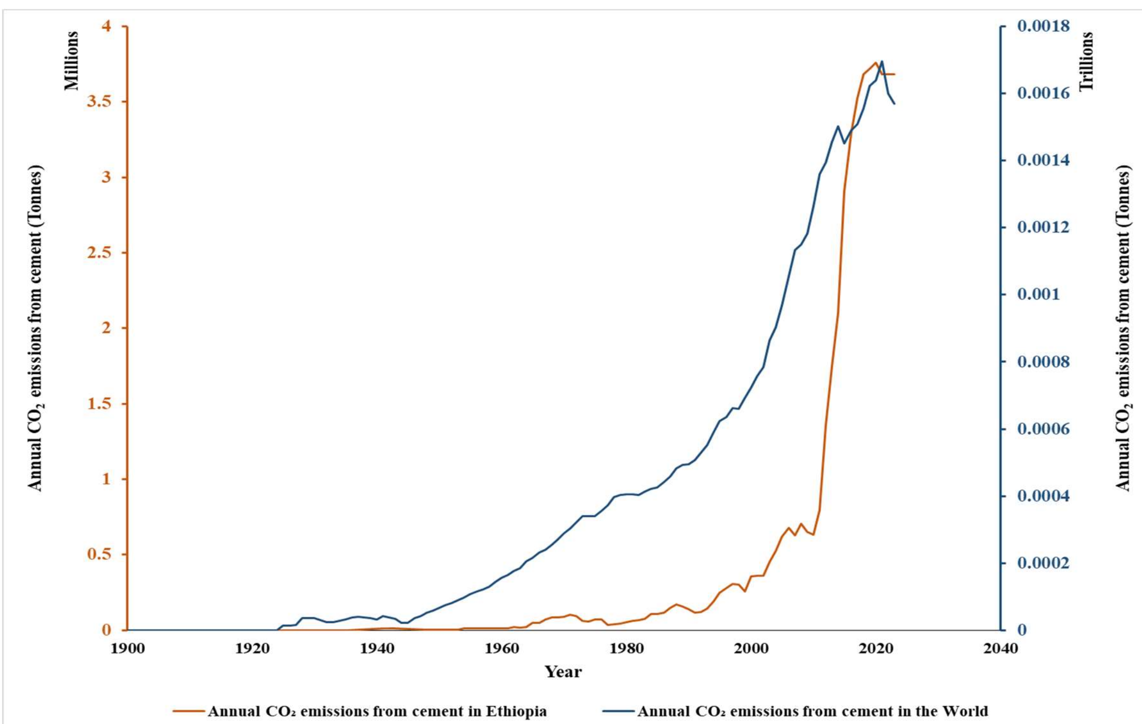

c)

Figure 1.1 CO_2 emission trend; a) cumulative emission, b) annual emission, c) annual emission from cement production data source from [7] and processed for presentation.

Beyond emissions, the industry also places immense pressure on natural resources through large scale extraction of sand, gravel, and other aggregates, which alters landscapes, disrupts ecosystems, and accelerates the depletion of nonrenewable materials [19]. NAs, such as crushed stone and sand, represent essential mineral resources extracted from the earth. These materials are typically obtained through the mechanical crushing of bedrock or by processing naturally occurring deposits of gravel and sand [20, 21]. As fundamental components of construction, aggregates contribute significantly to resource and energy demands, with their extraction, processing, transportation, and utilization accounting for approximately 7% of global energy consumption [22]. Current estimates suggest that annual worldwide aggregate consumption reaches nearly 50 billion tonnes [23]. Of this volume, the construction sector alone is responsible for approximately 40% of the demand [24]. Furthermore, global requirements for construction aggregates are projected to rise substantially, with extraction expected to increase from 24 million to 55 million tonnes per year by the years till 2060 [25].

Coupled with rapid urbanization, this leads to unprecedented consumption of raw materials and the generation of enormous quantities of C&D waste [26]. With the rapid pace of construction, renovation, and infrastructure upgrades, the generation of C&D waste has escalated worldwide [26, 27]. Each year, more than 3 billion tonnes of such waste are produced, and this figure continues to grow steadily [27]. C&D waste typically includes materials discarded during the construction, modification, or dismantling of buildings and other structures [28]. In addition to human driven activities, natural disasters and war related activities also contribute significantly to the production of C&D debris [29]. Such waste not only strains landfills and harms local environments but also reduces the availability of quality resources for future use.

Another important thing in the construction industry to be considered well is application of technological advancements to simplify tiresome, time consuming and costly processes. For engineering structures to perform safely and reliably throughout their intended lifespan, it is essential to understand the mechanical behavior of concrete. Among its various properties, mix design; compressive, split and flexural strength are regarded as the most critical parameters. Therefore, the ability to assess concrete strength both quickly and accurately is crucial for ensuring construction quality and maintaining project timelines [30].

Predicting physical and mechanical properties of concrete is inherently difficult due to the material's complex nature and the highly nonlinear interactions between its constituents [31]. Traditionally, these properties has been measured through experimental testing, where standardized testing protocols and methods passed to determine their capacity [32]. While this method is reliable, it is also time consuming and costly. To overcome these limitations, researchers have explored empirical regression techniques for predicting strength based on mixture proportions [33]. However, because the relationship between mixture components and compressive strength is strongly nonlinear, regression based approaches often fail to provide accurate generalized models [34].

With advancements in artificial intelligence, ML has emerged as a powerful alternative. These techniques have been applied across multiple areas of structural engineering, including the prediction of concrete strength [35, 36]. Unlike conventional regression methods, ML can capture complex, nonlinear relationships through sophisticated algorithms, offering more accurate predictive models [37].

Similar to the global trend anthropogenic activities in Ethiopia are contributing to the worldwide climate change ((see Figure. 1.1, a), b), and c)). The cumulative and annual CO_2 emission in Ethiopia has reached 20 million tonnes and 4 million tonnes respectively by 2023 [7]. This indicated that Ethiopia has contributed 0.05% of the annual global emissions in 2023. Cement production in Ethiopia emitted 20% of the country's annual CO_2 emission by 2023, which is very high compared to the global value of 4.5%. According to a study by Tafesse et al. [38], construction waste in Ethiopian construction projects accounts for up to 13% of total material usage, which is significantly higher than the national waste limit of 5%. Similarly 45% of the total waste from construction projects in shire Endaslassie, Ethiopia accounts for construction and demolition waste [39]. Even though, there are no literature studies describing and quantifying the trends in aggregate availability in Ethiopia, in urban areas such as Addis Ababa, the availability and quality of construction materials like sand and coarse aggregates are steadily declining. As a result, stakeholders are forced to transport materials over long distances to secure acceptable quality, which raises transportation costs, energy consumption, and the overall price of materials per cubic meters. Furthermore, the Ethiopian government's urbanization and corridor development plans indicate that there will be increased urban restructuring and housing construction over the next years. This process will require large amounts of natural materials and, at the same time, generates substantial volumes of C&D wastes.

Addressing these issues necessitates a paradigm shift towards sustainable construction practices. Decarbonization of cement and concrete materials, through alternative energy efficient processes, and carbon capture technologies, offers a pathway to significantly reduce the carbon intensity of construction. At the same time, circular economy approaches such as the recycling of C&D waste into secondary aggregates can reduce the sector's reliance on virgin raw materials while minimizing landfill burdens. These strategies not only contribute to the conservation of finite resources but also support the preservation of ecosystems and biodiversity.

Recycling C&D waste into RCA offers clear environmental benefits by conserving natural resources, lowering embodied impacts, and reducing the burden on landfills [40]. Over the years, a range of processing methods has been developed to convert C&D waste into RCA with the aim of extending its use in higher value engineering applications [41-43]. Despite these efforts, RCA still presents notable drawbacks compared with natural aggregates, including higher porosity, increased water absorption, and reduced mechanical and durability performance due to adhered mortar and micro cracks [44-46]. To overcome these challenges, researchers have investigated several treatment techniques such as microwave heating [47], acid dissolution [44, 48], thermal mechanical abrasion [49], microbial carbonation [5], and mechanical abrasion [51]. However, many of these approaches face practical barriers related to cost, energy demand, or scalability [40].

Among the available options, accelerated carbonation has emerged as one of the most effective and environmentally sustainable methods for improving RCA quality [40]. Through the precipitation of calcium carbonate ($CaCO_3$) within the adhered mortar, carbonation refines pore structures, reduces water absorption, and enhances durability while simultaneously providing a cost effective and technically viable solution [44, 52, 53].

Importantly, this process also enables permanent CO_2 sequestration by storing carbon within the aggregate's pore network.

In parallel, machine learning (ML) methods, particularly regression based approaches such as multiple linear regression, random forests, gradient boosting, and neural networks have shown strong potential for predicting the performance of RCA concrete, including compressive strength and other key properties [54-56]. Yet, studies that combine the effects of PC strength, carbonation treatment, and RCA enhancement with ML driven predictive modeling remain scarce. This gap underscores the need for integrated experimental and data driven strategies to better evaluate and optimize the performance of carbonated RAC. The present study integrates the investigation of parent concrete strength, carbonation treatment, microstructural characterization, and machine learning modeling within a unified framework to comprehensively evaluate the performance of RAC. The influence of PC strength was examined to understand its effect on the quality and mechanical behavior of RCA and the resulting RAC properties. Carbonation treatment was subsequently employed as a strengthening and densification approach to improve the performance of RCA through microstructural modification. To support this, microstructural analyses were conducted to identify the physical and morphological changes associated with carbonation and their relationship to the observed macroscopic properties. Finally, machine learning techniques were incorporated to develop predictive models capable of capturing the complex interactions among the studied parameters and accurately estimating compressive strength performance.

1.2.Problem statement

As described well in the introduction section, the transition towards sustainable construction demands a systematic reduction of natural resource consumption and greenhouse gas emissions, particularly from cement and concrete production. Utilization of RCA from C&D wastes is one of the sustainable methods and has been widely studied as a substitute for NAs [57-61]. To overcome the reduced capabilities of RCAs compared to NAs, accelerated carbonation treatment has emerged as a promising technique to both improve RCA quality and sequester CO_2 [62-65]. Despite decades of research, however, key uncertainties continue to limit the structural use of carbonated RCA and impede reliable quantification of its environmental benefits.

One of the central challenge lies in understanding the influence of PC strength on RCA and RAC performance. Multiple studies have demonstrated that PC strength significantly affects RCA physical and mechanical properties [66]. However, the literature reports contradictory findings. Some studies argue that high strength PC yield superior RCA due to reduced porosity and higher crushing resistance, while others contend that aggregates from lower strength concretes perform better because their attached mortar detaches more easily during crushing, producing cleaner particles. The lack of consensus creates uncertainty for researchers, practitioners, and regulators, complicating material selection and hindering the development of standards and guidelines.

Further unconsidered gap is the interaction between PC strength and carbonation. Accelerated carbonation treatment alters the microstructure and pore of RCA and improves their characteristics [63, 65]. But, Literature studies have not considered the PC strength effects on the carbonation capacity of RCAs. Most studies have not systematically compared aggregates sourced from different PC levels under controlled carbonation protocols. The extent to which carbonation can offset quality differences, or whether high strength aggregates respond differently to their counter parts is not investigated. This absence of systematic evidence prevents generalization of laboratory results across diverse feedstocks and processing conditions.

Another gap to be considered is preprocessing ambient carbonation prior to accelerate carbonation. RCAs are often exposed to ambient conditions during storage and handling, leading to partial carbonation before formal treatment. This ambient carbonation, along with variables such as moisture conditioning and mechanical abrasion, can significantly influence carbonation efficiency and CO_2 uptake. Yet, few studies if not none integrated these preprocessing effects into experimental programs. The optimization space for variability in aggregate sources therefore remains largely unexplored. Finally, predictive modelling for carbonated RAC performance is lacking. While machine learning has been applied to general RAC strength prediction and to carbonation depth in conventional concretes [67-70], to the authors knowledge, no established frameworks exist for modelling the compressive strength of RAC incorporating carbonated RCAs. Such models would require explicit integration of CO_2 uptake and RCA property changes. Without predictive tools, it is difficult to rapidly screen materials and transfer findings across projects, which constrains both practical adoption and policy development.

Together, these gaps restrict the reliable specification and structural integration of RCA, and their treatment methods to understand and estimate RCAs true environmental and technical potentials. Addressing these issues is therefore essential to establish robust processing to performance knowledge and to support the development of standards that enable sustainable deployment of RCA in structural concrete.

1.3.Research objectives and questions

To address the literature gaps identified in the problem statement section, this research sets out a series of objectives and guiding questions. The comprehensive goal is to contribute to the sustainability of the construction industry by systematically investigating one potential pathway which is the recycling of C&D waste as aggregate. Specifically, the study aims to examine the influence of PC strength and carbonation treatment on the properties and performance of RCAs, and to develop predictive modeling approaches that support the sustainable use of recycled RCA in concrete construction.

The primary research question guiding this study is: How can the construction industry become more sustainable and environmentally responsible by reducing emissions, conserving natural resources, and minimizing waste? This central question is further broken down into several sub questions. First, Can recycling C&D waste contribute to the sustainability of the construction industry? More specifically, as the properties of RCA produced from C&D waste inferior to those of natural aggregates; How does the strength of PC influence the characteristics of RCA and RAC? And why do existing research findings on this topic often appear inconsistent? To address these issues, a systematic literature review was conducted. Based on its findings, another question was raised: What experimental and observational techniques can be applied to resolve contradictions in the literature? A detailed experimental program was then designed and executed to provide evidence based answers.

The next stage of the research focused on enhancing the properties of RCA derived from PCs of varying strengths. A review of treatment methods identified carbonation as a promising approach. This led to additional questions: How does ambient carbonation during storage and handling affect the efficiency of subsequent accelerated carbonation treatment? And how does PC strength influence the carbonation capacity of RCA? A comprehensive experimental study was performed to answer these questions and provide insights into the potential of carbonation treatment as a sustainable enhancement methods.

Finally, the study explored ways to minimize reliance on labor intensive and time consuming laboratory experiments. The guiding question was: How can predictive modelling, including ML approaches, be used to estimate the compressive strength of RAC incorporating carbonated RCAs? And can predictive models integrate CO_2 uptake and RAC property changes to use carbonated RCA in concrete applications? To investigate this, experimental datasets were used to develop ML based predictive models. The results demonstrated that ML models can accurately predict the expected strength of carbonated RACs, effectively reducing both experimental time and cost while supporting faster and more efficient decision making for sustainable construction practices.

Based on the above general objective and questions, the specific objectives of this dissertation were:

- To conduct an in-depth literature review on the effect of PC strength on the properties of RCA and RAC, in order to address the inconsistencies reported in the existing literature.
- To evaluate the influence of PC strength on the physical and mechanical properties of RCA.
- To examine the effect of PC strength on the carbonation capacity and performance improvements of RCA under accelerated carbonation, and to investigate the role of natural preprocessing carbonation in influencing the efficiency of accelerated carbonation treatments.
- To develop and validate predictive models for estimating RAC performance incorporating carbonated RCAs, and to provide scientific evidence to support the

formulation of standards and guidelines for the sustainable use of RCA in concrete applications.

1.4.Significance of the study

This research's significance lays on its capability to respond to one of the most urgent challenges, the reduction of environmental impact of the construction industry while meeting growing demand for materials. Globally, recycling C&D waste into RCAs can offer a clear pathway towards resource conservation, waste reduction, and carbon emission mitigation. However, uncertainties around the performance of RCA and RAC continue to limit its widespread adoption. This work tackles these concerns and adds fresh data to support the global argument for sustainable concrete manufacturing by examining the effects of PC strength and carbonation treatments on RCA qualities.

Construction industry in Ethiopia is expanding rapidly, generating large volumes of C&D waste while placing intense pressure on natural aggregate sources. But, recycling and reusing practices are unregulated, and the advantage and application of RCA is poorly understood among construction stakeholders. In practice, most waste is still discarded in landfills or dumped on city outskirts, if reused in base and sub base course in roads with no technical guidelines or standards to promote its reuse. This study provides the scientific foundation needed to close that gap by demonstrating both the technical feasibility and the environmental benefits of RCA. The findings from this study can support the development of local standards and encourage a cultural shift toward more sustainable construction practices in Ethiopia.

The study's methodological contributions highlights the dual environmental benefits of carbonation treatment by evaluating it as a carbon sequestration method as well as a procedure that improves performance. Additionally, the use of ML as a predictive tool lessens the need for laborious experimental work, which makes sustainability both feasible and economical. All things considered, the importance of this research resides in its ability to close important knowledge gaps, by impacting current standardization practices, and offering instruments that connect science, practice, and policy. This can advance a vision of a resource efficient, ecologically conscious construction industry that is ready to meet the needs of sustainability in Ethiopia and around the world.

1.5.Scope and limitations

As discussed in the objectives section, this study focused on developing sustainable concrete by partially replacing NAs with C&D waste derived materials. The work encompassed several key objectives including identifying research gaps, characterizing locally available RCAs, treating them for property enhancement, designing concrete mixes incorporating these materials, and conducting laboratory tests on their fresh and hardened properties. It also involved ML modeling to predict the strength of RAC, aiming to reduce the reliance on extensive laboratory testing.

However, the experimental program for RCA property enhancement was limited to PC strengths of only 25 MPa and 67 MPa due to the high cost of the experiments. Similarly, the important parameters like coarse aggregate size and variability in fine aggregate properties were not considered in this study. While the literature suggests the optimal gas pressure for accelerated carbonation is in the range of 0.01 to 0.2 MPa, investigating pressures up to 0.5 MPa may be important. This study was limited to a maximum pressure of 0.15 MPa due to the capacity of the custom built chamber. Additionally, high strength PC aggregates were not completely carbonated, suggesting that other methods beyond pressurized accelerated carbonation should be considered for full carbonation. Even though linear regression, tree based and ensemble based ML models perform good with the current datasets, having a large volume of datasets that are well distributed across all strength levels may increase accuracy and avoid overfitting in the models. Finally, this study did not include a life cycle analysis of the RCA experimental program. While the findings provide a strong foundation for the development of standards and guidelines for RCA applications, the creation of formal guidelines and standards was outside the scope of this work.

1.6.General methodology

This comprehensive methodology outlines a multi phased approach to investigate the properties of RCAs, treatment methods for enhancing their property, characteristics of RAC produced from these aggregates and ML modeling of the RAC incorporating the carbonated RCAs. The study specifically focuses on how PC characteristics and accelerated carbonation influence material behavior. A thorough literature review was conducted to establish the current state of knowledge, utilizing academic databases like Scopus and Google Scholar to identify relevant research in the study area. Then, experimental programs were designed to characterize and determine the behavioral relationships. To make a controlled study, concrete of different mix ratios and target strengths were produced. To produce the RCA, PCs were prepared in the laboratory with target 28 day cube compressive strengths of 25 MPa, 37 MPa, 45 MPa, and 67 MPa, in accordance with ACI 211.1-91. Additionally, samples were sourced from demolished structures to account for real world variability. The crushing procedure was controlled to produce RCA with a particle size range of 4.75-25 mm, complying with ASTM C136 and ASTM C33.

The physical and mechanical properties of the RCA were evaluated using relevant ASTM standards to understand how the source concrete's strength and age influence the quality of the resulting RCA. These tests included water absorption and specific gravity (ASTM C 127) to assess porosity, and Los Angeles abrasion, aggregate crushing, and aggregate impact value tests to determine resistance to mechanical stress. Carbonation treatment of the aggregates was designed for the aggregates from two PCs with cube compressive strengths of 25 Mpa and 67 Mpa to consider PC strength on the property enhancement of the RCAs. Sample were exposed to ambient environmental conditions for 1.5 years to consider the preprocessing ambient carbonation contributions in the controlled pressurized accelerated carbonation process. Then, samples were subjected to accelerated carbonation in a custom built, cost effective carbonation chamber maintained at a relative humidity, a CO_2 gas pressure, and a temperature for 3 and 7 days. The extent of carbonation was subsequently verified using a phenolphthalein indicator test.

Following the carbonation process, microstructural changes in the RCA were analyzed using fine powdered samples extracted from the adhered mortar. TGA-DTA tests were performed to quantify the weight loss of the heated samples, which helped in estimating the amount of CO_2 uptake and confirming the formation of calcium carbonate. XRD was conducted to identify changes in the crystalline composition, specifically looking for a decrease in portlandite peaks and an increase in calcite peaks. FTIR was used to detect shifts in chemical bonding in hydroxyl (O-H) signals and carbonate bands further confirming the chemical transformation. The next phase of the study involved designing and preparing RAC mixes to evaluate their mechanical properties, including fresh and hardened properties, taking into account the effects of carbonation, PC strength and aggregate replacement ratios. Concrete sample were prepared for compressive and tensile strength tests following appropriate standards. Another component of this study involved a data driven approach to model and predict the compressive strength of RAC. Datasets of concrete samples with eight distinct properties including cement to aggregate ratios, water absorption, crushing value, PC strength, carbonation degree, and replacement ratio, were used for modeling. To overcome challenge of multicollinearity, where predictor variables were highly correlated, a novel composite index approach was implemented. This involved creating two new variables: a Proportioning Index, which combines mix design ratios, and a Performance Index, which combines aggregate quality indicators. This data transformation was used to ensure the stability and reliability of the predictive models. The study then evaluated the predictive performance of various ML models, including traditional statistical methods like Multiple Linear Regression, Ridge regression and more advanced algorithms like Random Forest and LightGBM, on both the original and composite datasets. Model performance was assessed using a range of quantitative metrics and visual diagnostic tools, and the SHAP framework was utilized to interpret the contribution of each feature to the final prediction.

1.7.Outline

The dissertation is structured into six chapters. The core of the thesis, excluding the introductory and concluding chapters, directly addresses the four research questions set out in Section 1.3.

Chapter 1: Introduction and research methodology introduces the research context, problem statement, and significance of the study. It also provides an overview of the comprehensive methodology and scope of the work.

Chapter 2: Literature review and research gap analysis which synthesizes the current knowledge on the characteristics of C&D waste and the influence of PC strength on RCAs. It focuses on identification of specific gaps in the existing literature that the present study aims to fill. An article prepared for this section has already been published.

Chapter 3: Experimental program on RCAs and RACs that details the extensive experimental program presented the production and characterization of RCAs. An article prepared for this section has already been published.

Chapter 4: Deals with sustainable enhancement of RCAs via accelerated carbonation which examines the property enhancement and CO_2 sequestration potential of RCAs. This chapter presents the experimental work on both the microstructural and mesoscale levels to validate the effects of carbonation. Design of the concrete mixes and experimental tests on concrete for evaluating physical and mechanical properties were also performed in this chapter. A manuscript has been prepared for this section and is under review at Cleaner Waste systems, Elsevier.

Chapter 5: Examined the predictive modeling of RAC strengths exploring the development and implementation of ML models to accurately predict the compressive strength of RACs, utilizing the comprehensive dataset from the experimental programs were the core performances of this chapter. A manuscript has been prepared for this section and is under review at Scientific Reports, Springer.

Chapter 6: The conclusion and recommendations section which presented the key findings of the entire dissertation, discussed their implications, and offered actionable recommendations for future research and practical applications.

CHAPTER 2

PARENT CONCRETE STRENGTH EFFECTS ON THE QUALITY OF RECYCLED AGGREG ATE CONCRETE: A REVIEW

Original publication on Heliyon and can be sited as:

"Hintsa G. Gebremariam, Shifferaw Taye, Abrham Gebre Tarekegn (2024). Parent Concrete Strength Effects on the Quality of Recycled Aggregate Concrete: A Review, Heliyon, Volume 10, Issue 4, e26212, https://doi.org/10.1016/j.heliyon.2024.e26212"

2.1. Introduction

Concrete has been used more widely in modern construction projects due to its durability, affordability, and safety. The production of concrete requires a significant amount of nonreplenishable natural materials, such as fine sand and coarse aggregate gravels. Sand and gravel mining and preparation also need a significant amount of energy. The energy consumption involves those required during quarry production, transportation and aggregate crushing. Ittepie et al. [1] determined the energy consumption per ton of virgin aggregates and RCAs. They discovered that the energy consumed during the making of one ton of virgin aggregates (21,112 kJ/t) is about 30.5% higher than the energy consumed during the production of recycled concrete aggregate (16,178 kJ/t).

Similarly, a substantial amount of concrete waste is being produced by the construction firm causing the scarcity of natural materials, massive energy usage and environmental degradation [2]. The construction and building industry is, thus, considered a vital source of environmental deterioration and is associated with the production of construction waste [2]. Concrete structures generally also have a service life limited only to a few decades [3] and, consequently, the adverse environmental effects come to play continuously in shorter spans of time. According to a study by the authors [4], the construction sector solely produces roughly 75 billion metric tons (mt) of concrete by product annually. China alone produced 2.36 billion mt of C&D waste in 2018, then comes the United States (USA) (approximately 600 million mt) and the federal state of India (about 530 million mt) [5]. A significant amount of C&D waste was also produced by European countries with France and Germany contributing the most, with 240 and 225 million mt, respectively [5]. In many developing countries, handling solid waste is a problem for most, and construction junk is emerging as a serious environmental issue. More than half of Sub Saharan Africa's population now lives in cities, which is predicted to increase garbage production by up to 1 kg per person [6]. Additionally, in other African nations such as Zimbabwe, Tanzania, and Mauritius, mixed municipal solid waste generation rates range from 0.7 kg per person per day in Zimbabwe to 1.1 kg per person per day, of which up to 30% is construction and demolition waste [6].

A global solution is needed immediately to deal with the pressing problem of the deposition and disposal of these huge amounts of wastes. On the other hand, the traditional practice of sending a major proportion of construction and demolition wastes to landfills is being hampered by a sharp price increase and environmental concerns [7]. Furthermore, C&D wastes are very likely going to contain potentially harmful materials, including varnishes, sealants, adhesives, and mercury; these will undoubtedly contaminate the soil and groundwater reserves. Therefore, more sound technologies, such as, for example, working on waste recycling process and those converting wastes for potential reuse, are urgently needed to handle these vast amounts of construction and demolition wastes.

RAC can minimize greenhouse gas release by 65% and nonreplenishable energy by 58% compared to natural aggregate concrete (NAC), according to a study in Hong Kong [8]. The higher proportion of accumulated concrete waste from demolition is made up of aggregates [5]. On the other hand, aggregates are finite resources, and as urbanization in developing nations picks up speed, demand for them will only rise. Future availability of these construction materials will very likely catastrophic as a result of their shortage. The necessity to become more sustainable has become clear as a result of the problems the building sector has been facing. Consequently, reusing some of the RCAs from the C&D waste in the manufacture of fresh concrete material is one potential approach for the wise use of materials. By protecting virgin aggregate reserves, reducing greenhouse gas release, minimizing nonrenewable energy use during aggregate production process, and protecting useable land from being a landfill site, this will help the building sector become more sustainable [9].

It has been proposed to use RCAs in place of NAs when producing structural concrete. These aggregates are mostly derived from construction waste and demolished concrete buildings. Despite the fact that RAC, which is made by partially or entirely substituting NAs with RCAs, has notable financial and environmental advantages [10–12], its application in the construction industry has been restricted thus far due to worries about RCA's lower quality when compared to NAs [13]. The performance of RAC is impacted by the varying features of RCAs from different sources [14–16]. For instance, Liu et al. [14] and Zhou et al. [15] discovered that the shear capacity, compressive behavior, and modulus of rapture of concrete produced from various types of RCAs varied. Numerous investigations were performed over the last thirty years to comprehend the performance of RAC applying coarse RCAs [13]. Reviewing the body of literature on RCAs and RACs reveals that even though there are contradictory results, high quantity of research have been reported thus far on the effect of source concrete. It has, indeed, been demonstrated that the characteristics of RCAs and RACs' mechanical and long term properties are affected by the quality of the PC.

Researchers have observed contradictory findings in various literature sources regarding the influence of variable source concrete quality on the characteristics of RCA and RAC. A thorough review of different research and examination on the mater revealed that varying outcomes and conclusions on the subject, leading to an inconsistency in understanding the influence of increased source concrete quality on the characteristics of RCA and RAC. With respect to RCA and RAC behaviors, different studies report contrasting results when PC strength is increased. Some sources indicate that values of these properties increase, while others suggest no effect or even a decrease. Specifically, the density of RCA is reported to improve [17] with a rise in the source concrete quality while [18–20] reported an increase in density as the source concrete quality decreased.

The specific gravity of RCA is reported to improve in quality [17, 21, 22] with the rise in the PC quality while [20, 23] reported an increase in specific gravity as the PC strength tended to decrease. Water absorption of RCA might increase [20, 23–25] or decrease [17, 21, 22, 26, 27]; Los Angeles coefficient of RCA can either increase [26] or remain the same [28, 29]; and adhered hardened paste quantity of RCA can either show a rise [17, 18, 20, 21, 23] or a fall [30–32] with the increment in source concrete quality.

Furthermore, the influence of increased source concrete quality on the properties of RAC also presents conflicting results across different studies. Compressive strength of RAC can either increase [22–24, 26, 29, 30], have no effect [18, 35], or decrease [20, 21], while split tensile strength of RAC might either increase [22–24, 26, 29, 30] or remain the same [18]. Drying shrinkage of RAC can either stay the same [26, 36] or increase [22, 30, 37, 38], and the slump of fresh RAC can either decrease [30] or show no change [18, 39]. Similarly, Young's modulus of RAC might increase [26, 30] or show no effect [35, 37].

These contradictory findings highlight the need for a comprehensive perception of the interaction between PC strength and the characteristics of RCA and RAC. These inconsistencies might arise due to variations in methodologies used in different studies, which could contribute to the divergent conclusions. Understanding the implications of these contradictory results is crucial for the practical application of RCA and RAC in construction projects.

Summarized literature studies have presented three main arguments to demonstrate the impact of source concrete quality on RAC characteristics. The first argument posits that high quality source concrete yields better quality RAC due to a denser and stronger bond connecting the adhered mortar and virgin aggregates. The second argument suggests that lower parent concrete strength leads to higher-quality RCA, as the low-strength attached mortar can be easily separated from the aggregates, resulting in cleaner aggregates for high-quality RAC. The third argument contends that PC strength has no bearing on RAC quality, with the primary determinant being the type and number of crushers used to process the waste concrete, irrespective of PC strength. Consequently, brainstorming the mechanics governing the influence of source concrete quality on the characteristics of RCAs and RACs is quite important.

This section provides a thorough analysis of the research exploring the effects of source concrete grade on the behavior of RCA and RAC. Numerous studies have focused on physical and strength characteristics of recycled aggregates and RAC including water absorption, specific gravity, compressive behavior, elastic modulus, splitting tensile behavior, flexural capacity, durability, and microstructure. However, this study presents the cutting-edge analysis and, hence, it is the first literature review to discuss how parent concrete strength affects RCA and RAC features.

2.2. Research goal, extent, and originality

Various researches have been conducted to date to demonstrate by what means the strength of PC from various sources affects the properties of RCAs and RACs [17, 18, 23, 24, 32, 38]. But there are inconsistencies in the findings of these literary works as described in the introduction section of this chapter. Due to these and other similar inconsistencies given in the published works, investigators and construction collaborators may have difficulty deciding which of these ideas to adopt in their practical applications.

The objective of this literature review is to investigate the connection between PC strength and the characteristics of RCAs and RACs. The review seeks to address the inconsistencies found in previous studies and provide directions for future research.

The scope of this study includes an analysis of the physical, mechanical, and long term attributes of RCAs and RAC blends. Key characteristics such as water absorption, load carrying capacity in compression, modulus of elasticity, tensile capacity, modulus of rupture, and microstructure are explored. The review aims to determine the impact of PC strength on these properties and identify the optimal conditions for producing high-performance RAC without the need for additional NAs. The novelty of this review lies in its focus on investigating the relationship between PC strength and the qualities of RCAs and RACs, which has not been extensively reviewed previously. While there have been numerous review studies [5, 40–42] focusing on physical and mechanical properties, long term behaviors, and system performance of RAC, none of them have specifically examined the impact of PC quality on the properties of RCAs and RACs.

By addressing these gaps in the existing literature, this review provides valuable insights for researchers, construction stakeholders, and policymakers interested in employing RCA in concrete production. Furthermore, the review will contribute to a more sustainable approach in dealing with the effects of the manufacturing of concrete upon the ecosystem, as it highlights the potential of RAC as a more sustainable alternative to NAC.

2.3. Methods

The characteristics of RCAs and RAC and their relationship to the quality of the PC were the subject of the comprehensive literature review. To identify relevant research articles, reports, and publications, the search examined academic journals in the disciplines of civil engineering, construction, and materials science as well as databases like Google Scholar and Scopus. In accordance with the already established inclusion and exclusion criteria, the literature search results were reviewed. In this review, researches that specifically examined the features of RCAs and RAC in relation to PC strength were considered. Studies that did not offer thorough details on the durability, microstructure, or mechanical characteristics of recycled aggregates and concrete were disregarded.

The research objectives were used to extract and organize the relevant information from the studies that were selected. Water absorption characteristics, load carrying capacity in compression, modulus of elasticity, tensile capacity, modulus of rupture, and microstructure features of RCAs and RAC blends were among the most significant data retrieved. Additionally, information was extracted on the PC's quality and how it affected the characteristics of the RCA and RAC. To uncover any conflicts or inconsistencies in earlier research findings, the extracted data was examined. Trends and patterns in the correlations between PC strength and the RCA and RAC parameters were examined. Any gaps in the current body of research were also noted. Based on the outcomes of the state of the art review, suggestions for more research were put forward. These suggestions were made in an effort to rectify the shortcomings of earlier research and offer suggestions for further study. The areas of research that were deemed to be insufficient or in need of more thorough investigation were underlined.

2.4. Review of the state of the art

The characteristics of RCA and the results of their integration in RAC have attracted the interest of numerous studies in recent years [5, 6, 9, 13, 25, 26]. It is common knowledge that the PC's quality, the production process, and the aggregate size distribution all have variable impacts on the amount and calibre of mortar adhering as well as water absorption [18]. A sizable number of studies on the behavior of RACs has been published in the literature during the past three decades [12, 15, 19, 21, 23, 28]. Particularly, there have been numerous studies done on the effect of PC strength on the behavior of RCAs and RAC blends. Different researchers [19, 21, 24, 26, 27, 29] arrived at different conclusions about the impact of source concrete grade on RAC behavior. To visualize and identify the causes of variability in findings in the literature, subsequent sections discuss the impact of source concrete strength to the physical, mechanical, and durability behavior of recycled aggregates and concrete.

2.4.1 Impact of source concrete strength on physical characteristics of RCA

2.4.1.1 Aggregate shape and appearance

The characteristics of concrete both in plastic and hardened state may be substantially impacted by the form and appearance of the aggregates [43]. As the aggregate surface becomes more angular and rough, the connection between adhered mortar and aggregates becomes stronger. This will consequently influence the compressive behavior and modulus of rupture of concrete to increase. On the other hand, utilizing this kind of material with angular and rough surface makes concrete less workable thereby calling for more water to improve workability. Regarding of RCA, the attached mortar strength can also influence the morphological characteristics of the aggregates [44]. Figure 2.2. Shows the roundness and irregularity characteristics of some granular materials.

There hasn't been any investigation in the literature that indicates how the quality of the source concrete of the RCA affects the configuration of RCAs except the study by Marie and Mujalli [44]. They [44] carried out a study on the impact of the design characteristics of PC on the morphological behavior of RCA. In their study, they used three distinct varieties of coarse aggregates made from crushed laboratory cubes that have been produced from concrete samples of various PC strength and crushed natural limestone. The three PC mixtures they used were: NA concrete with 0% RCA replacement; RAC with 20% replacement of NA with RCA (M-RCA-NA-0); RAC with 20% replacement of new RCA with old RCAs (aggregate are recycled for the second time) (M-RCA-RCA-0) and concrete made with rubber (RC), which substitutes fragmented rubber for 20% of the virgin fine aggregates (M-RCA-RC-0). The angularity number (AN) of coarse aggregates, the index of aggregate particle shape and texture (IAPST), and the residual mortar content (RMC) were impacted by the properties of the source concrete (Figure. 2.1).

The angularity number, which was first proposed by Shergold [46], could be calculated using the concept of the proportion of empty spaces or voids. The percentage by cubic measure of voids in the single size aggregate that are greater than the proportion by cubic measure of voids in the precisely shaped aggregate (33%) can be used to calculate the angularity value, which is a measurement of the shape's property [44]. This means that aggregates that were perfectly round and of a single size had voids that were around 33% by volume. It can also be inferred that less porous concrete is produced using aggregates with higher angularity numbers. Similarly, one can understand from this study [44] that RCAs have more angularity number than virgin aggregates. This may be as a result of the hardened cement plaster glued to the aggregates that makes the elongated NA more angular by filling the gaps in the recycled aggregates.

Another behavior that can be observed from the findings of the article [44] is that RCAs manufactured from stronger source concrete have a higher angularity number because weaker parent concretes had less attached mortar (Figure. 2.1). Because the crushing procedure easily removes the less dense attached mortars, the quantity of the latter in low strength PC RCA is generally low.

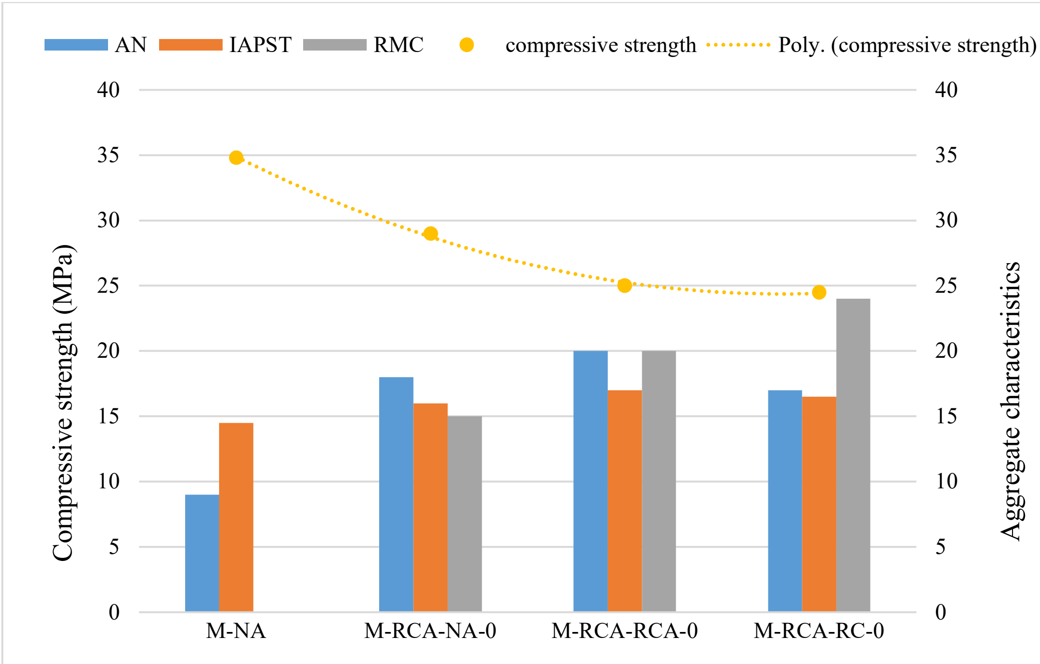

Figure 2.1 The relationship between the morphological characteristics AN, IAPST, and RMC and the compressive load carrying behavior of source concrete [44]

Note: The left vertical axis of the graph shows the compressive load carrying capacity of parent concrete, while the right vertical axis shows the values of AN, IAPST, and RMC. The polyline graph shows the compressive load carrying capacity of RAC.

The IAPST is another metric for particle shape and surface texture. This value is a quantitative evaluation of the recycled aggregate morphology and textural properties that could influence aggregate performance [47]. Recycled aggregates have a higher IAPST than natural aggregates because recycled particles tend to shatter into little blocks rather than flaky particles. Generally, the morphological properties of RCA are superior to those of virgin aggregates, while increased PC strength improves the morphological characteristics of the RCAs in contrast to low-strength parent concrete. Conversely, though, the compressive load carrying capacity of RAC decreased with increased PC (Figure 2.1). Because of the higher amount of attached cement paste in the RCAs manufactured from better quality source concretes, the shape and texture of the RCAs have higher angularity number, and the flakiness index of these aggregates is low in contrast to natural aggregates and weak strength PC aggregates. This enhances the morphological behavior of these aggregates. But since the degree of cement paste adhered to these RCAs is high in volume compared to low-strength PC aggregates, the compressive load carrying capacity of those aggregates is lower with the contrast to virgin aggregates and weaker PC RCAs [44].

Even though a comprehensive examination of the form and external appearance properties of RCAs made from various types of aged PC was already conducted [44], conclusions were more general as it was reported, quote, "both parent concrete and crushing procedures affected the aggregate morphology [44]." As a result, a more detailed research on the consequence of strength of source concrete on the aggregates' morphological behavior while considering a constant crushing procedure should be conducted. Testing the validity of the existing techniques and developing more direct and simple methods of study are also areas for further research.

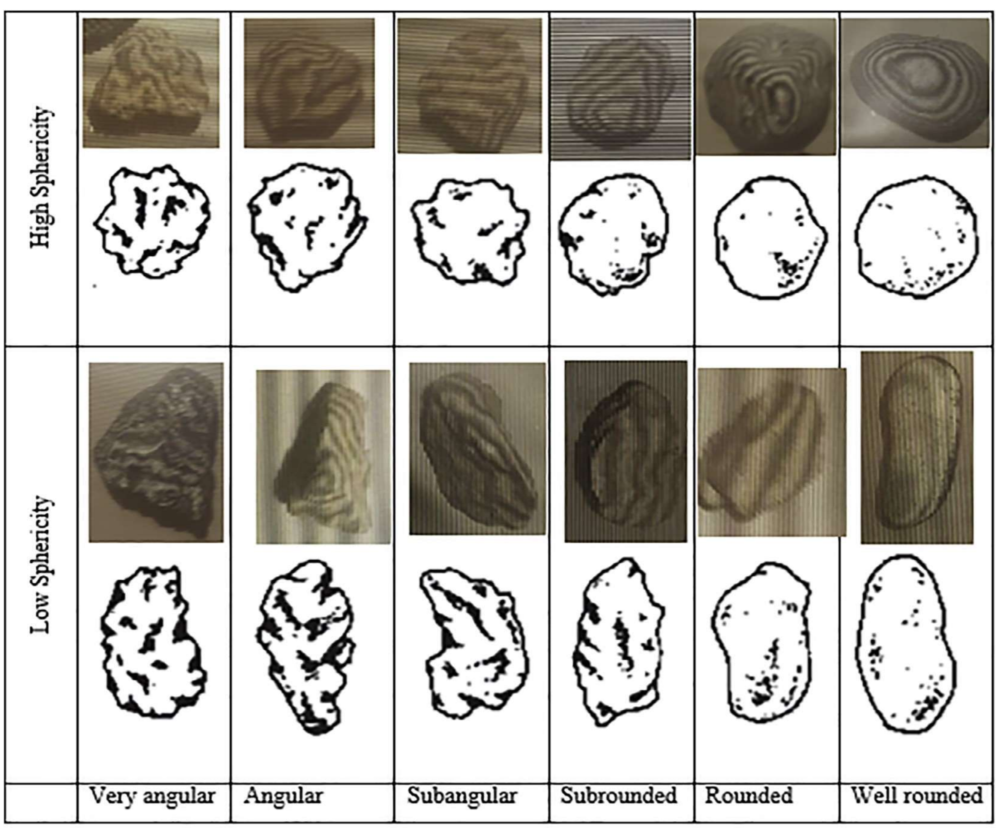

Figure 2.2 Comparing the Moiré visual assessment of aggregates' roundness and irregularity to Powers' [45] visual assessment of granular materials, obtained from Marie and Mujalli [44].

2.4.1.2 Water absorption

The water absorption of RCA refers to the amount of water that the aggregate may retain while submerged in water. There are various techniques for calculating RCA's hygroscopicity. The saturated surface dry (SSD) approach is one such technique. The aggregate is first dried to a consistent mass. The mass is then measured again after being submerged in water for a predetermined amount of time. The volume of water that the aggregate absorbs is represented by the difference in mass.

The hygroscopicity rate can have an impact on the behavior of both plastic and hardened states of concrete [48, 49]. Concrete manufactured from recycled materials exhibited reduced strength in compression and thawing and freezing resilience when compared to concrete produced from virgin aggregates [50, 51]. Nevertheless, the aggregate's ability to absorb water also impacts the fresh properties of concrete [52]. As a result, the Spanish Structural Concrete Code EHE-08 [53] limits the values for natural aggregates on this attribute to those that are lower than 5% while allowing values of not more than 7% for the RCAs applied in the production of structural concrete.

Aggregates' capacity for absorbing water is dependent upon either a fixed level of porosity in the particles or a mean number for a mix of different materials with varying degrees of absorption [23]. More moisture is often absorbed by RCAs than by NAs. Generally, in order to get the same workability, concrete manufactured using RCA and virgin fine aggregates typically consumes nearly 5% additional water than natural aggregate concrete [48]. This is because there is more absorption with recycled aggregates. Some researchers contend that because weaker strength concretes have an elevated water to cement ratio and the RCAs are produced from low strength original concretes, the standard of the cement paste that had set and adhered to these RCAs can generally be low. Hence, the mortar obtained with them is more porous, leading to increased water absorption [23, 26]. According to a study [20], because there is higher mortar employed, RCAs constructed from harder PCs have higher water absorption. Contrary to [20], but, because higher strength source concrete aggregates are not as porous as aggregates from weaker strength parent concrete, recycled aggregates from high strength source concrete with higher mortar content had shown less water absorption behavior. [17, 21].

According to Kou and Poon [30], RCA manufactured using source concrete with low grade has greater degree of water absorption compared to RCA made from stronger source concrete. Andreu & Miren [27] used RCA from diverse sources to create high performance concrete mixtures. The aggregates from the PCs with compressive load carrying capacity of 40 MPa, 60 Mpa, and 100 MPa absorbed water at rates of 5.91%, 4.90%, and 3.74%, respectively, with a maximum variance of 58%. The rise in the grade of source concrete increases the submerged water absorption capacity (from 33% to 38% [25, 54, 55]) and through a capillary (from 75% to 85% [33]). The findings of some references reported, as illustrated in Figure. 2.3, provide information on how different PC strengths might cause distinctions between specific gravity and water absorption. The studies on reference number [20, 23] found an increase in water absorption, while studies [21, 22] discovered that when source concrete strength boosted there was a decline in water absorption. Similarly, studies [21, 22] found an increase in specific gravity, while [20, 23] discovered that when source concrete strength increased, its specific gravity dropped.

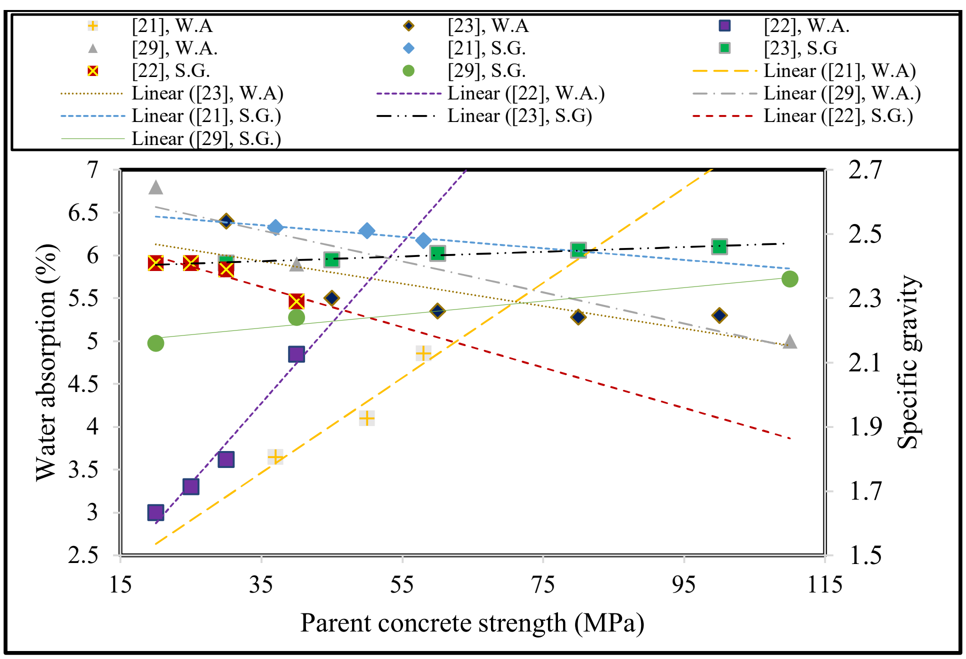

Figure 2.3 Figure shows how the absorption of water and specific gravity of RCAs vary inconsistently with the strength of the source concrete.

Note: W.A in the legend of this table represents the water absorption value of recycled aggregates; S.G. represents the specific gravity of recycled aggregates and values in square brackets are the reference numbers.

Working with RCA is quite difficult because of its heterogeneous nature. RCAs have a variety of origins and qualities compared to natural aggregates which often come from the same resource. This results in quality variations across various batches of RCAs. NA type and size used in the manufacturing of source concrete, service time and loading condition of the source concrete, aggregate crushing type and number of crushing operations, and grades of the source concrete all impact the characteristics of RCAs, including the moisture absorbance of RCAs. Researchers' exposure to these inconvenient situations may be the corollary to the divergent results of the above studies. For instance, Pedamini et al [20] used a jaw crusher to produce their recycled aggregates and found a rise in the moisture absorption of RCA with the rise in the quality of the source concrete. On the other hand, Duan et al [21] produced their aggregates by crushing the source concrete by hammer and then by mini crusher, and they concluded that aggregates from stronger parent concrete have less water absorption. In this case, the crushing procedure is the cause of the divergence in the results reported by the authors. As a result, more detailed and systematic research on the source-concrete impact on RCA characteristics is expected.

There have been no studies found in the literature that specifically study the impact of the quality of source concrete and hardened cement paste content of RCAs on the water absorption of RAC. However, it is evident that introducing adhered hardened cement paste to RCA will enhance the RAC's capacity to absorb water. This is because the availability of adhered mortar in the recycled aggregates applied in the manufacturing of RAC will absorb additional water in contrast to virgin aggregates. Consequently, this absorption of extra water by the recycled aggregates incorporated in RAC leads to a rise in the overall moisture absorption of the RAC. But a further experimental study to prove the provided argument is needed.

2.4.1.3 Density and specific gravity

The density of a particle of an aggregate is defined as the total weight of the particle substance divided by the amount of space covered by its individual particles. Because the porosity of the hardened cement paste phase is higher compared to the aggregate phase, the relative density and density of RCA are substantially lower. In fact, the great quantity of hardened cement paste that is attached to each piece of crushed clay brick minimizes the particle density and rise the moisture intake value [56]. Rao [23] found that the mass over volume and relative density of RCA made from parent concrete with elevated grade are comparatively smaller, and the moisture intake is generally a little higher, however insignificant it can be, than those made from source concrete with lower strength. They hypothesized that this was due to RCAs found from higher-strength source concrete adhering to a comparatively significant quantity of distant, permeable, lighter cement paste as opposed to lower-strength parent concrete.

Similarly, for comparable aggregate dimensions, RCAs produced from low strength source concrete have higher dry state densities [18, 19]. Furthermore, De Juan and Gutiérrez [24] discovered that the density of recycled aggregates dropped as their strength and adhered hardened cement past content increased. Contrarily, it was determined that as the source concrete strength increased, the dry density and relative density of the RCAs increased [17].

Figure 2.3 illustrates how the strengths of different PC might cause variations in specific gravity. The density of particles can be taken as an indirect measure to determine the volume of pores with respect to the total volume of a particle. A single natural aggregate particle has a small volume of pores compared to its total volume. Regarding RCAs, the mortar adhered to the aggregates influences the density and the porosity of the aggregate particle. The ambiguity here is whether the grade of the adhered mortar influences the density of RCAs (high strength PC produces high quality aggregates [17]) or whether the amount of attached mortar influences the properties of RCAs (lower strength source concrete produces high quality recycled aggregates [18, 20, 23]). This inconsistency could result from a number of causes, such as the type of crusher used, the number of times the material is crushed, and the presence of impurities in the parent concrete. As a result, developing consistent methods for determining the effects of source concrete on the density and relative density of RCAs is an area for future research.

2.4.1.4 Mortar content

Natural aggregates and RCAs differ primarily in that the latter, as obtained from C&D wastes, have some amount of mortar attached to them. This mortar makes the aggregates weaker in quality compared to the corresponding natural aggregates [5, 7, 15, 18, 19]. The quality and amount of this adhered mortar depend mainly on the source concrete's strength and the technique of crushing the aggregates. In this section, the review of available literature on the impact of source concrete quality on the mortar content of RCAs is discussed.

Some experts believe that in the crushing procedure of the low strength source concrete, most of the mortar that was used separates from the primary aggregate due to a weakened bonding between the aggregate and the cement mortar. This hardened cement paste is broken down into small fragments, whereby the filtering and sieving procedure subsequently takes off. Consequently, there is less mortar in the RCA made from this parent low quality concrete. Because of this, the mortar composition of the RCAs increases in a manner consistent with the PC's increasing strength [18, 20, 21, 23]. Conversely, several studies have demonstrated a reverse trend, wherein fewer mortars are attached due to the stronger source concrete grade [30–32]. The crushing procedure is to blame for this opposing trend. Because of the extensive automated crushing procedures, RA supplied from the crusher facility often has less associated mortar [57].

Construction and demolition wastes pass through a number of crushing steps in aggregate crushing plants to remove and reduce the quantity of hardened mortar adhered to the RCA. Aggregates passing through a two-step crushing process contain less mortar adhered than aggregates collected from demolition waste manually. Additionally, de Juan et al. [24] discovered that there wasn't any obvious correlation between the strength of source concrete and the recycled concrete mortar content. The inconsistent findings inside the written works on the effect of source concrete on mortar content call for further studies to identify the underlying causes.

2.4.1.5 The role of parent concrete strength in aggregate abrasion, crushing, and impact resistances

The resistance of aggregates to abrasion, aggregate crushing strength, and impact value are other important parameters that heavily influence the quality of an aggregate. Abrasion resistance measures the degree of degradation of aggregates affected by impact and abrasion in an abrasion machine against the abrasive impact of steel balls. Likewise, the crushing value of aggregates offers a relative measurement of RCAs resistance to crushing by applying a compressive stress progressively. In a similar manner, the particles impact resistance offers a relative assessment of the resilience of an aggregate against sudden shock or damage. Parent concrete quality has, thus, an effect on the materials' abrasion value, crushing value, and impact. According to a study by Nagataki et al. [29], particle Los Angeles abrasion loss is independent of source concrete's strength. However, a study by Gebremariam et al. [58] discovered that the Los Angeles resistance of RCA was benefited by an increase in source concrete strength.

Impact resistance of aggregates decreased with the increase in parent concrete strength [23, 44], and the crushing resistance of aggregates also decreased as the strength of the parent concrete increases [24]. On the other hand, as strength of source concrete increased, recycled aggregates' impact and breaking ability rose as well [58]. Additional study on aggregate abrasion resistance, crushing resistance, and impact resistance is needed on aggregates produced from multiple sources to further strengthen those study results from the literature.

2.4.2 Impact of source concrete strength on fresh and hardened qualities of RAC

The mechanical characteristics of concrete on plastic and hardened state RAC include workability, compressive strength, split tensile strength, flexural strength, and elastic modulus. The determination of these mechanical properties involves conducting various tests on the RAC samples. These tests are performed in accordance with standardized procedures and guidelines. It is important to note that the mechanical behavior of RAC can be influenced by factors such as the strength of the source concrete and mortar content. Therefore, it is crucial to consider these factors when evaluating and determining the mechanical characteristics of RAC. The subsequent sections will discuss these properties in detail.

2.4.2.1 Workability (Slump values)

Slump value of concrete refers to how quickly freshly mixed concrete may be mixed, placed, solidified, and finished with little loss of homogeneity [59]. Quality, aesthetics, and even manpower cost for refining and placing techniques are all strongly impacted by workability. The slump value and other factors of each concrete mix design are impacted by the quantity, caliber, and characteristics of the water reducing admixtures. Particle size and morphology, water/cement ratio and admixtures properties are some of the elements influencing the serviceableness and workability of concrete [30, 59].

High amount of mortar is required to completely cover the surface of the aggregates as their surface area grows. As a result, mixes containing smaller particles are less workable than those containing bigger aggregates under similar conditions of water-cement ratio. Aggregates that are long, angular, and flaky are also more challenging to mix and placement because they exhibit comparatively larger surface area which, thus, reduces workability [60]. In the case of the percentage of water to cement, greater volume of paste covers the outermost layer of the aggregates with the correct quantity of water for speedier consolidation and a better finish. Strength is often indicated by the percentage of cement or cement-based substances in the mixture. The malleability of newly mixed concrete is changed by many admixtures, either on purpose or as an unintended consequence. Surfactants, similar to superplasticizers, reduce the binding force between aggregate and cement particles, enabling flowable mixtures without the negative effects of too much water on strength and segregation [60]. In RAC, the workability is more influenced by the quality of the parent concrete, the size of recycled aggregates, the mortar content of the particles, and the number of pores in the RCAs.

By the increase in source concrete's compressive load carrying capacity from where the various RCAs were obtained, increased, it was noted that the slump of the concrete mixtures reduced [30]. This is because RCAs with lower water absorption values come from PC with higher strengths. Contrary to the above argument, however, Akbarnezhad et al [18] commented on the findings of Grubl and Ruhl [39] where, the latter, argued that the load carrying capacity of the source concrete had almost little bearing on the strength of either the fresh and hardened concrete. Based on the authors' perspective, the method used for crushing the parent concrete a significant effect on these characteristics [18]. It was determined that the initial free water content of the concrete mixes had a huge impact on the workability of the mix, as determined by Kou and Poon [30]. Two series of mixes were created by Kou and Poon [30], one for high strength RAC (Series II) with a 0.35 percentage of water to cement and compressive strength of 65 MPa and the other for normal strength (Series I), which had a 0.5 percentage of water to cement and compressive load carrying capacity of 45 MPa. Their objective was to investigate how the strength of the original concrete affects the slump value of the RCA concrete. The initial slump of superior performing RAC mixes was decreased because RCA, which was created from source concrete with an increased strength, has a minimum moisture intake capacity. Additionally, it was discovered that raising the source concrete's strength decreased the slump of normal grade RAC mixes [30]. Recycled aggregates' workability is generally determined by their ability to absorb water and the crushing process used to create them, according to studies on the qualities of fresh RCA concrete that were conducted. Therefore, when using these properties, the utmost caution should be used.

2.4.2.2 Compressive strength

The compressive strength of concrete is a measure used to establish the ability of the concrete to withstand the applied compressive loads and stresses. As a result of the adhering mortar porous behavior, RACs compressive strength is affected by factors like water absorption, density, PC grade, and porosity [26]. Studies conducted on the compressive cube and cylinder load carrying capacity of RAC produced from variable parent concrete grades are reviewed subsequently.

According to reports from Pedro et al. [26], the compressive load carrying capacity of RAC decreased more in RAC with lower parent concrete strengths. They examined the desired compressive load carrying capacity of weak strength (20 MPa), medium strength (45 MPa), and high load carrying capacity (65 MP) RCA concrete by Appling 100% RCA obtained from two distinct origins; namely, samples examined in a laboratory and discarded precast components with same goal strengths. It was found that there was a noteworthy reduction in load carrying capacity in contrast to corresponding values from conventional concrete [26]. Because of the use of weak strength recycled aggregates, the big reduction observed in the low capacity RAC element may be proved to be reasonable. The microstructural interactions in the RAC significantly impair the concrete behavior [61]. When it comes to standard NAC, there is only one surface of contact between the natural material and the adhered hardened cement paste. But with RAC, there are two distinct connections: one is within the attaching cement paste and virgin aggregate, and the other is among the new concrete paste and the aggregate. Therefore, the compressive load carrying capacity of the RAC is adversely affected by the rise in weak microstructural interfaces.

Padmini et al. [20] investigated the characteristics of RCAs made from source concrete that had three grades and was composed of three aggregate sizes at their maximums (10, 20, and 40 mm). A general correlation has been established for RAC between the cement content, aggregate relative to cement ratio, compressive load carrying capacity, and water to cement proportion, and it has been contrasted to the relationship for PC. It was determined that for a given compressive load carrying capacity, the RAC demanded a smaller w/c ratio compared to the source concrete whereby the RAC was formed, and the difference between the two materials' strengths grew as strength levels increased. The authors also came to the conclusion that, for a certain target mean strength, the achieved strength rose with an increase in the RCA's maximum size. With increasing concrete strength, the strength gap between PC and RAC widened. Their conclusion, therefore, was that the reduced strength of RAC was not significantly affected by the presence of adhering mortar.

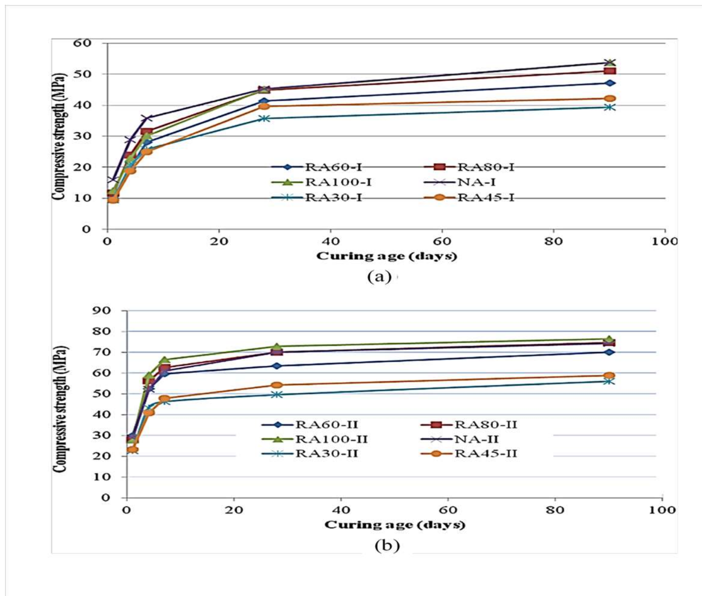

Figure 2.4 Compressive strength increases with ageing (a) in Series I mixes and (b) in Series II mixes. Note: [Reprinted from [30] with permission from Elsevier].

Kou and Poon [30] developed two series of mixes: normal strength concrete, with a w/c mix ratio of 0.5 and 45 MPa compressive load carrying capacity, and high strength RCA made with a w/c mix ratio of 0.35 and a 28day compressive load carrying capacity of 65 MPa, using RCAs obtained from source concretes with capacity of 30, 45, 60, 80, and 100 MPa. It was discovered that the compressive load carrying capacity of RAC mixes from PC of 80 MPa and 100 MPa was similar or even a little more elevated at 28 days in contrast to NAC (Figure. 2.4). But, at all curing times, the compressive load carrying capacity of the normal and high strength RAC made with PC aggregates of 30 and 45 MPa load carrying capacity was significantly decreased from that of the correlated NAC.

In the normal strength concrete, it was seen that 0.4 and 1.1% of the compressive load carrying capacity of RAC made with source concretes of grade 100 MPa and 80 MPa, respectively, were reduced in contrast to NAC. However, in the high strength concrete, the compressive load carrying capacity of concrete made with aggregates with 100 MPa and 80 MPa strengths was comparable to or some 3.9% larger than the concrete made with conventional aggregates. This could be due to the fact that RCA obtained from high strength parent concrete is of higher quality and the internal water curing process had an enhanced hydration process, because of the inclusion of RCAs [30]. Similar increases in results were also observed by other authors with the application of high strength parent concrete aggregates [22-24, 26, 28, 30]. The findings by Kou and Poon [43] showed that source concrete with higher strength (not less than 80 MPa) may be applied to manufacture high strength concrete without using any additional natural aggregates.

Luisa Pani et al. [35] and Akbarnezhad et al. [18] investigated that the mechanical properties of source concrete do not influence the quality of RAC. They reasoned that the method used for crushing concrete substantially influences how much mortar is contained in RCA, not the parent concrete strength. Andreu G. & Miren [27] performed mechanical and durability tests to see how the efficiency of recycled concrete was impacted by the source concrete. They determined that for the highest degree of substitution, all mixes using RCAs from the 60 MPa compressive load carrying capacity and 100 MPa compressive load carrying capacity source concrete achieved compressive load carrying capacity values that were identical to those of the recycled concrete (around 100 MPa). Only 20% and 50% of the RCA from the 40 MPa parent concrete experienced this, though. For the 100% ratio, there was a 20% difference in strength inside the interval of the mixes Appling RCA with the 40 MPa parent concrete and that of the 100 MPa parent concrete. According to a review of works from different authors [62–64] by D. Pedro et al. [26], compressive strengths of RAC losses in the interval of 6% to 25% were found for natural aggregate replacement with different parent strength recycled aggregates at 100%. Similarly, the strength level achieved for a particular goal decreases when the strength of the source concrete, from where the RCA is produced, increases [20]. This decrease in strength may be resulted from the existence of high quantity of adhered hardened cement paste in the high load carrying capacity PC aggregates.

It is claimed that RCA concrete strength increases with increasing source concrete strength; but it begins to decrease once the source concrete strength reaches 45 MPa [21]. This binominal trend in the strength may be because of the different quality and quantity of the RCAs used in their study. There is a third argument in the literature that says source concrete strength has no visible effect on the characteristics of RAC. According to microstructural investigations by Nagataki et al. [29], contrary to usual expectations, adherent mortar is not necessarily the primary factor influencing the quality of the RCA. Similarly, Akbarenezihad [18] also found that the compressive load carrying capacity of recycled aggregate concretes was not highly impacted by an increase in mortar content; it was argued that this was because the positive effects of increased load carrying capacity and mass to volume ratio of the hardened cement paste, and harder concretes with improved adherence to natural aggregates, partially outweighed the negative effects of the increase in adhered mortar.

Incorporation of RCAs from different sources, aiming to assess the capability of producing concrete with a predetermined level of performance (mechanical strength) using laboratory produced concrete as well as precast industry rejected elements, demonstrated that, for the greatest levels of the required strength, there were no appreciable mechanical or durability variations comparing precast waste aggregates and those from monitored sources [26]. The invisible difference in results reported in the study findings [26] may indicate that the application of waste products from deconstruction in the manufacture of new concrete could not hinder the achievement of the new concrete if the samples taken were controlled and free of impurities. Furthermore, using medium or high strength source concrete significantly reduces the performance losses brought on by the integration of the RCAs [26]. These reductions induced by increases in parent concrete may be because the fact that a rise in the mass to volume ratio and the fall in porosity of RCA in high strength PC leads to the production of good quality RAC.

The impact of the PC quality, from where the coarse RCA particles were found, on the mechanical characteristics of three strengths of RAC were examined by Ahmad Bhat [28]. He used two phases of weight replacements of NA with RCAs of 50% and 100%. The RCAs PCs were intended to withstand the cube compressive load at 28 days at nominal strengths of 20 MPa (normal load carrying capacity), 40 MPa (medium load carrying capacity), and 60 MPa (high load carrying capacity). The RACs were prepared at target strengths of 20 MPa (normal strength RAC), 40 MPa (medium load carrying capacity RAC), and 60 MPa (high load carrying capacity RAC). The findings showed that none of the mentioned strengths of RAC's compressive load carrying capacity was significantly impacted by the grade of the original concrete. The aforementioned characteristics were not as good as the control concrete that included solely NA. However, the mechanical qualities of the resulting RAC generated with high load carrying capacity of source concrete were higher than those created with normal and medium strength PC.

Figure 2.5(a) demonstrated that for normal strength RCAs with replacement threshold of 50%, the RAC's compressive strength produced from the 60 MPa (N-50, 60) parent concrete had 4.5% greater strength compared to ordinary concrete (OC-20). This showed that, in some cases, RAC can have a better quality than NAC at specified optimum replacement levels.

Figure 2.5(a) also shows that RAC constructed with RCAs from high load carrying capacity source concrete has greater compressive capacity than RAC produced with RCAs from normal and medium strength parent concrete. It could also be observed from Figure 2.5(a) that the replacement of RCA in high strength RAC has greater variation in compressive strength (H-100, 20, 40 had 23% less strength than OC-60) than the normal (N-100, 20, had 21% less strength than OC-20) and medium strength (M-100, 20, had 18.5% less strength than the OC-40) RACs. Additionally, Figure 2.5 showed that, at a 100% RCA substitution limit, the corresponding compressive load carrying capacity of RAC produced from RCAs obtained from high load carrying capacity source concrete (N, M, H-50-60) has a reduction of 12%, 11.6%, and 20% of the ordinary concrete-20, ordinary concrete -40, and ordinary concrete -60 strengths, respectively. These findings suggest that RACs of lower grades should be made with high strength parent concrete aggregate so that RACs with better quality than NAC are produced.

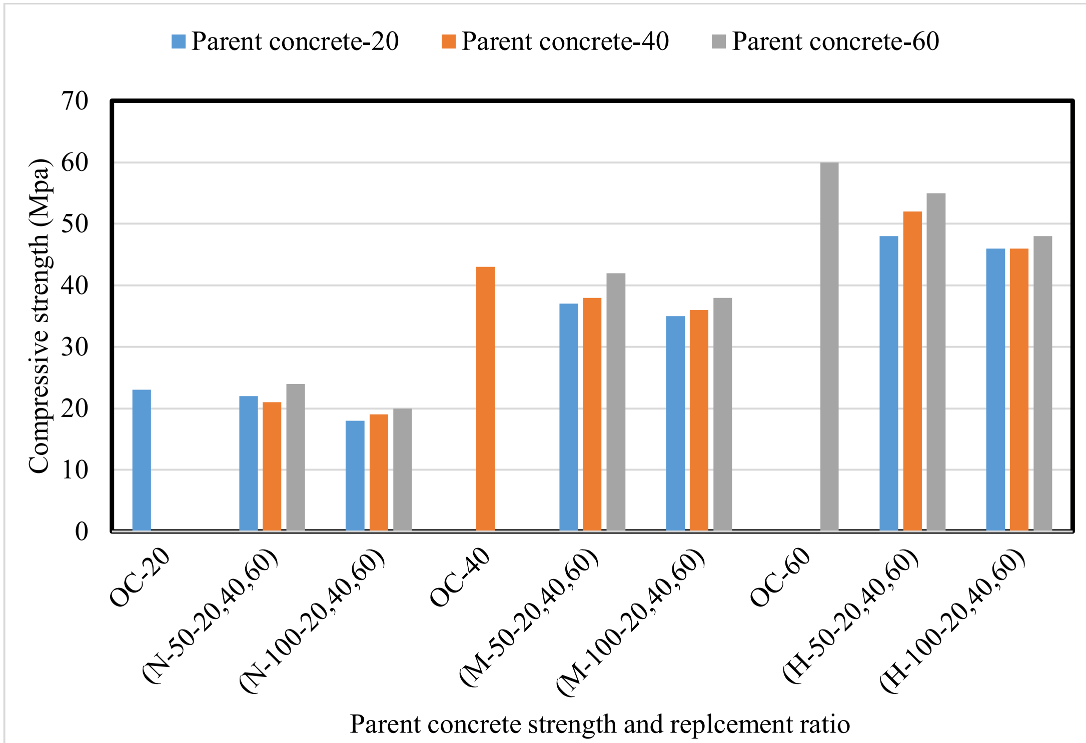
Parent concrete-20
Parent concrete-40
Parent concrete-60
Compressive strength (Mpa)
70
60
50
40
30
20
10
0
OC-20
(N-50-20,40,60)
(N-100-20,40,60)
OC-40
(M-50-20,40,60)
(M-100-20,40,60)
OC-60
(H-50-20,40,60)
(H-100-20,40,60)
Parent concrete strength and replcement ratio

(a)

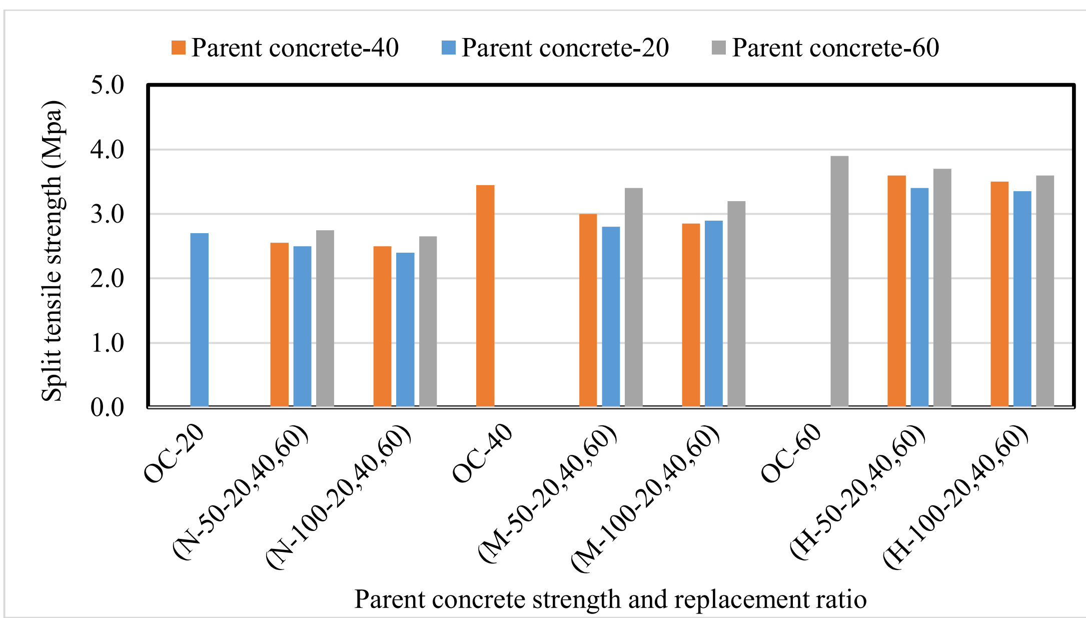
Parent concrete-40
Parent concrete-20
Parent concrete-60
Split tensile strength (Mpa)
5.0
4.0
3.0
2.0
1.0
0.0
OC-20
(N-50-20,40,60)
(N-100-20,40,60)
OC-40
(M-50-20,40,60)
(M-100-20,40,60)
OC-60
(H-50-20,40,60)
(H-100-20,40,60)
Parent concrete strength and replacement ratio

(b)

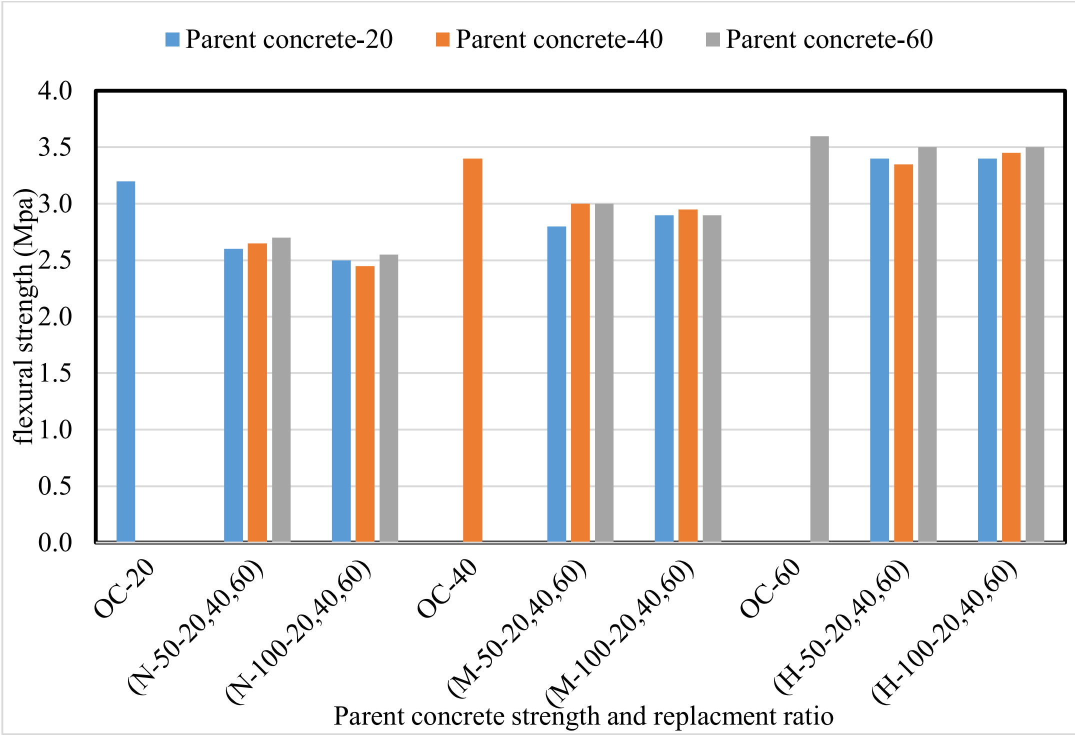

(c)

Figure 2.5. Parent concrete strength effects on strength properties of RAC. (a) Variation of the recycled aggregate concrete's compressive load carrying capacity of the (low, medium and high-strength concrete) with source concrete compressive strength. (b) Disparity of tensile load carrying capacity of RAC concrete (normal, medium, and high-strength) with compressive strength of the source concrete. (c) Variation of RAC concrete's flexural strength (normal, medium, and high-strength) with source concrete compressive strength.

Notes: OC-20, 40, 60: Original concrete strengths of 20, 40, 60 MPa. RACs (N, M, H-50,100-20, 40, 60): Concrete grades (Normal, Medium, High) with 50% or 100% RCA substitution, from source concrete strengths of 20, 40, 60 MPa. [Reprinted with some arrangements from [28] with permission from Elsevier].

Generally, even though there are contradicting results, most of the test results from the published papers stated that RAC's compressive strength manufactured from RCA produced with relatively higher load carrying capacity source concrete was slightly higher compared to regular concrete. However, RAC constructed using RCA produced from similar strength of source concrete consistently had a lower compressive strength compared to the source concrete throughout the entire curing time. This means that RAC created from PC aggregate that has a substantially higher strength may yield a strength that is comparable to NAC of equal strength. Similarly, higher strength source concrete yields RAC of greater strength. The rise in compressive load carrying capacity may be attributable to the cement mortar relative strength (bond) with the aggregates.

The majority of the study findings suggest that, at high performance levels, PC aggregates produce comparable or better compressive strength with RAC than NAC. This finding is very interesting for making sustainable structural concrete with 100% RCAs. Despite the fact that many Research has been done to improve the RCA and RAC characteristics, they have been more general in nature, focusing on the enhancement of all RCA types without taking into account the parent concrete strength effects. Therefore, enhancement methods targeting the parent concrete quality to increase the compressive load carrying capacity of low strength source concrete aggregates could be the target of future research.

2.4.2.3. Tensile load carrying capacity of RAC

One of the methods to measure the tensile load carrying capacity of concrete is the splitting tensile strength (STS). In this test, a normal cylindrical sample is laid out horizontally, and force is applied radially along its surface until a vertical crack develops along the specimen's diameter. The STS of RAC is influenced by numerous parameters, encompassing the kind of cement used, the amount of RA used, the process of blending, the source concrete grade, and the age of the RAC [33]. Research has been done to investigate the impact of source concrete strength on the STS of RAC. A tensile load carrying capacity of two distinct RCA mixed concretes, Concrete mix design 1 with an expected load carrying capacity of 30 MPa and design mix of concrete 2 with 50 Mpa expected strength, was studied by Tabsh and Abdelfatah [65]. The STS test outputs for concrete from Mix 1 demonstrates that concrete manufactured with coarse recycled aggregates from the 50 MPa parent concrete has similar STS as equivalent concrete produced from conventional coarse aggregates. Nevertheless, the tensile strength of concrete produced with RCA which came from concrete with a goal strength defined by Mix 1 (30 MPa) or coarse aggregate made from crushed concrete from unidentified sources decreased by 25 to 30%.

The experimental outputs from the second Mix exhibited a pattern that is comparable to that of Mix 1 except for a lesser decline in strength. The concrete produced with RCAs from the 50 MPa source concrete exhibited about similar STS as concrete produced with conventional aggregate. The tensile strength of RAC was shown to be dependent on the load carrying capacity of the concrete accustomed to create the recycled aggregate and to have a greater significance when it comes to concrete with a lower strength. It is clear from the findings of the article [66] that the usage of high strength PC aggregates in the production of concrete by replacing natural aggregates is useful in the manufacture of better quality RAC.

Ahmed Bhat [28] illustrated the connection among the STS and the PC compressive load carrying capacity. Tensile strength was found to be reduced by 2% - 25% throughout the RACs where RCA substitution is 100% in contrast to the source concrete. Looking at Figure 2.5 (b), it is evident that the three grades of STS for RCA concrete with 50% RCA replacement level were very slightly impacted by the quality of original concrete. Additionally, it ought to be pointed out that (Figure 2.5(b)) RACs produced from recycled aggregates of high strength parent concrete have stronger tensile strength properties than RACs manufactured with RCAs from normal and medium load carrying capacity source concrete. Figure 2.5(b) demonstrated that for normal strength concrete with 50% substitution level, the STS of the RAC produced from the 60 MPa (N-50, 60) parent concrete had 1.85% greater strength compared to the ordinary concrete (OC-20). The reason for the increased tensile strength achieved by the application of high load carrying capacity parent concrete may be the drop in porosity of the high strength source concrete.

Kou and Poon [30] developed two series of RAC: high strength RAC (Series II), made with a w/c proportion of 0.35 and a 65 MPa 28-day compressive load carrying capacity, and normal strength (Series I), with a w/c proportion of 0.5 and a 45 MPa 28-day compressive load carrying capacity, using RCA derived from PCs with strengths of 30, 45, 60, 80, and 100 MPa. In high performance RAC, the STS of RCA concrete produced from source concretes with load carrying capacity ranging from 30 to 100 MPa was found to be 11.1 to 26.0% higher compared to equivalent conventional aggregate concrete, respectively. Whereas in normal capacity RAC, it was discovered that RAC produced with RCA obtained from source concrete strengths varying from 30 to 100 MPa had split tensile strengths that were, correspondingly, 2.1 to 12.2% greater than the comparable concrete made with conventional aggregates. The rougher and permeable surface of RCAs may have strengthened the interfacial transition zone (ITZ) among the RCAs and hardened cement paste, increasing the STS of RAC. This gives a clue to use recycled aggregates rather than natural aggregates in areas highly stressed by tensile forces. However, further research into practical applications is required.

Another significant element that influences how concrete behaves structurally is its flexural load carrying capacity. Regardless of any of the factors, the compressive and STS load carrying capacity of the RACs were often inferior to those of the original concrete [28]. Bhat [28] on his study has implemented to determine the interaction among the RAC modulus of rupture and the compressive load carrying capacity of the original concrete. (Figure 2.5 (c)) demonstrated that the source concrete grade had less discernible impact on the flexural strength of the three grades of the RCA concrete at either the 50% or 100% RCA substitution levels. Conversely, the modulus of rupture was found to be reduced by 7%–23% in the aggregates with a 100% RCA substitution level in contrast to the conventional NAC. The reduction in modulus of rupture may be due to the inability of RACs to withstand moment loads. Slip and bonding behavior of reinforced recycled aggregate concrete under tensile and flexural loading is an important characteristics of recycled aggregate concrete that is not investigated so far.

2.4.2.4 Static elastic modulus

An additional crucial mechanical characteristics that defines concrete's resilience is its static modulus of elasticity. Numerous factors, including the density of the aggregate, grade of PC, and characteristics of the ITZ, impacts the concrete modulus of elasticity. This is so because the porosity and density of the aggregate dictate the bulk matrix stiffness. The substitution of RCA for NA has an influence on the static elastic modulus. However, the modulus of elasticity is more significantly impacted by RCA porosity [67]. The elasticity of the concrete formed using RCA was inferior to the conventional concrete because of the weaker modulus of the previous hardened mortar that was glued to the RCAs.

The largest change in loss of modulus of elasticity resulted from variable source concrete strength and was shown to be between 11% and 80% [25, 48, 68, 69]. Kou and Poon [30] determined the impact of source concrete strength on RACs static elastic modulus (Figure 2.6). It was discovered that the RAC with RCAs had a lower elastic modulus compared to ordinary concrete; this is regardless of the parent concrete's load carrying capacity. However, the drop in static modulus was lessened by the source concrete's increased strength, from which the RCA was produced. For instance, considering Series II concrete of Kou and Poon [30] , the static elastic modulus of the RACs cured for 90 days at 100 MPa and 30 MPa PC strengths have a drop of 6% and 23%, correspondingly, in contrast with the corresponding natural aggregate concrete (Figure 2.6). Considering similar parent concrete strength, RAC produced with RCA having higher amounts of attached mortar had a lower 28 and 90 days elastic modulus compared to those produced with RCA with lower amounts of adhered mortar and conventional aggregates [30]. According to Kou et al. [61], RAC produced using low grade RCA has a considerably lower elastic modulus than regular concrete.

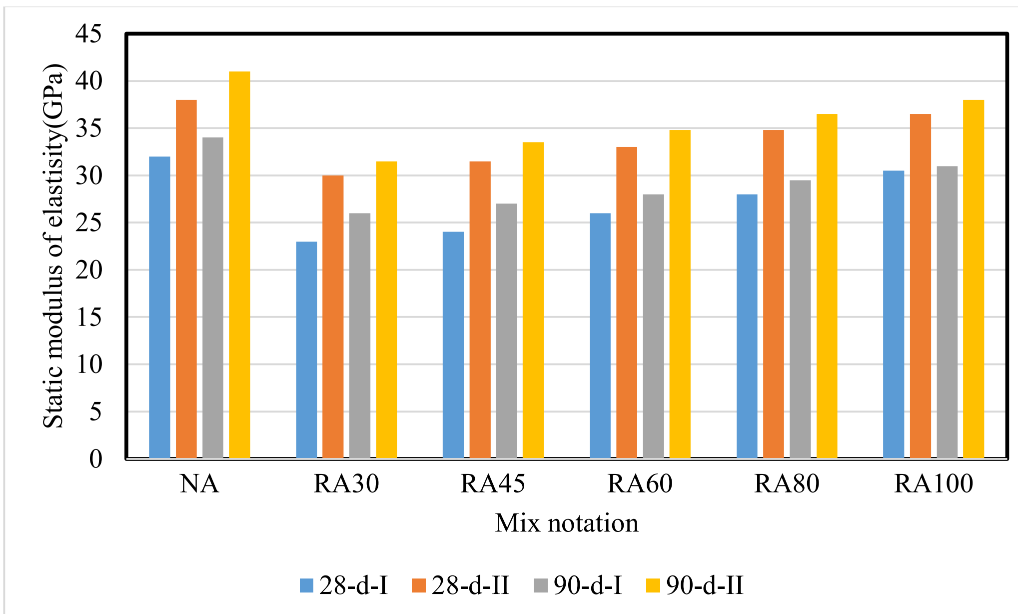

Figure 2.6 Static elastic modulus of concrete combinations in normal strength RAC (Series I) and high performance RAC (series II). [Reprinted from [30] with permission from Elsevier].

This output was anticipated since low grade RCAs have a reduced elastic modulus than conventional and industrially manufactured RCAs, because it is widely recognized that aggregate elastic modulus has a greater influence on the elastic modulus of concrete [48]. Generally, it can be seen from earlier works that the static elastic modulus is negatively impacted by the load carrying capacity of the source concrete if the aggregates are manufactured from low-strength source concrete. However, at an increased capacity of parent material, its effect on the elastic modulus is low. Future research should focus on the use of recycled aggregate concrete with varied source concrete strength considering dynamic elastic modulus, as it was not taken into account in the all previous literature studies.

2.4.3 Effects of parent concrete strength on long term and durability properties of recycled aggregate concrete

The durability of concrete can be expressed in terms of its capacity to withstand abrasion, harsh environmental attack, chloride penetration, carbonation, frost resistance and weathering while retaining the desired engineering qualities [70]. All concrete projects must fulfill their intended purposes and maintain appropriate strength and serviceability requirements throughout their service period. Concrete should, therefore, possess the ability to withstand the deteriorating degree to which it will likely be subjected [70]. RACs are more vulnerable to abrasion, chemical attack, chloride penetration, carbonation, frost action and weathering attacks because of the existence of attached porous mortar. It is obvious that the capacity of the parent concrete has a visible impact on the durability characteristics of RAC. The effects of the source concrete's strength on the durability and long-term behavior of RAC are addressed in the following sub-sections.

2.4.3.1 Drying shrinkage

One of the notable characteristics of a RAC is shrinkage of the material upon drying. This is the reduction in cubic volume of the concrete caused by the concrete's reduction in capillary water which, in turn, promotes the growth of cracks in osmotic stress inside the cement mortar's structure of the mesopores [69]. The residual mortar quality, which is mostly defined by the life time and load carrying capacity of the source concrete, may affect the drying induced shrinkage of RAC. Pedro et al. [26] and Geng et al. [36] stated that the source concrete strength showed no noticeable effect on the drying induced shrinkage of the final concrete. They reasoned out that the crushing procedure is the key parameter that removes the porous mortar attached to the natural aggregates; their finding is that the amount of attached mortar has negative influence on the shrinkage resistance of the RAC more than the grade of the source concrete.

Kou and Poon [30], Gonzalez-Corominas and Etxeberria [38], and Gholampour and Ozbakkaloglu [22] discovered that concrete products made with RCA derived from higher strength source concrete experienced less drying induced shrinkage than concrete mixtures produced with RCA derived from reduced strength source concrete. It is because the less porous nature of good strength source concrete in contrast to low grade source concrete, that sucks less capillary water and losses less water during drying causing less shrinkage in the RAC was their reason for their conclusion [22, 30, 38]. In cases of normal to medium-load carrying capacity source concrete aggregates, to increase the shrinkage resistance of RAC to a level that is similar to that of regular concrete, it may be necessary to incorporate additional crushing steps into the RCA process, which reduces the amount of deformable older mortar and effectively controls concrete shrinkage.

The amount of adhered mortar gives a clue on the detrimental effect on the ability of RAC to withstand shrinkage. The best crushing technique for removing the adhered mortar and minimizing drying shrinkage can be determined by comparing several crushing techniques. Admixtures can also be used to modify concrete's drying shrinkage and other properties. The development of new admixtures specifically designed to reduce drying shrinkage can lead to the production of more durable RCA. Therefore, future studies should focus on minimizing the drying induced shrinkage of RAC through the application of different crushing techniques and admixtures.

2.4.3.2 Freezing and thawing

Frequent exposure to moisture, high relative humidity, and low ambient temperature can lead to concrete elements degrading due to cyclic frost and thaw. The corrosion of the rebar begins as a result of this damage, which makes it possible for hostile external agents (such as sulphates and chlorides) to penetrate [35, 61, 71, 72]. In the case of RCAs, the connected mortar's porous character worsens the freezing thawing effect. PC strength variations may also introduce variability in the capacity of the recycled concrete to resist the freeze and thaw effects.

Liu et al. [17] clarified how the source concrete and the technique of mixing affected the resilience of concrete with air-entrained RCA to thawing and freezing conditions. The qualities of the RAC were heavily dependent on the source concrete. The frost resistance of the air entrained concrete and regular RAC were comparable because the RCAs used in the sample was derived from frost resistant PC. The air entrained RAC sample showed high freeze and thaw resistivity in addition to almost similar freeze and thaw durability as natural air contained concrete. However, the second air entrained RAC sample, on the other hand, was manufactured with RCA derived from non-air contained concrete and low strength concrete, and it had a low resistance to frost. The development of strategies to improve the freeze and thaw resistance of RAC needs further study. This will enable RAC to be used more widely in a variety of climates and applications.

2.4.3.3 Creep

Numerous studies [33, 73, 74] have demonstrated that, because of the existence of weak adhered mortar, employing RCA in concrete causes greater shrinkage and creep than NAC. Additionally, it has been found that the volume, composition, and qualities of the previous adhering mortar have a substantial impact on the RAC creep [32]. Lower strength RAC mixes have poorer mechanical characteristics and exhibit greater shrinkage strain and creep deformation than higher strength RAC mixes. This is resulted from the low strength source concrete aggregates, less dense and more permeable behavior compared to stronger parent concrete aggregates, allowing them to drain and lose water during temperature variations.

Because the characteristics of the low strength source concrete RAC are more vulnerable to variation due to environmental factors, the RAC produced from them wears and degrades over time. Additionally, it has been demonstrated that high strength RACs, which are made by completely substituting conventional aggregates with RCAs of higher source concrete strength, have either a long term and time varying mechanical qualities that are comparable to or superior to those of associated NAC [34]. The increased durability due to increased parent concrete strength could be due to the presence of less capillary pores with less moisture intake, making the RAC resistant to weathering degradations.

Future research could concentrate on the Establishment of models that estimate the creep behavior of RAC based on the load carrying capacity of the source concrete. This can help in understanding the relationship between the long term deformation characteristics of RAC and the load carrying capacity of the PC without experimental studies.

2.4.3.4 Resistance to chloride ion infiltration and carbonation

Carbonation resistance and resistance to chloride ion penetrations of RAC were influenced by the quality of the source concrete in a similar manner with other properties of RAC. As described by Rao et al. [75], the outcomes of two RAC mixes' defense against penetration of chloride ions (w/c proportions of 0.5 and 0.35) made with RCAs and gained various strengths ranging from 30 to 100 MPa of PC were reported by Kou and Poon [30] and are shown in Figure 2.7. The results showed that adding RCA, which is made from a mix of various strengths of PC, increases chloride penetrability in comparison to the NAC mixture. However, compared to concrete manufactured with RCA that was collected from PC with inferior strength, the chloride penetrability of mixtures produced with RCA from source concrete with greater strength was lower due to the denser attached mortar in the high strength parent concrete. Carbonation resistance levels ranged widely, from a 3% increase [56] to a 67% decrease [52], and resistance to chloride penetration decreased by 10% to 32% [25, 33, 34] due to PC strength variations. This variation could be caused by the uncontrolled parallel effects of other variables such as the crushing procedure and size of aggregates. The draw backs of using different parent concrete strength recycled aggregates in RAC's opposition to carbonation and chloride ion infiltration could be the subject of future studies.

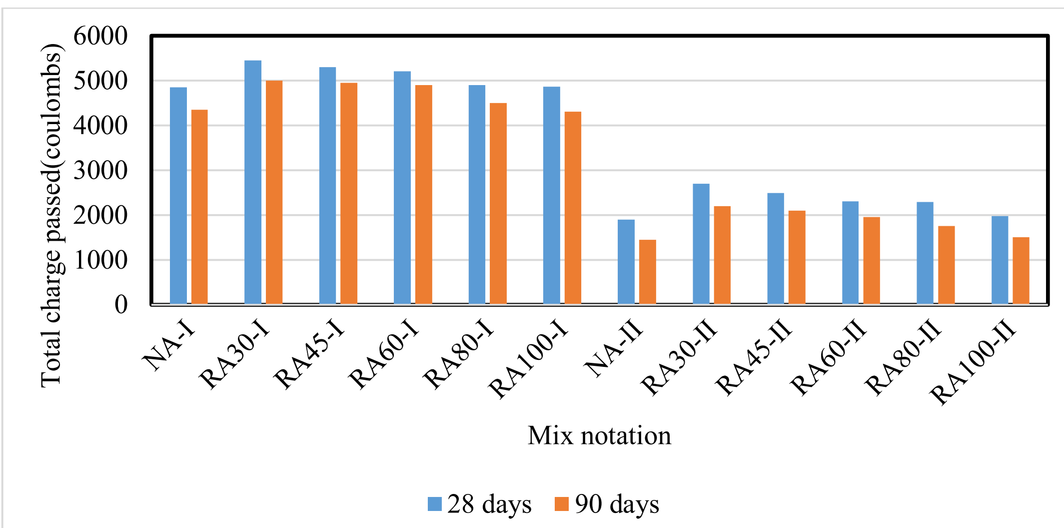

Figure 2.7 Penetrability potential of concrete by chloride ions (w/c proportions of 0.5) and (w/c proportions of 0.35) [Reprinted from [30], with permission from Elsevier].

2.4.4. Impact of strength of source concrete on the microstructure of RAC

There are a total of three phases in the microstructure of concrete: the aggregate phase, the bulk hardened mortar phase, and the ITZ [76]. Because of RACs have increased number of interface zones than conventional concrete, studying the interface of attached mortar and aggregate is especially important in this type of concrete. Contrary to conventional concrete, which has single ITZ; located between the aggregate and cement paste, there is additional interface zone in RCAs: ITZ between the adherent hardened cement paste and the new cement paste matrix (the new ITZ) and between the natural aggregate and the old connected mortar (the old ITZ) [75].

Poon et al. [77] produced concrete specimens using a recycled high strength concrete aggregates, a recycled normal strength concrete aggregates (compressive strength between 20 and 40MPa), and a conventional aggregate as a control and, subsequently investigated the effect of those particles on the micro scale organization of the resulting concrete. Generally, the scanning electron microscope (SEM) findings revealed that the normal strength RCA and cement matrix had a weak and permeable interfacial layer, whereas the high strength RCAs and cement matrix had a stronger interfaces (Figure 2.8(3)). The increased porosity and absorption capacity of RCAs are the causes for the inferior ITZ in RAC with regular strength concrete aggregate, and under higher magnification, the ITZ extreme porosity could be detected [77] (Figure 2.8(2(b))). Additionally, from Figure 2.8((1(a)) and Figure 2.8 (1(b)), the dimension of the ITZ ranged over the aggregate surface, as can be seen obviously, and the interface between the granite aggregate and mortar was rather loose. It was found that the ITZ between the mortar matrix and the aggregates made from regular load carrying capacity concrete was approximately 45 μm wide and mostly comprised loose particles [77]. Under higher magnification, the ITZ extreme porosity could also be detected (Figure 2.8(2(a)) and Figure2.8 (2(b)) [77].

Leite and Monteiro [78] examined the RAC morphology utilizing sophisticated light source synchrotron microtomography (μCT) and SEM analysis. In their research, the authors used compressive strengths of the parent concrete of 40 MPa and 80 MPa with the initial water content conditions of saturated surface dry (SSD) and oven dry states of the RCAs. Based on the microstructural findings, they suggested that it would be possible to produce recycled concrete by using RCA from high load carrying capacity source concrete (greater than 80 MPa) that was employed in the SSD condition and whose mechanical, physical, and microstructural qualities could be comparable to those of the standard concrete used as a reference. Because there is less porosity in the RAC at higher levels of source concrete strength, the standard of the RAC improves. There are few microstructural studies in the literature considering parent concrete effects; accordingly further studies on the microstructural attribute of RAC incorporating various strengths of parent concrete is needed to strengthen the current findings.

Another crucial area of study was the analysis of the bond attribute of reinforced RCAs and geopolymer RCAs that contained aggregates from various PC strengths. The effects of source concrete calibre on RCA characteristics such as durability and steel concrete bondage were examined by Joseph et al. [79]. The test findings demonstrated that the PC grade has a visible impact on the ultimate bonding strength and stress transmission to inserted rebars. Similarly the workability of geopolymer concrete can be significantly enhanced by the application of good quality RCAs, according to a study by Blessen et al. [80]. A further review and investigation on the impact of source concrete grade on bond to steel reinforcement, on geopolymer and engineered cementitious composts should be the areas of future studies.

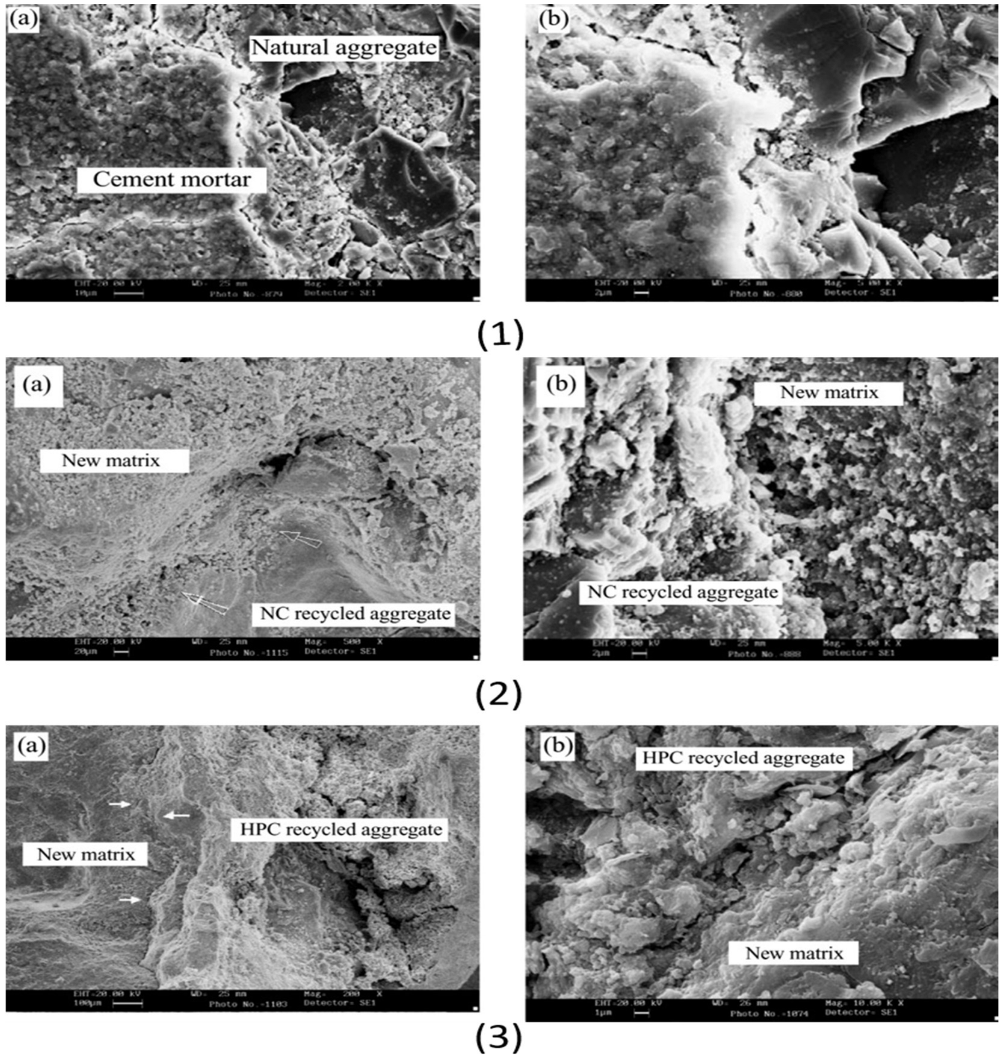

Figure 2.8 Microstructure of RAC. (1) RCA concrete made of crushed raw granite, (2) RCA concrete made with recycled ordinary-strength parent concrete aggregates. (3) RCA concrete made with recycled high-strength parent concrete). [Reprinted from [77] with permission from Elsevier].

2.5. Conclusions and Future Remarks

A number of researches on the impact of source concrete strength on RCAs and concrete have been carried out so far, producing informative findings that can add value to the recycling world. However, there are inconsistencies in the findings from these studies in terms of the influence of source concrete quality on RCA characteristics. The objective of the study reported in this paper has been to review the investigations carried out to date on the potential effects of source concrete properties on RAC qualities in order to identify the possible causes of variability and inconsistency in those findings.

Based on the reviewed findings, it is not fully and conclusively clear yet in what manner PC load carrying capacity affects the behavior of RCAs and RAC. But, the porosity of the source concrete, and the crushing methodology of the source concrete aggregate were the two primary causes of variabilities in the results of the literary works on RAC. In view of these developments, it is found that more in depth experimental work and research are required, including developing norms and standards for parent concrete strength effects while taking into account the constraints and competing claims in the studies, in order to arrive at a dependable conclusion regarding the core issue of the subject matter.

The key specific findings and recommendations from this review are as follows:

– Several factors contribute to the heterogeneity in RAC properties of literature outcomes. Firstly, the qualities of RAC are significantly impacted by the PC's porosity. Porosity is affected by shape and texture, with angular and rough surfaces encouraging a stronger connection with cement pastes. Second, different researchers used different NA types in PC, which results in diverse qualities of RCAs. The method of crushing also has an impact on how much mortar is adhered to RCAs. Different crushing methods result in variable quantity of mortar. On top of that, the porosity of attached mortar might vary based on the compaction of the RAC and the type of cement, among other factors. For comprehensive studies in this subject, researchers must take these elements into account.

– After reviewing the research carried out on the effects of source concrete strength on RAC characteristics, it has been found that, contrary to the popular belief that "RACs in general have lower quality than natural aggregate concrete", RACs produced using high strength source concrete (not less than 80 MPa) can have equivalent or better strength properties than NAC. Therefore, aggregates produced from PC with higher strength could be applied to produce good physical and mechanical property concrete without using any additional NAs. But, with the addition of the high strength source concrete aggregates, it was seen that the long term behavior of the RAC began to deteriorate after 50% replacement level.

Therefore, consideration of approaches for durability enhancement should be the subject of further research.

- The findings of the tensile load carrying capacity of RAC studies in the literature showed that, at higher strengths of the PC, RAC has better tensile capacity than NAC. This could be because of the rough and porous nature of the RCA, which creates an interlocking bond in the weak ITZ that makes the tensile strength of the RAC better. Similarly, a rise in the strength of the source concrete produces RAC with better tensile strength than low quality PC because the attached mortar in the high strength RAC is dense and resistant to tension.

- Employing high strength PC as the source material for RAC can demonstrably enhance its structural integrity, with potential strength gains exceeding 20% relative to RACs produced from weaker parent concrete.

- It has been seen from the literature that the rise in the aggregates' source concrete strength clearly enhanced the durability properties of RAC. Upcoming studies should concentrate on the efficacy of various RCA property improvement techniques and their impact on the durability performance of RCA and RAC made from low strength PC. Similarly, enhancement methods for the microstructure of RCAs and RACs at new and old ITZs of the low strength PCs should be considered because the characteristics of RCA and the micro scale organization of concrete are what generally determine the durability capacity of RAC.

- Many models have been established to forecast the performance of RAC in order to guarantee both economy as well as safety of the developments with usability in mind. The models mainly targeted on modulus of elasticity, compressive load carrying capacity, split tensile strength, or stress strain behavior of concrete without considering the impact of the source concrete's strength on those properties. Therefore, new performance based models for recycled aggregate concrete considering the variability in properties induced by the PC strength should be developed for a better prediction of the performance of RAC.

- According to recent literature, the porous nature of RCA and the dimensions of ITZ have the most significant effects on the microstructure of RAC. The quality of the source concrete also has an influence on the porosity and ITZ dimensions.

Considering the strength of the source concrete, however, the microstructure of RAC is not sufficiently researched.

– A further study on the influences of source concrete strength on the flexural, shear, and torsional behavior of reinforced RAC structures should be carried out. Because the previous studies were conducted on a plain concrete cube cast in the laboratory, the bond and interaction between the various strength parent concrete aggregates and the reinforcement bars were not investigated. The studies could involve both experimental testing, analysis techniques and simulations to evaluate these properties of reinforced RAC structures.

2.6. References

[1]. Ittyeipe, AV., Thomas AV, Ramaswamy KP., (2020). Comparison of the energy consumption in the production of natural and recycled concrete aggregate: A case study in Kerala, India. IOP Conf Ser.: Mater Sci. Eng'.989(1),012011. https://doi.org/10.1088/1757-899X/989/1/012011.

[2]. De Magalhães RF, Danilevicz ÂMF, Saurin TA., (2017). Reducing construction waste: A study of urban infrastructure projects. Waste Manag. 67,265-77, 28551278 https://doi.org/10.1016/j.wasman.2017.05.025

[3]. S'aez PV, C'esar PA, Del Río MM., (2020). Estimation of construction and demolition waste. In: Torgal P, Ding Y, Colangelo F, Tuladhar R, Koutamanis A, editors. Available from: https://www.elsevier.com/books/advances-in-construction-and-demolition-waste-recycling/pacheco-torgal/978-0-12-819055-5. Advances in construction and demolition waste recycling, management, processing and environmental assessment.1,13-30.

[4]. Kaarthik M, Maruthachalam D., (2021). A sustainable approach of characteristic strength of concrete using recycled fine aggregate. Mater Today Proc.45(7),6377-80. https://doi.org/10.1016/j.matpr.2020.11.058.

[5]. Wang B, Yan L, Fu Q, Kasal B. (2021). A comprehensive review on recycled aggregate and recycled aggregate concrete. Resour Conserv Recycl.171,105565. https://doi.org/10.1016/j.resconrec.2021.105565.

[6]. Aboginije A, Aigbavboa C, Thwala W., (2020). Determining the Impact of Construction and Demolition Waste Reduction practices on Green Building Projects in Gauteng Province, South Africa. Paper presented at: Proceedings of the International Conference on Industrial Engineering and Operations Management Dubai. UAE, March 10-12. IEOM Society International; 2020. Available from: https://www.researchgate.net/publication/340129188.

[7]. Liang Z, Hu Z, Zhou Y, Wu Y, Zhou X, Hu B, et al., (2022). Improving recycled aggregate concrete by compression casting and nano-silica. Nanotechnol Rev. 11(1),1273-90. https://doi.org/10.1515/ntrev-2022-0065.

[8]. Hossain MU, Poon CS, Lo IMC, Cheng JCP. (2016). Comparative environmental evaluation of aggregate production from recycled waste materials and virgin sources by LCA. Resour Conserv Recycl. 109, 67-77. https://doi.org/10.1016/j.resconrec.2016.02.009.

[9]. Sajan KC, Adhikari R, Mandal B, Gautam D. (2022). Mechanical characterization of recycled concrete under various aggregate replacement scenarios. Cleaner Eng Technol. 7, 100428. https://doi.org/10.1016/j.clet.2022.100428.

[10]. Wang Y, Chen J, Geng Y., (2015). Testing and analysis of axially loaded normal-strength recycled aggregate concrete filled steel tubular stub columns. Eng Struct. 86,192-212. https://doi.org/10.1016/j.engstruct.2015.01.007.

[11]. Ignjatović IS, Marinković SB, Tošić N., (2017). Shear behavior of recycled aggregate concrete beams with and without shear reinforcement. Eng Struct.141,386-401. https://doi.org/10.1016/j.engstruct.2017.03.026.

[12]. Gholampour A, Gandomi AH, Ozbakkaloglu T., (2017). New formulations for mechanical properties of recycled aggregate concrete using gene expression programming. Constr Build Mater. 130, 122-45. https://doi.org/10.1016/j.conbuildmat.2016.10.114.

[13]. Ozbakkaloglu T, Gholampour A, Xie T. (2017). Toward the development of sustainable concretes with recycled concrete aggregates: a comprehensive review of studies on mechanical properties. J Mater Civ Eng.. https://doi.org/10.1061/(ASCE)MT.1943-5533.0002304.

[14]. Liu B, Feng C, Deng ZH., (2019). Shear behavior of three types of recycled aggregate concrete. Constr Build Mater.217,557-72. https://doi.org/10.1016/j.conbuildmat.2019.05.079.

[15]. Zhou CH, Chen ZP., (2017). Mechanical properties of recycled concrete made with different types of coarse aggregate. Constr Build Mater.134,497-506. https://doi.org/10.1016/j.conbuildmat.2016.12.163

[16]. Abdulla NA., (2015). Effect of recycled coarse aggregate type on concrete. J Mater Civ Eng. 27(10), 04014273. https://doi.org/10.1061/(ASCE)MT.1943-5533.0001247.

[17]. Liu K, Yan J, Hu Q, Sun Y, Zou C., (2016). Effects of parent concrete and mixing method on the resistance to freezing and thawing of air-entrained recycled aggregate concrete. Constr Build Mater.106, 264-73. https://doi.org/10.1016/j.conbuildmat.2015.12.074.

[18]. Akbarnezhad A, Ong KCG, Tam CT, (2013). Zhang MH. Effects of the parent concrete properties and crushing procedure on the properties of coarse recycled concrete aggregates. J Mater Civ Eng. 25, 1795-802. https://doi.org/10.1061/(ASCE)MT.1943-5533.0000789.

[19]. Xie T, Gholampour A, Ozbakkaloglu T. (2018). Toward the development of sustainable concretes with recycled concrete aggregates: comprehensive review of studies on mechanical properties. J Mater Civ Eng, 30(9). https://doi.org/10.1061/(ASCE)MT.1943-5533.0002304.

[20]. Padmini AK, Ramamurthy K, Mathews MS., (2009). Influence of parent concrete on the properties of recycled aggregate concrete. Constr Build Mater. 23(2), 829-36. https://doi.org/10.1016/j.conbuildmat.2008.03.006.

[21]. Duan Z, Han N, Singh A, Xiao J., (2020). Multi-scale investigation on concrete prepared with recycled aggregates from different parent concrete. J Renew Mater. 8(11),1375-90. https://doi.org/10.32604/jrm.2020.013044

[22]. Gholampour A, Ozbakkaloglu T. (2018). Time-dependent and long-term mechanical properties of concretes incorporating different grades of coarse recycled concrete aggregates. Eng Struct.157, 224-34. https://doi.org/10.1016/j.engstruct.2017.12.015.

[23]. Chakradhara Rao MC. (2018). Properties of recycled aggregate and recycled aggregate concrete: effect of parent concrete. Asian J Civ Eng. 19(1), 103-10. https://doi.org/10.1007/s42107-018-0011-x.

[24]. De Juan MS, Gutiérrez PA., (2009). Study on the influence of attached mortar content on the properties of recycled concrete aggregate. Constr Build Mater. 23(2)872-7. https://doi.org/10.1016/j.conbuildmat.2008.04.012

[25]. Chakradhara Rao M, Bhattacharyya SK, Barai SV. (2011). Influence of field recycled coarse aggregate on properties of concrete. Mater Struct. 44(1), 205-20. https://doi.org/10.1617/s11527-010-9620-x.

[26]. Pedro D, de Brito J, Evangelista L. (2014). Influence of the use of recycled concrete aggregates from different sources on structural concrete. Constr Build Mater.71,141-51. https://doi.org/10.1016/j.conbuildmat.2014.08.030.

[27]. Andreu G, Miren E., (2014). Experimental analysis of properties of high performance recycled aggregate concrete. Constr Build Mater. 52,227-35. https://doi.org/10.1016/j.conbuildmat.2013.11.054.

[28]. Ahmad Bhat JA., (2021). Effect of strength of parent concrete on the mechanical properties of recycled aggregate concrete. Mater Today Proc.42:1462-9. https://doi.org/10.1016/j.matpr.2021.01.310.

[29]. Nagataki S, Gokce A, Saeki T, Hisada M. (2004). Assessment of recycling process induced damage sensitivity of recycled concrete aggregates. Cem Concr Res. 34(6),965-71. https://doi.org/10.1016/j.cemconres.2003.11.008.

[30]. Kou SC, Poon CS., (2015). Effect of the quality of parent concrete on the properties of high performance recycled aggregate concrete. Constr Build Mater. 77,501-8. https://doi.org/10.1016/j.conbuildmat.2014.12.035.

[31]. Seo DS, Choi HB., (2014). Effects of the old cement mortar attached to the recycled aggregate surface on the bond characteristics between aggregate and cement mortar. Constr Build Mater. 59,72-7. https://doi.org/10.1016/j.conbuildmat.2014.02.047.

[32]. Fan Y, Xiao J, Tam VWY., (2014). Effect of old attached mortar on the creep of recycled aggregate concrete. Struct Concr. 15(2), 169-78. https://doi.org/10.1002/suco.201300055.

[33]. Kou SC, Poon CS., (2012). Enhancing the durability properties on concrete prepared with coarse recycled aggregate. Constr Build Mater. 35,69-76. https://doi.org/10.1016/j.conbuildmat.2012.02.032.

[34]. Limbachiya MC, Meddah MS, Ouchagour Y. (2011). Use of recycled concrete aggregate in fly-ash concrete. Constr Build Mater. 27(1),439-49. https://doi.org/10.1016/j.conbuildmat.2011.07.023.

[35]. Pani L, Francesconi L, Rombi J, Mistretta F, Sassu M, Stochino F., (2020). Effect of parent concrete on the performance of recycled aggregate concrete. Sustainability. 12(22), 9399. https://doi.org/10.3390/su12229399

[36]. Geng Y, Wang Q, Wang Y, Zhang H., (2019). Influence of service time of recycled coarse aggregate on the mechanical properties of recycled aggregate concrete. Mater Struct. 52(5), 97. https://doi.org/10.1617/s11527-019-1395-0.

[37]. Wang Q, Geng Y, Wang Y, Zhang H., (2020). Drying shrinkage model for recycled aggregate concrete accounting for the influence of parent concrete. Eng Struct. 202, 109888. https://doi.org/10.1016/j.engstruct.2019.109888.

[38]. Gonzalez-Corominas A, Etxeberria M., (2016). Effects of using recycled concrete aggregates on the shrinkage of high performance concrete. Constr Build Mater.115(4), 32-41. https://doi.org/10.1016/j.conbuildmat.2016.04.031.

[39]. Grubl P, Ruhl M. (1998). German committee for reinforced concrete (DAfStb) code: concrete with recycled aggregates. University of Dundee; Proceedings of the international symposium on sustainable construction: use of Recycled Concrete Aggregate, Concrete Technology Unit. Available from: http://worldcat.org/isbn/0727727265.

[40]. Upshaw M, Cai CS., (2020). Critical review of recycled aggregate concrete properties, improvements, and numerical models. J Mater Civ Eng. 32(11),03120005. https://doi.org/10.1061/(ASCE)MT.1943-5533.0003394.

[41]. Guo H, Shi C, Guan X, Zhu J, Ding Y, Ling T et al. (2018). Durability of recycled aggregate concrete – a review. Cem Concr Compos. 89,251-9. https://doi.org/10.1016/j.cemconcomp.2018.03.008.

[42]. VWY, Soomro M, Evangelista ACJ. (2018). A review of recycled aggregate in concrete applications (2000-2017). Constr Build Mater. 172,272-92. https://doi.org/10.1016/j.conbuildmat.2018.03.240.

[43]. Mo civil engineering. Shape and texture of aggregate for concrete [cited Feb 27, 2024]. Available from: https://mocivilengineering.com/shape-and-texture-of-aggregate-for-concrete/.

[44]. Marie I, Mujalli R. (2018). Effect of design properties of parent concrete on the morphological properties of recycled concrete aggregates, Eng. sci. Tech. Int J. https://doi.org/10.1016/j.jestch.2018.08.014.

[45]. Powers MC., (1953). A new roundness scale for sedimentary particles, SEPM J. J Sediment Res. 117-119 23 (2). https://doi.org/10.1306/D4269567-2B26-11D7-8648000102C1865D.

[46]. Shergold FA. (1953). The percentage voids in compacted gravel as a measure of its angularity. Magazine of Concrete Research. 5(13):3-10. https://doi.org/10.1680/macr.1953.5.13.3.

[47]. ASTM D-3398 (2004). Standard Test Method for Index of Aggregate Particle Shape and Texture. West Conshohocken, PA: ASTM International; Available from: http://www.astm.org.

[48]. Etxeberria M, Vázquez E, Marí A, Barra M., (2007). Influence of amount of recycled coarse aggregates and production process on properties of recycled aggregate concrete. Cem Concr Res. 37(5) 735-42. https://doi.org/10.1016/j.cemconres.2007.02.002.

[49]. Lamond JF, Campbell RL, Campbell JA, Giraldi A, Halczak W, Hale HC. (2002). Removal and reuse of hardened concrete: reported by ACI committee 555. ACI Mater J. 99,300-25.

[50]. Tam VWY, Wang K, Tam CM.(2008). Assessing relationship among properties of demolished concrete, recycled aggregate and recycled aggregate concrete using regression analysis. J Hazard Mater. 152(2),703-14. https://doi.org/10.1016/j.jhazmat.2007.07.061.

[51]. Tam VWY, Gao XF, Tam CM, Chan CH., (2008). New approach in measuring water absorption of recycled aggregates. Constr Build Mater. 22(3),364-9. https://doi.org/10.1016/j.conbuildmat.2006.08.009.

[52]. Rao A, Jha KN, Misra S., (2007). Use of aggregates from recycled construction and demolition waste in concrete. Resour Conserv Recycl. 50(1), 71-81. https://doi.org/10.1016/j.resconrec.2006.05.010

[53]. Spanish minister of public works. Vol. 2008; 2008. Instrucción de hormigón estructural EHE-08 [Spanish structural concrete code]. Available from: http://asidac.es/asidac-en/wp-content/uploads/2016/07/EHE-ENG.pdf.

[54]. Thomas C, Setién J, Polanco JA, Alaejos P, Sánchez de Juan M., (2013). Durability of recycled aggregate concrete. Constr Build Mater. 40,1054-65. https://doi.org/10.1016/j.conbuildmat.2012.11.106.

[55]. Levy SM, Helene P., (2004). Durability of recycled aggregates concrete: a safe way to sustainable development. Cem Concr Res. 34(11)1975-80. doi: 10.1016/j.cemconres.2004.02.009.

[56]. Poon CS, Chan D., (2006). Feasible use of recycled concrete aggregates and crushed clay brick as unbound road sub-base. Constr Build Mater.20(8),578-85. https://doi.org/10.1016/j.conbuildmat.2005.01.045.

[57]. Liu Q, Xiao J, Sun Z., (2011). Experimental study on the failure mechanism of recycled concrete. Cem Concr Res. 41(10),1050-7. https://doi.org/10.1016/j.cemconres.2011.06.007.

[58]. Gebremariam HG, Taye S, Tarekegn AG., (2023). Disparity in research findings on parent concrete strength effects on recycled aggregate quality as a challenge in aggregate recycling. Case Stud Constr Mater.19,e02342. https://doi.org/10.1016/j.cscm.2023.e02342

[59]. Backus BE., (2023). What is workability of concrete? Materials testing equipment, Gilson Company, ILC; [cited Feb 16 2023]. Available from: https://www.globalgilson.com/blog/what-is-workability-of-concrete.

[60]. Ghasemi Y, Emborg M, Cwirzen A., (2019). Exploring the relation between the flow of mortar and specific surface area of its constituents. Constr Build Mater. 211,492-501. https://doi.org/10.1016/j.conbuildmat.2019.03.260

[61]. Guedes M, Evangelista L, de Brito J, Ferro AC. (2013). Microstructural characterization of concrete prepared with recycled aggregates. Microsc Microanal. 19(5), 1222-30. https://doi.org/10.1017/S1431927613001463, PMID 23673273.

[62]. Poon CS, Shui ZH, Lam L, Fok H, Kou SC., (2004a). Influence of moisture states of natural and recycled aggregates on the slump and compressive strength

of concrete. Cem Concr Res. 34(1), 31-6. https://doi.org/10.1016/S0008-8846(03)00186-8.

[63]. Rahal K., (2007). Mechanical properties of concrete with recycled coarse aggregate. Build Environ. 42(1), 407-15. https://doi.org/10.1016/j.buildenv.2005.07.033.

[64]. Kisku N, Joshi H, Ansari M, Panda SK, Nayak S, Dutta SC., (2017). A critical review and assessment for usage of recycled aggregate as sustainable construction material. Constr Build Mater. 131,721-40. https://doi.org/10.1016/j.conbuildmat.2016.11.029.

[65]. Tabsh SW, Abdelfatah AS., (2009). Influence of recycled concrete aggregates on strength properties of concrete. Constr Build Mater. 23(2), 1163-7. https://doi.org/10.1016/j.conbuildmat.2008.06.007.

[66]. Bairagi NK, Ravande K, Pareek VK., (1993). Behavior of concrete with different proportions of natural and recycled aggregates. Resour Conserv Recy. 9(1-2),109-26. https://doi.org/10.1016/0921-3449(93)90036-F.

[67]. Behera M, Bhattacharyya SK, Minocha AK, Deoliya R, Maiti S., (2014). Recycled aggregate from C&D waste & its use in concrete – A breakthrough towards sustainability in construction sector: a review. Constr Build Mater. 68,501-16. https://doi.org/10.1016/j.conbuildmat.2014.07.003.

[68]. Xiao J, Li J, Zhang C., (2005). Mechanical properties of recycled aggregate concrete under uniaxial loading. Cem Concr Res. 35(6), 1187-94. https://doi.org/10.1016/j.cemconres.2004.09.020.

[69]. Topçu IB, Günçan NF., (1995). Using waste concrete as aggregate. Cem Concr Res. 25(7), 1385-90. https://doi.org/10.1016/0008-8846(95)00131-U.

[70]. Neville AM. London, UK: Pearson Education; 2006. Properties of concrete. 4th ed. Available from: https://scholar.google.pl/scholar?hl=en&as_sdt=0%2C5&as_vis=1&q=properties+of+concrete+neville&oq=+Properties+of+concrete.

[71]. Hanjari KZ, Utgenannt P, Lundgren K., (2011). Experimental study of the material and bond properties of frost-damaged concrete. Cem Concr Res. 41(3), 244-54. https://doi.org/10.1016/j.cemconres.2010.11.007.

[72]. Harrison TA, Dewar JD, Brown BV., (2001). Freeze-thaw resisting concrete: its achievement in the UK. London, UK: CIRIA.

[73]. Domingo-Cabo A, Lázaro C, López-Gayarre F, Serrano-López MA, Serna P, Castaño-Tabares JO., (2009). Creep and shrinkage of recycled aggregate concrete. Constr Build Mater. 23(7),2545-53. https://doi.org/10.1016/j.conbuildmat.2009.02.018.

[74]. Fathifazl G, Ghani Razaqpur A, Burkan Isgor O, Abbas A, Fournier B, Foo S., (2011). Creep and drying shrinkage characteristics of concrete produced with coarse recycled concrete aggregate. Cem Concr Compos. 33(10), 1026-37. https://doi.org/10.1016/j.cemconcomp.2011.08.004.

[75]. Rao MC, Bhattacharyya SK, Barai SV., (2019). Systematic approach of characterization and behavior of recycled aggregate concrete. STICEE. Available from: https://link.springer.com/book/10.1007/978-981-10-6686-3.

[76]. Mehta PK, Monteiro PJM., (2006). Concrete: microstructure, properties and materials. McGraw-Hill professional. 3rd ed. Available from: https://books.google.com.et/books/about/Concrete.html?id=Y4zlKBBW7nEC&redir_esc=y.

[77]. Poon CS, Shui ZH, Lam L., (2004b). Effect of microstructure of ITZ on compressive strength of concrete prepared with recycled aggregates. Constr Build Mater. 18(6):461-8. https://doi.org/10.1016/j.conbuildmat.2004.03.005.

[78]. Leite MB, Monteiro PJM., (2016). Microstructural analysis of recycled concrete using X-ray microtomography. Cem Concr Res. 81, 38-48. https://doi.org/10.1016/j.cemconres.2015.11.010.

[79]. Assaad JJ, Matar P, Gergess A., (2020). Effect of quality of recycled aggregates on bond strength between concrete and embedded steel reinforcement. J Sustain Cem Based Mater. 9(2), 94-111. https://doi.org/10.1080/21650373.2019.1692315.

[80]. Skariah Thomas B, Yang J, Bahurudeen A, Chinnu SN, Abdalla JA, Hawileh RA et al., (2022). Geopolymer concrete incorporating recycled aggregates: A comprehensive review. Cleaner Materials.3. https://doi.org/10.1016/j.clema.2022.100056.

CHAPTER 3

DISPARITY IN RESEARCH FINDINGS ON PARENT CONCRETE STRENGTH EFFECTS ON RECYCLED AGGREGATE QUALITY AS A CHALLENGE IN AGGREGATE RECYCLING

Original publication on Case Studies in Construction Materials and can be sited as:
Hintsa G. Gebremariam, Shifferaw Taye, Abrham Gebre Tarekegn, (2023). Disparity in research findings on parent concrete strength effects on recycled aggregate quality as a challenge in aggregate recycling, Case Studies in Construction Materials, Volume 19, e02342, https://doi.org/10.1016/j.cscm.2023.e02342”

3.1. Introduction

As highlighted in the literature review in chapter two, the conflicting findings regarding the characteristics of RCAs create ambiguity in the current understanding. To address this, it is essential to conduct controlled experimental studies aimed at examining how the strength of the original concrete influences the quality of RCAs. Accordingly, the following sections of this chapter will identify the existing research gaps, present the experimental methodology, analyze and compare the findings with those reported in the literature, and ultimately provide conclusions along with a clear roadmap for future work on this topic.

3.2. Research aim, scope and novelty

As we tried to mention in the previous sections, the contradictions in the outputs of the literary works on the effect of PC strength on the properties of the RCAs were downsides to the application of RAC in new construction projects. According to some research, "high strength parent concrete RCA application helps to produce better quality RAC because RCA produced from high strength PC is less porous and has a greater density than low strength PC, leading to lower water absorption and high fragmentation resistance of the resulted RAC [1]. The results of other studies, however, revealed that, quote, "RCAs produced from low strength parent concrete give better quality RCA and RAC because the mortar attached to the aggregates in low strength parent concrete easily detaches during the aggregate crushing process, producing clean aggregates." [1]. Because of the absence of a clear consensus on the parent concrete strength effects on the properties of the material, researchers, construction stockholders, and consumers may find it difficult to decide which literature work to refer to in the application of RCA in construction. The contradictions in results in the literature may result from the uncontrolled and non-uniform behavior of construction and demolition remnant's used in the manufacturing of the RAC, the differences in production processes, and not considering the effects of other variables other than the PC strength. Therefore, it is mandatory to investigate the matter, taking into account the above mentioned factors. Additionally, most nations in the world have not developed legal regulations and standards for recycled aggregates, except for a few developed nations. The few developed legal regulations, standards, specifications, and guidelines on RCAs and RAC also did not clearly describe the effect of PC strength on the RCA properties. This is because of the inconsistency in the results of the research findings, which hindered the development of regulations and guidelines for the use of RCA in construction. First, if there is no clear consensus on the relationship between PC strength and RCA quality, then it is difficult to know what properties RCA should have in order to meet a given standard. Second, the inconsistency in research findings can make it difficult to determine which factors are most important in determining the quality of RCA. If different studies find that different factors are important, then it is difficult to know which factors should be considered when establishing standards. For example, some studies find that the method used to produce RCA is more important than the PC strength [2], while other studies find that the PC strength is an important factor in determining the properties of RCAs [3, 4, 5, 6, 7, 8]. In order to establish standards in countries with no standards, like Ethiopia, for RCA quality, it is crucial to have a clear understanding of the relationship between PC strength and RCA quality, as well as the factors that most influence the quality of RCAs. Therefore, it is necessary to continue research in this area in order to improve the understanding of RCA quality and develop more reliable standards, especially in areas where there is no study. In addition to conducting research, it is also important to communicate the results of research to consumers and develop educational materials that will help them understand the quality of recycled aggregate. This will help build confidence in RCA and promote its use.

In order to avoid ambiguity in the results of the conflicting theories on the matter, it is vital to perform controlled experimental tests to investigate the impact of PC strength on the quality of RCAs in the Ethiopian context. Therefore, this research conducted new physical and mechanical property tests on RCAs derived from various strengths of PC laboratory cubes and concrete remnants found from demolished buildings in Ethiopia. The crushing procedure, aggregate size and type, and cement type were considered the same for all PCs. The novelty of the research lies in the identification of the inconsistencies in results in studies and the methodology followed in performing the assessment and examination of the study tests. The scope of the study is limited to the PC strength effects only. This paper is therefore an important contribution to the literature on aggregate recycling and will be of interest to researchers, engineers, and policymakers who are working in this field.

3.3. Material and methods

All of the raw and recycled materials used in this experimental study are described in this section. It also identified and explained the constituent material properties of the PC and all the concrete mix compositions for the PC. The tests that were run to evaluate how the PC affects the properties of the recycled aggregates are also reported.

3.3.1. Production of parent concrete and recycled concrete aggregates

One of the causes of variability in the behavior of RCA is the source concrete that the aggregates are extracted. In order to study the effects of the strength of the PC on RCA properties, it was mandatory to prepare PCs with controlled properties in the laboratory. Therefore, PC with cube characteristic compressive strengths of 25 MPa, 37 MPa, 45 MPa, and 67 MPa was prepared considering the constituent material properties studied as follows.

3.3.1.1 Parent concrete material properties

The material properties of each material of the PC were studied before the mix design was prepared. Because it directly affects concrete's workability, porosity, permeability, strength, level of compaction, and durability, investigating the properties of each constituent materials is crucial. A continuous particle size distribution shows that the aggregate is evenly graded in all sizes, allowing for more opportunities for particle contact and enhancing both mechanical strength and compactness [9, 10].

The mix design was prepared according to American Concrete Institute, Committee 211. 1977 (ACI 211.1-91) [17]. In connection with Sieve analysis, unit weight, specific gravity (bulk, apparent, and SSD), water absorption, moisture content, silt content, and fineness modulus, which are very important parameters in aggregate property testing, were all performed in the laboratory for fine and coarse aggregates (Table 3.1 and Figure 3.1).

For the PCs made in the laboratory, a source concrete mix was made utilizing a maximum coarse aggregate (basalt) size of 37 mm, fine aggregates (river sand) with a fineness modulus of 2.85, Dangote OPC 42.5 R with a specific gravity of 3.1 cement, and natural tap water.

Table 3.1 Physical characteristics of natural aggregates for PC production

	Physical properties	value	Limit
Coarse aggregates	Rodded Dry density	1543 kg/m^3	ASTM C 29 [11]
	Dry Specific gravity	2.56	ASTM C 127 [13]
	Specific gravity @ SSD	2.62	
	Apparent specific gravity	2.72	
	Water absorption	2.25%	
	Moisture content	2%	ASTM C 566 [15]

	Physical properties	value	limit
Fine aggregates	Dry Specific gravity	2.6	ASTM C 128 [12]
	Specific gravity @ SSD	2.65	
	Apparent specific gravity	2.73	
	Water absorption	1.83%	
	Fineness modulus	2.85	ASTM C136 [14]
	Moisture content	1.46%	ASTM C70 [16]

In particular, four sets of PC with cylinder or cube compressive strengths of 20/25 MPa, 30/37 MPa, 35/45 MPa, and 55/67 MPa were prepared. The designed mix proportion for these concretes is shown in Table 3.2, and the source concrete compressive strength is shown in Table 3.3.

In this investigation, PCs made in the laboratory and from actual demolition projects were employed to show the variability in the properties of RCAs induced by variations in loading and lifetime in practical applications. Samples were taken from 25 MPa parent concrete strength of a G+3 residential building demolished for replacement purposes after 5 years of service time and from the 30 MPa parent concrete strength obtained from a 23 year old pedestrian bridge demolished for the purpose of new roundabout construction (Table 3.4). The G+3 building was initially constructed for residential purposes, but after 5 years of service, the owners of the building changed their minds and decided that a G+15 commercial building must be constructed in place of the residential building; therefore, they demolished the residential building, and samples were taken from the demolished building's concrete waste for testing. These two demolished structures served as examples of typical structures made of normal strength concrete that were destroyed after serving their purpose.

Table 3.2 Material proportion for parent concrete production

Strength concrete grade	Volume of concrete (m^3)	Water (kg)	Cement (kg)	Admixture (kg)	Coarse aggregate (kg)	Fine aggregate (kg)
C20/25	1	174.76	291.23	0.00	1117.59	869.50
C30/37	1	174.44	377.27	0.00	1117.59	782.20
C35/45	1	174.34	404.88	0.00	1117.59	754.19
C55/67	1	154.79	596.43	5.57	1163.42	510.93

3.3.1.2 Production of recycled aggregates and their properties

To produce a correct quality and size fraction complying with ASTM C136 [14] and ASTM C33 [18], with a particle size range of 4.75 mm to 25 mm, the six groups of PCs underwent a crushing procedure using a Sam Young aggregate crushing plant found at Addis Ababa City Roads Authority. Experiments were conducted on the RCA produced by crushing the lab cast concrete and samples from demolished structures. Concrete cube specimens (standard 15 cm cubes) that were 28 days old were broken in a jaw crusher to create RCA in a lab setting. Various RCA samples were created by varying the strength of the PC in order to examine the impact of the PC strength on the properties of RCA (Tables 3.4 and 3.5). Samples were given the designations based on Table 3.4. Each category's RCA samples were broken down into three size fractions: 4.75-12.5 mm, 12.5-19 mm, and 19-25 mm. Samples were gathered from each size fraction in accordance with the ASTM C702 [19] sampling methodology.

Table 3.3 Slump and compression strength test results of parent concrete

Strength of concrete (MPa)	Dimension of cube (mm)	Slump (mm)	Ultimate applied load(KN)	Ultimate strength (MPa)	Average strength (MPa)
		45	616.5	27.40	
C20/25	150 × 150 × 150	45	533.8	23.73	25.54
		45	573.4	25.48	
		50	921.0	38.10	
C30/37	150 × 150 × 150	50	814.7	40.93	38.41
		50	857.5	36.21	
		40	1081.4	48.06	
C35/45	150 × 150 × 150	40	987.6	43.90	45.59
		40	1008	44.80	
		65	1635.2	72.66	
C55/67	150 × 150 × 150	65	1439.6	63.98	67.50
		65	1481.6	65.85	

After the preparation of the needed aggregate samples was completed, the physical and mechanical properties of the RCAs were studied following the laboratory procedures stated in the ASTM standard.

a. Recycled aggregate water absorption and specific gravity

In computations of aggregate productivity, the percentage of voids and the solid volume of the aggregates are determined using the specific gravity of the material. The net water to cement ratio in the concrete mix is determined in large part by absorption. In this study, the specific gravity and water absorption of RCAs are determined based on the recommendations of ASTM C 127 [13]. The test sample was thoroughly washed to remove dust or other coatings from the surface. Then samples were dried in a suitable pan, and after 24 hrs of soaking in water, the bulk specific gravity and absorption were determined.

b. Determination of Aggregates resistance to abrasion

This test provides a measurement of the aggregate's resistance to abrasive surface wear. The Los Angeles abrasion test is the most commonly utilized abrasion test. When an aggregate sample is put in a steel drum with several 4.8 mm steel balls, the drum is set to rotate a predetermined number of times at a predetermined speed. The percentage of fines that pass through an ASTM 1.7 mm sieve to determine an aggregate's abrasion resistance is known as the Los Angeles abrasion value. While hard aggregates lose little mass, soft aggregates are easily pulverized into dust. The test sample used in this study is made up of aggregate that has been kept on a 9.5 mm flake sorting sieve after passing a 25 mm test sieve. Samples are cleaned, dried in an oven at 107 °C for 24 hrs and their mass is measured before being placed in the abrasion machine with 12 standard balls. 500 spins of the drum are made at a speed of 28 to 30 rpm. The samples are sieved on a 1.7 mm ASTM sieve after being removed from the drum, and the samples that were retained are then cleaned and dried [20, 21]. Each samples' total abrasion value is determined as follows:

$$\left(\frac{A-B}{A}\right) \times 100 \tag{3.1}$$

Where A is mass of sample before abrasion = 5,000g

B is mass of sample after abrasion.

c. Determination of aggregate crushing value

The aggregate crushing value provides a comparative assessment of an aggregate's resistance to crushing under a compressive load that is gradually applied. The typical aggregate crushing test must be performed on aggregate that has been kept on a 9.5 mm ASTM test sieve after passing a 12.5 mm ASTM test sieve. Before testing, aggregates are cooled to ambient temperature after being heated for four hours at a temperature that does not exceed 110°C. The amount of aggregate needed for a single test is such that the material in the cylinder must be at a depth of 10 mm after tamping. The convenient way to determine the correct amount is to fill the cylindrical measure with material, tamp it 25 times with the rounded end of the tamping rod from a height of about 50 mm above the surface of the aggregate, and then level it off with the tamping rod acting as a straight edge. It is found that the test sample's material mass is 2,000g (mass A). Using compression testing equipment, the device is positioned with the test sample, plunged into position, loaded with a constant load of 667 kN/min for 10 minutes, and halted when the force reaches 400 kN. By holding the cylinder over a flat tray and hammering on the sides, the burden is then released, and the crushed materials are removed. The sample is finally sieved through a 2.36 mm sieve, and the portion that passes through is weighed [20].

The ratio of the mass of fines formed to the total mass of the sample in each test expressed as a percentage,

$$Percentage\ fines\ = (\frac{B}{A}) \times 100 \qquad (3.2)$$

Where:

A= the mass of surface dry sample (g)

B = the mass of the fraction passing the 2.36 mm test sieve (g)

d. Determination of Aggregate Impact Value

The aggregate impact value provides a comparative assessment of an aggregate's resistance to abrupt shock or impact, which can vary depending on the aggregate and on its resistance to a slowly applied compressive stress. The typical aggregate impact test must be performed on aggregate that has been kept on a 9.5 mm ASTM test sieve after clearing a 12.5 mm ASTM test sieve. The aggregate is examined in a surface dry state. A scoop is used to scoop the aggregate into the measuring cup until it is one third full. Then, by letting the tamping rod descend freely from a height of about 50mm above the surface of the aggregate, the aggregate is stamped 25 times. Additionally, the strikes were dispersed equally across the surface. The measured net mass of aggregate is 300g, and the same mass was applied to the second and third tests. The impact machine is loaded with the entire test sample, and the hammer is set up with a 380 mm lower face. It is permitted to freely tumble 15 times onto the aggregate on the cup's upper surface. The crushed aggregate is then transferred into a clean tray by holding the cup and hammering on the outside, and the entire sample is then sieved through a 2.36mm ASTM test sieve until no more appreciable amount is present. Finally, the fraction passed and retained is weighed [20]. The ratio of the mass of fines formed to the total sample mass in each test is expressed as a percentage,

$$Percentage\ fines\ = \left(\frac{B}{A}\right) \times\ 100 \tag{3.3}$$

Where:

A = the mass of surface dry sample (g)

B = the mass of the fraction passing the2.36 mm (g)

e. Estimation of attached mortar on recycled coarse aggregate by hybrid acid and mechanical method

Recycled aggregates are composed of aggregates that have been attached or separated and coated with primary mortar. The difference in behavior between RACs and NACs is caused by the presence of this main mortar. The extent of these modifications depends on how much original mortar is present on the recycled pieces. The literature discusses various methods for separating basic aggregate and mortars [5]. These techniques take advantage of the different characteristics between the aggregates and the cement paste, which are based on mechanical (wear, fragmentation, etc.), chemical (acid attack), or physical (heat treatment) principles.

The measurement of connected mortar content in this study was done using a modified hybrid hydrochloric acid dissolving and mechanical method, as there is no accepted method for determining the old cement mortar contents of RCAs [22]. For the acid test, RCAs with a size range of 25 to 19 mm, 19 to 12.5 mm, and 12.5 to 4.75 mm were utilized to determine how much mortar had adhered to each size range. The 35% pure hydrochloric acid that was made accessible in the Addis Ababa market was utilized for the acid treatment. A total of 54 samples, three weighing approximately 100 g each, were tested for each type and size of RCA in order to get the average value. In this process, the prepared RCA is washed in distilled water and dried in an oven for 24 hours at 105°C (m1). The oven dried RCA was then submerged in a 2 molar solution of 35% hydrochloric acid distilled in 500 ml of water for 24 hrs, then washed to remove the loose and smaller particles, and then dried in the oven for a further 24 hours. The samples were gently rammed to remove the acid left adhered to the mortar after oven drying. The samples were then run through a 4.75 mm sieve to determine the aggregate's mass (m2). The following equation was used to determine the mortar content (Mc) in percent.

$$Mc = (\frac{m1-m2}{m1}) \times 100 \qquad (3.4)$$

3.4. Result and discussion

3.4.1. Properties of RCAs from concrete of various parent strengths

3.4.1.1. Particle size distribution

Table 3.4 General information about the source concrete to be recycled

Designation	Sample taken from.	Date of construction	Date of demolition	Life time	Reason for demolition
C20/25	Samples taken from concrete cubes casted in laboratory	9/3/2022	7/4/2022	28 days	28 day cube compression test
C20/25, 5 years old	Sample taken from a G + 3 Residential building around Jemo, Addis Ababa	2017	May-21	5 years	Replacement
C30/37	Samples taken from concrete cubes casted in laboratory	9/3/2022	7/4/2022	28 days	28 day cube compression test
C30/37,23 years old	Sample taken from pedestrian bridge around Bob Marley Square, Addis Ababa	1999	Feb-22	23 years	New round about construction
C35/45	Samples taken from concrete cubes casted in laboratory	9/3/2022	7/4/2022	28 days	28 day cube compression test
C55/67	Samples taken from concrete cubes casted in laboratory	9/3/2022	7/4/2022	28 days	28 day cube compression test

Table 3.5 Gradation of recycled concrete aggregates.

Concrete type and strength	Designation	Mass in % retained on 19.5 to 25 mm sieve	Mass in % retained on 12.5 to 19.5 mm sieve	Mass in % retained on 4.75 to 12.5 mm sieve	% finer than 4.75 mm
Concrete with characteristic cylinder and cube strength of 20 and 25 MPa respectively.	C20/25	41.91	32.64	13.66	11.79
Concrete with characteristic cylinder and cube strength of 20 and 25 MPa respectively with 5 years old life time.	C20/25, 5 years old	41.13	33.53	18.52	6.82
Concrete with characteristic cylinder and cube strength of 30 and 37 MPa respectively.	C30/37	45.22	31.47	14.87	8.44
Concrete with characteristic cylinder and cube strength of 30 and 37 MPa respectively with 23 years old life time.	C 30/37, 23 years old	45.89	28.67	13.94	11.50
Concrete with characteristic cylinder and cube strength of 35 and 45 MPa respectively.	C35/45	46.46	25.78	12.31	15.45
Concrete with characteristic cylinder and cube strength of 55 and 67 MPa respectively.	C50/67	35.55	35.23	18.11	11.10

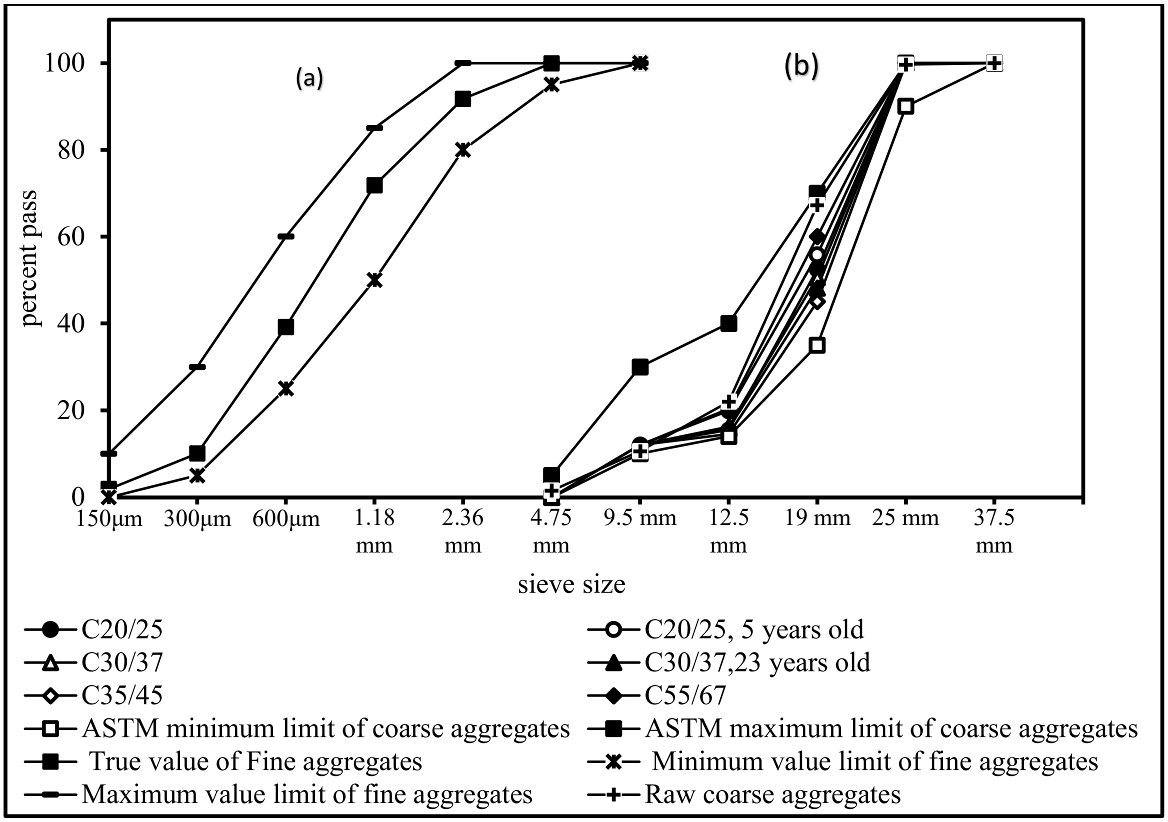

Figure 3.1 Particle size distribution of aggregates (a) fine aggregates, (b) virgin coarse aggregates and recycled concrete coarse aggregates

Note; all concrete grades are 28 days strength except specified

Particle size distribution indicates the percentage of particles of a given size at certain intervals. Particle size distribution affects the strength and load bearing behavior of RCAs. A continuous particle size distribution shows that the aggregates are evenly graded in all sizes, allowing for more opportunities for particle contact and enhancing both mechanical strength and compactness [21]. The grading and particle distribution of the virgin aggregates and the crushed products of this study were compared with ASTM grading regulations for aggregates. As can be seen in Table 3.5 and Figure 3.1, it is clear that all the aggregates (fine aggregates, coarse aggregates, and recycled coarse aggregates) have met ASTM C 33 grading requirements [18].

3.4.1.2. Water absorption and specific gravity

Recycled aggregates have a significantly lower specific gravity and density than new aggregates because the porosity of the mortar phase is higher than that of the aggregate phase. As a result, RCAs are more water absorbent than NAs [22]. The EHE-08 [23] limits the values for RCA water absorption to less than 7% for structural concrete applications. Table 3.6's analysis of water absorption and specific gravity as a function of PC strength revealed that as PC strength increased, specific gravity rose while water absorption fell. According to the findings of this study, the water absorption rate of the RCA dropped as the PC's strength increased, which is in agreement with the results of [24-27]. These results contradicted the findings of [5, 6, 7, 8], where the water absorption capacity of RCAs increased with an increase in PC strength. The increase in specific gravity with an increase in PC strength found by this study supports the findings of Liu et al. [24] but disagrees with the outcomes of the studies by Pedamini et al. [22] and Dejuan et al. [28]. In cases of greater than 45 MPa source concrete strength, the increase in strength of the PC yields no appreciable increase in specific gravity (Table 3.6). The effect of Age and service time on water absorption and specific gravity showed that the 5 year old concrete with 25 Mpa strength aggregates had 0.8% less specific gravity and an 11.4% increase in water absorption than the 28 day old 25 Mpa strength PC aggregates. The decrease in water absorption with an increase in PC showed us that high strength PC aggregates are less porous. The RCAs employed in this study's water absorption and specific gravity both fell within the allowable ranges specified in EHE-08 [23].

Generally, the strength of the original concrete has a significant impact on the water absorption and specific gravity of the recycled particles. The specific gravity of the RCAs increases and water absorption reduces when the strength of the PC improves, as shown by the results of the specific gravity and water absorption tests conducted in this study [23]. This is because high strength PC has lower porosity than low strength concrete. The porosity of a material is a measure of the number of voids in the material. The higher the porosity, the more cavities there are and the lower the specific gravity. Water absorption is also a measure of how much water a material can absorb. The higher the water absorption, the more water the material can absorb. In RCAs, the mortar phase is more porous than the aggregate phase. This means that RCA has more voids that can hold water. In the case of PC's effect on the water absorption of the RCAs, it is clearly shown that the more porosity in the aggregates, the more water it can absorb. The decrease in water absorption with increasing PC also tells us that high strength PC aggregates are less porous. This is because high strength concrete has a lower water to cement ratio, which means there is less water available for pore formation in the concrete and finer particles of cement to close the void formation inside the aggregate cement matrix. As a result, recycled high strength concrete aggregates have lower water absorption. In conclusion, the porosity of the RCAs can be used to explain the relationship between the strength of the PC, the specific gravity, and the water absorption of the RCAs. As the strength of the PC increases, the bond matrix of the mortar in the RCA increases, resulting in lower porosity and reduced water absorption.

Table 3. 6 Water absorption and specific gravity of recycled aggregates

parent concrete grade	specific gravity(SSD)	Water absorption (%)
C20/25	2.49	5.91
C20/25, 5 years	2.47	6.67
C30/37	2.50	5.75
C30/37, 23 years old	2.49	5.88
C35/45	2.51	4.64
C55/67	2.51	4.41
Natural aggregates	2.63	2.25

3.4.1.3. Shape of the aggregates

Optimal compaction, deformation resistance, and workability depend on the shape of the aggregate particles and the texture of their surfaces. ASTM D3398 [29] introduced an index for assessing the suitability of aggregate shape and texture for different applications. Concrete quality is decreased by Smooth Surfaced and elongated aggregates [21]. This decreases the concrete's strength and uses an excessive amount of cement. As a result, the particles shatter more quickly, and additionally, the slab formations frequently concentrate on a horizontal plane where air and water collect. Therefore, Concrete's durability is negatively impacted by this [30]. The flakiness index is a measure of the shape of RAC. An essential characteristic of RCAs is their flakiness index, which has an impact on the characteristics of the concrete produced with these aggregates. The flakiness index of RCA is affected by a number of factors, including the type of concrete from which the aggregate is made, the type of processing, and the size of the aggregates. Observationally, RCA made from high strength concrete has a lower flakiness index than aggregate made from low strength concrete. This is because aggregates produced from high strength PC have a lower water to cement ratio and a better bond between aggregate and mortar than lower strength PC aggregates.

The flakiness index, which is used to determine the particle form of aggregates, should be, less than 35% for coarse aggregates [6]. The flakiness index of natural aggregate is 5-9% greater than that of RCA [22, 31]. This is because round particles often become more angular as a result of the mortar adhering to the corners of RCAs. The crushing equipment has a significant role in determining the particle shape of RCAs. In this study, Aggregates in the shape of cubes were produced by the crushing mills used in the recycling plant. Concrete usually breaks into smaller particles at the recycling plant rather than forming slabs. Because the samples under study were produced at a recycling plant using an impact mill, the flakiness index does not need to be calculated [30]. Therefore, it would not be difficult to confirm that the aggregate samples used in our investigation complied with the ASTM D3398 limitations for particle shape. But in the case of RCA production by manually hammering or other methods that can fragment the aggregates into round and flaky shapes, the flakiness and elongation index tests of the samples must be carried out.

3.4.1.4. Los Angeles abrasion resistance

A measurement used for the determination of the aggregate's resistance to abrasive surface wear is called abrasion resistance [32]. It's crucial that the aggregate used to make concrete be robust in general [30]. In most circumstances, aggregate toughness, a characteristic that is generally comparable to impact strength, is a prerequisite for intrinsic aggregate strength. The interconnected qualities of crushing strength, abrasion resistance, and elastic modulus of aggregate are all significantly controlled by porosity. NAs are often dense and strong, according to experience, so they rarely pose a threat to the strength of concrete. Under physical strain or abrasion, RCAs may deteriorate and experience particle fracture, losing their strength and durability. The laboratory experiment result of this study (Figure 3.2) lists the outcomes of the Los Angeles abrasion test for the samples examined. The results were comparable to previous analyzed aggregates [30] in terms of values. As can be seen from Figure 3.2, as PC strength increases, the abrasion loss of the resultant aggregates decreases. Therefore, the abrasion resistance of RCAs is influenced by the strength of the PC; stronger concrete causes less loss. This is so because high strength PC has mortar that is stronger than low strength PC when it attaches to aggregates. Because of this, when RCAs are subjected to abrasion, they are less likely to break off.

The mortar that holds RCAs in place is more durable in high strength concrete than it is in low strength concrete for a number of reasons. First, since there is a greater hydration induced link between the aggregate and mortar as well as inside the mortar itself because high strength concrete is made with a lower water to cement ratio, Second, because high strength concrete contains more cement, the mortar is denser and more resilient.

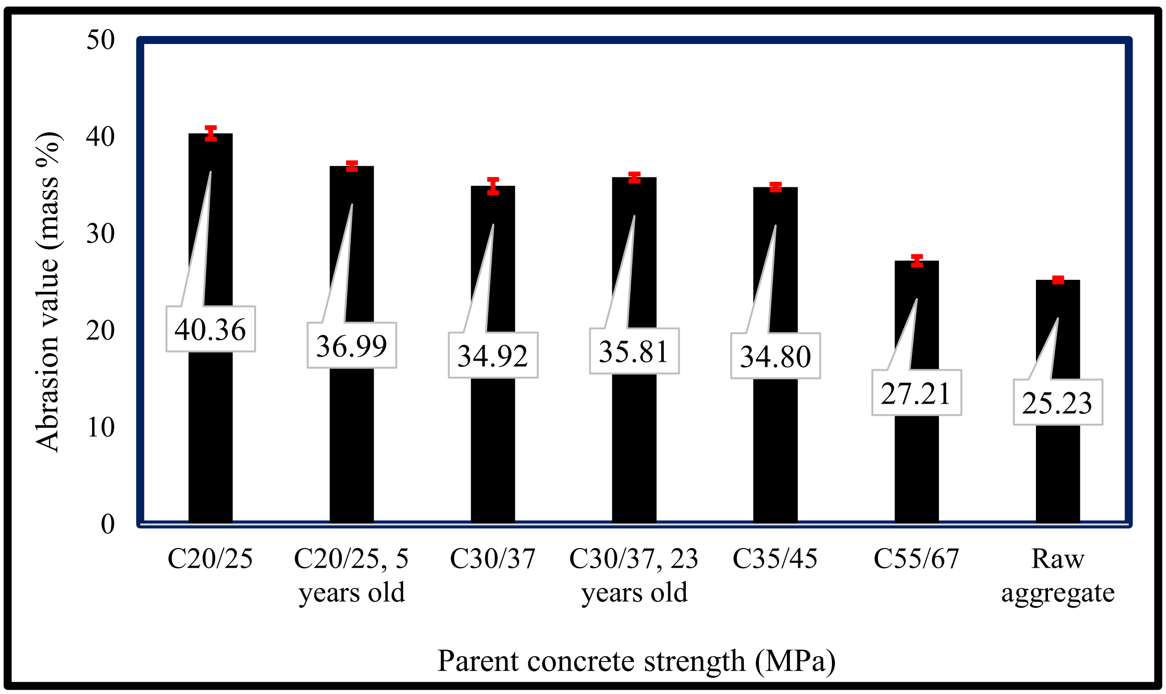

Figure 3.2 Mechanical characterization of recycled concrete aggregates (abrasion loss of aggregates)

Sajan et al. [32] found that the abrasion resistance of RCAs increases with an increase in the strength of the PC, which fits with the finding of this study. On the other hand, a study by Nagataki et al. [33] concluded that the strength of PC has no influence on the abrasion resistance of RCAs. Further, the effect of service time of the source concrete on abrasion loss is not clear, as the loss in the C20/25 crushed after 28 days of source concrete aggregate (40%) is greater than the 5 years of source concrete aggregate (37%), but in the case of the C30/37 crushed concrete, the 23 year old concrete aggregates have more loss (36% vs. 35% for the 28 day source concrete). However, all of the outcomes of RCA fall within ASTM C33's [18] permissible range of less than 50% for buildings.

3.4.1.5. Aggregate crushing value test

Aggregate strength can be estimated by looking at the aggregate crushing value (ACV). To make sure that the aggregate will be able to withstand imposed loads, using lower ACV aggregate is advised. The ACV is determined as the difference between the initial weight and the weight passing through a sieve size of 2.36 mm. As can be seen in Figure 3.3, the aggregate crushing value decreased with the increase in PC strength of the RCAs. This increase in resistance of the aggregates produced from high strength PCs was due to the high density and low porosity of the attached mortar in the aggregates produced from the high strength PCs compared to low strength PC RCAs. Pedamini et al. [22] and Extreberia et al. [9] found that the increase in PC strength led to a decreased crushing value of the RCAs, which is a similar finding to this study. But De Juan et al. [28], on the contrary, found out that low strength PC aggregates had better crushing resistance. They reasoned out that the low quantity of mortar attached to the aggregates made the aggregate more resistant to crushing. The aggregate crushing value of C20/25, which is 5 year old concrete aggregate, which is the highest value in this test, was 34%, 25% for C55/67 material, and 18% for natural aggregates. This demonstrates that the deviation in aggregate crushing values of NAs and RCAs are getting narrowed at an enhanced PC strength. The high aggregate crushing value of low PC strength aggregates suggests that they have the maximum number of pores, and the bond in the aggregates is very weak, which leads to low resistance to crushing loads.

In general, the ACV of RCAs is influenced by the PC's strength and age. The ACV of the recycled particles diminishes as the PC's strength rises. This is because the mortar bond that is attached to the RCAs is stronger in high strength concrete than in low strength concrete. Because of this, when RCAs are crushed, they are less prone to break off. The ACV of RCAs is also influenced by the age of the concrete. Ageing tends to cause the

ACV of these aggregates to rise. This is because the mortar used to bind the aggregates has a propensity to degrade over time. The highest number of pores and weak link in the aggregates, which results in low resistance to crushing stresses, are suggested by the high ACV of low PC strength aggregates. For concrete mixes where high strength is required, it is crucial to incorporate RCAs from high strength concrete or enhancing the quality of the aggregates produced from low strength parent concrete is mandatory. The crushing values of all the RCAs tested in this study were within the limit of the ASTM standard for non-wearing surfaces, which is less than 45%.

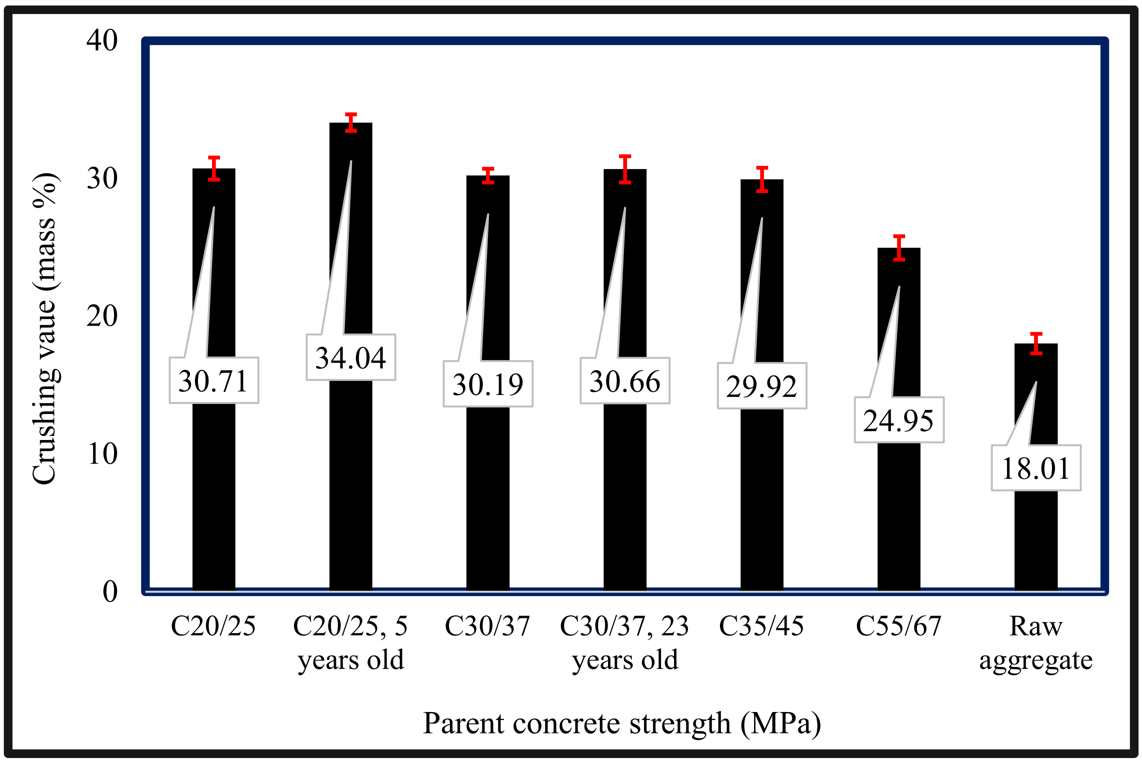

Figure 3.3 Mechanical characterization of recycled concrete aggregates (aggregate crushing value test)

3.4.1.6. Aggregate impact value

The impact test is a reliable predictor of durability and strength. It was discovered that the impact value of RCAs is higher than the impact value of RAs. Consequently, RCA is less durable than NA [22]. According to the results of the experimental impact value test on six RCA types and a NA, the impact value of the RCA decreased with an increase in parent concrete strength (Figure 3.4). This result matched the test results of some researchers [9, 22, 24]. In contrast, stronger PC reduces the impact resistance of the resultant aggregates, according to other researchers' findings [28, 31, 34]. According to this study, the impact value of the NAs is around 22%, that of the C55/67 compressive strength PC is 24%, and that of the C20/25 compressive strength PC aggregates is 36%. This showed us that at increased PC strength, the impact values of NAs and RCAs are comparable. Low parent concrete strength aggregates' impact values are high, indicating that the aggregates are more porous and easily degradable. The strength and longevity of the RCAs are influenced by the water to cement ratio of the PC. Aggregates are stronger and more longlasting when concrete has a lower w/c ratio.

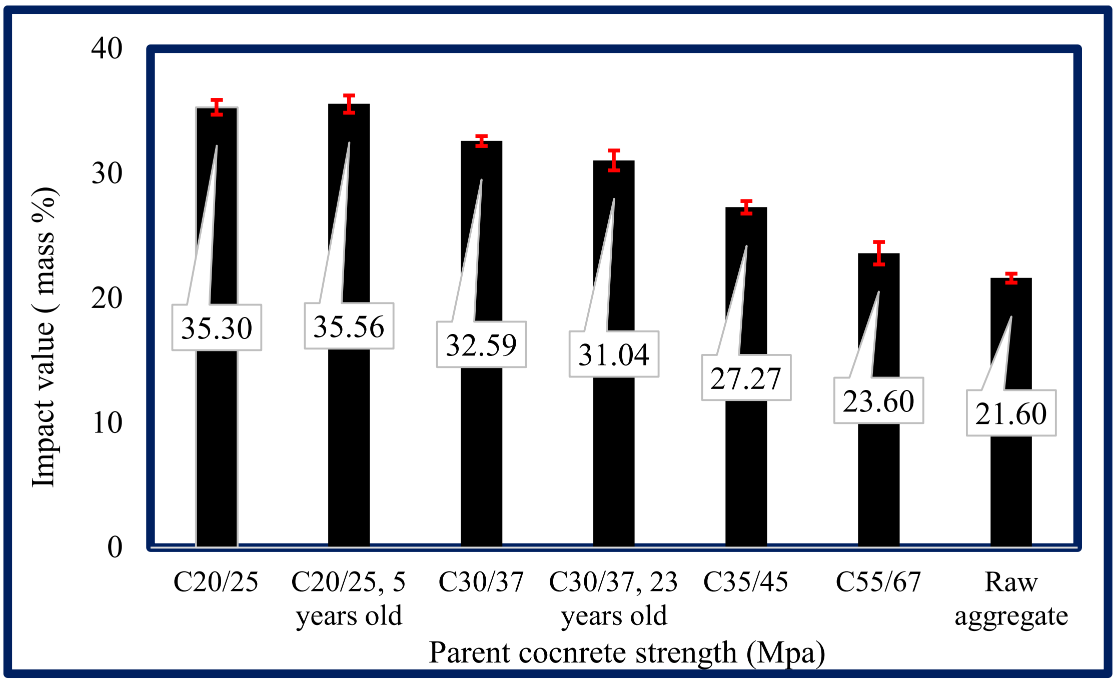

Figure 3.4 Mechanical characterization of recycled concrete aggregates (aggregate impact value test results)

The usage of RCA in concrete can be affected in a number of ways by the decrease in impact value with increased PC strength. As a result, concrete created with PC aggregates of low strength may be less impact resistant than concrete made with PC aggregates of high strength. It is crucial to remember that the impact value is only one indicator of the resilience and toughness of RCAs. Other elements, such as RCA's resistance to abrasion and water absorption, may also be crucial. The impact value of RCA is simply one of several variables that must be taken into account when discussing the use of RCA as a whole. All of the evaluated RCAs impact values fell within the ASTM standards' tolerances.

3.4.1.7. Quantification of mortar content of the recycled aggregates from Concrete of various parent Strengths

After the old concrete is crushed, some mortar from the original concrete is still connected to the stone particles in the RCA. The inferiority of recycled aggregate RCAs over natural NAs is caused by this hardened cement paste [26]. Some researchers claim that the volume of RCA mortar was boosted by the PC's increased strength [6, 22, 25, 31]. Table 3.7 and Figure 3.5 of this study display the test findings of old mortar contents for RCAs from various PCs. As can be seen, the adhered mortar content in each type of RCA made from a certain PC increases with the PC's strength. In the case of high strength PC, the water to cement ratio used in the production of the concrete is low. The more cement particles in the concrete, the faster the hydration process and the higher the bondage between the aggregate and cement paste. This strong bond reduces the breakdown of the attached mortar from the aggregates during the aggregate crushing process, leaving more adhered mortar in the aggregates produced from high strength PC. Therefore, the conclusion from the experimental test in the quantification of mortar, which said that as PC strength increases, so does the mortar content of the resultant RCAs, is logical. Other researchers have shown the opposite pattern, whereby the stronger parent concrete causes less mortar to be used [26, 35, 36].

The particle size of RCAs is one of the influential parameters in the quantification of the mortar content of RCAs. As the size of the RCAs particles shrank, the adhering mortar content of the RCAs rose. This is mostly due to the fact that the RCA's weaker components, mostly the mortars, were easily removed during the initial interactions with the crusher's jaws and ended up in the smaller size fractions. Observations during the experimental study showed that some aggregates in all sizes of particles were entirely made up of mortar, especially in the smaller aggregates. Therefore, it is reasonable to conclude that smaller RCAs contained more adhered mortar compared to larger aggregate particles.

Table 3.7 Results of mortar content quantification

Grades of PC	Size of aggregates (mm)	Total weight of sample (Grams)				Weight of mortar (Grams)				Mortar content of recycled aggregates in (%)
		T 1	T 2	T 3	Average	T 1	T 2	T 3	Average	
C20/25	4.75 -12.5	100	100	100	100	59.00	60.20	57.85	59.02	59.02
	12.5- 19.0	100	100	100	100	41.02	42.19	42.56	41.92	41.92
	19.0 -25.0	100	100	100	100	35.00	36.45	34.48	35.31	35.31
C20/25, 5 years old	4.75 -12.5	100	100	100	100	59.00	58.50	58.94	58.81	58.81
	12.5- 19.0	100	100	100	100	46.50	46.98	45.94	46.47	46.47
	19.0 -25.0	100	100	100	100	37.98	39.06	38.76	38.60	38.60
C30/37	4.75 -12.5	100	100	100	100	59.22	59.87	58.63	59.24	59.24
	12.5- 19.0	100	100	100	100	45.96	46.95	46.83	46.58	46.58
	19.0 -25.0	100	100	100	100	45.23	45.67	46.24	45.71	45.71
C30/37, 23 years old	4.75 -12.5	100	100	100	100	61.69	60.83	61.59	61.37	61.37
	12.5- 19.0	100	100	100	100	48.06	47.65	48.95	48.22	48.22
	19.0 -25.0	100	100	100	100	43.00	42.00	43.68	42.89	42.89
C35/45	4.75 -12.5	100	100	100	100	63.25	63.98	64.16	63.80	63.80
	12.5- 19.0	100	100	100	100	47.56	48.64	48.72	48.31	48.31
	19.0 -25.0	100	100	100	100	50.00	52.02	50.68	50.90	50.90
C55/67	4.75 -12.5	100	100	100	100	65.03	66.78	66.91	66.24	66.24
	12.5- 19.0	100	100	100	100	56.51	57.88	58.62	57.67	57.67
	19.0 -25.0	100	100	100	100	54.63	55.35	56.48	55.49	55.49

Note; T1, T2, T3 represent for trials numbers 1, 2, and 3., all concrete grades are 28 days strength except specified.

As can be seen from Table 3.7 and Figure 3.5, the mortar content increased by about 8% (4.75 to 12.5 mm), 27%(12.5 to 19 mm), and 36% (19 to 25 mm) as the 28 day strength of PC increased from C20/25 to C55/67. This shows us that an increase in aggregate size can increase the difference in mortar content resulting from variable PC strength. Similarly, the variation in size of aggregates with a constant grade of PC can lead to a variable quantity of mortar. The PC with strength C20/25 RCA had a 15% increase in mortar content as a result of the reduction in aggregate size from (19.0–25 mm) to (12.5–19.0 mm) and a 29% increase in mortar content as a result of the reduction in particle size from (12.5-19.0 mm) to (4.75-12.5 mm). The PC's strength of C55/67 aggregate resulted in a 4% increase in mortar content due to the aggregate's size reduction from (19.0–25 mm) to (12.5–19.0

mm) and increased by 13% as particle size reduced from (12.5–19.0 mm) to (4.75–12.5 mm). The outcome from the mortar content test of the C35/45 parent concrete strength aggregates shows a decrease in mortar content as the particle size decreases.

This may be due to the sampling uncertainty. In general, this study's findings showed that low strength parent concrete's mortar is easily removable during the concrete's crushing process, resulting in RCA with less mortar.

During the experimental test performed to quantify the mortar adhered to the RCA, it was observed that there were pure NA fragments that passed the 4.75 mm sieve. These mortar free and mortar adhered aggregates that passed the 4.75 mm sieve were produced during the hammering process of the RCA samples. Therefore, it is important to consider that the quantified attached mortar includes these smaller fragmented aggregate particles.

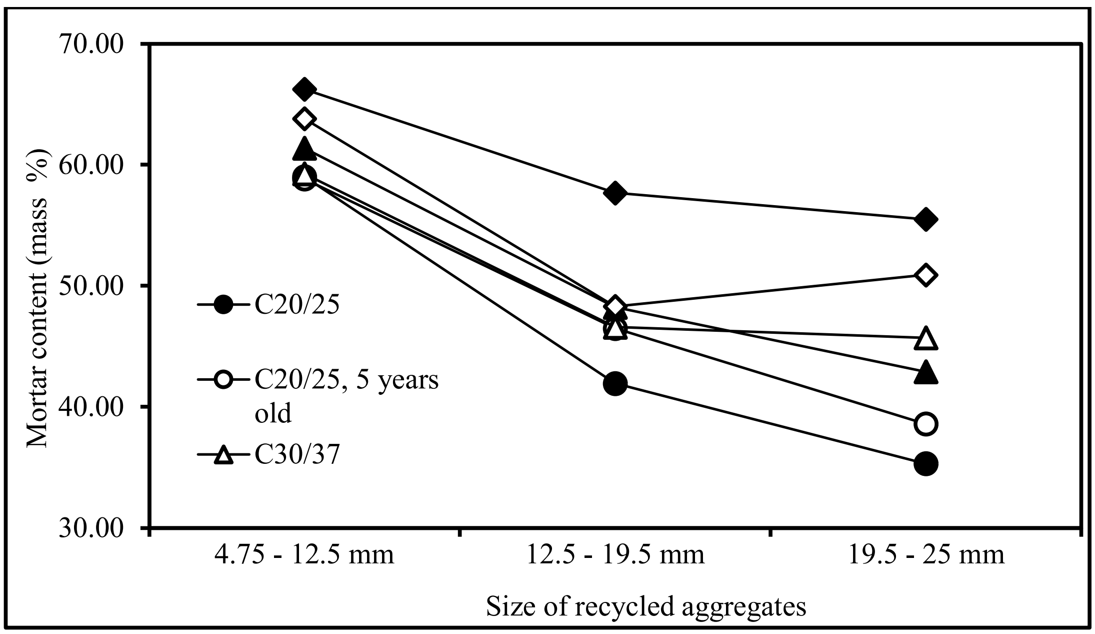

Figure 3.5 Mechanical characterization of recycled concrete (quantification of mortar attached to aggregates)

Generally, as can be seen from this research, PC grade had a great influence on the properties of RCAs. The increase in PC strength led to increased mortar content, but even though the mortar content increased, its density, bond, and specific gravity increased, leading to decreased water absorption. Similarly, the mechanical properties, such as resistance to abrasion loss, impact, and crushing strength, of the recycled aggregates increased with the increase in PC grades. Therefore, one might draw the conclusion that RCAs from PC with high strength have superior properties to those of PC with lesser quality.

3.5. Conclusion

In addition to preventing landfill disposal and promoting a closed cycle economy, concrete recycling may be a very popular choice in developing countries and war torn areas like the Tigray region of Ethiopia, where the challenge of rebuilding and reconstruction follows the end of the war.

The study of RCA utilization in the construction industry is not particularly new today. For more than 40 years, researchers have been looking into the topic, and they've discovered some fascinating results that might help the building sector stay sustainable. Many researchers have also examined the effects of RCA and RAC properties on the strength of PC. However, the findings drawn from these literary works about the influence of PC strength on the characteristics of RCA lacked uniformity.

In regions where there have been few or no studies on the topic, like Ethiopia, these associated conflicts in the literature may make it challenging for researchers and construction stakeholders to choose which of these principles to apply in their everyday work. Therefore, it is vital to carry out thorough experimental research in the area, taking into account the precise influencing elements that may cause the results of the literary work to vary in connection with the geographical factors.

In this study, the expected influencing factors, such as the NA types (coarse and fine), the cement type and properties used in the PC, the method of crushing the PC wastes, and the PC mixing techniques, were taken into consideration as constants. New physical and mechanical property tests on RCAs derived from various strengths of PC laboratory cubes and concrete remnants found from demolished buildings in Ethiopia were carried out in order to investigate the impact PC strength on the properties of RCAs. Based on the experimental results, the following conclusions were drawn:

- Despite the contradictory results of the literary works, this investigation discovered that the presence of additional mortar linked to the RCAs was made possible by the PC's increased strength. The density, bond strength, and specific gravity of the RCAs were improved, despite the fact that the amount of bonded mortar to the aggregates grows as the original concrete's strength increases. With the PC's strength increasing, the recycled particles' water absorption likewise decreased. This improvement in RCA quality brought about by the PC's higher strength was the outcome of the attached mortar's firm and less porous behavior in PCs of high strength.

- The PC's strength has an impact on the RCAs resistance to abrasion; stronger concrete results in less loss. The abrasion loss of the weaker PC aggregates was considerably high due to the poor adhesion and connection between the mortar and aggregate. NAs and RCAs had comparable aggregate crushing and impact values at increased PC strength classes. High aggregate crushing and impact values in low PC strength aggregates suggest that they are easily broken down by external loads while in use.

- The amount of mortar that is attached to the RCAs may vary depending on the size of the aggregates and the PC's grade. As the size of the RCAs gets smaller, the mortar content goes up. As a result, employing RCA in bigger sizes can improve the quality of concrete made with RCAs.

- This study found that the overall quality of RCAs can be improved by using high strength PC aggregates rather than low strength PC aggregates. Therefore, to manufacture RAC of higher quality, researchers and building stakeholders should think about using high strength PC aggregates. Special processing methods that can enhance the quality of these aggregates may be taken into account when employing aggregates from low strength PC.

3.6. References

[1]. Gebremariam, H.G., Taye, S., Tarekegn, A.G., (2023). Disparity in research findings on parent concrete strength effects on recycled aggregate quality as a challenge in aggregate recycling, Case Stud. Constr. Mater., 19, e02342, https://doi.org/10.1016/j.cscm.2023.e02342

[2]. Xie T, Gholampour A, Ozbakkaloglu T., (2018. Toward the development of sustainable concretes with recycled concrete aggregates: comprehensive review of studies on mechanical properties. J Mater Civ Eng, ISSN 0899-1561. 30(9). https://doi.org/10.1061/(ASCE)MT.1943-5533.0002304

[3]. Pedro D, de Brito J, Evangelista L., (2014). Influence of the use of recycled concrete aggregates from different sources on structural concrete. Constr Build Mater. 71, 141-51. https://doi.org/10.1016/j.conbuildmat.2014.08.030.

[4]. Zhao XY, Chen J-X, Chen GM, Xu J-J, Zhang L-W., (2023. Prediction of ultimate condition of FRP-confined recycled aggregate concrete using a hybrid boosting model enriched with tabular generative adversarial networks. Thin Walled Struct. 182(B),110318. https://doi.org/10.1016/j.tws.2022.110318

[5]. Chakradhara Rao M, Bhattacharyya SK, Barai SV.,(2011). Influence of field recycled coarse aggregate on properties of concrete. Mater Struct. 44(1):205-20. https://doi.org/10.1617/s11527-010-9620-x.

[6]. Akbarnezhad A, Ong KCG, Tam CT, Zhang MH., (2013). Effects of the parent concrete properties and crushing procedure on the properties of coarse recycled concrete aggregates. J Mater Civ Eng. 25(12), 1795-802. https://doi.org/10.1061/(ASCE)MT.1943-5533.0000789.

[7]. Thomas C, Setién J, Polanco JA, Alaejos P, Sánchez de Juan M., (2013). Durability of recycled aggregate concrete. Constr Build Mater. 40, 1054-65. https://doi.org/10.1016/j.conbuildmat.2012.11.106.

[8]. Levy SM, Helene P., (2004). Durability of recycled aggregates concrete: a safe way to sustainable development. Cem Concr Res. 34(11), 1975-80. https://doi.org/10.1016/j.cemconres.2004.02.009

[9]. Etxeberria M, Vázquez E, Marí A, Barra M., (2007). Influence of amount of recycled coarse aggregates and production process on properties of recycled aggregate concrete. Cem Concr Res. 37(5), 735-42. https://doi.org/10.1016/j.cemconres.2007.02.002.

[10]. Tam VWY, Wang K, Tam CM., (2008). Assessing relationship among properties of demolished concrete, recycled aggregate and recycled aggregate concrete using regression analysis. J Hazard Mater. 152(2):703-14. https://doi.org/10.1016/j.jhazmat.2007.07.061.

[11]. ASTM C29/C29M. Standard test method for bulk density (unit weight) and voids in aggregate. West Conshohocken, PA: ASTM; 2009.

[12]. ASTM C128/C128M-01. Standard test method for density, relative density (specific gravity), and absorption of fine aggregate. West Conshohocken, PA: ASTM; 2004.

[13]. ASTM C127-12. Standard test method for density, relative density (specific gravity), and absorption of coarse aggregate. West Conshohocken, PA: ASTM; 2012.

[14]. ASTM C136-06. Standard test method for sieve analysis of fine and coarse aggregates. West Conshohocken, PA: ASTM; 2006.

[15]. ASTM C566/C566M-97. Standard test method for total evaporable moisture content of aggregate by drying. West Conshohocken, PA: ASTM; 2004.

[16]. ASTM C70/C70M-94. Standard test method for surface moisture in fine aggregate. West Conshohocken, PA: ASTM; 2004.

[17]. American Concrete Institute. Committee 211. Recommended Practice for Selecting Proportions for Normal and Heavyweight Concrete. (ACI 211.1-91)" Reapproved. 1977;2009.

[18]. ASTM C33/C33M-11. Standard Specification for Concrete Aggregates. West Conshohocken, PA: ASTM; 2011. Available from: http://www.astm.org.

[19]. ASTM C702/C702M-98. Standard practice for reducing samples of aggregate to testing size. West Conshohocken, PA: ASTM; 2004.

[20]. Dinku A., (2000.) Construction materials laboratory manual. Available from: https://www.scribd.com/document/367438254/Construction-Materials-Labratory-Manual-by-Abebe-Dinku.

[21]. Spanish standard UNE-EN 933-3. Test for geometrical properties of aggregates. Part 3: determination of particle shape. Flakiness index.

[22]. Padmini AK, Ramamurthy K, Mathews MS. (2009). Influence of parent concrete on the properties of recycled aggregate concrete. Constr Build Mater. 23(2), 829-36. https://doi.org/10.1016/j.conbuildmat.2008.03.006

[23]. Spanish minister of public works. Vol. 2008; 2008. Instrucción de hormigón estructural EHE-08 [Spanish structural concrete Code]. Available from: http://asidac.es/asidac-en/wpcontent/uploads/2016/07/EHE-ENG.pdf.

[24]. Liu K, Yan J, Hu Q, Sun Y, Zou C., (2016). Effects of parent concrete and mixing method on the resistance to freezing and thawing of air-entrained recycled aggregate concrete. Constr Build Mater. 106, 264-73. https://doi.org/10.1016/j.conbuildmat.2015.12.074.

[25]. Duan Z, Han N, Singh A, Xiao J., (20202). Multi-scale investigation on concrete prepared with recycled aggregates from different parent concrete. J Renew Mater. 8(11), 1375-90. https://doi.org/10.32604/jrm.2020.013044.

[26]. Kou SC, Poon CS., (2015). Effect of the quality of parent concrete on the properties of high performance recycled aggregate concrete. Constr Build Mater. 77, 501-8. https://doi.org/10.1016/j.conbuildmat.2014.12.035.

[27]. Andreu G, Miren E., (2014). Experimental analysis of properties of high performance recycled aggregate concrete. Constr Build Mater. 52,227-35. https://doi.org/10.1016/j.conbuildmat.2013.11.054.

[28]. De Juan MS, Gutiérrez PA., (2009). Study on the influence of attached mortar content on the properties of recycled concrete aggregate. Constr Build Mater. 23(2),872-7. https://doi.org/10.1016/j.conbuildmat.2008.04.012

[29]. ASTM D3398-00. Standard test method for index of aggregate particle shape and texture. West Conshohocken, PA: ASTM; 2004.

[30]. Martín-Morales M, Zamorano M, Ruiz-Moyano A, Valverde-Espinosa I., (2011). Characterization of recycled aggregates construction and demolition waste for concrete production following the Spanish Structural Concrete Code EHE-08. Constr Build Mater. 25(2),742-8. https://doi.org/10.1016/j.conbuildmat.2010.07.012.

[31]. Chakradhara Rao MC., (2018). Properties of recycled aggregate and recycled aggregate concrete: effect of parent concrete. Asian J Civ Eng. 19(1), 103-10. https://doi.org/10.1007/s42107-018-0011-x.

[32]. Sajan KC, Adhikari R, Mandal B, Gautam D.,(2022). Mechanical characterization of recycled concrete under various aggregate replacement scenarios. Cleaner Eng Technol. 7,100428. https://doi.org/10.1016/j.clet.2022.100428.

[33]. Nagataki S, Gokce A, Saeki T, Hisada M.,(2004). Assessment of recycling process induced damage sensitivity of recycled concrete aggregates. Cem Concr Res. 34(6),965-71. https://doi.org/10.1016/j.cemconres.2003.11.008.

[34]. Marie R Mujalli., (2018). Effect of design properties of parent concrete on the morphological properties of recycled concrete aggregates, Eng. Sci. Tech. Int J. https://doi.org/10.1016/j.jestch.2018.08.014

[35]. Fan Y, Xiao J, Tam VWY. (2014). Effect of old attached mortar on the creep of recycled aggregate concrete. Struct Concr. 15(2), 169-78. https://doi.org/10.1002/suco.201300055.

[36]. Seo DS, Choi HB., (2014). Effects of the old cement mortar attached to the recycled aggregate surface on the bond characteristics between aggregate and cement mortar. Constr Build Mater. 59, 72-7. https://doi.org/10.1016/j.conbuildmat.2014.02.047.

CHAPTER 4

CARBON SMART CONCRETE: RECYCLED AGGREGATES AS CO_2 SINKS THROUGH NATURAL AND ACCELERATED CARBONATION PATHWAYS

Original publication: “Manuscript under review.”

4.1. Introduction

Technological advancements such as carbonation treatment, nano silica impregnation, and bio deposition have been shown to enhance the mechanical and durability properties of RCAs [1]. Among these, carbonation stands out for its dual benefits: it improves RCA quality and serves as an environmentally friendly method for long term CO_2 storage, making it a promising solution for industrial scale applications [2].

The carbonation process in cement based materials involves a complex sequence of physical and chemical interactions, primarily driven by the presence of CO_2 in the environment. Initially, CO_2 gas diffuses into the pore network of the cementitious matrix. Once inside, it dissolves into a thin film of water that naturally exists within these pores as can be seen in Equation 4.1 [2]. Simultaneously, $Ca(OH)_2$, a common hydration product within the cement matrix, begins to dissolve into the pore water. Within the pore solution, the dissolved CO_2 chemically reacts with the dissolved $Ca(OH)_2$, leading to the formation of calcium carbonate as can be seen in Equation 4.2. In addition to reacting with $Ca(OH)_2$, the CO_2 also interacts with other calcium containing phases, both hydrated and unhydrated, particularly calcium silicates (Equation 4.3). As a result of these reactions, solid carbonation products precipitate and gradually fill the pores, reducing the overall pore volume and altering the microstructure of the material. Eventually, as these reactions progress, condensation of water occurs along the pore walls, further influencing the moisture conditions and potentially impacting subsequent stages of carbonation [2, 3].

$$CO_2 + H_2O = H_2CO_3 \tag{4.1}$$

$$Ca(OH)_2 + H_2CO_3 = CaCO_3 + 2H_2O \tag{4.2}$$

$$C_3S_2H_3 + 3H_2CO_3 = 3CaCO_3 + 2SiO_2 + \ 6H_2O \tag{4.3}$$

This process fills micro cracks and pores, increases aggregate density, improves interfacial bonding, reduces water absorption and ultimately strengthening the mechanical and durability properties of RCA [4]. This enhancement in physical and mechanical properties of RCAs helps to use more construction and demolition concrete wastes for environmental sustainability and natural aggregate preservations.

Additionally, Carbonation technology is a promising method, offering significant potential for carbon sequestration and energy conservation, and gaining substantial industry interest [5]. The statistics regarding global anthropogenic CO_2 emissions paint a stark picture of the urgent need for action to mitigate climate change. With emissions reaching around 37.4 billion tons in 2024 and growing rapidly since the mid-20th century, it's evident that decisive measures are essential to curb this trajectory [6]. The International Energy Agency's [7] estimation that cement production contributes roughly 7% of these emissions underscores the importance of addressing emissions from this sector. Achieving significant emission reductions by 2050, as outlined in net-zero scenarios, is imperative to limit global warming and its associated impacts. Fortunately, research [8-10] offers a promise in the form of concrete structures, which have the potential to absorb between 11 to 30% of CO2 emissions during their service life. This inherent carbon sequestration capacity presents a promising opportunity to reduce the lifecycle carbon footprint of concrete. Moreover, the theoretical potential of RCA to capture 70% to 80% of the original CO_2 emitted during clinker production highlights the untapped potential of this sustainable material [8]. However, to fully harness the CO_2 sequestration benefits of RCA, it is crucial to quantify their real degree of carbon capture through rigorous experimental studies. By doing so, we can understand and find the full potential of RCAs in mitigating CO_2 emissions and contribute significantly to global efforts to combat climate change.

Currently, there are two types of carbonation: accelerated or rapid carbonation and ambient carbonation. When concrete hardens and demolished after service time, as well as when aggregates are crushed into the appropriate shapes, carbonation occurs at a comparatively slow pace in the presence of air, this process is referred to as ambient carbonation [11]. The second carbonation type that occurs under specific pressure, CO_2 level, and humidity circumstances, which is accelerated carbonation often yields increased surface hardness as well as initial strength for concrete samples [12]. Accelerated carbonation is a more efficient approach for enhancing the functionality of leftover old mortar in RCA cases. Accelerated carbonation enhances the properties of old mortar in the RCA, influenced by both internal and external circumstances. These conditions can affect the rate of the carbonation process. 'Internal circumstances' refer to the inherent properties of RCA, such as the source material's grade, activated calcium ions, degree of preprocessing ambient carbonation, and particle size. 'External circumstances' primarily include relative humidity, gas pressure, carbonation time, and CO_2 concentration [4]. Therefore, carbonation of RCA, when optimized with these conditions, is a promising method for improving RCA strength, sequestering atmospheric CO_2, and promoting energy conservation.

4.2. Research gap

The existing body of research on the accelerated carbonation of RCAs has encountered limitations by overlooking crucial factors in the carbonation process. Many studies have failed to account for the preprocessing ambient carbonation status that occurs in RCAs before the initiation of accelerated carbonation. RCAs are typically sourced from demolished buildings, which have been subjected to initial ambient carbonation throughout their entire service life. Even after demolition, these aggregates continue to undergo ambient carbonation, and when crushed into aggregate forms, they remain in a natural air-dry condition for weeks, if not months or years. Consequently, the degree of carbonation in accelerated carbonation studies reflects the cumulative impact of both initial preprocessing ambient carbonation and accelerated processes. Surprisingly, the existing literature lacks comprehensive mapping of the genuine carbonation journey of RCAs during accelerated carbonation.

Certain studies have opted for the use of RCAs derived from laboratory produced cubes, strategically sidestepping the impact of initial preprocessing ambient carbonation before the onset of accelerated carbonation. However, this approach falls short of capturing the authentic scenario encountered in the actual production of RCAs, where a significant degree of preprocessing ambient carbonation is inherent. The reliance on laboratory produced cubes undermines the realism of these studies, neglecting the vital interplay of initial preprocessing natural and accelerated carbonation that takes place in RCAs during their real world production. This oversight introduces a critical gap in understanding and fails to mirror the complexities and nuances present in the genuine production and utilization of RCAs. To truly advance our understanding and application of RCAs, it is imperative to address these limitations and embrace a more realistic representation of the carbonation processes involved in their lifecycle. Furthermore, the strength of the PC emerges as a significant determinant influencing the carbonation degree of RCAs. RCAs originating from high strength PC exhibit more alkaline behavior, coupled with lower porosity compared to their counterparts from low strength PC. This inherent property variation induced by the strength of the PC can significantly impact the carbonation degree of RCA. Unfortunately, this crucial aspect has been consistently overlooked in prior literature studies.

To address these gaps in knowledge, this study is proposed, aiming to comprehensively understand the carbonation process of RCAs during accelerated carbonation. This study will take into account the intricate interplay between initial preprocessing ambient and accelerated carbonation, acknowledging the real world conditions in which RCAs are exposed. Additionally, the study will systematically evaluate the impact of the PC strength on the carbonation degree of RCAs, offering a more accurate representation of the carbonation process. Furthermore, this study will quantify the real CO_2 sequestration potential of RCA and study the effect of the stored crystal CO_2 by products on the physical and mechanical properties of RCA concrete.

This study conducted an in depth investigation into the microstructural and mineralogical characteristics of RCAs exposed to both preprocessing ambient carbonation and accelerated carbonation using XRD, TGA, and FTIR techniques. The research also explored how the carbonation process interacts with the aggregates by analyzing parameters such as pH levels. In addition, the effects of carbonation on the physical and mechanical performance of the aggregates were evaluated through water absorption, crushing resistance, compressive and tensile strength testing. The ultimate goal of this study is charting a roadmap for advanced CO_2 capture by integrating essential factors and addressing knowledge gaps, offering significant insights for sustainable construction and environmental preservation.

4.3. Materials and methods

4.3.1. Materials

As this research builds upon the foundation established in our earlier work, comprehensive information regarding the characteristics of the PC including the mix proportions, material properties, testing protocols for the constituent components, and the procedures followed for producing the RCAs has already been thoroughly documented in the study by Gebremariam et al. [13]. Readers are encouraged to refer to that publication for a full understanding of the experimental background and material preparation, which forms the basis for the current investigation. The carbonation testes were carried out in RCA samples from the PCs with cube compressive strength of 25 Mpa and 67 Mpa to consider the effect of source concrete strength on the carbonation degree of the RCAs.

4.3.2 Carbonation chamber production

In the field of civil engineering, carbonation chambers play a critical role in simulating and accelerating the carbonation process of cementitious materials. These chambers are widely employed in laboratory settings for two main purposes: evaluating the durability and service life of concrete, and conducting CO_2 curing experiments, especially for unreinforced materials [2]. Commercially available carbonation chambers are highly specialized and technologically advanced; however, they are often prohibitively expensive for many research institutions. In our case, the absence of a preinstalled carbonation chamber and the high cost of purchasing one from a specialized supplier presented a significant challenge. To overcome this limitation, we designed and constructed a custom carbonation chamber using readily available local materials and practical engineering solutions.

The initial attempt to develop the carbonation chamber involved embedding a reinforced concrete box in the ground, which served as the primary containment unit. A reinforced concrete lid was fabricated to act as a sealable cover, and the interior surfaces, including the lid, were lined with polyethylene sheets to enhance airtightness and prevent CO_2 leakage. Inside the chamber, two layers of wire mesh were strategically placed to support baskets filled with RCA, while also allowing for even distribution and circulation of CO_2 gas throughout the chamber.

Once assembled, the entire setup was sealed using high strength cement mortar at all junctions and allowed to cure for three days. After curing, an air tightness test was conducted using a compressor to check for any potential leaks under pressurized conditions. Unfortunately, the test revealed that air was escaping from the chamber, indicating a failure in achieving the necessary seal. To address this, we replaced the concrete cover with a wooden lid and used industrial grade contact adhesives to reinforce the joints. Despite these efforts, air leakage persisted, rendering the setup ineffective for controlled carbonation.

Realizing the need for a more robust and pressure resistant structure, we moved forward with the design and fabrication of a second chamber, this time constructed from 3 mm thick steel sheets, resulting in a cylindrical chamber with a volume of approximately 0.8 m^3 as can be seen on Figure 4.1. The new steel chamber featured a top loading inlet for easy placement of RCA samples. A steel inlet pipe was integrated into the chamber's upper section to facilitate CO_2 gas injection, and a pressure gauge was installed on the side to monitor the internal pressure during carbonation.

To regulate the humidity levels within the chamber, a salt solution was introduced at the bottom, maintaining a controlled environment conducive to carbonation. Two layers of wire mesh were installed horizontally at 30 cm intervals to hold the RCA baskets securely above the humidity control solution. Prior to the actual testing, the new setup underwent a leakage test under 2 bar pressure using an air compressor. This time, the chamber successfully retained the pressure, confirming its airtight integrity. A thermo-hygrometer was placed inside the chamber to record the humidity and temperature fluctuations in the chamber and it was found that the humidity and temperature variations were within the proposed limits.

Subsequently, a CO_2 cylinder was procured from a local supplier and connected to the chamber through a plastic hose. The cylinder was equipped with a regulator gauge to control the flow of CO_2 into the chamber. For each carbonation cycle, approximately 80 kg of RCA was loaded into the chamber. Once the inlet was sealed using gasket materials,

CO_2 gas was released into the chamber until the internal pressure reached 1.5 bar (0.15 MPa).

The RCA samples were left inside the chamber for a duration of three days to ensure thorough carbonation. After the exposure period, the extent of carbonation was verified using phenolphthalein indicator tests. This process was repeated in cycles until a sufficient quantity of fully carbonated aggregates was obtained for use in subsequent experimental phases. This practical and cost effective approach to chamber construction not only enabled us to carry out accelerated carbonation under controlled conditions but also demonstrated the potential of low cost, locally fabricated setups for advanced material research in resource constrained settings.

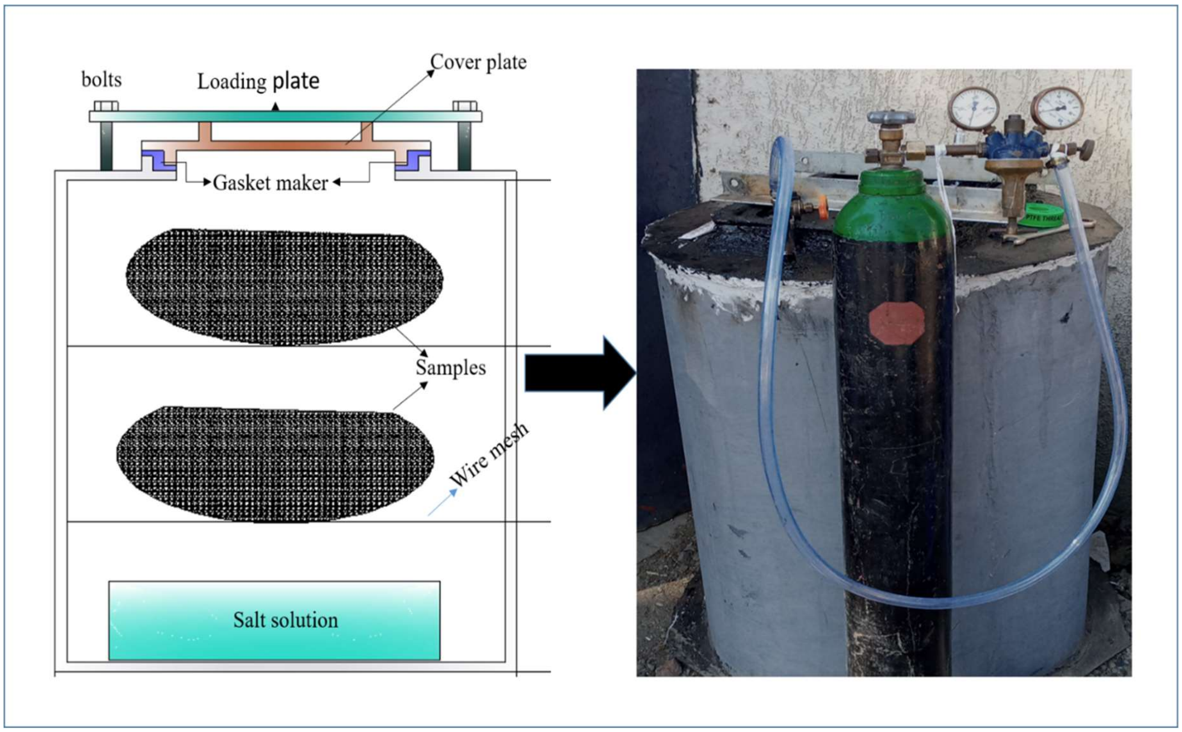

Figure 4.1 Carbonation chamber setup

4.3.3 Internal circumstances affecting carbonation degree

4.3.3.1 Effect of moisture content of RCA

After the production of the RCAs, to account for the ambient carbonation that occurs in RCA before the initiation of accelerated carbonation, the aggregates were stored in an open environment placed inside of sacks and covered with plastic sheeting to protect freezing and thawing for one and half years to be naturally carbonated. Then the materials were tested for water absorption and specific gravity according to ASTM C 127 [14] to estimate the percentage of moisture the RCAs must have, to have an optimum moisture for better accelerated carbonation. According to the studies [8, 15] optimum moisture in the RCAs must not be greater than 60% of the water absorption capacity of the aggregates. RCAs with maximum aggregate size of 25 mm were used in this study. Initially, aggregate samples were immersed in water for 24 hrs to be fully saturated and were oven dried at 110 °C for 24 hrs to determine the saturated surface dry water absorption of the aggregates. Concurrently, Sample aggregates in their natural moisture contents were oven dried at 110 °C to determine the available moisture in the aggregates. The optimal moisture content for RCA to maximize carbonation during accelerated carbonation is typically around 30 to 65 % saturation of their water absorption capacity [15, 16]. Then the percent addition or subtraction of water from the aggregates according to 50% of the aggregates water absorption capacity were performed. Then the aggregates were stored in sealed plastic bags. The bags were then air tightly sealed, and the samples were left undisturbed for 3 days to allow uniform distribution and stabilization of moisture content across all RCA particles.

4.3.4 External circumstances affecting carbonation degree

4.3.4.1 Effect of relative humidity

The efficiency of RCA carbonation is strongly influenced by the chamber's relative humidity. Both very low and very high humidity levels hinder CO_2 absorption, either by reducing its solubility or blocking its diffusion [17]. Carbonation improves with increasing humidity up to a certain point, after which it declines. An optimal humidity range of 50-80% is generally effective for accelerated carbonation, [18-20]. A study by Young [21] proved that salt solutions can control humidity in a sealed environments. In the present study the relative humidity of 70 to 78 % was achieved using sodium chloride solution at water to salt mix ratio of 1.5:2 by weight.

4.3.4.2 Effect of CO_2 gas pressure

The degree of carbonation in RCAs is notably affected by gas pressure. A modest rise in pressure up to around 0.01 Mpa, leads to a sharp increase in carbonation. Beyond this point, however, further pressure increments yield only marginal improvements [22]. Identifying an optimal pressure range, ideally below 0.5 MPa, is essential for maximizing the efficiency of accelerated carbonation processes [21]. Therefore in this research, we have used a CO_2 gas pressure of 0.15 Mpa.

4.3.4.3 Effect of carbonation duration

It is evident that extending the carbonation duration generally enhances the degree of carbonation in RCAs. However, the reaction does not progress at a constant rate. A significant portion of carbonation occurs rapidly within the early phase, particularly in the first 24 hours, after which the reaction rate gradually diminishes [23]. This decline is primarily attributed to the densification of the adhered mortar as carbonation progresses, reducing its porosity and forming a more compact microstructure that restricts the diffusion of CO_2 into the inner layers [24]. As highlighted in [20, 24-26], this rapid initial reaction slows noticeably after the first day and continues at a much reduced pace, eventually plateauing around 72 hrs. In the present study, the carbonation duration was 72 hrs.

4.3.4.4 Effect of CO_2 concentrations

The concentration of carbon dioxide is a crucial factor influencing the carbonation behavior of RCAs. As noted in [27], the rate at which CO_2 penetrates the material depends not only on its concentration but also on the internal pathways available for gas movement. Initially, before pore spaces begin to close due to the formation of carbonation products, a higher CO_2 concentration promotes more effective gas diffusion and reaction throughout the porous matrix [28]. Although previous research [20] indicates that a concentration as low as 25% can sufficiently support the carbonation process, this study employed high purity CO_2 gas of 99.9% readily available from Ethiopian local commercial sources, to ensure consistency and to avoid variability in the experimental setup.

4.3.4.5 Effect of temperature variations

Although elevated temperatures can promote the formation of metastable polymorphs of calcium carbonate, maintaining a relatively low temperature is essential to favor the generation of stable calcite, as carbonation is an exothermic reaction that releases heat during the process [12]. Controlling temperature is therefore crucial, not only to regulate the type of carbonate phases formed, but also to ensure a consistent reaction environment. Moreover, temperature fluctuations within the carbonation chamber can influence the relative humidity, which in turn indirectly affects CO_2 diffusion and the overall carbonation performance of RCAs [29]. For these reasons, numerous studies have adopted a temperature range of 20-30 °C as optimal for accelerated carbonation treatments [29, 30], as this range provides a balanced environment for CO_2 reactivity, moisture stability, and formation of durable carbonation products. On the present study the carbonation temperature was 23 ±5 °C.

4.3.5 Physical property testes of RCA after carbonation

Upon completion of the accelerated carbonation process for the required RCA samples, a comprehensive evaluation of their physical and mechanical properties was conducted. These assessments were carried out in accordance with the standardized laboratory testing procedures outlined by ASTM, as detailed in the methodology of Gebremariam et al. [13]. Specifically, key parameters such as water absorption and specific gravity were measured to understand changes in porosity and density of the aggregates post carbonation. In addition, mechanical strength indicators including aggregate crushing value were determined.

4.3.6 Microstructural testes of carbonated RCA samples

This section focuses on analyzing the microstructural changes in RCAs after exposure to accelerated carbonation, before their use in concrete. The goal was to examine how carbonation alters the material at the microscopic level in terms of crystallinity, weight changes, and chemical bonding. To achieve this, fine powdered samples extracted from the adhered mortar of RCA particles were tested for TGA-DTA, XRD, and FTIR.

4.3.7 Sample preparation

After the accelerated carbonation process was completed, samples from naturally carbonated recycled concrete aggregate (NRCA) and accelerated carbonated recycled concrete aggregate (ARCA) particles were dried and the attached mortar was carefully extracted. This mortar was then ground into a fine powder passing through a 75 µm sieve to ensure uniformity. These powders were stored in sealed containers until testing to avoid unwanted CO_2 or moisture interference.

TGA and DTA were used to track weight changes as the samples were gradually heated. Around 10 mg of each powder was tested using DTA-60H detector from Shimadzu Japan by placing it in a crucible and heated from room temperature to 900°C at a flow rate of 50 milliliter per minute in a nitrogen atmosphere. Mass loss at specific temperature points revealed the breakdown of compounds like calcium hydroxide and calcium carbonate. The DTA curve helped pinpoint the temperatures where the most significant changes occurred, offering a clearer view of carbonation effects.

The mass loss observed within the temperature range of 550°C to 950°C, which corresponds to the decarbonation process of calcite polymorphs, is generally taken as the estimated amount of CO_2 absorbed [31]. In our case, however, as can be seen from the DTA curve, the relevant temperature range was 500°C to 750°C. The CO_2 uptake capacity of the NRCA and ARCAs with respect to the attached mortar mass was determined from the TGA graph using the following equations:

$$CO_2\ uptake\ by\ NRCA\ (\%) = (\frac{m_{750} - m_{500}}{M_{mortar}}) \times 100 \quad (4.4)$$

$$CO_2\ uptake\ by\ ARCA\ (\%) = ((\frac{M_{750} - M_{500}}{M_{mortar}}) \times 100) - CO_2 uptake\ by\ NRCA(\%) \quad (4.5)$$

Where CO_2 uptake by ARCA (%) is the mass of CO_2 uptake by the accelerated carbonation, CO_2 uptake by NRCA (%) is the mass of CO_2 uptake by the preprocessing ambient carbonation, m_{750} and m_{500} are the masses of naturally preprocessing carbonated samples at 750 and 500°C, and M_{750} and M_{500} are the masses of pressurized accelerated carbonated samples at 750 and 500°C, and M_{mortar} is the mass of the attached mortar sample.

To identify changes in crystalline composition, XRD scans were conducted using XRD7000 from Shimadhu, Japan. Patterns were recorded between 10° and 70° (2θ), and the data was compared between NRCA and CRCA samples. A drop in portlandite peaks and an increase in calcite indicated the shift from hydration to carbonation products.

FTIR from PerkinElmer 65, PerkinElmer, Inc. Waltham, USA, helped detect shifts in chemical bonding caused by carbonation. Powdered samples scanned in the 4000-400 cm^{-1} range. Key attention was given to changes in hydroxyl and carbonate peaks. A shift in O-H signals and carbonate bands confirmed the chemical transformation during carbonation.

4.3.7 Mix design and testing methodology of carbonated RCA concrete

To systematically examine the effects of carbonation degree, PC strength, and aggregate replacement ratio on the mechanical properties of both NRAC and ARAC, a comprehensive experimental program was developed.

Firstly, RCA were sourced from two different PCs which were prepared according to the methodology in [13], with cube compressive strengths of 25 MPa and 67 MPa, respectively, in order to capture the influence of original concrete quality. Secondly, three replacement ratios of NAs with NRCA and ARCA were selected namely, 0%, 30%, and 100%. This allowed evaluation of the mechanical behavior across a range of RCA incorporation levels. Thirdly, two target concrete strength levels were designed: a normal strength mix (25 MPa) and a high strength mix (67 MPa), enabling the assessment of water to cement ratio effects on the performance of NRAC and ARAC. A target NRAC and ARAC concrete mix was prepared using a maximum aggregate size of 25 mm. Fine aggregates used were river sand with a fineness modulus of 2.85. The binder material was Dangote Ordinary Portland Cement 42.5R with a specific gravity of 3.1. Natural tap water was employed as the mixing water. All constituent materials were obtained from the same sources as those characterized in our previous study [13].

To avoid unintentional water addition caused by the water absorption of RCA all aggregates were conditioned to a SSD state prior to mixing. Workability of the fresh concrete was assessed for each of the 18 mix designs using the slump test method, with good slump values ranging from 40 to 80 mm. Following satisfactory trial mixes and workability tests, concrete specimens were cast for mechanical performance evaluation. A total of 108 cube specimens (150 mm × 150 mm × 150 mm) were prepared for compressive strength testing. In addition, 54 cylindrical specimens (100 mm diameter × 200 mm height) were prepared for split tensile strength testing, and 54 prismatic beam specimens (100 mm

× 100 mm × 500 mm) were cast for flexural strength testing. Each specimen was labeled with a unique mix code, as shown in table 4.1, to ensure clear identification and traceability.

After casting, all specimens were kept at room temperature for 24 hours to set. They were then demolded and submerged in tap water for a standard curing period of 28 days. This carefully structured methodology ensured that all variables were well controlled, enabling a reliable assessment of the individual and combined effects of carbonation treatment, PC strength, and RCA replacement ratio on the mechanical properties of NRAC and ARAC. This comprehensive experimental plan was designed according to American Concrete Institute, Committee 211. 1977 (ACI 211.1-91) [32].

After the 28 day curing period, the concrete specimens were subjected to mechanical testing to evaluate their compressive strength, split tensile strength, and flexural strength. All tests were conducted using a universal testing machine in accordance with the procedures outlined by Dinku A. [33].

Table 4.1 Sample designation names for ease of use.

Designation	Full sample name
NA	Natural aggregate
NRCA	Naturally carbonated recycled concrete aggregate
ARCA	Accelerated carbonated recycled concrete aggregate
NA(25)-control	25 MPa concrete strength produced from natural aggregates
NRAC(25)-(30)-(25)	25 MPa concrete strength produced by 30% replacement of NA by NRCA from 25 MPa parent concrete
NRAC(25)-(100)-(25)	25 MPa concrete strength produced by 100% replacement of NA by NRCA from 25 MPa parent concrete
NRAC(25)-(30)-(67)	67 MPa concrete strength produced by 30% replacement of NA by NRCA from 25 MPa parent concrete
NRAC(25)-(100)-(67)	67 MPa concrete strength produced by 100% replacement of NA by NRCA from 25 MPa parent concede
ARAC(25)-(30)-(25)	25 MPa concrete strength produced by 30% replacement of NA by ARCA from 25 MPa parent concrete
ARAC(25)-(100)-(25)	25MPa concrete strength produced by 100% replacement of NA by ARCA from 25 MPa parent concrete

Designation	Full sample name
ARAC(25)-(30)-(67)	67 MPa concrete strength produced by 30% replacement of NA by ARCA from 25 MPa parent concrete
ARAC(25)-(100)-(67)	67 MPa concrete strength produced by 100% replacement of NA by ARCA from 25 MPa parent concrete
N(67)-control	67 MPa concrete strength produced from natural aggregates
NRAC(67)-(30)-(25)	25MPa concrete strength produced by 30% replacement of NA by NRCA from 67 MPa parent concrete
NRAC(67)-(100)-(25)	25MPa concrete strength produced by 100% replacement of NA by NRCA from 67 MPa parent concrete
NRAC(67)-(30)-(67)	67 MPa concrete strength produced by 30% replacement of NA by NRCA from 67 MPa parent concrete
NRAC(67)-(100)-(67)	67 MPa concrete strength produced by 100% replacement of NA by NRCA from 67 MPa parent concrete
ARAC(67)-(30)-(25)	25 MPa concrete strength produced by 30% replacement of NA by ARCA from 67 MPa parent concrete
ARAC(67)-(100)-(25)	25MPa concrete strength produced by 100% replacement of NA by ARCA from 67 MPa parent concrete
ARAC(67)-(30)-(67)	67 MPa concrete strength produced by 30% replacement of NA by ARCA from 67 MPa parent concrete
ARAC(67)-(100)-(67)	67 MPa concrete strength produced by 100% replacement of NA by ARCA from 67 MPa parent concrete

4.4. Result and discussion

4.4.1 PH changes related to carbonation

Phenolphthalein is a widely used PH indicator that changes its appearance depending on the alkalinity of the material. When the pH is above approximately 8.2, conditions where $Ca(OH)_2$ is present in significant amounts, it develops a deep pink coloration. In contrast, when the pH drops below 8.2, typically due to the conversion of $Ca(OH)_2$ into calcium carbonate through carbonation, the indicator remains clear and colorless [34]. The PH tests done before the accelerated carbonation, showed clear differences between the RCAs from low strength (25 MPa) and high strength (67 MPa) parent concretes. For the 25 MPa RCAs, spraying phenolphthalein on the outer mortar surfaces caused no color change, meaning those surfaces were already carbonated before the test. Looking at the cross section of the aggregates, the color change was seen far from the surface. This likely happened because the lower strength concrete is more porous, allowing natural CO_2 from the air to enter and react with the alkaline materials over time. For the 67 MPa RCAs, the outer mortar surfaces was color less but the cross section showed turned a weak, dull pink up starting from the near surface and changed to bright pink after that which indicates uncarbonated mortar. This shows that some carbonation had taken place on the surface, but not fully, there were still some hydroxide products near the surface. The denser structure of high strength concrete makes it harder for CO_2 to enter naturally, which explains this partial carbonation.

The inner mortar parts of both RCA types turned bright pink before accelerated carbonation, meaning carbonation had not reached the core in either case. This shows that the inside is protected from ambient carbonation by the mortar's density. After three days of pressurized accelerated carbonation, the 25 MPa RCAs showed almost complete carbonation, although some very small areas within the thick mortar still displayed pink coloration, indicating uncarbonated regions. This confirms that their higher porosity allows CO_2 to pass through easily under pressure. However, the 67 MPa RCAs still had pink cores after the same treatment, meaning the carbonation did not reach all the way inside. This is because the dense, low porosity structure blocks CO_2 from moving deep into the material, even under pressure. The pictures showing this process can be found from the appendix of this dissertation. The aggregates from the high strength were then allowed to stay in the carbonation chamber for seven days to check if they can be carbonated on elongated time. But the aggregates were not full carbonated. These results show that the carbonation level of RCAs strongly depends on the strength and porosity of the original concrete. Low strength RCAs can carbonate more easily, both naturally and under accelerated conditions, while high strength RCAs resist carbonation in their inner parts. This shows us that, high strength RCAs would need extra treatment such as mechanical breaking or alternative better treatment methods other than stable pressurized carbonation to achieve full carbonation.

4.4.2 Water absorption and crushing resistance of the NRCA and ARCA

The effects of accelerated carbonation on the water absorption and crushing value of RCAs derived from PCs of different strengths are shown in Figure 4.2. The NRCA from the 25

MPa PC exhibited an 18% reduction in water absorption after undergoing accelerated carbonation, producing ARCA. In comparison, the NRCA from the 67 MPa parent concrete showed only a 2.3% reduction after the same treatment. This clear difference highlights the role of initial porosity and degree of carbonation, the more porous 25 MPa aggregates allowed CO_2 to penetrate more effectively, promoting pore filling through carbonation products such as $CaCO_3$, which in turn reduces water uptake.

When comparing the two NRCAs prior to carbonation, the 25 MPa aggregates had 33% higher water absorption than the 67 MPa aggregates. This large difference is consistent with the expectation that lower strength concrete has a more open pore structure and higher permeability. After accelerated carbonation, the gap in water absorption between the two aggregate types decreased from 33% to 18%. This narrowing suggests that carbonation treatment benefits the lower strength aggregates more significantly, improving their quality and narrowing performance differences relative to the high strength aggregates. This supports the idea that high strength aggregates do not get fully carbonated due to the denser porosity they exhibit by the obvious pressurized accelerated carbonation.

A similar trend was observed in the crushing value results. For the 25 MPa NRCA, accelerated carbonation reduced the crushing value by 6.9%, indicating an improvement in aggregate strength. For the 67 MPa NRCA, the reduction was 11.78%, suggesting that, while high strength aggregates already have lower porosity, carbonation can still densify the microstructure and enhance mechanical integrity. Initially, the crushing value of NRCA-25 was 18.75% higher than that of NRCA-67, reflecting the inherent lower strength of aggregates from weaker PC. After carbonation, this difference was reduced to 12.75%, again showing that the process helps close the performance gap between low and high strength aggregates.

Overall, these results demonstrate that accelerated carbonation can improve both water absorption and mechanical performance of RCAs, with more pronounced effects in low strength, high porosity aggregates. These findings align with the understanding that carbonation products primarily calcium carbonate precipitate within the pore structure, reducing porosity and micro cracking while enhancing particle cohesion [20, 24, 29].

However, the denser microstructure of high strength aggregates limits CO_2 penetration, explaining the smaller water absorption changes compared to low strength aggregates. This highlights the importance of tailoring carbonation treatment methods and conditions to the original concrete's properties to maximize performance gains.

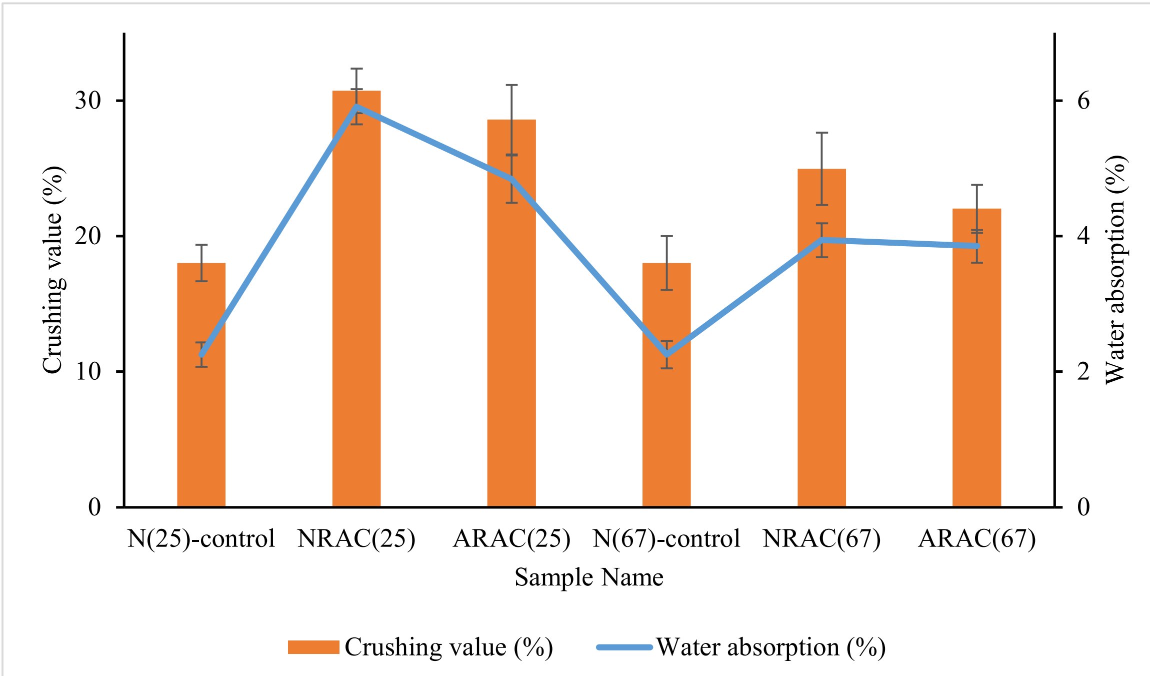

Figure 4.2 Physical and mechanical properties of aggregates before and after accelerated carbonation

4.4.3 TGA-DTA analysis

Figure 4.3 shows the TGA-DTA results of the NRCAs and ARCAs from the 25 Mpa and 67 Mpa PC strength concretes. The peaks observed in the DTG curves correspond to three distinct phase specific thermal events. The first peak, occurring at approximately between 23°C and 340°C, and is associated with the loss of moisture, the dehydration of calcium silicate hydrate phases along with gypsum and other hydration products. The second thermal band, between 340 °C and 500 °C, corresponds to the decomposition of $Ca(OH)_2$. The third thermal band, from 500 °C to 750 °C, is linked to the decomposition of $CaCO_3$. In TGA analysis, the weight loss over a particular temperature range is taken as the mass loss of the specific mineral phase that decomposes in that range. This approach, which has been widely used in previous studies [35], allows for the comparison of the relative content of specific phases among different samples and methods.

As can be seen in Figure 4.3, the percentage mass loss within each decomposition range varies for the different aggregate types. This variation is primarily due to differences in alkalinity behavior and the quantity and composition of calcium carbonate crystals present in each sample. For the NRCA-25, the mass loss in the $CaCO_3$ decomposition range (third band) was measured at 7.42% of the attached mortar mass. After accelerated carbonation (ARCA-25), this value increased to 11.93%, representing an increase of approximately 4.5% by mass. This indicates that accelerated carbonation enhanced the formation of carbonate products in the mortar attached to the low strength aggregates. For the NRCA-67, the mass loss in the same decomposition range was 4.00% prior to accelerated carbonation and increased to 5.12% after accelerated carbonation (ARCA-67), corresponding to a smaller increase of 1.12%. This relatively low increase in carbonate content confirms that aggregates derived from high strength PC have a much denser pore structure, which hinders the diffusion of CO_2 gas into the internal pores, even under controlled, pressurized carbonation conditions. These results are consistent with the findings from the pH tests and the physical and mechanical property measurements, where the high strength aggregates exhibited incomplete carbonation under similar treatment conditions.

Previous studies found similar trend in CO_2 consumption capacities of RCAs and concretes. For example, Farahani et al. [36] investigated the carbonation reaction of RCAs to quantify CO_2 uptake under different treatment conditions, and reported that RCAs can store up to 3% CO_2 by their mass. Similarly, Zhan et al. [37] examined the influence of carbonation treatment on the transport properties and steel corrosion behavior of RAC, finding that carbonation treatment enabled a CO_2 uptake of up to 18.55% by the mass of mortar. In addition, Leemann et al. [8] observed that carbonation treatment of RCAs can sequester approximately 21 kg of CO_2 per ton of dry RCA mass. Along the same line, Hu et al. [31] developed sustainable low carbon engineered cementitious composites (ECC) incorporating waste polyethylene fiber, sisal fiber, and carbonation curing. Their results demonstrated that carbonation curing of ECC, when sisal fiber was used as a diffusion medium, achieved a CO_2 uptake of up to 21% by the mass of cement.

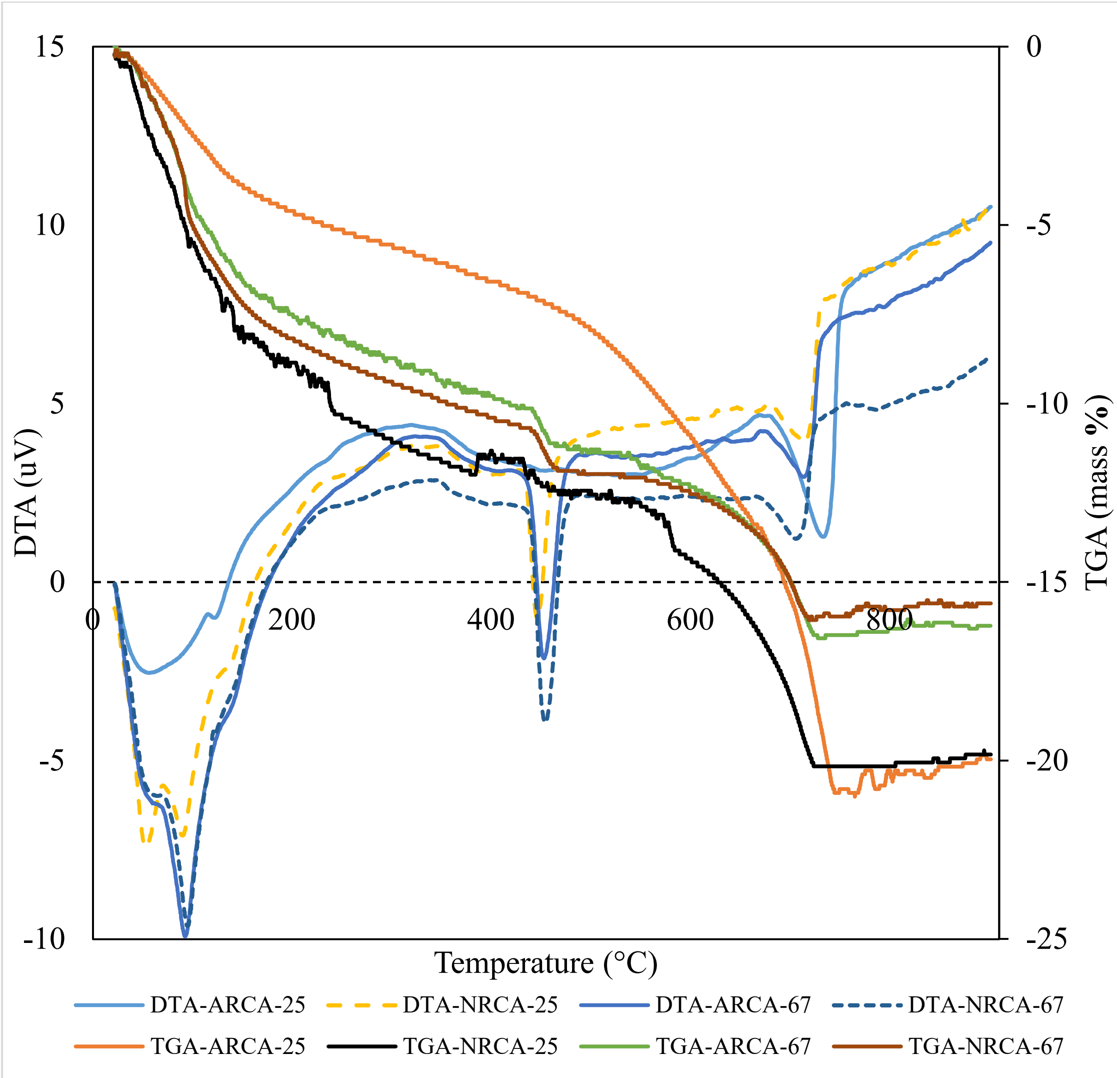

Figure 4.3 TGA-DTA outputs of aggregates before and after accelerated carbonation

4.4.4 XRD analysis

The XRD patterns of the NRCA and ARCA samples are presented in Figure 4.4. As shown in the figure, the diffraction profiles display numerous identifiable peaks corresponding to quartz and other crystalline phases. However, the analysis in this study focused primarily on peaks associated with portlandite and its related phases, as well as the various polymorphs of calcite. This focus was chosen because the primary objective was to evaluate the effect of carbonation treatment on calcite precipitation and the consequent reduction in aggregate alkalinity. The diffraction profiles showed that the carbonation treatment effectively reduced the alkalinity of the aggregates and promoted substantial calcite precipitation, thereby densifying the pore structure. In the accelerated carbonation specimens, the characteristic portlandite ($Ca(OH)_2$) peaks located at approximately 2θ = 18°, 23°, and 34°, [38] exhibited markedly lower intensities compared with those of aggregates subjected to only natural pre carbonation. Conversely, the diffraction peaks corresponding to calcium carbonate polymorphs observed at approximately 2θ = 29°, 39°, 43°, and 49° [35] were more prominent in the accelerated carbonation treated aggregates than in their naturally carbonated counterparts.

Consistent with the TGA-DTA findings, the XRD results further indicate that aggregates derived from high strength PC (67 MPa cube compressive strength) exhibited relatively higher portlandite peak intensities compared with those obtained from normal strength PC (25 MPa). This difference is attributed to incomplete carbonation within aggregates from high strength concrete, likely due to their denser microstructure, which restricts CO_2 diffusion into the interior mortar phases. Overall, the XRD observations of this study align closely with trends reported in previous investigations [35, 38-39], reinforcing the conclusion that accelerated carbonation significantly alters the mineralogical composition of RCAs by promoting portlandite consumption and calcite formation.

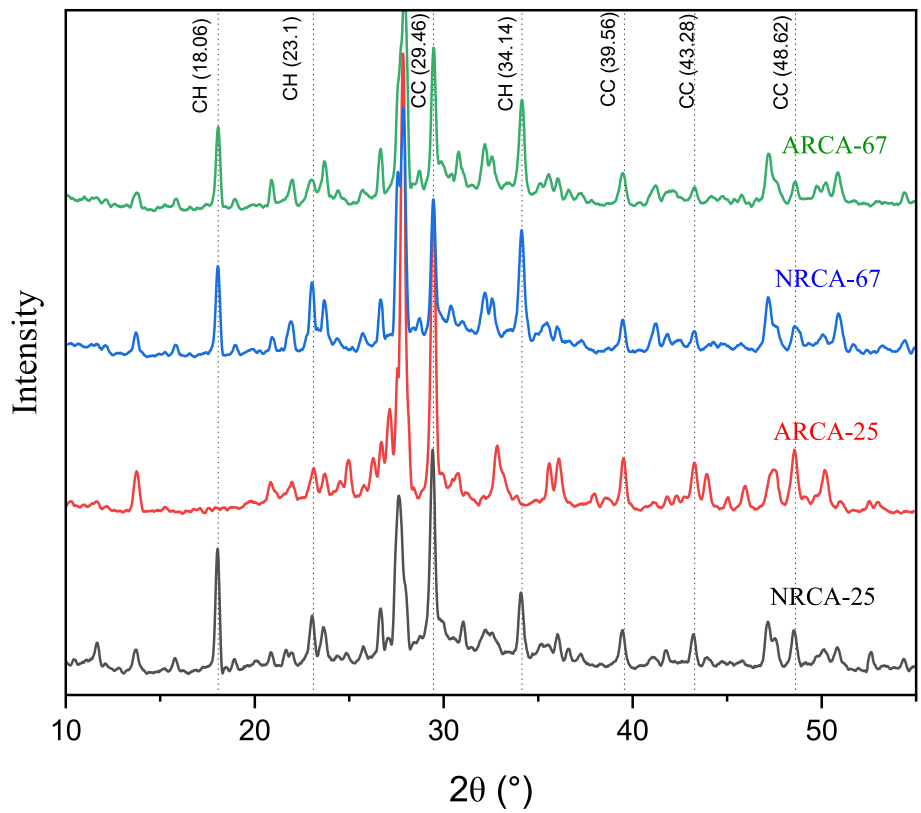

Figure 4.4 XRD outputs of aggregates before and after accelerated carbonation**,** where: CH: Portlandite CC: Calcium carbonate polymorphs and the number followed them represents the corresponding 2θ value.

4.4.5 FTiR analysis

The FTIR spectra of the NRCA and ARCA samples subjected to preprocessing carbonation and controlled pressurized accelerated carbonation are shown in Figure 4.5. Peak assignments for the identified functional groups are also indicated in the figure. In the NRCA specimens, a prominent absorption band at approximately 963 cm^{-1} was attributed to portlandite and the silicate component of C-S-H [40]. Following pressurized accelerated carbonation, this band exhibited a noticeable shift towards a higher wavenumber, with post treatment peaks positioned at around 1028 cm^{-1}. This shift was particularly pronounced in aggregates derived from normal strength PC.

Previous studies have reported that a reduction in portlandite content and a decrease in the Ca/Si ratio cause the Si-O bond vibrations in C-S-H and O-H groups to shift towards higher wavenumbers. This observation supports the interpretation that during carbonation, Ca-rich C-S-H reacts with CO_2 to form $CaCO_3$ and Si-rich C-S-H. The increase in the Si-rich C-S-H fraction results in the observed spectral shift [41].

Furthermore, pressurized accelerated carbonation produced a distinct increase in the intensity of peaks corresponding to calcite and its polymorphs. This is particularly evident at the band near 874 cm^{-1}, which became more pronounced after treatment. This change is attributed to the further reaction of C-S-H and portlandite with CO_2, yielding $CaCO_3$ (various calcite polymorphs) and calcium modified silica gel [42]. The carbonate bands characteristic of calcite polymorphs, observed at around 874 cm^{-1} [43], also showed substantial intensification in the range of 1410-1440 cm^{-1}, with stronger signals detected in aggregates sourced from normal strength PC. Finally, the absence of a distinct portlandite signal in aggregates from normal strength PC was evident from the lack of absorption bands at approximately 3642 cm^{-1}, confirming the near complete consumption of portlandite during carbonation.

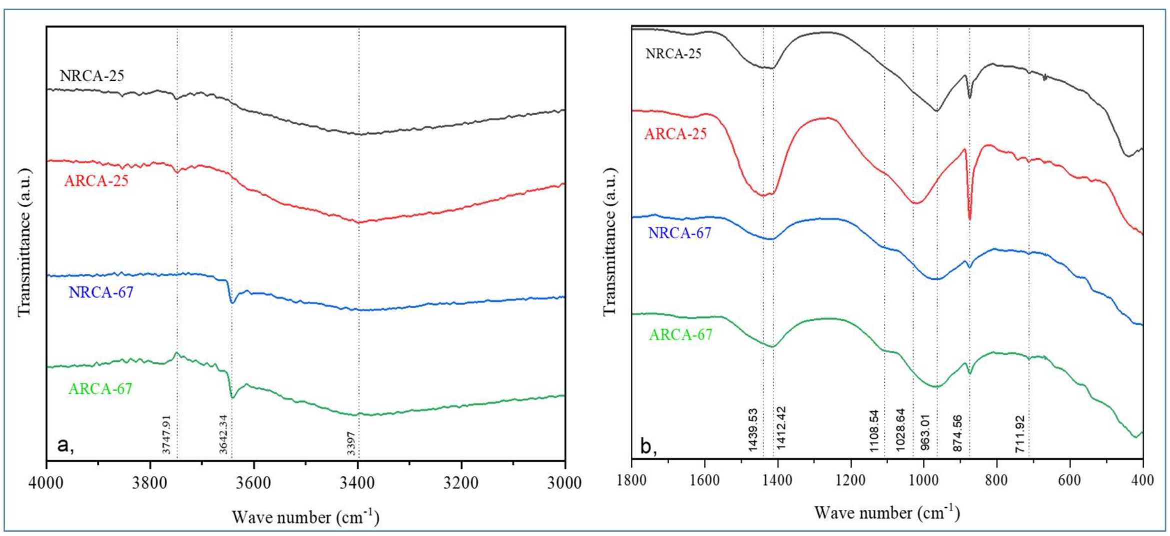

Figure 4.5 FTIR spectra of the NRCA and ARCA samples

4.4.6 Mechanical characteristics of carbonated recycled aggregate concrete

Figure 4.6 summarizes the strength differences in cube compressive strength at 28 days, between various concrete mixtures incorporating NAs, NRCAs, and ARCAs. When compared to the NA controls, NRCA mixtures consistently showed a reduction in compressive strength, reflecting the inherently lower quality of RCAs due to residual mortar and higher porosity. For example, NRCA (25)-(30)-(25) exhibited a 14.49% lower strength than N (25)-control, and NRCA (67)-(30)-(67) had 11.16% lower strength than N (67)-control. The reduction became slightly larger when the replacement level increased from 30% to 100%, confirming that higher replacement ratios lead to greater performance loss. This aligns with the known influence of aggregate quality on concrete strength. NRCA sourced from high strength PC (67 MPa) provided better performance than that from lower strength PC (25 MPa) for the same target strength. For instance, replacing NRCA (25)-(100)-(25) with NRCA (67)-(100)-(25) reduced the strength loss from 14.39% to 12.63%, while in the 67 MPa target group, NRCA (67)-(100)-(67) outperformed NRCA (25)-(100)-(67) by 18.09%. This improvement is attributed to the denser microstructure and lower porosity of aggregates from higher strength PC, which translates into better load transfer in the new mix.

Accelerated carbonation treatment also improved RCA quality, resulting in higher compressive strengths compared to their NRCA counterparts. For 25 MPa target concrete, ARCA (25)-(100)-(25) achieved an 8.85% increase relative to NRCA (25)-(100)-(25). Likewise, ARCA (67)-(100)-(25) outperformed ARCA (25)-(100)-(25) by 9.51%, reflecting the combined benefits of accelerated carbonation and high PC strength. Even though, the ARCA from the high strength PC was not fully carbonated according to the results from microstructural testes, it showed an increase in compressive strength. The peak improvement was recorded for ARCA (67)-(100)-(67), which had a 21.35% higher strength than ARCA (25)-(100)-(67).

In ARCA mixtures, the negative effect of increasing replacement ratio was still evident. ARCA (25)-(30)-(25) had 15.84% higher strength compared to ARCA (25)-(100)-(25), highlighting that partial replacement allows better retention of mechanical properties. These results are in agreement with existing literature, which attributes the performance improvements of ARCA to mineralogical changes such as portlandite consumption and calcite precipitation, leading to reduced porosity and enhanced aggregate mortar bonding. Several studies have investigated this effect, showing that carbonation can mitigate or even reverse the strength reduction typically associated with using recycled materials.

According to the study [41], "a research by Thomas et al [44] found that replacing 100% of NAs with untreated RCAs led to an 11-19% decrease in compressive strength. This finding aligns with Ozbakkaloglu et al [45] observation that higher replacement ratios of RCAs generally result in lower compressive strength". However, treating the RCAs with carbonation introduces a key difference. A similar study, noted that while untreated RCAs caused a significant 26.3% strength reduction at a 100% replacement rate, carbonating the RCAs reversed this trend [46]. Their research [46] showed a substantial 22.6% increase in compressive strength for concrete made with 100% carbonated RCAs compared to concrete with noncarbonated RCAs.

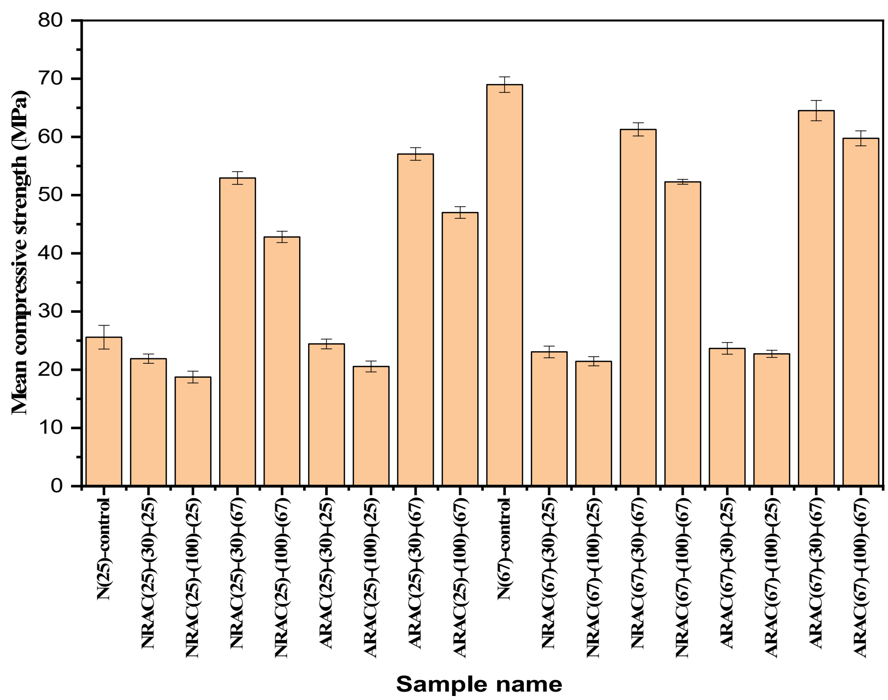

Figure 4.6 Mean compressive strengths of different samples

Similarly, the mechanical performance of the concretes in terms of split tensile and flexural strength was evaluated to assess the effects of replacing NA with NRAC and ARAC as shown on Figure 4.7 and Figure 4.8. The reference mix, N (25)-control, composed entirely of NAs, achieved the highest performance, reaffirming the well established fact that NA concrete possesses superior strength characteristics compared to its NRCA and ARCA counterparts. Compared to this control, NRAC (25)-(30)-(25) exhibited a 10.68% reduction in split tensile strength and 8.70% reduction in flexural strength. Increasing the replacement level from 30% to full replacement (100%) in NRAC(25)-(100)-(25) caused a further 8.13% decrease in split tensile strength and a 3.30% decrease in flexural strength, illustrating the direct negative influence of higher RCA content on both tensile and bending performance. PC strength also emerged as a key factor. When comparing NRAC(25)-(100)-(25) to NRAC(67)-(100)-(25), a 3.03% increase in split tensile strength was observed, alongside a modest 1.15% decrease in flexural strength, suggesting that high strength parent concrete (67 MPa) can partly offset the losses associated with RCA use in tensile performance. A similar trend appeared when comparing NRAC (25)-(100)-(67) with NRAC (67)-(100)-(67) where, split tensile and flexural strength rise drastically by 25.98% and 30.04%, respectively.

When accelerated carbonation was applied to NRAC, consistent improvements were observed. ARAC(25)-(100)-(25) achieved 8.57% higher split tensile strength and 3.30% higher flexural strength compared to the noncarbonated NRAC(25)-(100)-(25). Similarly, ARAC (25)-(30)-(25) surpassed ARAC (25)-(100)-(25) by 3.23% in split tensile strength and 7.77% in flexural strength, highlighting that both lower replacement percentages and carbonation treatment enhance mechanical performance. ARAC(25)-(100)-(67) exhibited a 24.21% lower split tensile strength and a 24.96% lower flexural strength compared to ARAC(67)-(100)-(67), clearly indicating the crucial role of PC quality in RCA performance enhancement, even after carbonation. A notable exception in the dataset is the 1.15% decrease in flexural strength recorded in the concrete from high strength PC compared to normal strength PC, indicating that the low strength PC NRAC unexpectedly outperformed the NRAC from high strength PC. This could be attributed to experimental variability, batching inconsistencies, or human error, and does not align with the broader trends observed. Similarly, it has been seen that at higher strength PC the tensile load resistance of the RAC has reached equivalent to NAC.

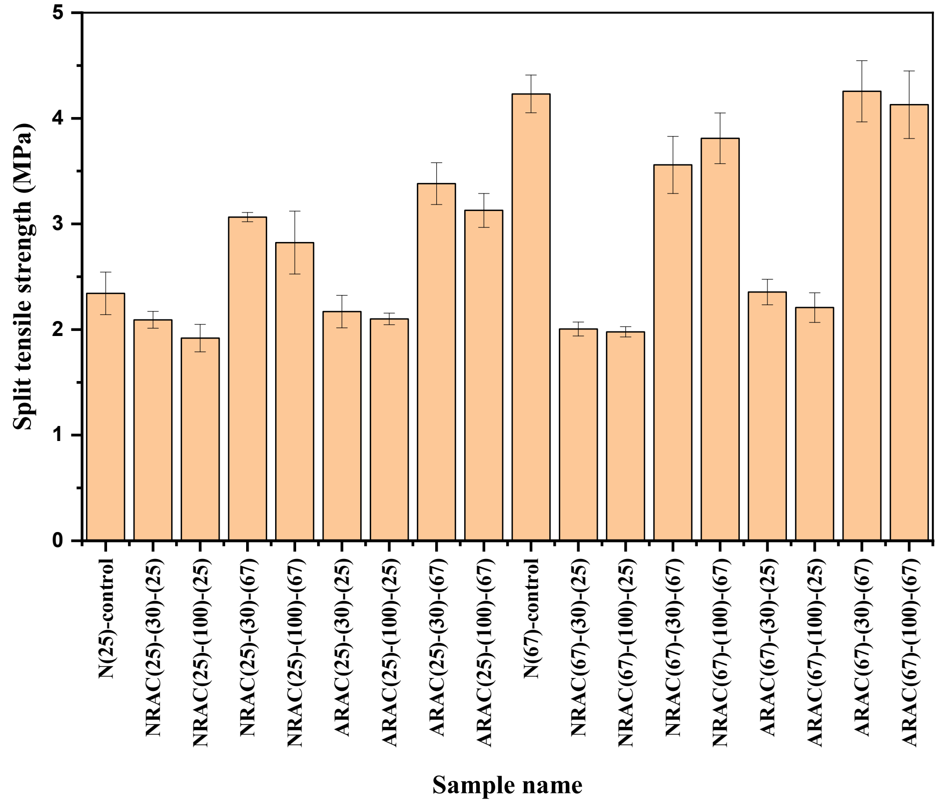

Figure 4.7 Mean split tensile strengths of samples

Previous studies conducted on mechanical properties enhancement by using accelerated carbonation showed that the split tensile and flexural strengths of carbonation treated RCA concrete had enhanced strength compared with the untreated aggregate concrete. For example, Tong et al [47] conducted a study on the effect of carbonated RCAs on the strength properties of 3D printed concrete, and found that, at the RCAs replacement level of 100 %, the flexural strength and splitting tensile strength increased by a maximum of 24.71 % in the X direction, 12.95 % in the Y direction and 18.27 % in the Z direction after RCA carbonation. on the other hand, Hadjari et al [48] investigated on the mechanical and fracture properties of RAC and found that compressive and tensile behavior of the RCA concrete remain comparable to, or even slightly greater than, those of NA concrete, with optimal performance at a 60% replacement rate.

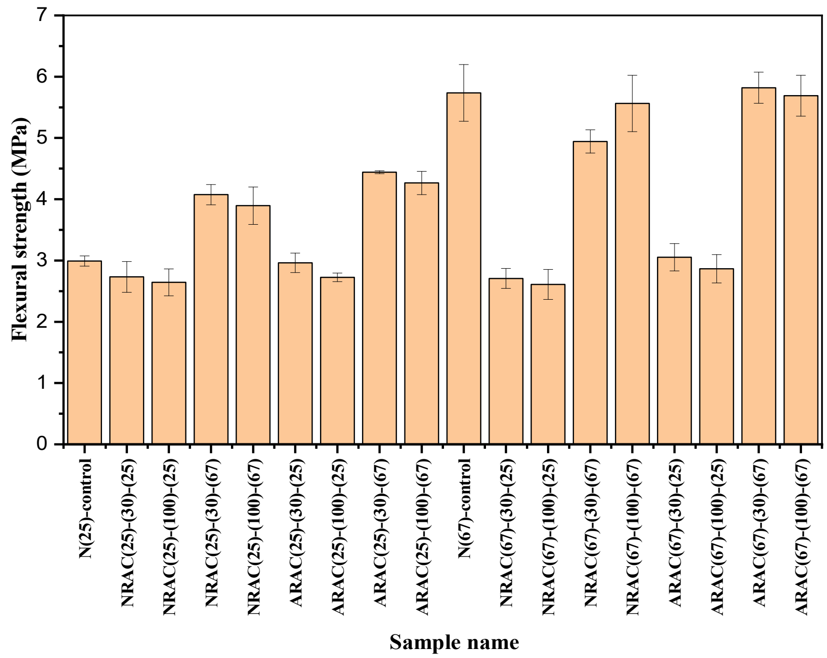

Figure 4.8 Mean flexural strengths of samples

The limitations in the range of PC strength used (normal strength and high strength) are due to limitations related to budget. But using wide varieties including very low strength, medium strength and high strength PC of greater than 70 Mpa can increase the accuracy and generalizability of the results.

4.5. Conclusion and recommendation

The current body of knowledge offers limited understanding of how material source characteristics influence the carbonation process, as well as the effect of pre accelerated carbonation of RCAs on CO_2 storage capacity, often overlooking precise behavioral interactions and the accurate estimation of CO_2 sequestration and storage potential in RCAs. To address this gap, this study conducted an extensive experimental investigation on NRCA and ARCA derived from PCs of varying strengths, as well as on concretes produced from these aggregates. Based on the findings, the following conclusions and recommendations are presented.

- Preprocessing carbonation, which is common in real world scenarios, significantly impacts the pressurized accelerated carbonation capacity of RCAs.

- Variations in PC strength also significantly impact the CO_2 storage capacity of RCAs.
- Carbonation reduces the water absorption and crushing value of the RCAs.
- RCAs from high strength PC are unable to fully carbonate even after pressurized accelerated carbonation extended from 3 to 7 days. This may be due to their dense pore structure hindering CO_2 diffusion within the aggregates.
- The preprocessing carbonation stored up to 7.5 % by mass of mortar of CO_2, while the pressurize carbonation stored up to 12% by mass of mortar of CO_2 in the form of calcium carbonate polymorphs
- Compressive, split tensile and flexural strengths increased by maximum of 12.5%, 8.59% and 3.3% respectively by carbonation treatment. The change in aggregate source from normal strength to high strength induced an increase in compressive, split tensile and flexural strength of 18%, 25.96% and 30 % respectively.
- Aggregate size effect, a limitation which was not considered in this study, could also impact the carbonation degree of RCAs from high strength PC.
- Futures studies should focus on finding alternative carbonation methodologies that help in carbonation treatment of RCAs sourced from high strength PCs.
- Since this study was conducted on a small, laboratory scale, future research should consider expanding it to industrial scale mass production of carbonated RCAs.

4.6. References

[1]. Peiris, D., Gunasekara, C., Law, D.W. et al. (2025). Impact of treatment methods on recycled concrete aggregate performance: a comprehensive review. Environ Sci Pollut Res 32, 14405–14438. https://doi.org/10.1007/s11356-025-36497-y.

[2]. Fortunato, L.R., Parsekian, G.A., Junior, A.N. (2023). Developing an easy-to-build laboratory chamber for CO2 experiments. Matéria (Rio J.) 28 (2). https://doi.org/10.1590/1517-7076-RMAT-2023-0078

[3]. Bui, H., Delattre, F., & Levacher, D. (2023). Experimental Methods to Evaluate the Carbonation Degree in Concrete—State of the Art Review. Applied Sciences, 13(4), 2533. https://doi.org/10.3390/app13042533

[4]. Liu K., Xu W., Sun, D., Tang, J., Wang, A., Dong Chen, D. (2021). Carbonation of recycled aggregate and its effect on properties of recycled aggregate concrete: A review. Mater. Express 11 (9), 1439-1452(14). https://doi.org/10.1166/mex.2021.2045

[5]. Feng, R., Xian, X. (2025).A review for accelerated carbonation improvement of recycled concrete coarse aggregates and the meta-analysis of environmental benefit assessment and cost analysis of concrete so produced, J. Build. Eng., 106,112649, https://doi.org/10.1016/j.jobe.2025.112649

[6]. Friedlingstein, P., O'Sullivan, M., Jones W., Robbie M. Andrew, R., Hauck, J., Landschützer, P., et al. [2024]. Global Carbon Budget 2024. Earth Syst. Sci. Data, 17 (3), 965–1039. https://doi.org/10.5194/essd-17-965-2025

[7]. International Energy Agency. Net Zero by 2050, a Roadmap for the Global Energy Sector. https://iea.blob.core.windows.net/assets/deebef5d-0c34-4539-9d0c-10b13d840027/NetZeroby2050-ARoadmapfortheGlobalEnergySector_CORR.pdf

[8]. Leemann,a., Winnefeld, F., Münch, B., Tiefenthaler, J.(2023) Accelerated carbonation of recycled concrete aggregates and its implications for the production of recycling concrete. J. Build. Eng., 79,107779. https://doi.org/10.1016/j.jobe.2023.107779.

[9]. Pade C., Guimaraes, M. (2007). The CO2 uptake of concrete in a 100 year perspective, Cement Concr. Res. 37, 1348–1356. https://doi.org/10.1016/j.cemconres.2007.06.009

[10]. Leemann, A. (2019). CO2 absorption of concrete based on the boundary conditions of Switzerland, in: Proceedings of International Workshop on the CO2 Storage in Concrete-CO2STO2019Marne La Vall´ee, 2019. https://www.rilem.net/publication/publication/536?id_papier=13371

[11]. Sanjuán, M.A., Andrade, C. and Cheyrezy, M. (2003). Concrete carbonation tests in natural and accelerated conditions. Adv. Cem. Res, 15(4), 171–180. https://doi.org/10.1680/adcr.2003.15.4.171

[12]. Kaliyavaradhan, S.K. and Ling, T. (2017). Potential of CO2 sequestration through construction and demolition (C&D) waste-an overview. J. CO2 Util, 20, 234–242. https://doi.org/10.1016/j.jcou.2017.05.014

[13]. Gebremariam, HG., Taye, S., Tarekegn AG., (2023).Disparity in research findings on parent concrete strength effects on recycled aggregate quality as a challenge in aggregate recycling.CSCM, 19, e02342, https://doi.org/10.1016/j.cscm.2023.e02342

[14]. ASTM C127-12. Standard test method for density, relative density (specific gravity), and absorption of coarse aggregate. West Conshohocken, PA: ASTM; 2012

[15]. Sereng, M., Djerbi, A., Metalssi, O., Dangla, P., Torrenti, J. (2021). Improvement of Recycled Aggregates Properties by Means of CO2 Uptake Appl. Sci. 11 (14), 6571. https://doi.org/10.3390/app11146571

[16]. Zhan, B., Poon, C.S., Liu, Q., Kou, S., Shi, C. (2013). Experimental study on CO2 curing for enhancement of recycled aggregate properties, Constr. Build. Mater., 67, Part A, 3-7, https://doi.org/10.1016/j.conbuildmat.2013.09.008

[17]. Fernández Bertos, M., Simons, S.J.R., Hills, C.D., Carey, P.J (2004). A review of accelerated carbonation technology in the treatment of cement-based materials and sequestration of CO2, J. Hazard. Mater. 112 (3) (2004) 193-205, https://doi.org/10.1016/j.jhazmat.2004.04.019.

[18]. Liang, C., Pan, B., Ma, Z., He, Z., Duan, Z. (2020). Utilization of CO2 curing to enhance the properties of recycled aggregate and prepared concrete: a review, Cem. Concr. Compos. 105, https://doi.org/10.1016/j.cemconcomp.2019.103446.

[19]. Fang, X., Xuan, D., Poon, C.S. (2017). Empirical modelling of CO2 uptake by recycled concrete aggregates under accelerated carbonation conditions, Mater. Struct. 50 (4) 200, https://doi.org/10.1617/s11527-017-1066-y

[20]. Pu, Y., Li, L., Wang, Q., Shi, X., Luan,C., Zhang, G., et al. (2021). Accelerated carbonation technology for enhanced treatment of recycled concrete aggregates: A state-of-the-art review, Constr. Build. Mater, 282, 122671. https://doi.org/10.1016/j.conbuildmat.2021.122671

[21]. Young, J.F. (1967), Humidity control in the laboratory using salt solutions-a review. J. Appl. Chem., 17: 241-245. https://doi.org/10.1002/jctb.5010170901

[22]. Zhan, B.J., Xuan, D.X., Poon, C.S., Shi, C.J. (2016). Effect of curing parameters on CO2 curing of concrete blocks containing recycled aggregates, Cem. Concr. Compos. 71 (2016) 122-130, https://doi.org/10.1016/j.cemconcomp.2016.05.002

[23]. Zhang, J., Shi, C., Li, Y., Pan, X., Poon, C.S., Xie, . (2015). Performance enhancement of recycled concrete aggregates through carbonation, J. Mater. Civ. Eng. 27 (11), 04015029, https://doi.org/10.1061/(ASCE)MT.1943-5533.0001296.

[24]. Kou, S.C., Zhan, B.., Poon, C.S. (2014). Use of a CO2 curing step to improve the properties of concrete prepared with recycled aggregates, Cem. Concr. Compos. 45, 22-28, https://doi.org/10.1016/j.cemconcomp.2013.09.008.

[25]. Luo, S., Wu, W., Wu, K. (2018). Effect of recycled coarse aggregates enhanced by CO2 on the mechanical properties of recycled aggregate concrete, IOP Conf.

Ser., Mater. Sci. Eng. 431 (8), 102006. https://doi.org/10.1088/1757-899x/431/10/102006

[26]. Luo, S., Ye, S., Xiao, J., Zheng, J., Zhu, Y. (2018). Carbonated recycled coarse aggregate and uniaxial compressive stress-strain relation of recycled aggregate concrete, Constr. Build. Mater. 188,956-965, https://doi.org/10.1016/j.conbuildmat.2018.08.159.

[27]. Hyvert, N., ASellier, A., Duprat, F., Rougeau, P., Francisco, P. (2010). Dependency of C-S–H carbonation rate on CO2 pressure to explain transition from accelerated tests to ambient carbonation, Cem. Concr. Res. 40 (11) (2010) 1582–1589, https://doi.org/10.1016/j.cemconres.2010.06.010.

[28]. Mo, L., Zhang, F., Deng, M., Panesar, D.K. (2016). Effectiveness of using CO2 pressure to enhance the carbonation of Portland cement-fly ash-MgO mortars, Cem. Concr. Compos. 70 (2016) 78–85, https://doi.org/10.1016/j.cemconcomp.2016.03.013

[29]. Lu, B., Shi, C., Cao, Z., Guo, J.M. (2019). Zheng, Effect of carbonated coarse recycled concrete aggregate on the properties and microstructure of recycled concrete, J. Clean Prod. 233, 421–428, https://doi.org/10.1016/j.jclepro.2019.05.350

[30]. Wang, J., Zhang, J., Cao, D., Dang, H., Ding, B. (2020). Comparison of recycled aggregate treatment methods on the performance for recycled concrete, Constr. Build. Mater. 234, https://doi.org/10.1016/j.conbuildmat.2019.117366

[31]. Hu, W., Zhang, D., Ftwi, E., Ellis, B.R., Li, V.C., (2023). Development of sustainable low carbon Engineered Cementitious Composites (ECC) with waste polyethylene fiber (WPE), sisal fiber and carbonation curing. Resour. Conserv. Recycl. 197, 107096. https://doi.org/10.1016/j.resconrec.2023.107096

[32]. American Concrete Institute. Committee 211. Recommended Practice for Selecting Proportions for Normal and Heavyweight Concrete. (ACI 211.1-91)" Reapproved. 1977; 2009.

[33]. Dinku A. (2002). Construction materials laboratory manual. Available from: https://www.scribd.com/document/367438254/Construction-Materials-LabratoryManual-by-Abebe-Dinku

[34]. Silva, B.A., Ferreira Pinto, A.P., Gomes, A., Candeias, A. (2021). Effects of natural and accelerated carbonation on the properties of lime-based materials. J. CO2 Util., 49, 101552. https://doi.org/10.1016/j.jcou.2021.101552

[35]. Li, L., Ziyabek, N., Jiang, Y., Xiao, J., Poon, C.H. (2023). Effect of carbonation duration on properties of recycled aggregate concrete. CSCM. 19, e02640. https://doi.org/10.1016/j.cscm.2023.e02640

[36]. Farahani, H.S., Zadeh, A.H., Hu, J., Hawkins, C.H., Kim, S., (2025). Carbonation reaction of recycled concrete aggregates (RCA): CO2 mass

consumption under various treatment conditions, Cleaner Materials, 15, 100296, https://doi.org/10.1016/j.clema.2025.100296

[37]. Zhan, B.J., Xuan, D.X., Zeng, W., Poon, C.S. (2019). Carbonation treatment of recycled concrete aggregate: Effect on transport properties and steel corrosion of recycled aggregate concrete, Cement and Concrete Composites, 104, 103360, https://doi.org/10.1016/j.cemconcomp.2019.103360

[38]. WU, J., DING, Y., XU, P., ZHANG, M., GUO, M., GUO, S. (2022). Effects of carbonated recycled concrete aggregates on the mechanical properties of concrete and the micro-properties of the interfacial transition zone. Ceram. Silik. 66 (1), 113-127. https://doi.org/10.13168/cs.2022.0006

[39]. Singh, M., Danie Roy, A. B., Waseem, S., Singh, H. (2020). Feasibility and performance analysis of carbonated recycled aggregate concrete. Int. J. Sustain. Eng., 14(4), 761–775. https://doi.org/10.1080/19397038.2020.1856967

[40]. Shen, P., Zhang, Y., Jiang, Y., Zhan,B., Lu, J., Zhang S., Poon, C.S. (2022). Phase assemblance evolution during wet carbonation of recycled concrete fines, Cem. Concr. Res. 154, 106733. https://doi.org/10.1016/j.cemconres.2022.106733

[41]. Sáez del Bosque, I.F., Van den Heede, P., De Belie, N., Sánchez de Rojas, M.I., Medina, C. (2020). Carbonation of concrete with construction and demolition waste based recycled aggregates and cement with recycled content. Constr. Build. Mater, 234,117336. https://doi.org/10.1016/j.conbuildmat.2019.117336.

[42]. Liu, X., Feng, P., Cai, Y., Yu, X., Yu, C., Ran, Q. (2022). Carbonation behavior of calcium silicate hydrate (C-S-H): Its potential for CO2 capture, Chem. Eng. J. 431, 134243. https://doi.org/10.1016/j.cej.2021.134243

[43]. Cizer, O., Rodriguez-Navarro, C., Ruiz-Agudo,E., Elsen, ., Van Gemert, D., Van Balen, K. (2012). Phase and morphology evolution of calcium carbonate precipitated by carbonation of hydrated lime, J. Mater. Sci. 47, 6151-6165. https://doi.org/10.1007/s10853-012-6535-7

[44]. Thomas, J., Thaickavil, N.N., Wilson P.M. (2018). Strength and Durability of Concrete Containing Recycled Concrete Aggregates. J. Build. Eng. 19, 349-365. https://doi.org/10.1016/j.jobe.2018.05.007

[45]. Ozbakkaloglu, T., Gholampour, A., Xie, T. (2017). Mechanical and Durability Properties of Recycled Aggregate Concrete: Effect of Recycled Aggregate Properties and Content. J. Mater. Civ. Eng. 30 (2), 4017275. https://doi.org/10.1061/%28ASCE%29MT.1943-5533.0002142

[46]. Xuan, D., Zhan, B., Poon, C.S. (2016). Assessment of Mechanical Properties of Concrete Incorporating Carbonated Recycled Concrete Aggregates. Cem. Concr. Compos. 65, 67-74. https://doi.org/10.1016/j.cemconcomp.2015.10.018

[47]. Tong, J., Ding, Y., Lv, X., Ning, W. (2023). Effect of carbonated recycled coarse aggregates on the mechanical properties of 3D printed recycled concrete. J. Build. Eng., 80,107959, https://doi.org/10.1016/j.jobe.2023.107959.

[48]. Hadjari, M., Marouf, H., Dahou, Z., Maherzi, W. (2025). Investigation of the Mechanical and Fracture Properties of Recycled Aggregate Concrete. Bldgs., 15(7), 1155. https://doi.org/10.3390/buildings15071155

CHAPTER 5

COMPRESSIVE STRENGTH PREDICTION OF CARBONATED RECYCLED AGGREGATE CONCRETE USING REGRESSION BASED MACHINE LEARNING MODELS

Original publication: “Gebremariam, H.G., Taye, S. & Tarekegn, A.G. Compressive strength prediction of carbonated recycled aggregate concrete using regression based machine learning models. Sci Rep 16, 5825 (2026). https://doi.org/10.1038/s41598-026-36197-8.”

5.1. Introduction

As already discussed in the previous sections in detail, concrete and other materials recycling coordinated with carbonation is increasingly recognized as a vital strategy in sustainable construction [1-13]. While the benefits of carbonated RAC are well established, traditional laboratory testing of its mechanical properties is labor intensive, costly, and time consuming [14]. These constraints hinder rapid mix optimization and large scale adoption. Predictive modeling offers a practical alternative by enabling accurate property estimation based on mix proportions, material properties, and carbonation parameters, thereby reducing the need for exhaustive experimental testing [15-17]. Classical regression techniques, such as multiple linear regression (MLR), Ridge regression and polynomial MLR, have been widely applied in predicting concrete strengths due to their interpretability and ability to quantify linear and simple nonlinear relationships [18-20]. However, these methods performs less when dealing with complex, nonlinear interactions.

Recent advances in deep ML and ensemble learning offer powerful tools for overcoming these limitations. Models such as Random Forest, Decision Tree, and LightGBM can capture nonlinearities, handle high dimensional data, and automatically identify important input features [21-24]. Optimization frameworks such as k-fold cross validation enable systematic hyper parameter tuning and Shapley Additive explanations (SHAP) for interpretability [25].

Despite the growing body of research on predictive modeling for conventional concrete and RAC, there is a notable gap. To the best of the authors' knowledge, no study to date has developed predictive models considering parameters like carbonation treatment and PC strength effects on the characteristics of RCAs and ARACs. Additionally, effects of multicollinearity and correlation between data sets on the predictive capacity of regression based and deep learning models are not explored. Furthermore, systematic comparisons between classical regression based ML models and new ensemble and deep learning based ML approaches for carbonated RCA remain unexplored.

The present study aims to fill these gaps by developing and evaluating predictive models for the compressive strength of carbonated RCA concrete. Composite indices for correlated data will be developed and a comparison of the ML data outputs using the individual dataset and aggregated datasets will be explored. Both classical regression based ML methods (MLR, Ridge and Polynomial MLR) and advanced ML techniques (Random Forest, Decision Tree, and LightGBM) are employed. These models have been selected due to their simplicity for justification, including their suitability for nonlinear material behavior prediction and their performance on relatively limited experimental datasets. Model performance is compared in terms of predictive accuracy, robustness, interpretability, and computational efficiency. The research further seeks to identify the most influential parameters governing carbonated RAC performance.

5.2. Methodology

5.2.1. Source of data

The data used for strength predictions in this study were obtained from an experimental program reported in a previous work by the present authors [26]. In that study, 108 concrete samples were tested for compressive strength. The datasets were categorized into five groups: (i) mix design proportioning of the target concrete, (ii) physical and mechanical properties of the coarse aggregates, (iii) PC strength effects on RCA carbonation degree, (iv) quantified CO_2 stored by carbonation (expressed as percent by mass of mortar attached to RCAs), and (v) percentage replacement of RAs with RCAs. The eight individual data sets from the 5 categories were, water to cement ratio (W/C), cement to Coarse aggregate ratio (C/C_a), cement to fine aggregate ratio (C/F_a), water absorption (W_a) of NA and RCA in percent, crushing value (C_v) of NA and RCAs in percent, PC strength (P_{cs}) of RCA, degree of carbonation (D_c) of RCA, and Replacement ratio (R_r) of NAs by RCAs. The descriptive statistics of these data sets and the output variable which is compressive strength (CS) are shown in table 5.1.

Table 5.1 Descriptive statistics of the predictor variables and target variable

Variable	Mean	St. Dev	Minimum	Maximum	Skewness	Kurtosis
C/C_a	0.3855	0.1251	0.2610	0.5100	-0.00	-2.04
C/Fa	0.7510	0.4179	0.3350	1.1670	-0.00	-2.04
W/C	0.4150	0.1557	0.2600	0.5700	0.00	-2.04
W_a (%)	3.629	1.096	2.250	5.910	0.82	-0.28
C_v (%)	22.952	4.073	18.010	30.710	0.76	-0.71
R_r (%)	57.89	38.83	1.00	100.00	0.05	-1.76
D_c (%)	4.141	3.500	0.100	11.930	1.06	0.25
P_{cs} (Mpa)	26.57	23.19	0.10	67.00	0.91	-0.58
CS (Mpa)	39.38	17.98	18.07	70.42	0.26	-1.63

5.2.2. Data validity and assumption checks prior to regression based machine learning modeling

Prior to modeling, a series of statistical validity checks were conducted to ensure that the predictor variables were accurately represented in the models and that the fundamental assumptions of multiple regression and data processing were reasonably met [27, 28]. The initial step involved was examining the pairwise correlations among the predictor variables as shown in figure 5.1. It was observed that C/C_a, W/C, and C/F_a exhibited high intercorrelation to each other. In addition, a strong correlation was found between W_a, C_v, R_r, and D_c suggesting a high degree of correlation in the information provided by these predictors.

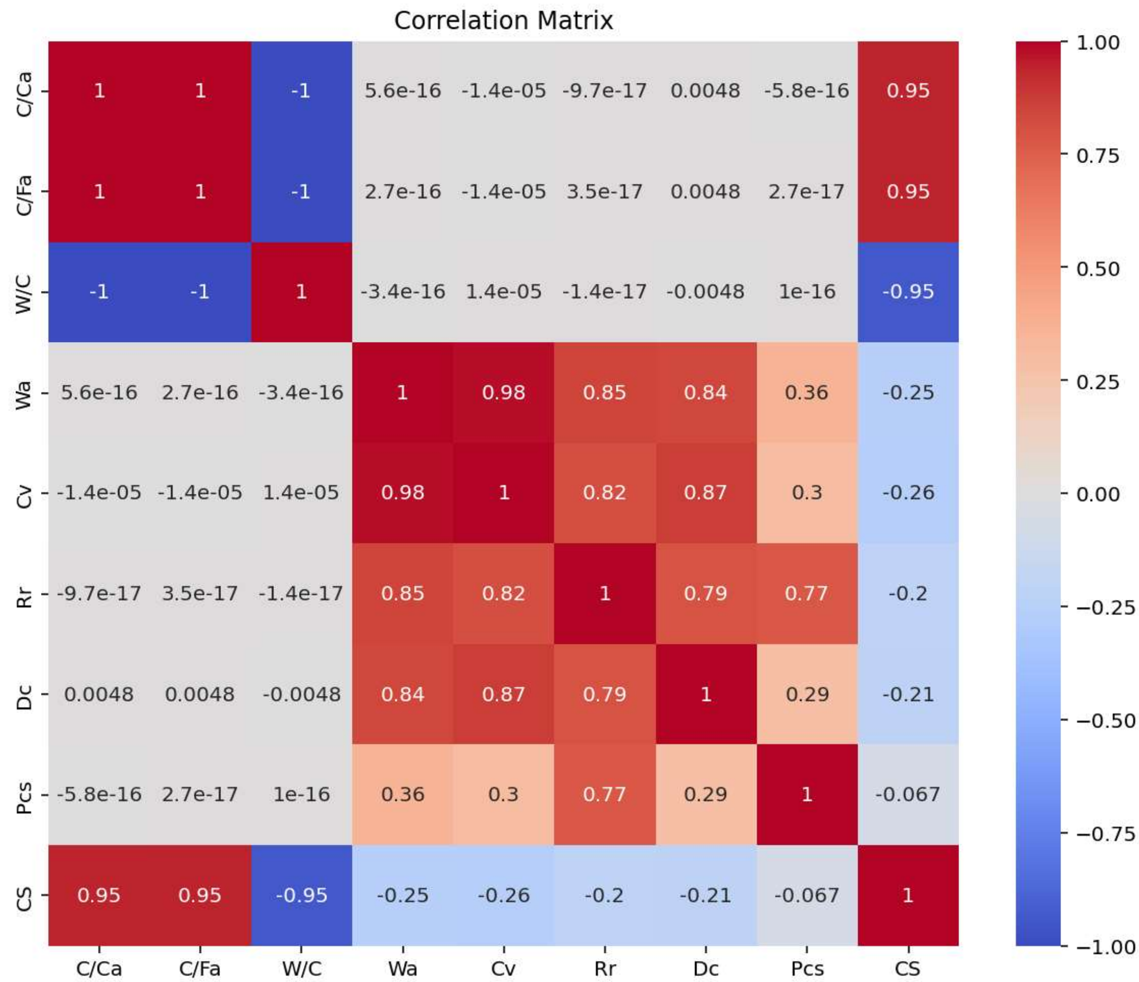

Figure 5.1 Pearson's correlation matrix between predictor variables before aggregation

The presence of such high correlations raised a substantial concern regarding multicollinearity, which was further confirmed through Variance Inflation Factor (VIF) analysis as shown in table 5.2 [29]. Extremely large VIF values (see table 5.2), were seen in the data sets, indicating multicollinearity and may lead to unstable coefficient estimates, inflate standard errors, and difficulties in determining the relative importance of individual predictors.

Table 5.2 Significance and multicollinearity between predictors before aggregation

Term	Constant	C/C_a	C/C_a	W/C	W_a (%)	C_v (%)	R_r (%)	D_c (%)	P_{cs} (Mpa)	CS (Mpa)
VIF	0.00E+00	inf	inf	Inf	4.46E+03	4.32E+02	4.35E+04	3.60E+03	1.31E+04	3.37E+01

To address this issue, a combined index approach was implemented as a countermeasure [29, 30]. This involved aggregating highly correlated variables into composite indices, thereby retaining the essential information they contribute while reducing the interdependence between predictors. In this study, two composite predictors were developed to address multicollinearity among highly correlated variables, while retaining the essential engineering significance of each constituent parameter. The composites were formulated based on essential physical and mechanical characteristics of aggregates (Performance Index) and the strength governing proportions of the mix (proportioning Index) in a compact and statistically sound form using multiplicative, divisive, and exponential relationships informed by domain knowledge and statistical optimization [30]. The composite indices were created for the proportioning variables (W/C, C/C_a and C/F_a), and aggregate performance indicators (W_a, C_v and P_{cs}). The new data set after aggregation were then became, replacement ratio (x_1), degree of carbonation (x_2), proportioning index (x_3) and performance index (x_4).

To perform the aggregation, domain knowledge was used to derive the proportioning index and performance indices. A statistical optimization was then applied to ensure that the correlation between predictors was reduced to below 0.8 and the VIF to below 5. This step was necessary to minimize instability and overfitting caused by multicollinearity. Based on these criteria, the new indices were fed into a machine learning model, which was used to learn and determine the optimized exponents:

$$x_1 = {R_r}^{a_1} \tag{5.1}$$

$$x_2 = {D_c}^{a_2} \tag{5.2}$$

$$x_3 = \frac{\left(C/C_a\right)^{a_3} \times \left(C/F_a\right)^{a_4}}{\left(W/C\right)^{a_5}} \tag{5.3}$$

$$x_4 = \left(\frac{P_{cs}{}^{a_6}}{\left(W_a{}^{a_7} \times C_v{}^{a_8}\right)}\right)^{a_9} \tag{5.4}$$

After optimization using ML the values of the exponents were obtained as follows:

a_1 = 1.911, a_2 = 0.103, a_3 = 1.165, a_4 = 0.801, a_5= 1.481, a_6= 1.053, a_7= 1.752, a_8= 0.986, a_9= 0.659. All correlation values and VIFs fell below their respective limits, as shown in Table 3 and Figure 2.

The proportioning index (x_3) reflects the balance between binder content, coarse and fine aggregate mass, and water dosage in the RAC mix. The product of the cement to coarse aggregate and cement to fine aggregate ratios represents the overall binder richness of the mix relative to the aggregate mass. Dividing by the water to cement ratio adjusts the index to account for water content, a critical determinant of workability and strength development. Physically, a higher proportion index value corresponds to mixes with greater binder content, generally associated with higher strength and reduced porosity. The index therefore encapsulates the combined influence of mix composition parameters in a single value, reducing collinearity between the original ratios while retaining their collective predictive power.

The performance index (x_4) integrated three critical aggregate characteristics into a single measure of aggregate quality. PC strength, in the numerator, reflects the intrinsic load bearing capacity of the original aggregate source. The denominator combines water absorption, representing pore structure, and aggregate crushing value, representing resistance to mechanical breakdown. The physical interpretation of this composite is straightforward where higher parent strength increases the index, while higher porosity or lower mechanical durability reduces it. Thus, the index expresses a net measure of aggregate performance. Statistically, combining these collinear parameters into one variable mitigates redundancy in regression modelling, ensuring VIF remain within acceptable limits while preserving the behavioral influence of each individual property. The exponents in each predictor are determined based on the statistical optimization that the data fulfils all the statistical checks (see (tables 5.3 and fig 5.2) before processing machine learning modeling.

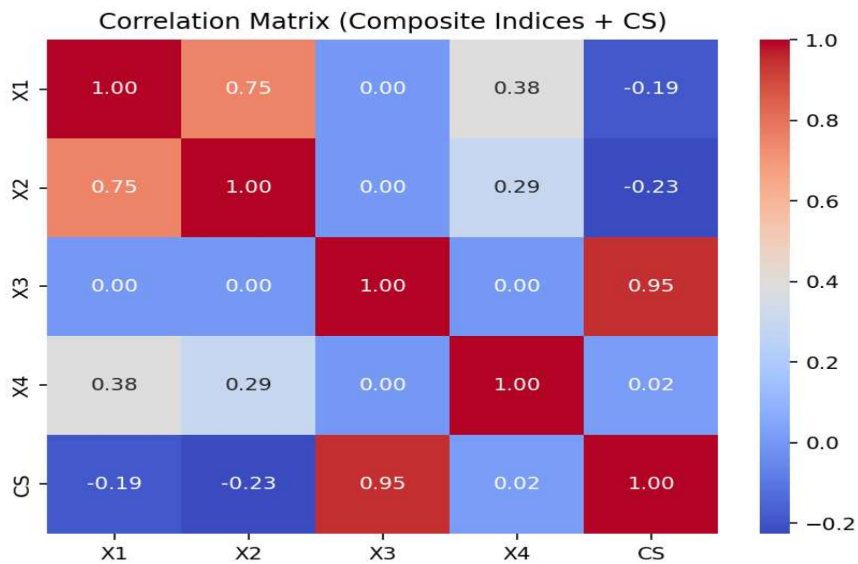

Figure 5.2 Pearson's correlation matrix after aggregation

Table 5.3 VIF after aggregation.

Feature	X1	X2	X3	X4
VIF	2.4911	2.3209	1.0001	1.1732

To prevent the composite indexes from becoming infinite, small insignificant values were assumed instead of using zero for the NAC. For replacement ratio, a value of 1% was used instead of 0%. For the degree of carbonation and PC effects, 0.1% was used. These small adjustments avoid division by zero while ensuring the composite indexes remain finite. Importantly, these assumed values do not affect the characteristics or behavior of the models being developed.

Following the construction of composite indices for highly correlated predictors, two separate modeling pathways were pursued. The aim of this stage was to determine whether the presence of intercorrelation among predictors influences the predictive performance of regression based ML models. In the first pathway, models were trained using the original dataset containing the individual predictors. In the second pathway, models were trained using the composite dataset, in which correlated predictors had been aggregated into indices. Both modeling pathways were implemented under identical conditions where the same data preprocessing steps, including training and testing partitioning, and algorithm settings were applied to ensure fair comparison. Model performance was assessed using standard regression evaluation metrics. Comparing the predictive outcomes of the two models, we can see if intercorrelation among predictors, has a significant effect on the models' accuracy and stability.

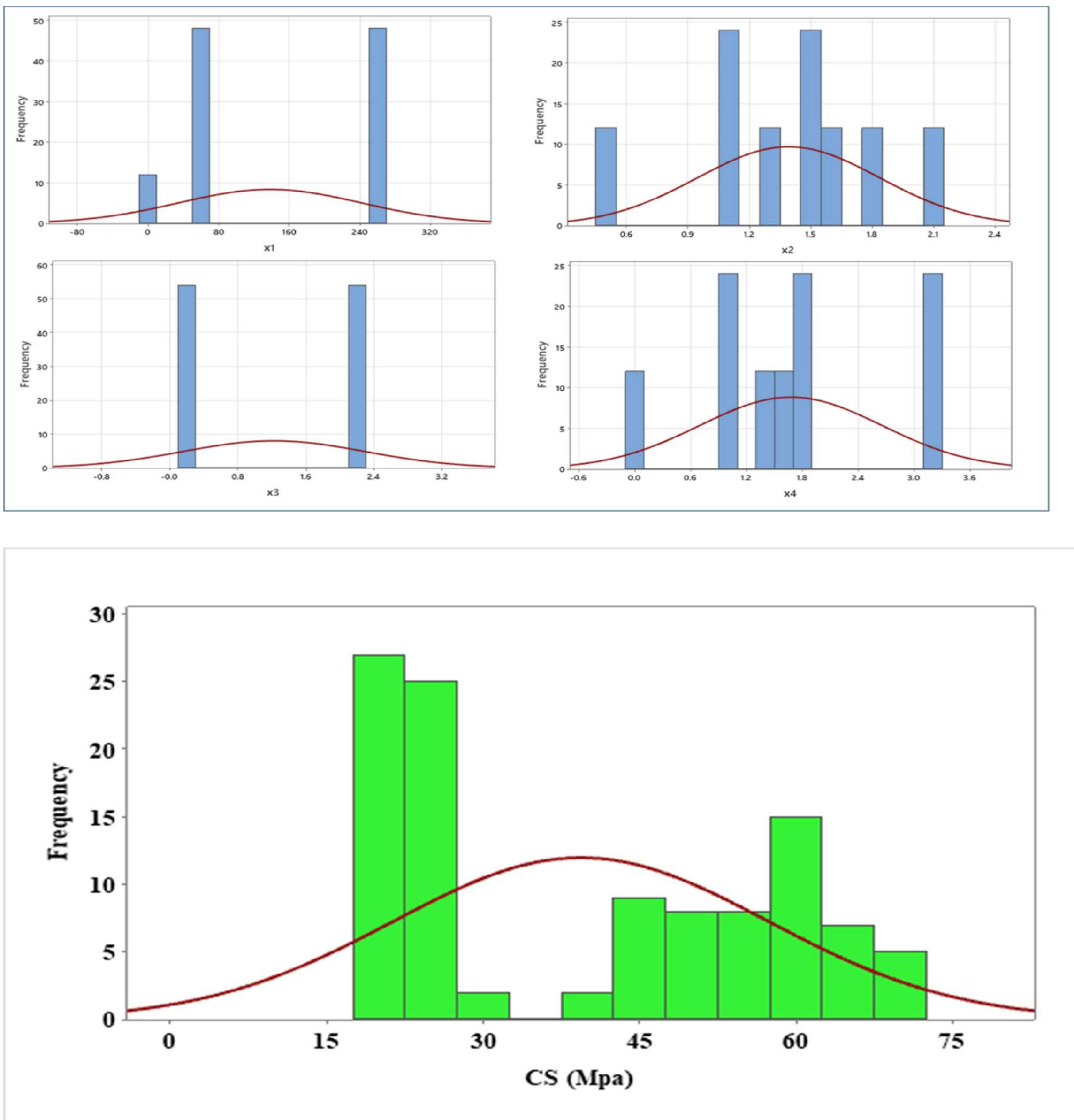

Figure 5.3 Frequency distribution of features after aggregation

5.2.3. Principles of the classical statistical models and deep learning algorisms

In numerical modeling, selecting the right regression approach depends not only on the nature of the data but also on the underlying assumptions about how features influence the target [31]. This section explores a spectrum of regression methods from classical statistical models to advanced machine learning architectures. Each technique is briefly outlined, focusing on its internal logic, typical use cases, and how it adapts to different data structures. Three classical regression-based algorism and three ensemble and deep learning-based algorisms were used in this study and these were, MLR, Ridge, ploy MLR, Random Forest, Decision Tree, and LightGBM.

5.2.3.1 Classical MLR models

A regression model provides a mathematical framework for describing how one variable of interest changes in relation to one or more influencing factors. If the model incorporates only a single predictor, it is termed a simple regression. But, when it includes two or more predictors, it becomes a multiple regression model. Such models are widely used to quantify the degree and nature of association between explanatory variables and the response, with the aim of revealing patterns and dependencies that might otherwise remain hidden [31].

In a simple regression scenario, the model seeks a single straight line that best represents the relationship between the dependent and independent variable across all observations. Multiple regression extends this principle to higher dimensions that, instead of fitting a line, it estimates a hyperplane that best represents the combined effect of several predictors. While the inclusion of multiple variables increases analytical complexity, it also allows for richer interpretations, including the possibility that the influence of one predictor may vary depending on the level of another. These dependencies may manifest as linear trends, curvature, or conditional effects [32].

The general structure of MLR model can be expressed as:

$$y = b_0 + \sum_{j=1}^{n} b_j x_j \tag{5.5}$$

b_0 is the intercept, and b_j are the partial regression coefficients reflecting the marginal contribution of each predictor. The coefficients are typically estimated using the least squares method, which minimizes the sum of squared differences between observed and predicted values [32]. Ridge regression is a type of regularized linear regression that helps prevent overfitting by adding a penalty on the size of the model coefficients.

Polynomial regression builds on the MLR framework by introducing higher order and interaction terms, enabling the model to capture curved relationships without discarding the linear estimation approach. This enhancement increases the model's flexibility in fitting data that exhibit nonlinear patterns. However, the inclusion of many polynomial terms also increases the likelihood of overfitting, particularly when the number of predictors or polynomial degree is high. Nevertheless, for datasets with relatively smooth curvature, polynomial MLR can yield highly accurate and interpretable fits. The polynomial MLR equation of degree two is expressed as:

$$y = b_0 + \sum_{j=1}^{n} b_j x_j + \sum_{j=1}^{n} b_{jj} {x_j}^2 + \sum_{1\le i\le j\le n} b_{ij} x_i x_j \tag{5.6}$$

Where b_{jj}, denotes coefficients for the squared terms of each predictor, and b_{ij}, corresponds to coefficients for interaction terms between predictors.

5.2.3.2 Tree based learning algorisms

a. Decision Tree

The algorithm works by recursively splitting the dataset based on feature values that provides the best discriminatory power, resulting in a tree like structure [33]. Each internal node represents a decision based on the input feature, and the leaves represent the specific classification outcome or value of the tested attribute. The tree is constructed using a greedy approach, selecting the best feature to split the data at each step [34]. Decision Trees partition the feature space into regions using recursive binary splits. For input x, prediction is the average of target values in the corresponding region:

$$y(x) = \sum_{n=1}^{n} c_n \, 1(x \in R_n) \tag{5.7}$$

Where, R_n are regions (leaf nodes), C_n is the mean response in R_n, and $1(x \in R_n)$ is the indicator function. Splits are chosen to minimize impurity measures.

b. Random Forest

Random Forest, an ensemble learning technique, builds multiple decision trees and aggregates their results to improve predictive performance and reduce overfitting [33, 35]. Each tree in the forest is trained on a random subset of the data, and predictions of each are combined through majority voting to produce the final classification. The Random Forest model was used to compare its performance to the Decision Tree, with expectations of improved accuracy and reduced variance. This method is often preferred in situations where robustness and generalization are important [33]. Random Forest's average predictions are generated from many decision trees built on bootstrapped data samples and random feature subsets [36, 37]:

$$y(x) = \frac{1}{T}\sum_{t=1}^{T} y_t(x) \tag{5.8}$$

Where, $y_t(x)$ is the prediction of the t^{th} tree and T is the total number of trees. This reduces variance and overfitting compared to a single decision tree [37, 39].

c. LightGBM

LightGBM is a gradient boosting framework that builds decision trees sequentially, each one correcting errors of the previous. It uses advanced optimizations such as leaf wise tree growth, gradient based one side sampling, and exclusive feature bundling, making it highly efficient for large scale tabular data [38]. LightGBM achieves better performance on many tabular tasks, handling complex nonlinear relationships with minimal manual feature engineering. Interpretability is moderate, with tools like SHAP often needed to explain predictions. Overfitting is possible, but well controlled with parameters like tree depth, learning rate, and regularization. It is highly scalable and computationally efficient, though essentially a black box model. The model results are found by adding the prediction of all the ensemble trees (Equation 5.9), where $f_n(x)$ indicates the prediction from the n^{th} individual tree [38, 39].

$$y_{(x)} = \sum_{1}^{n} f_n(x) \tag{5.9}$$

During the training and testing of the models; in the MLR model, Ordinary Least Squares estimation was applied directly to the original feature set. In the Polynomial MLR, nonlinear feature interactions were introduced through a second degree polynomial expansion (excluding the bias term), followed by linear regression. The Random Forest model was implemented as an ensemble of 100 decision trees (n-estimators = 100) with fixed randomization to ensure reproducibility. For LightGBM, a gradient boosting based ensemble approach was employed with default parameters and a fixed random seed. All models were trained independently within each fold, using only the corresponding training subset, with hyperparameters fixed to ensure fair and consistent comparisons.

5.2.3.3 Cross validation strategy

Model evaluation employed fivefold cross validation to ensure robust performance assessment and minimize bias due to data partitioning. The dataset was randomly shuffled prior to splitting, with a fixed seed (random state = 42) to maintain reproducibility. Each fold consisted of mutually exclusive training (80%) and testing (20%).

5.2.3.4 Quantitative performance metrics

To provide a comprehensive evaluation of predictive accuracy and robustness, multiple statistical metrics were computed for both training and testing sets:

Coefficient of determination (R^2) was applied to assess explanatory power, with adjustment for the number of predictors. Root Mean Square Error (RMSE) used to measure prediction error in absolute terms. While Mean Absolute Error (MAE) used to determine average magnitude of error. The expected values for the indice R^2 should ideally be 1, indicating good prediction level, while RMSE, and MAE should ideally be 0, indicating less errors in the predictions. In general, a predictive model is ideal if its performance indices are close to or strictly at these values [40]. The equations for calculating these indices are presented in Eqs. (5.10-5.12) as follows [40, 41]:

$$R^2 = 1 - \frac{\sum_{n=1}^{n}(y_i - \hat{y})^2}{\sum_{n=1}^{n}(y_i - \bar{y})^2} \tag{5.10}$$

Where, y_i are observed value, $\hat{y}$ are predicted value and $\bar{y}$ are mean of observed value.

$$RMSE = \sqrt{\frac{1}{n}\sum_{n=1}^{n}(y_i - \hat{y})^2} \tag{5.11}$$

$$MAE = \frac{1}{n}\sum_{n=1}^{n}|y_i - \hat{y}| \tag{5.12}$$

5.2.3.5 Visual performance metrics

When evaluating models, visual checks are extremely useful because they make complex statistics easier to understand at a glance [40]. To complement the numerical evaluation of model performance, visual diagnostic techniques were applied. These techniques were, scatter plots, residual plots, histograms of residuals, and quantile-quantile (Q-Q) plots. Scatter plots, in which predicted values were plotted against the observed data, provided an overview of how closely the model output followed the actual trend. Ideally, points cluster around the line, and noticeable departures from this line highlight areas of reduced reliability. Residual plots offered further insight by presenting the distribution of prediction errors. Systematic patterns, such as consistent underestimation or overestimation in certain ranges or increasing error spread with larger values, were examined to identify potential weaknesses in the models.

Histograms of the residuals were used to evaluate the overall error distribution. A distribution centered near zero with a roughly symmetric shape indicates unbiased predictions, while skewed or shifted distributions suggest bias. In addition, Q-Q plots were generated to compare the residuals with a theoretical normal distribution for the test dataset. Alignment of points along the diagonal indicated that the normality assumption was reasonable, whereas systematic deviations reflected no normal error structures.

5.2.3.6. Feature importance analysis

To investigate the sensitivity of machine learning models and to interpret their behavior at both broad and granular levels, the SHAP framework, grounded in cooperative game theory principles, was applied [42]. This method was used to evaluate the relative contribution of each input variable to the model's predictions. As a sophisticated tool within explainable artificial intelligence, SHAP provides a transparent view of how input features interact and influence the output. By quantifying feature impacts, it highlights which variables play the most significant roles in shaping predictions and clarifies the direction and magnitude of their effects on the model's results [40, 43].

5.2.3.7. Pipeline and scientific libraries

The experimental pipeline was implemented in Python 3.10 with a notebook of Spider version 6, using Scikit-learn, LightGBM, and supporting scientific libraries.

5.3. Result and discussion

5.3.1 Data correlation effects on model performance

The outputs from different machine learning modeling approaches showed that the predictions using the individual datasets and composite indices on the MLR based models have shown some differences. But in the tree based models there have not shown tangible differences. Figures 5.4 shows the effects of data type on the residual compressive strength outputs of different ML. The residual are scattered following the same line on the tree based models for both datasets but some deviations are seen on MLR, Ridge regression and Poly MLR. It is shown that the individual data performed well on these models.

The quantitative matrices comparisons between models trained on individual predictors and those using composite indices are shown on table 5.4 and table 5.5. With the composite predictors, MLR, Ridge regression and Poly MLR achieved fair accuracy with test R^2 of 0.965, 0.967 and 0.983 respectively. Similarly with the individual predictors they achieved a test R^2 values of 0.975, 0.975 and 0.991 respectively. Decision Tree, Random Forest and LightGBM models all achieved very high predictive performance (test R^2 >0.991) under both datasets, with minimal train-test differences. Overall, the results indicate that predictor intercorrelation is a minimal concern for classical linear models, where it can contribute to overfitting and unstable parameter estimates. For more advanced models, particularly ensemble tree methods, multicollinearity had little to no effect, as they inherently manage redundancy among predictors. This suggests that while composite indexing can improve the stability of simpler models such as MLR, modern ML algorithms can reliably predict concrete compressive strength even in the presence of highly correlated predictors. Nonetheless, the composite indices continue to demonstrate substantial value by greatly simplifying model variables. Equations. (5.15) and (5.16) reveal that prediction equations from classical models, especially polynomial MLR models are often long. Using composite indices, as shown in Equations. (5.13) and (5.14), has reduce this complexity. The indices condensed multiple variables into single, coherent metrics, making the models far more manageable and actionable.

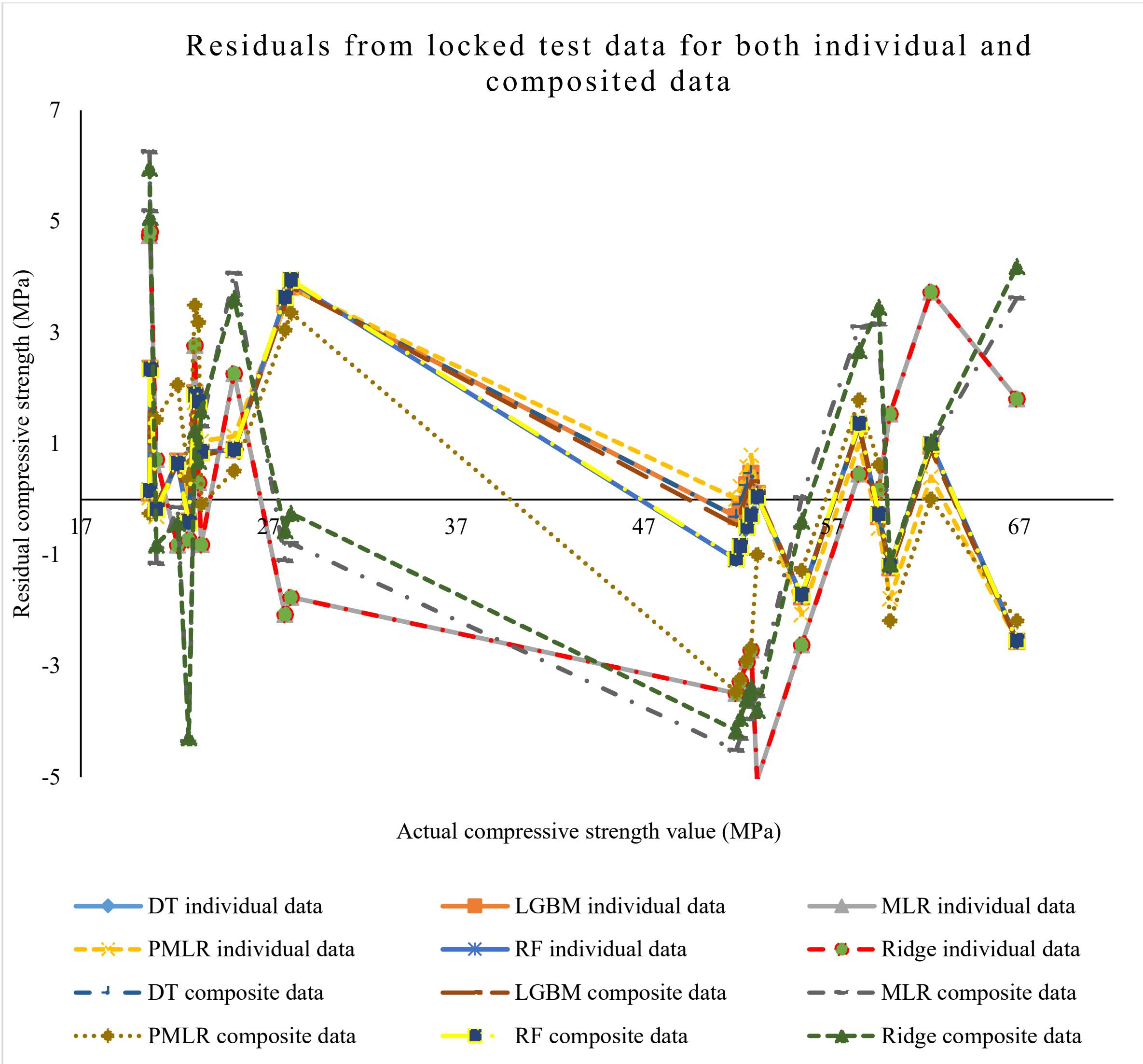

Figure 5.4 Model output comparisons between individual and aggregated data for locked test datasets.

Where, DT is decision tree, PMLR is polynomial MLR, LGBM is lightGBM, RF is random forest.

$$MLR\ CS_{Agg,} = 48.150 - 0.00048x_1 - 26.935x_2 + 9.525x_3 + 13.573x_4 \quad (5.13)$$

Where MLR $CS_{Agg.}$, is the compressive strength prediction equation derived from multilinear regression based machine learning and aggregated composite predictors.

$$poly\ MLR\ CS_{Agg.} = 6435.953 + 1.417x_1 - 12271.462x_2 + 1.2448x_3 - 5030.874x_4 - 0.000144x_1{}^2 - 0.294x_1x_2 - 0.000018x_1x_3 - 0.110x_1x_4 + 5275.472x_2{}^2 - 11.267x_2x_3 + 4889.829x_2x_4 + 4.975x_3{}^2 + 4.125x_3x_4 - 174.564x_4{}^2$$
(5.14)

Where, poly MLR $CS_{Agg.}$, is the compressive strength prediction equation derived from polynomial multilinear regression based machine learning and aggregated composite predictors.

$$MLR\ CS_{indv.} = 374.051 + 10.277\frac{C}{C_a} + 34.339\frac{C}{F_a} - 12.794\frac{W}{C} - 91.591W_a - 8.310C_v + 8.076R_r - 25.664D_c - 7.424P_{cs} \quad (5.15)$$

Where MLR $CS_{Indv.}$, is the compressive strength prediction equation derived from multilinear regression based machine learning with individual predictor data sets.

$$Poly\ MLR\ CS_{Indv.} == 792224.051 - 170.639\frac{C}{C_a} - 570.167\frac{C}{F_a} + 212.442\frac{W}{C} - 1425.529W_a - 187.573C_v - 1523.173R_r - 529.283D_c - 1756.424P_{cs} - 131.562(\frac{C}{C_a})^2 - 347.949\frac{C}{C_a}\frac{C}{F_a} + 11.081\frac{C}{C_a}\frac{W}{C} - 138.582\frac{C}{C_a}W_a - 28.542\frac{C}{C_a}C_V - 337.069\frac{C}{C_a}R_r - 67.744\frac{C}{C_a}D_c - 359.610\frac{C}{C_a}P_{cs} - 856.391\left(\frac{C}{F_a}\right)^2 - 77.075\frac{C}{F_a}\frac{W}{C} + 302.591\frac{C}{C_a}W_a + 5.373\frac{C}{F_a}C_v - 308.182\frac{C}{F_a}R_r + 57.918\frac{C}{F_a}D_c - 258.222\frac{C}{F_a}P_{CS} + 176.327(\frac{W}{C})^2 - 1103.230\frac{W}{C}W_a - 132.331\frac{W}{C}C_v - 943.503\frac{W}{C}R_r - 389.336\frac{W}{C}D_c - 1124.185\frac{W}{C}P_{cs} - 5794.084W_a{}^2 - 23828.927W_aC_v + 9449.029W_aR_r + 425.264W_aD_c + 2064.348W_aP_{cs} + 581.360C_v{}^2 + 1165.162C_vR_r - 6957.866C_vD_c - 2097.720C_vP_{cs} - 555.217R_r{}^2 + 3997.994R_rD_c + 355.644R_rP_{cs} + 444.873D_c{}^2 - 7790.791D_cP_{cs} + 526.695P_{cs}{}^2 \quad (5.16)$$

Where, poly MLR CS_{Indv}, is the compressive strength prediction equation derived from polynomial multilinear regression based machine learning with individual predictor data sets.

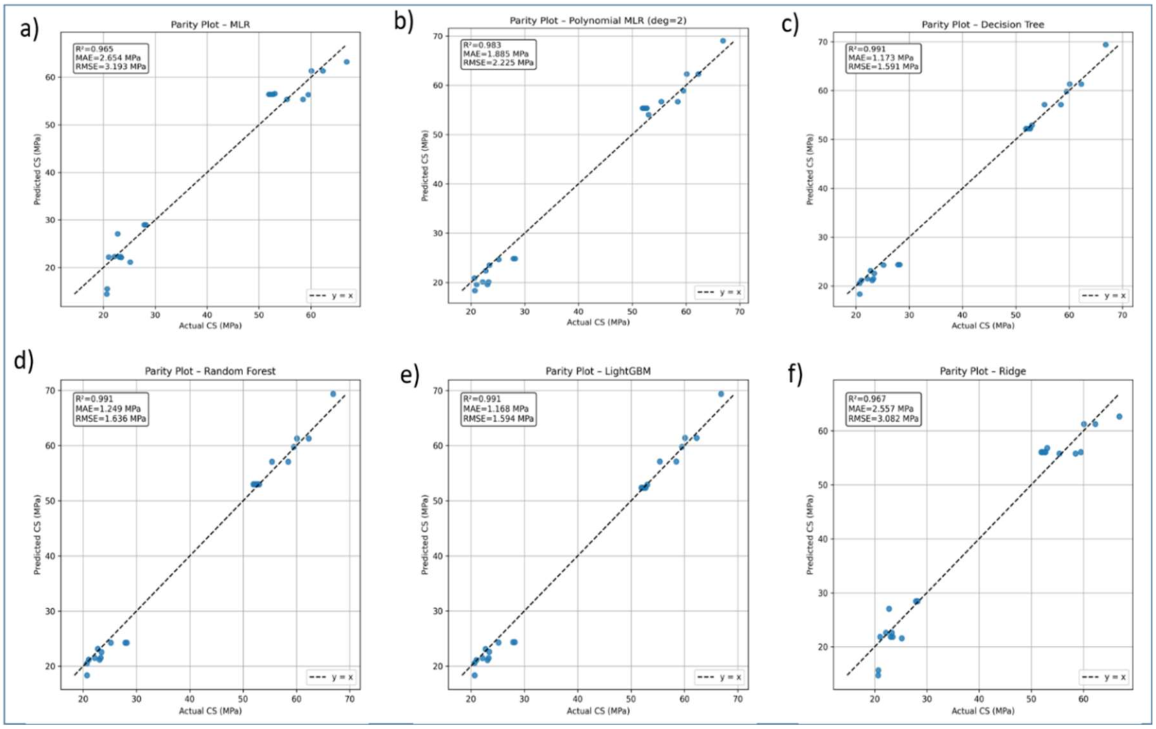

Figure 5.5 Relationship between actual experimental compressive strength and predicted values in multiple models.

5.3.2 Model performance comparisons

The series of plots comparing actual versus predicted compressive strength values for different models are shown on Figure 5.5 revealing distinct performance patterns across the methods. MLR, Ridge and Polynomial MLR (Figure 5.5, a, b and f) has shown reasonably good agreement between predicted and actual values. The points are largely clustered around the ideal 45° line, indicating that these models capture the general trend of the data. The polynomial MLR improves alignment for some values, suggesting that introducing a nonlinear term helps capture some curvature in the relationship. However, deviations at some values indicate some residual bias that these classical regression models may not fully capture [44-47].

Decision Tree, Random Forest (Figure 5.5, c, d and e) has demonstrated improved prediction accuracy over classical regression models. Decision Tree models already provide a better fit compared to MLR for nonlinear patterns, while Random Forest further enhance predictive performance by averaging multiple trees, reducing overfitting, and capturing complex interactions. The clustering of points near the ideal line in (Figure 5.5, c, d and e) confirms their robustness across test datasets. These models effectively manage the nonlinearity and heteroscedasticity in the data [46-48].

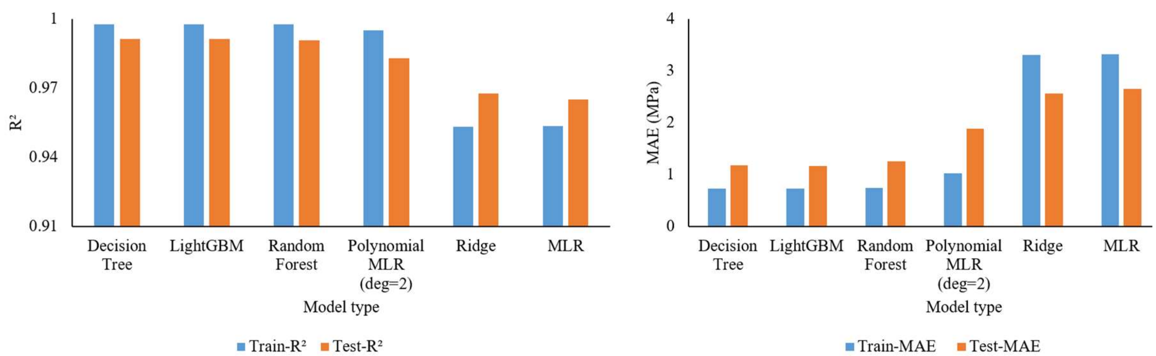

Figure 5.6 Models performance comparisons using adjusted R^2 and MAE.

The figural representations of the quantitative performance metrics (R^2 and MAE) and visual performance metrics (Q-Q plots and residual histograms) of the regression based ML models are shown on Figures 5.6, 5.7 and 5.8, as well as all quantitative performance metrics scores of these models are shown on table 5.4 for aggregated datasets and Table 5.5 for individual data sets. These results provides valuable insights into the predictive performance of the various ML models on the given dataset. The evaluation of the qualitative performance metrics R^2, MAE and RMSE for training and testing datasets, as well as an analysis of the visual performance metrics like the distribution of the models' residuals, revealed a clear hierarchy of model effectiveness, with nonlinear, tree based models outperforming traditional linear and polynomial regression methods. As shown in the performance metrics, the Decision Tree, Random Forest and LightGBM models demonstrated superior predictive accuracy and stability. Both models achieved the best qualitative metrics values on the test set, indicating that they were most effective at capturing the underlying patterns in the data and minimizing prediction error. The small discrepancy between their training and testing scores suggests strong generalization capabilities, indicating that these models are not overfitting the training data. This performance is consistent with the nature of these models, which are well suited to handle complex, nonlinear relationships and intricate feature interactions that linear models cannot. Many studies have compared different models for better performances based on their data types [49, 50].

Further evidence of the models' performance can be found by examining the distribution of their residuals using Q-Q plots and residual histograms. The histograms visually represent the frequency of different residual values, while the Q-Q plots compare the quantiles of the residuals to the quantiles of a theoretical normal distribution. For a well fitting model, both plots should demonstrate a bell shaped curve and a close alignment with the diagonal line, respectively [51].

The residual histograms for the Decision Tree, Random forest and LightGBM models show a fair distribution that is close to a bell shaped curve, with residuals centered around zero. This is a strong indication that these models are fairly capturing the systematic relationships in the data. The corresponding Q-Q plots for these models show that their residuals are close to a normal distribution, confirming that their predictions are both accurate and reliable.

Conversely, the MLR, Ridge regression models yielded the weakest performance, with the lowest test R^2 (0.965) and the highest MAE (2.65). This indicates that the relationship between the predictors and the target variable is likely not linear, and that a simple linear model is unable to model the data as accurate as tree based models. The residual histogram for the Linear MLR models is noticeably less centered and shows a wider spread, indicating less prediction capability compared to other models. An improvement in performance observed in the Polynomial MLR model which achieved a better qualitative performance than the standard MLR further supports the conclusion that nonlinear relationships are a key characteristic of this dataset. However, its residual histogram, while better than the standard MLR, is still not as well formed as the tree based models' histograms, suggesting that even with polynomial terms, a linear based model struggles to fully capture the data's structure.

Table 5.4 Quantitative performance indicators of models using aggregated data

Final test results (Aggregated composite data)												
Model	Training						Testing					
	MAE	RMSE	R2	95^{th} percentile error	99th percentile error	Max_error	MAE	RMSE	R2	95^{th} percentile error	99th percentile error	Max_error
Decision Tree	0.7276	0.9032	0.9975	1.7733	2.1496	2.3283	1.1732	1.5914	0.9913	3.4575	3.7499	3.8150
LightGBM	0.7247	0.9041	0.9975	1.8207	2.1463	2.2699	1.1683	1.5941	0.9913	3.4623	3.7551	3.8202
Random Forest	0.7349	0.9115	0.9975	1.7680	2.0993	2.3577	1.2493	1.6363	0.9908	3.5792	3.8788	3.9439
Polynomial MLR (deg=2)	1.0225	1.2883	0.9949	2.3979	2.9620	3.6508	1.8854	2.2251	0.9830	3.4555	3.4822	3.4879
Ridge	3.3034	3.9182	0.9531	7.1056	7.8891	8.6654	2.5568	3.0824	0.9675	5.0352	5.7710	5.9561
MLR	3.3152	3.9067	0.9534	6.8441	7.5090	8.5545	2.6536	3.1926	0.9651	5.1591	6.0281	6.2501

Analysis of average residuals for each model also showed that the poly MLR, Decision Tree, Random Forest and LightGBM models all demonstrated strong performance on the testing data, outperforming the standard linear MLR models.

Table 5.5 Quantitative performance indicators of models using individual data

Final test results (Individual data)

Model	Training						Testing					
	MAE	RMSE	R2	95^{th} percentile error	99th percentile error	Max_error	MAE	RMSE	R2	95^{th} percentile error	99th percentile error	Max_error
Decision Tree	0.7276	0.9032	0.9975	1.7733	2.1495	2.3283	1.1732	1.5914	0.9913	3.4574	3.7499	3.8150
LightGBM	0.7276	0.9032	0.9975	1.7733	2.1495	2.3283	1.1733	1.5914	0.9913	3.4578	3.7503	3.8154
Polynomial MLR (deg=2)	0.7439	0.9505	0.9972	1.9631	2.1576	2.3507	1.2056	1.6245	0.9910	3.4574	3.7499	3.8150
Random Forest	0.7364	0.9117	0.9975	1.7680	2.0993	2.3577	1.2497	1.6322	0.9909	3.5530	3.8513	3.9164
Ridge	2.6039	3.1980	0.9688	5.8326	6.3379	6.5610	2.2520	2.6890	0.9752	4.8088	4.9973	5.0464
MLR	2.6039	3.1980	0.9688	5.8326	6.3379	6.5611	2.2520	2.6890	0.9752	4.8087	4.9973	5.0465

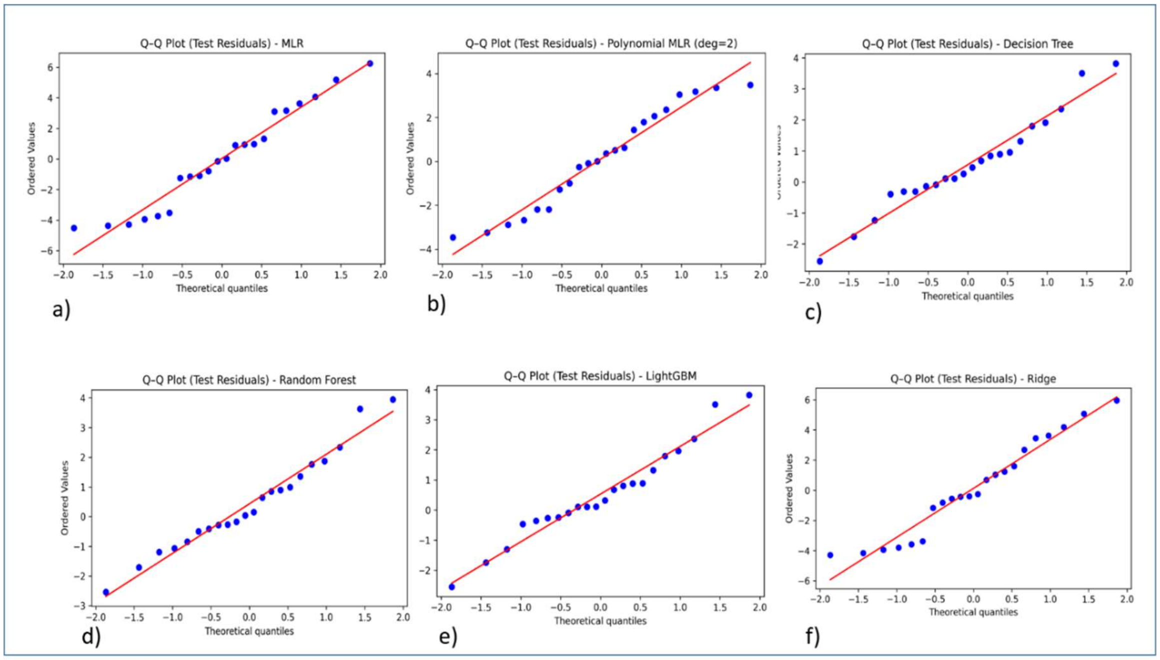

Figure 5.7 Q-Q plot of the test residuals of the models

The simple multilinear models exhibited an average locked test residual values of not less than 2.56 Mpa on the individual data and 2.65 Mpa on composite data. The scatter plots further confirm this performance, as the predictions from the MLR models show a wide deviation of up to 6.3 MPa, falling within a ±30% maximum error range from the actual experimental data. In contrast, the poly MLR model, which added complexity, achieved a lower testing average residual of 1.21 Mpa on the individual data and 1.88 Mpa on the composite data, showing its superior ability to generalize to new, unseen data. This model's better ability to generalize is further supported by its scatter plot analysis, which shows a significantly more accurate prediction with only a ±15% maximum error range.

Similarly, the Decision Tree, Random Forest and LightGBM models also performed well on the test set. The Decision Tree Random forest and LightGBM models testing average residuals were 1.17 Mpa, 1.25 MPa and 1.17 MPa, respectively, on both the individual and composited datasets. The scatter plots for Decision Tree, Random Forest and LightGBM models reinforce their accuracy, with both showing a tight error range of ±13% from the experimental data.

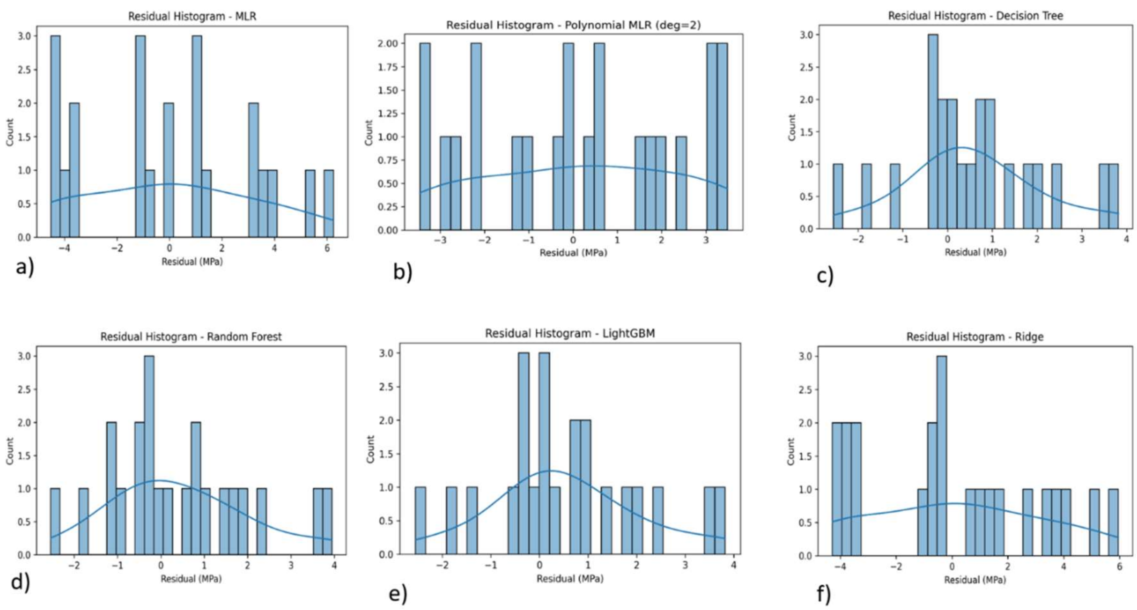

Figure 5.8 Histogram of residual of the prediction models

5.3.3. Sensitivity analysis

This section examines the SHAP summary plots of the individual predictors (C/C_a, C/F_a, W/C, W_a, C_v, D_c, P_{cs} and R_r) as can be seen on Figure 5.9 and the composite induced predictors (x_1, x_2, x_3 and x_4) as can be seen on Figure 5.10, to evaluate the influence of predictor variables on a machine learning model for concrete compressive strength [52]. SHAP values on the horizontal axis indicate each feature's contribution to model predictions were positive values enhance the output, and negative values reduce it. Data point colors reflect feature magnitude, with red for high values and blue for low values [14]. The analysis shows that all predictors impact the model, though to varying degrees. The most influential variables are the cement and water related ratios (W/C, C/C_a and C/F_a), forming a composite index x_3. High C/C_a and C/F_a ratios combined with low W/C strongly increase predicted compressive strength, consistent with standard mix design principles.

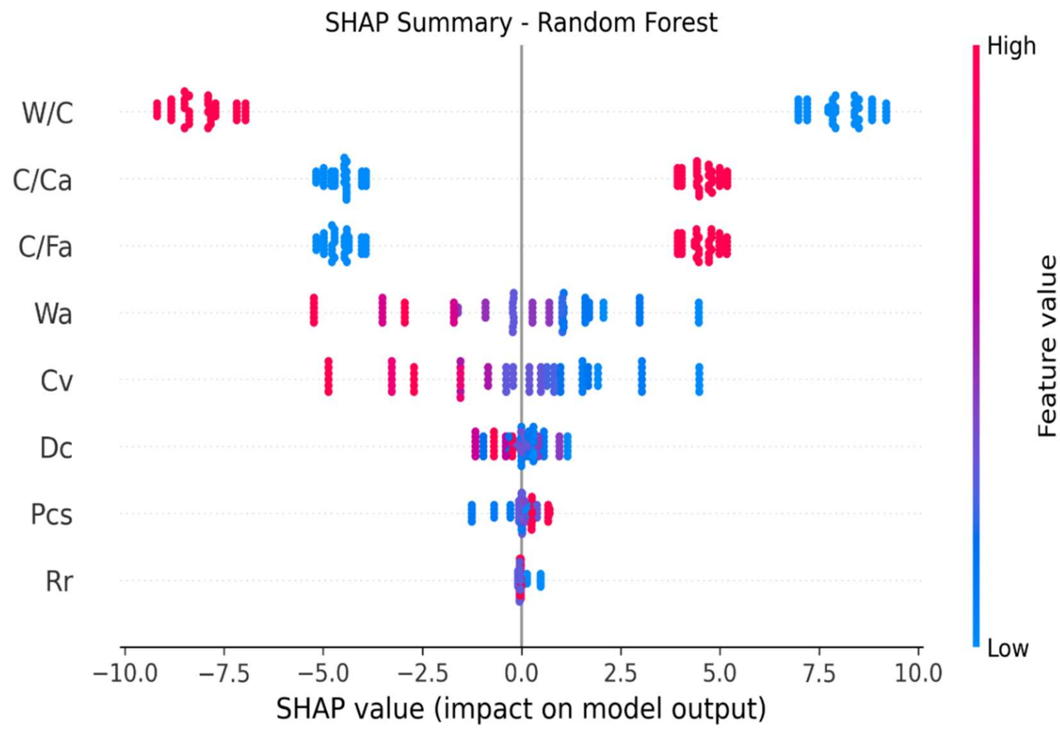

Figure 5.9 Random forest's SHAP analysis report of the individual predictors

The degree of carbonation ranks second in importance. Its effect looks complex and nonlinear, with both high and low values producing substantial positive and negative contributions. This was due to the incomplete carbonation of the high PC aggregates. The percentage of the carbonation byproducts in low strength PC aggregates were higher compared to aggregates sourced from high strength PC. But conversely, even though the amount of carbonation by products were less in the high strength PC aggregates, the resultant compressive strength of the concrete produced from these aggregates was higher compared to the aggregates produced from low strength PC. This behavior introduced the nonlinear behavior in the SHAP. Composite index x_4, encompassing (W_a and C_v along with P_{cs}), shows moderate influence. Individually these factors were impactful. However, collectively they exert less effect than the mix proportioning index variables and carbonation. The replacement ratio of NA with RCA (R_r, composite index x_1) has the least impact, with SHAP values clustered near zero. This insight can guide optimized concrete mix design for enhanced performance.

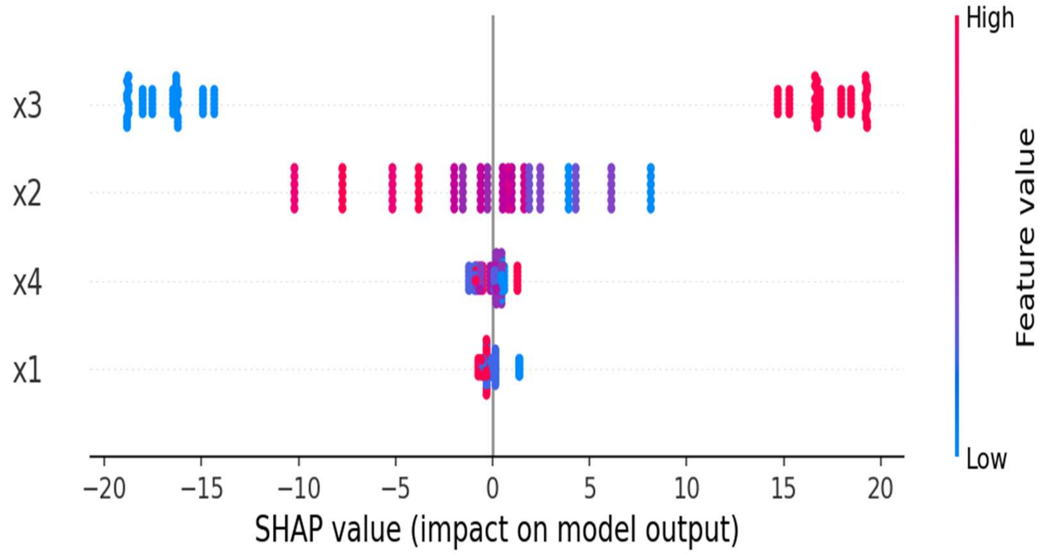

Figure 5.10 Random forest's SHAP analysis report of the aggregated predictors

Additionally, SHAP dependence plots were used to examine the marginal effects of the key input variables on the Random Forest predictions of compressive strength. Figure 5. 11 shows the dependence plots between variables x_1, x_2 and x_3. The variable x_1 showed SHAP values clustered near zero across its entire range, indicating that it contributed minimally to the model's predictions. In contrast, x_2 exhibited both positive and negative SHAP values (approximately -10 to +9 MPa), demonstrating a meaningful and nonlinear influence on compressive strength. Higher values of x_2 generally corresponded to positive SHAP contributions, while lower values were associated with reduced predicted strength. Among the evaluated predictors, x_3 displayed the strongest and most consistent effect, with SHAP values ranging from approximately -20 MPa at low x_3 levels to +20 MPa at higher levels. This indicates that increasing x_3 substantially increases the predicted compressive strength.

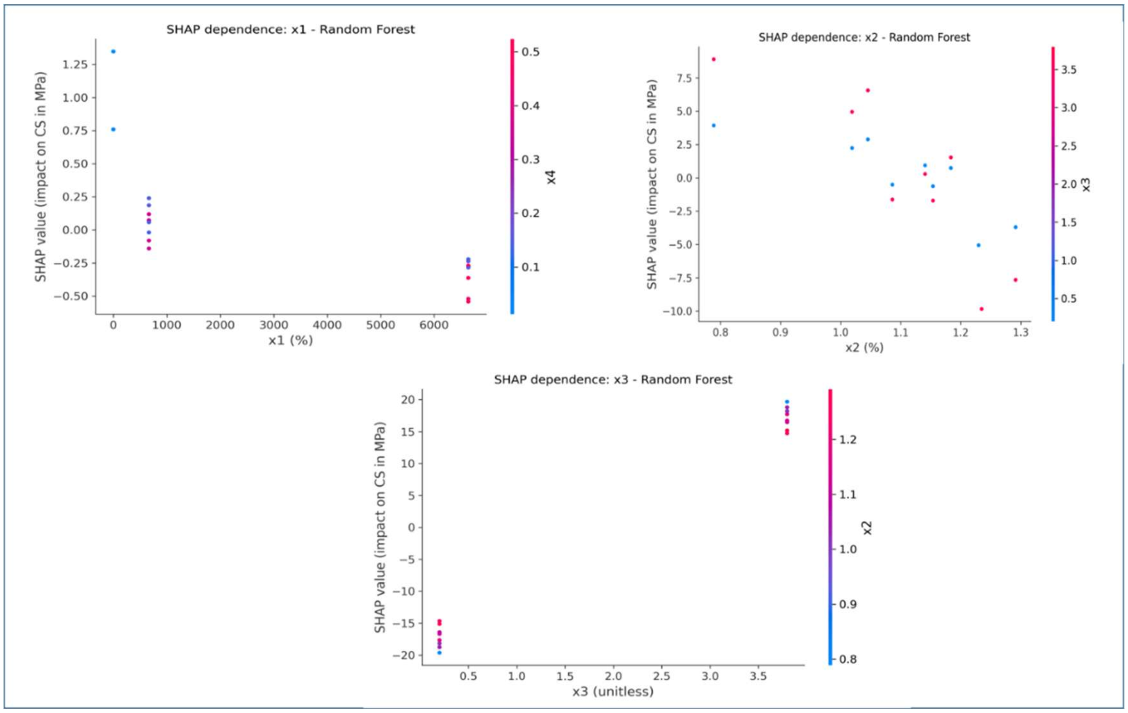

Figure 5.11 Sample SHAP dependence plots between aggregated variables

Table 5.6 shows an example of converting the individual predictors to composite indices then to predictions. It is clearly shown that the optimized indices predicted the outputs well.

Table 5.6. Example that converts raw inputs to an index and then to a prediction.

Individual predictors									Composite predictors				Predicted CS (MPa)					
C/C_a	C/F_a	W/C	W_a (%)	C_v (%)	R_r (%)	D_c (%)	P_{cs} (Mpa)	Actual CS (Mpa)	X_1	X_2	X_3	X_4	MLR	Ridge	Poly MLR	DT	RF	LightGBM
0.51	1.167	0.26	2.76	20.09	30	1.2	20.1	60.1	585.042	1.307	2.636	0.525	61.350	61.256	62.283	61.335	61.297	61.403
0.261	0.335	0.57	3.35	21.82	30	2.227	7.4	23.28	585.042	3.241	0.088	0.406	22.307	22.589	20.098	21.478	21.517	21.484
0.261	0.335	0.57	2.25	18.011	1	0.1	0.1	28.19	1.000	0.034	0.088	0.226	28.981	28.439	24.835	24.375	24.246	24.370

Individual predictors									Composite predictors				Predicted CS (MPa)					
C/C_a	C/F_a	W/C	W_a (%)	C_v (%)	R_r (%)	D_c (%)	P_{cs} (Mpa)	Actual CS (Mpa)	X_1	X_2	X_3	X_4	MLR	Ridge	Poly MLR	DT	RF	LightGBM
0.51	1.167	0.26	3.94	24.95	100	4	67	52.13	5581.222	7.659	2.636	0.549	56.425	56.064	55.371	52.220	52.976	52.373
0.261	0.335	0.57	2.76	20.09	30	1.2	20.1	22.74	585.042	1.307	0.088	0.525	27.097	27.027	22.376	23.134	23.150	23.098
0.261	0.335	0.57	3.94	24.95	100	4	67	23.07	5581.222	7.659	0.088	0.549	22.171	21.835	19.582	21.158	21.196	21.109
0.261	0.335	0.57	3.03	21.18	30	3.579	7.4	25.17	585.042	6.505	0.088	0.422	21.103	21.551	24.661	24.278	24.276	24.288
0.51	1.167	0.26	3.03	21.18	30	3.579	7.4	55.39	585.042	6.505	2.636	0.422	55.356	55.780	56.669	57.148	57.100	57.136
0.261	0.335	0.57	3.85	22.01	100	5.12	67	23.42	5581.222	11.006	0.088	0.573	22.098	21.826	23.510	22.580	22.571	22.612
0.261	0.335	0.57	3.35	21.82	30	2.227	7.4	22.16	585.042	3.241	0.088	0.406	22.307	22.589	20.098	21.478	21.517	21.484
0.51	1.167	0.26	3.94	24.95	100	4	67	51.91	5581.222	7.659	2.636	0.549	56.425	56.064	55.371	52.220	52.976	52.373
0.51	1.167	0.26	3.94	24.95	100	4	67	52.48	5581.222	7.659	2.636	0.549	56.425	56.064	55.371	52.220	52.976	52.373

Individual predictors									Composite predictors				Predicted CS (MPa)					
C/C_a	C/F_a	W/C	W_a (%)	C_v (%)	R_r (%)	D_c (%)	P_{cs} (Mpa)	Actual CS (Mpa)	X_1	X_2	X_3	X_4	MLR	Ridge	Poly MLR	DT	RF	LightGBM
0.261	0.335	0.57	2.25	18.011	1	0.1	0.1	27.88	1.000	0.034	0.088	0.226	28.981	28.439	24.835	24.375	24.246	24.370
0.51	1.167	0.26	3.94	24.95	100	4	67	52.69	5581.222	7.659	2.636	0.549	56.425	56.064	55.371	52.220	52.976	52.373
0.51	1.167	0.26	3.35	21.82	30	2.227	7.4	53.03	585.042	3.241	2.636	0.406	56.560	56.818	54.025	52.922	52.986	52.916
0.261	0.335	0.57	3.94	24.95	100	4	67	21.02	5581.222	7.659	0.088	0.549	22.171	21.835	19.582	21.158	21.196	21.109
0.51	1.167	0.26	2.25	18.01	1	0.1	0.1	66.86	1.000	0.034	2.636	0.226	63.234	62.668	69.046	69.414	69.399	69.413
0.51	1.167	0.26	2.76	20.09	30	1.2	20.1	62.29	585.042	1.307	2.636	0.525	61.350	61.256	62.283	61.335	61.297	61.403
0.51	1.167	0.26	3.85	22.01	100	5.12	67	59.51	5581.222	11.006	2.636	0.573	56.351	56.056	58.890	59.820	59.778	59.778
0.51	1.167	0.26	3.03	21.18	30	3.579	7.4	58.46	585.042	6.505	2.636	0.422	55.356	55.780	56.669	57.148	57.100	57.136
0.261	0.335	0.57	5.91	30.71	100	7.426	25	20.7	5581.222	19.001	0.088	0.386	15.507	15.625	18.346	18.346	18.360	18.332

Individual predictors									Composite predictors				Predicted CS (MPa)					
C/C_a	C/F_a	W/C	W_a (%)	C_v (%)	R_r (%)	D_c (%)	P_{cs} (Mpa)	Actual CS (Mpa)	X_1	X_2	X_3	X_4	MLR	Ridge	Poly MLR	DT	RF	LightGBM
0.261	0.335	0.57	4.84	28.59	100	11.93	25	20.66	5581.222	38.117	0.088	0.418	14.410	14.704	20.917	20.546	20.505	20.550

The ML models developed in this study were trained and validated using datasets that fall within the parameter ranges summarized in Table 5.7. These ranges define the domain in which the models can make predictions. Inputs that fall outside these intervals may lead to extrapolation, which may reduce prediction accuracy.

Table 5.7. The ML models prediction ranges

C/C_a	C/F_a	W/C	W_a (%)	C_v (%)	R_r (%)	D_c (%)	P_{cs} (Mpa)
0.261-0.51	0.335-1.167	0.26-0.58	2.25-5.91	18-31	1-100	0.1-12	25-67

Table 5.8 show the global SHAP values of each model. SHAP values quantify the contribution of each feature to the model's prediction and are expressed in the same units as the model output. In this study, the model predicts compressive strength (MPa), so a SHAP value represents how many Mpa a feature increases or decreases the predicted strength. For example, a mean absolute SHAP value of approximately 17 for feature x_3 (see table 5.8) indicates that this variable changes the prediction by about 17 MPa on average, whereas a value around 3 for x_2 reflects a smaller influence of roughly 3 MPa. Importantly. Polynomial regression models can exhibit very large SHAP magnitudes due to the presence of squared and interaction terms, which increase the internal numerical scale of the model. These inflated SHAP values do not imply disproportionately higher importance; instead, they reflect the model's expanded feature space and sensitivity to unscaled polynomial terms. Therefore, comparisons of absolute SHAP magnitudes should be made within the same model, while cross model comparisons should rely primarily on relative rankings rather than numerical size.

Table 5.8. Mean global SHAP of models

Models	Feature	SHAP global mean
MLR	x_1	1.446
MLR	x_2	2.920
MLR	x_3	17.127
MLR	x_4	2.002
Polynomial MLR (deg=2)	x_1	4264.070
Polynomial MLR (deg=2)	x_2	1330.491
Polynomial MLR (deg=2)	x_3	2.238
Polynomial MLR (deg=2)	x_4	742.073
Polynomial MLR (deg=2)	x_1^2	3101.106
Polynomial MLR (deg=2)	$x_1 x_2$	1096.625
Polynomial MLR (deg=2)	$x_1 x_3$	0.147
Polynomial MLR (deg=2)	$x_1 x_4$	102.858
Polynomial MLR (deg=2)	x_2^2	1232.142
Polynomial MLR (deg=2)	$x_2 x_3$	22.456
Polynomial MLR (deg=2)	$x_2 x_4$	771.937
Polynomial MLR (deg=2)	x_3^2	35.755
Polynomial MLR (deg=2)	$x_3 x_4$	1.984
Polynomial MLR (deg=2)	x_4^2	14.255
Ridge	x_1	1.766
Ridge	x_2	2.567
Ridge	x_3	17.115
Ridge	x_4	1.912
Decision Tree	x_1	0.187
Decision Tree	x_2	4.003
Decision Tree	x_3	17.064
Decision Tree	x_4	0.697
Random Forest	x_1	0.303

Random Forest	x_2	3.838
Random Forest	x_3	17.079
Random Forest	x_4	0.592
LightGBM	x_1	0.775
LightGBM	x_2	3.532
LightGBM	x_3	17.417
LightGBM	x_4	1.138

5.4 Conclusion and Recommendation

This study demonstrated that carbonation treatment of RCAs can be effectively integrated with ML to support sustainable construction practices. The investigation showed that, unlike conventional testing methods that are expensive and time consuming, regression based ML models provide an efficient and accurate alternative. For the first time, predictive modeling was applied specifically to concretes containing carbonated RCAs, filling a gap in existing research. Using 108 experimental tests of individual datasets that are later composited to indices representing mix proportioning, aggregate performance, carbonation degree, and replacement percentage, six ML algorithms were evaluated for their predictive ability. Based on the outputs of the study the authors concluded and recommended the following:

- ML models predicted the compressive strength of carbonated RAC with good accuracy.
- Intercorrelation and multicollinearity within the datasets have no noticeable effect on the performance of the ML models, especially tree based and ensemble based models.
- Comparing classical regression based and tree based models on the same dataset, it was found that tree based models performed better.
- Numerical prediction equations developed using polynomial MLR performed well after the ensemble based models and may be applied in practical compressive strength predictions.

- Based on the quantitative metrics, qualitative assessments, and SHAP analyses, the Random Forest model outperformed all other models.
- Variations in fine aggregate type and properties, variations in cement type, addition of super plasticizers and coarse aggregate size effect were not considered in this study. Therefore, future studies can work on compressive strength prediction of carbonated RCA concrete considering these properties together with deep learning models and sufficient datasets.
- Since the datasets used in this study are limited and the available strength ranges are extreme, normal strength (17-29 MPa) and high strength (40-72 MPa), including additional values both in between these ranges and outside these ranges may improve accuracy and reduce overfitting, instability and noise in the model outputs.
- Modeling of Tensile strength, modulus of elasticity and other durability properties of carbonated RCA concrete can be another area for future research.
- The models in this study produced relatively high R^2 values, which should be interpreted with caution. Although the dataset includes 18 mix combinations, one possible reason for the high accuracy is the limited variation in water to cement ratios, as only two values were used across all mixtures. Even with additional parameters such as carbonation degree, replacement ratio, and parent concrete strength, the restricted range of water to cement ratios may reduce the overall variability in the dataset and simplify the prediction task, allowing the models to achieve high goodness of fit scores. This limitation suggests that the results may reflect the narrow experimental conditions. Future studies would benefit from incorporating a wider range of water to cement ratios to better capture the diversity of concrete mix behavior and to more rigorously evaluate the robustness of the models.

5.5. References

[1]. Li, S., Wang, B., Gao, Y., Yu, Y. (2025). A Compressive Strength Prediction Model for Precast Recycled Aggregate Concrete Based on Machine Learning. AIP Adv., 15, 075133. https://doi.org/10.1063/5.0280234

[2]. Sinkhonde, D., Bezabih, T., Mirindi, D., Mashava, D., Mirindi, F. (2025). Ensemble machine learning algorithms for efficient prediction of compressive strength of concrete containing tyre rubber and brick powder, Clean Waste Syst., 10, 2025, 100236, https://doi.org/10.1016/j.clwas.2025.100236.

[3]. Lin, L., Xu, J., Ying, W. Yu, Y., Zhou, L. (2025). Post Fire Compressive Mechanical Behaviors of Concrete incorporating Coarse and Fine Recycled Aggregates. Constr. Build. Mater.461, 139948. https://doi.org/10.1016/j.conbuildmat.2025.139948

[4]. Yu, Y., Xu, J., Su, J., Xu, L., Luo, Y. (2024). Investigating Specimen Size and Shape Effects on Compressive Mechanical Behaviors of Recycled Aggregate Concrete Using Discrete Element Mesoscale Modeling, Constr. Build. Mater. 438, 137196. https://doi.org/10.1016/j.conbuildmat.2024.137196

[5]. Wang, D., Lu, C., Zhu, Z., Zhang, Z., Liu, S., Ji, Y., Xing, Z. (2023). Mechanical Performance of Recycled Aggregate Concrete in Green Civil Engineering: Review," Case Stud. Constr. Mater. 19, e02384. https://doi.org/10.1016/j.cscm.2023.e02384

[6]. Arora, S., Singh, B., Bhardwaj, B., (2019). Strength Performance of Recycled Aggregate Concretes Containing Mineral Admixtures and Their Performance Prediction through Various Modeling Techniques. J. Build. Eng. 24, 100741. https://doi.org/10.1016/j.jobe.2019.100741

[7]. Deng, F., He, Y., Zhou, S., Yu, Y., Cheng, H., Wu, X., (2018). Compressive Strength Prediction of Recycled Concrete Based on Deep Learning. Constr. Build. Mater. 175, 562-569. https://doi.org/10.1016/j.conbuildmat.2018.04.169

[8]. Duan, J., Asteris, P.G., Nguyen, H., Bui, X.-N., Moayedi, H., (2021). A Novel Artificial Intelligence Technique to Predict Compressive Strength of Recycled Aggregate Concrete Using ICA-XGBoost Model. Eng Comput. 37, 3329-3346. https://doi.org/10.1007/s00366-020-01003-0

[9]. Zhang, J., Huang, Y., Aslani, F., Ma, G., Nener, B., (2020). A hybrid intelligent system for designing optimal proportions of recycled aggregate concrete. J. Clean. Prod. 273, 122922. https://doi.org/10.1016/j.jclepro.2020.122922

[10]. Peiris, D., Gunasekara, C., Law, D.W., Patrisia, Y., Tam, V.W.Y., Setunge, Y., (2025). Impact of treatment methods on recycled concrete aggregate performance: a comprehensive review. *Environ Sci Pollut Res*. 32, 14405-14438. https://doi.org/10.1007/s11356-025-36497-y.

[11]. Fortunato, L.R., Parsekian, G.A., Junior, A.N. (2023). Developing an easy to build laboratory chamber for CO2 experiments. Matéria (Rio J.) 28 (2). https://doi.org/10.1590/1517-7076-RMAT-2023-0078

[12]. Bui, H., Delattre, F., & Levacher, D. (2023). Experimental Methods to Evaluate the Carbonation Degree in Concrete-State of the Art Review. Appl. Sci., 13(4), 2533. https://doi.org/10.3390/app13042533

[13]. Liu K., Xu W., Sun, D., Tang, J., Wang, A., Dong Chen, D. (2021). Carbonation of recycled aggregate and its effect on properties of recycled aggregate concrete: A review. Mater. Express 11 (9), 1439-1452(14). https://doi.org/10.1166/mex.2021.2045

[14]. Kashem, A., Karim, R., Chandra Malo, S., Das, P., Dip Datta, S., Alharthai, M., (2024). Hybrid data-driven approaches to predicting the compressive strength of ultra-high-performance concrete using SHAP and PDP analyses, Case Stud. Constr. Mater., 20, e02991. https://doi.org/10.1016/j.cscm.2024.e02991.

[15]. Alyami, M., Nassar, R.U.D., Khan, M., Hammad, A.W., Alabduljabbar, H., Nawaz, R., Fawad, M., Gamil, Y., (2024). Estimating compressive strength of concrete containing rice husk ash using interpretable machine learning-based models. Case Stud. Constr. Mater. 20, e02901. https://doi.org/10.1016/j.cscm.2024.e02901.

[16]. Philip, S., Nidhi, M., (2024). Performance comparison of artificial neural network and random forest models for predicting the compressive strength of fbre - reinforced GGBS - based geopolymer concrete composites. Mater. Circ. Econ. 6 (34), 1-18. https://doi.org/10.1007/s42824-024-00128-7

[17]. Tipu, R.K., Arora, R., Kumar, K., (2024). Machine learning-based prediction of concrete strength properties with coconut shell as partial aggregate replacement: A sustainable approach in construction engineering. Asian J. Civ. Eng. 25 (3), 2979-2992. https://doi.org/10.1007/s42107-023-00957-y.

[18]. Rusu, A., Bărbuță, M., Sabina, S. (2024). Multiple Linear Regression Model to Predict Compressive Strength of Concrete with Silica Fume and Metallic Fibers. In: Moldovan, L., Gligor, A. (eds) The 17th International Conference Interdisciplinarity in Engineering. Inter-ENG 2023. Lecture Notes in Networks and Systems, 926. Springer, Cham. https://doi.org/10.1007/978-3-031-54664-8_23

[19]. Chore, H., Shelke, N.L, (2013). Prediction of compressive strength of concrete using multiple regression model. STRUCT ENG MECH, 45(6). https://doi.org/10.12989/sem.2013.45.6.837

[20]. Aamir, H., Aamir, K., & Javed, M. F. (2023). Linear and Non-Linear Regression Analysis on the Prediction of Compressive Strength of Sodium Hydroxide Pre-Treated Crumb Rubber Concrete. Eng. Proc., 44(1), 5. https://doi.org/10.3390/engproc2023044005

[21]. Yuan, Y., Yang, M., Shang, X., Xiong, Y., Zhang, Y., (2023). Predicting the compressive strength of UHPC with coarse aggregates in the context of machine learning. Case Stud. Constr. Mater. 19, e02627. https://doi.org/10.1016/J.CSCM.2023.E02627

[22]. Abdellatief, M., Murali, G., Dixit, S., (2025). Leveraging machine learning to evaluate the effect of Raw materials on the compressive strength of ultra-high-performance concrete. Results Eng. 25, 104542. https://doi.org/10.1016/J.RINENG.2025.104542

[23]. Abdellatief, M., Youssef M. H., Mohamed T. E., Wong, L.S., Chin, R.J., Mo, K.H., (2024). Investigation of machine learning models in predicting compressive strength for ultra-high-performance geopolymer concrete: A comparative study. Constr. Build. Mater. 436, 136884. https://doi.org/10.1016/j.conbuildmat.2024.136884

[24]. Abuodeh, O. R., Abdalla, J. A., Hawileh, R. A., (2020). Assessment of compressive strength of Ultra-high performance concrete using deep machine learning techniques. Appl. of Comput. 95, 106552. https://doi.org/10.1016/J.ASOC.2020.106552

[25]. Salman, K.M., Tianbo, P., Adeel, K.M., Asad, K., Mahmood, M., Kamran, A., et al. (2025). Explainable AutoML models for predicting the strength of high-performance concrete using Optuna, SHAP and ensemble learning. Front. Mater, 12 -2025. https://doi.org/10.3389/fmats.2025.1542655

[26]. Gebremariam H.G., Taye, S., Tarekegn, A.G., (2025). CO_2 Uptake in Recycled Concrete Aggregates: Influence of Parent Concrete Strength and Preprocessing Carbonation. Unpublished manuscript.

[27]. Alahakoon, Y., Sajindra, H., Krishantha, A., Alawatugoda, J., Ekanayake, I.U., Rathnayake, U., (2025). Prediction of alkali-silica reaction expansion of concrete using explainable machine learning methods. Discov Appl Sci 7, 407. https://doi.org/10.1007/s42452-025-06880-y

[28]. Meddage D.P.P., Mohotti D., Wijesooriya K., Lee C.K., Kwok K.C.S., (2025). Interpolating wind pressure time-histories around a tall building - a deep learning-based approach. J Wind Eng Ind Aerodyn. 256: 105968. https://doi.org/10.1016/j.jweia.2024.105968

[29]. O'brien, R.M., (2007). A Caution Regarding Rules of Thumb for Variance Inflation Factors. Qual Quant 41, 673-690. https://doi.org/10.1007/s11135-006-9018-6

[30]. Singh, S.G., Kumar, S.V., (2021). Dealing with Multicollinearity Problem in Analysis of Side Friction Characteristics Under Urban Heterogeneous Traffic Conditions. Arab J Sci Eng 46, 10739-10755. https://doi.org/10.1007/s13369-020-05213-y

[31]. Loureiro, A.A.B., Stefani, R., (2024). Comparing the performance of machine learning models for predicting the compressive strength of concrete. Discov Civ Eng 1, 19. https://doi.org/10.1007/s44290-024-00022-w

[32]. Sah, A.K., (2024). Hong Y.M. Performance Comparison of Machine Learning Models for Concrete Compressive Strength Prediction. Materials (Basel).7(9), 2075. https://doi.org/10.3390/ma17092075

[33]. Gayathri, R., Rani, S. U., Čepová, L., Rajesh, M., & Kalita, K. (2022). A Comparative Analysis of Machine Learning Models in Prediction of Mortar Compressive Strength. Processes, 10(7), 1387. https://doi.org/10.3390/pr10071387

[34]. Biau, G.; Scornet, E., (2016) A random forest guided tour. TEST, 25, 197-227. https://doi.org/10.1007/s11749-016-0481-7

[35]. Padula, W. V., (2023). Introduction to decision tree modeling, in Bishai, D., Brenzel L., Padula, W. (eds), Handbook of Applied Health Economics in Vaccines, Handbooks in Health Economic Evaluation (Oxford Academic). , accessed 16 Aug. 2025. https://doi.org/10.1093/oso/9780192896087.003.0020

[36]. James, G., Witten, D., Hastie, T., Tibshirani, R., (2021). An Introduction to Statistical Learning with Applications in R. Part of the book series: Springer Texts in Statistics. Springer New York, NY. https://doi.org/10.1007/978-1-0716-1418-1

[37]. Breiman, L., (2001). Random Forests. Machine Learning 45, 5-32. https://doi.org/10.1023/A:1010933404324

[38]. Hajihosseinlou, M., Maghsoudi, A. & Ghezelbash, R., (2023). A Novel Scheme for Mapping of MVT-Type Pb-Zn Prospectivity: LightGBM, a Highly Efficient Gradient Boosting Decision Tree Machine Learning Algorithm. Nat Resour Res 32, 2417-2438. https://doi.org/10.1007/s11053-023-10249-6

[39]. Elshaarawy, M.K., Zeleňáková, M., Armanuos, A.M., (2025). Hydraulic Performance Modeling of Inclined Double Cutoff Walls Beneath Hydraulic Structures Using Optimized Ensemble Machine Learning. Sci Rep 15, 27592. https://doi.org/10.1038/s41598-025-10990-3

[40]. Elshaarawy, M.K., Alsaadawi, M.M. & Hamed, A.K., (2024). Machine learning and interactive GUI for concrete compressive strength prediction. Sci Rep 14, 16694 (2024). https://doi.org/10.1038/s41598-024-66957-3

[41]. Harith, I.K., Nadir, W., Salah, M.S. et al. (2024). Prediction of high-performance concrete strength using machine learning with hierarchical regression. Multiscale and Multidiscip. Model. Exp. and Des. 7, 4911-4922. https://doi.org/10.1007/s41939-024-00467-7

[42]. Das, P., Kashem, A., (2024). Hybrid machine learning approach to prediction of the compressive and fexural strengths of UHPC and parametric analysis with

Shapley additive explanations. Case Stud. Constr. Mater. 20, e02723. https://doi.org/10.1016/j.cscm.2023.e02723

[43]. Elhishi, S., Elashry, A.M., El-Metwally, S., (2023). Unboxing machine learning models for concrete strength prediction using XAI. Sci Rep 13, 19892. https://doi.org/10.1038/s41598-023-47169-7

[44]. Arunvivek, G.K., Anandaraj, S., Kumar, P, Pratap, B., Sembeta, R.Y., (2025). Compressive strength modelling of cenosphere and copper slag-based geopolymer concrete using deep learning model. Sci Rep 15, 27849 (2025). https://doi.org/10.1038/s41598-025-13176-z

[45]. Albostami, A. S., Al-Hamd, R. K. S., & Al-Matwari, A. A. (2024). Data-Driven Predictive Modeling of Steel Slag Concrete Strength for Sustainable Construction. *Buildings*, *14*(8), 2476. https://doi.org/10.3390/buildings14082476

[46]. Pratap, B., Kumar, P., Shubham, K., Chaudhary, N., (2024). Soft computing-based investigation of mechanical properties of concrete using ready-mix concrete waste water as partial replacement of mixing portable water. Asian J. Civil Eng. 25 (2), 1255-1266. https://doi.org/10.1007/s42107-023-00841-9

[47]. Kumar, P., Pratap, B., Sharma, S., Kumar, I., (2024). Compressive strength prediction of fly Ash and blast furnace slag-based geopolymer concrete using convolutional neural network. Asian J. Civil Eng. 25 (2), 1561-1569. https://doi.org/10.1007/s42107-023-00861-5

[48]. Gogineni, A., Panday, I. K., Kumar, P., Paswan, R. K., (2024). Predicting compressive strength of concrete with fly Ash and admixture using xgboost: a comparative study of machine learning algorithms. Asian J. Civil Eng. 25 (1), 685-698. https://doi.org/10.1007/s42107-023-00804-0

[49]. Anwar, M.K., Qurashi, M.A., Zhu, X., Raheel Shah, S.A., Siddiq, M.U., (2025). A comparative performance analysis of machine learning models for compressive strength prediction in fly ash-based geopolymers concrete using reference data, Case Stud. Constr. Mater, 22, e04207, https://doi.org/10.1016/j.cscm.2025.e04207.

[50]. Dhengare, S., Waghe, U., Yenurkar, G., Shyamala, A., (2025). A comprehensive model for concrete strength prediction using advanced learning techniques. Discov Appl Sci 7, 551. https://doi.org/10.1007/s42452-025-07095-x

[51]. Cho, S.J., De Boeck, P., Naveiras, M., Ervin,H., (2022). Level-specific residuals and diagnostic measures, plots, and tests for random effects selection in multilevel and mixed models. Behav Res 54, 2178-2220. https://doi.org/10.3758/s13428-021-01709-z

[52]. Haque, M. A., Chen, B., Kashem, A., Qureshi, T., Ahmed, A. A. M., (2023). Hybrid intelligence models for compressive strength prediction of MPC composites and parametric analysis with SHAP algorithm. Mater. Today Commun. 35, 105547 (2023). https://doi.org/10.1016/j.mtcomm.2023.105547

CHAPTER 6

GENERAL DISCUSSION, CONCLUSION AND RECOMMENDATION

6.1. General discussion

As discussed in the previous sections, concrete is the most widely consumed construction material, with annual production reaching nearly 30 million tons. However, its production process contributes significantly to environmental degradation and pollution [71]. During construction, up to 13% of materials are wasted in less developed countries such as Ethiopia. Additional sources of C&D waste include urbanization, infrastructure expansion, and structural replacement activities. Material testing laboratories also generate considerable amounts of concrete waste; once tested, specimens accumulate and become an environmental concern. Experimental and testing institutions, particularly universities and construction consulting firms, produce large volumes of waste from laboratory cast cubes and other concrete samples [72]. Furthermore, natural and human induced disasters, such as earthquakes and conflicts, contribute to the generation of substantial quantities of C&D waste. At the end of their service life, buildings also produce vast amounts of concrete debris, creating significant disposal and management challenges [71]. This concern was the motivation for initiating the present study.

From the literature review, one promising solution identified is the use of RAC, which supports the sustainable development of the concrete sector [71]. Nevertheless, integrating waste concrete into new concrete mixtures still presents considerable technical and practical challenges [71]. These challenges include the generally inferior quality of RCAs compared to NAs and the variability in properties among RCAs sourced from different PCs. To address these challenges, this study conducted an extensive literature review and experimental program. The investigations presented in this dissertation deepen the understanding of how the characteristics of PC influence the performance of RCAs and RAC.

Despite inconsistencies in prior studies, the findings of this study clarified that PC strength closely linked to porosity and residual mortar content governs RCA behavior. High strength concretes generally yield RCAs with lower porosity, higher density, and greater resistance to mechanical degradation. These improvements are reflected in RAC mixes through reduced water absorption as well as enhanced compressive and tensile capacities.

The effectiveness of accelerated carbonation as a material enhancement technique was also a central finding. This process densifies the porous adhered mortar on the RCA by converting unstable calcium hydroxide into a stable calcium carbonate matrix. This chemical transformation not only improves the physical properties of the aggregate but also sequesters a measurable amount of atmospheric CO_2, offering a tangible environmental benefit. However, the study identified a significant limitation where the dense microstructure of RCAs from high strength PC impedes CO_2 diffusion, preventing full carbonation. This suggests that the current pressurized carbonation method may not be universally effective and highlights the need for a more versatile approach. In general, results from this study indicated that, with very high strength PCs, the tensile strength of carbonated RAC can reach values comparable to those of NACs.

In addition, the incorporation of ML predictive modeling demonstrated that reliable forecasting of RAC behavior is possible, even under complex multivariable conditions. Ensemble algorithms, particularly Random Forest, achieved high predictive accuracy compared to conventional regression methods. Furthermore, prediction equations found from regression based ML models of Poly MLR can also predict the compressive strength well. On the contrary, deep learning based models require large datasets to completely capture the trends. Given that aggregate types, cement chemistries, and mixing practices vary across regions and nations, countries like Ethiopia should establish guideline based datasets to ensure reliable predictions.

The results from this thesis indicate that carbonated RCA has strong potential for practical use in sustainable concrete production. In engineering applications, carbonated RCA can be used in pavements, precast products, and even in medium to high strength concrete. Its use also supports sustainable and circular construction practices.

6.2. General conclusion and recommendations

The results of this study confirm that the strength of PC is a factor in determining the performance of RCAs and RAC. Stronger concretes yield aggregates with higher density, lower water absorption, and superior mechanical behavior. Reported inconsistencies in performance are largely attributable to differences in porosity, residual mortar content, and processing methods.

Carbonation treatment emerged as an effective approach for enhancing RCA quality while contributing to CO_2 storage. This dual benefit links recycling with climate objectives. However, the CO_2 uptake capacity is limited in aggregates derived from dense, high strength concretes, underscoring the need for alternative or optimized carbonation methods. The generalizability of current laboratory findings including this study are constrained by the controlled nature of most of the parameters. In practice, demolition waste often contains impurities such as ceramics, tiles, plaster, finishing materials, metals, and organic residues, which significantly affect RCA quality and durability. This gap between laboratory conditions and field realities represents a key limitation to large scale application, particularly in Ethiopia, where diverse waste streams and weak segregation practices governs.

Future research should therefore focus on systematic investigations that replicate the heterogeneity of real demolition waste and assess its impact on RCA performance. Additionally, the scope in this study should be broadened to systematically investigate the effects of RCA particle size and fine aggregate variability on the properties of RAC. Durability aspects like chloride resistance, freeze-thaw performance, shrinkage and creep behavior of RAC can also be an alternative focus on future studies. Similarly, Research should move beyond material properties to evaluate the performance of RAC in structural elements, including its flexural, shear, and torsional behavior, as well as the bond strength with reinforcement bars. A detailed life cycle assessment is essential to quantify the environmental benefits of carbonated RAC. This analysis should compare the embodied carbon and embodied energy of the entire process, from C&D waste collection and crushing to final construction, against that of conventional concrete. This will provide the robust data needed to support its widespread adoption. It can also provide a full accounting of the environmental benefits of RAC. Additionally, wider durability assessments, such as long-term chloride exposure, sulfate resistance, freeze-thaw performance, shrinkage and permeability related investigations are recommended for future works.

6.2.1. A roadmap for implementation in the Ethiopian context

To facilitate the widespread use of RAC in Ethiopia, a coordinated effort among key stakeholders is essential.

One important parameter for Ethiopia to consider is a policy development which is central to unlock the potential of RAC. The Ethiopian government should lead the charge by developing and enforcing a national standard for RCA and RAC based on its source and quality. Policy levers, such as tax incentives for companies using recycled materials and carbonation technologies or mandates for their use in public infrastructure projects, are crucial. Policies that promote selective demolition and source segregation will be essential to improve input quality.

Universities and research centers should prioritize creating a local knowledge base by characterizing C&D waste streams specific to the region. They should also provide technical guidance and training to industry professionals on best practices for handling and mix design with RAC. Major construction companies should initiate pilot projects to demonstrate the practical viability of RAC in both structural and nonstructural applications. This phased adoption will build confidence and provide valuable real world data. The waste management sector must modernize by investing in specialized sorting, crushing, and quality control equipment.

Another significant opportunity lies in coupling RCA carbonation with industrial CO_2 emitters, including cement plants, steel factories, and power stations. Capturing emissions at the source and using them in aggregate carbonation or concrete curing would transform waste gases into a valuable resource. Such integration prevents CO_2 release, enhances RCA properties, and provides an alternative curing method for fresh natural aggregate concrete and RAC. With Ethiopia's cement production and emissions increasing, these synergies could substantially advance both reconstruction and climate mitigation efforts.

6.3. Bibliography

[1]. Ige, O.E., Von Kallon, D.V. & Desai, D., (2024). Carbon emissions mitigation methods for cement industry using a systems dynamics model. Clean Techn Environ Policy 26, 579-597. https://doi.org/10.1007/s10098-023-02683-0

[2]. Masson-Delmotte, Zhai, V.P., Pörtner, H.O., Roberts, D., JSkea, J., Shukla, P.R., (2022). Global Warming of 1.5°C IPCC Special Report on Impacts of Global Warming of 1.5°C above Pre-industrial Levels in Context of Strengthening Response to Climate Change, Sustainable Development, and Efforts to Eradicate Poverty, Cambridge University Press pp. 1-24 https://doi.org/10.1017/9781009157940.001

[3]. IPCC (2021). Climate Change 2021: The Physical Science Basis. Contribution of Working Group I to the Sixth Assessment Report of the Intergovernmental Panel on Climate Change. Cambridge University Press, Cambridge, United Kingdom and New York, NY, USA. https://www.ipcc.ch/report/ar6/wg1/

[4]. Tang B, Hu W, Duan A, Gao K, Peng Y (2022). Reduced risks of temperature extremes from 0.5 C less global warming in the Earth's three poles. Earth's Futur. 10: e2021EF002525. https://doi.org/10.1029/2021EF002525

[5]. WMO (2023). WMO Statement on the State of the Global Climate in 2022. World Meteorological Organization, Geneva, Switzerland. https://library.wmo.int/idurl/4/68835

[6]. IPCC (2018). Global Warming of 1.5°C. An IPCC Special Report on the impacts of global warming of 1.5°C above pre-industrial levels and related global greenhouse gas emission pathways, in the context of strengthening the global response to the threat of climate change, sustainable development, and efforts to eradicate poverty. World Meteorological Organization, Geneva, Switzerland. https://www.ipcc.ch/sr15/

[7]. Global Carbon Budget (2024) – with major processing by Our World in Data. "Annual CO_2 emissions" [dataset]. Global Carbon Project, "Global Carbon Budget" [original data]. https://ourworldindata.org/co2-emissions

[8]. Liu, Z., Zhou, Q., Tian, Z., He, B., Jin, G., (2019). A comprehensive analysis on definitions, development, and policies of nearly zero energy buildings in China, Renew. Sustain. Energy Rev, 114, 109314. https://doi.org/10.1016/j.rser.2019.109314

[9]. He, B., Yang, L., Ye, M., Mou, B., Zhou, Y., (2014). Overview of rural building energy efficiency in China. Energy Policy, 69,385–96. https://doi.org/10.1016/j.enpol.2014.03.018

[10]. Rhodes C., (2016). The 2015 Paris climate change conference: COP21. Sci Prog, 99(97). https://doi.org/10.3184/003685016X14528569315192

[11]. Barbhuiya, S., Kanavaris, F., Bhusan Das, B., Idrees, M., (2024). Decarbonising cement and concrete production: Strategies, challenges and pathways for sustainable development. J. Build. Eng., 86, 108861, https://doi.org/10.1016/j.jobe.2024.108861

[12]. Shivaprasad, K.N., Yang, Hm. Singh, J.K., (2024). A path to carbon neutrality in construction: An overview of recent progress in recycled cement usage, J. CO2 Util., 83, 102816, https://doi.org/10.1016/j.jcou.2024.102816

[13]. Uwasu, M., Hara, K., Yabar, H., (2014). World cement production and environmental implications, Environ. Dev. 10, 36-47, https://doi.org/10.1016/j.envdev.2014.02.005

[14]. Horvath, A., (2004). Construction materials and the environment, Annu. Rev. Environ. Resour. 29, 181-204, https://doi.org/10.1146/annurev.energy.29.062403.102215

[15]. Huntzinger, D.N., Eatmon, T.D., (2009). A life cycle assessment of Portland cement manufacturing: comparing the traditional process with alternative technologies, J. Clean. Prod. 17, 668-675, https://doi.org/10.1016/J.JCLEPRO.2008.04.007

[16]. Chen, C., Habert, G., Bouzidi, Y., Jullien, A., (2010). Environmental impact of cement production: detail of the different processes and cement plant variability evaluation, J. Clean. Prod. 18 (2010) 478–485, https://doi.org/10.1016/J.JCLEPRO.2009.12.014

[17]. Ali, M.B., Saidur, R., Hossain, M.S., (2011). A review on emission analysis in cement industries, Renew. Sustain. Energy Rev. 15, 2252-2261, https://doi.org/10.1016/j.rser.2011.02.014

[18]. Li, L., Wu, M., (2022). An overview of utilizing CO2 for accelerated carbonation treatment in the concrete industry. J. CO2 Util., 60, 102000, https://doi.org/10.1016/j.jcou.2022.102000

[19]. Vijerathne, D., Wahala, S., & Illankoon, C. (2024). Impact of Crushed Natural Aggregate on Environmental Footprint of the Construction Industry: Enhancing Sustainability in Aggregate Production. Buildings, 14(9), 2770. https://doi.org/10.3390/buildings14092770

[20]. Langer, W., (2016). Sustainability of aggregates in construction. In Sustainability of Construction Materials; Elsevier: Amsterdam, The Netherlands, 181-207. https://doi.org/10.1016/B978-0-08-100370-1.00009-3

[21]. Linares, R., López-Uceda, A., Piccinali, A., Martínez-Ruedas, C., Galvín, A.P., (2024). LCA applied to comparative environmental evaluation of aggregate production from recycled waste materials and virgin sources. Environ. Sci. Pollut. Res. 2024, 31, 44023–44035. https://doi.org/10.1007/s11356-024-33868-9

[22]. Hossain, M.U., Poon, C.S., Lo, I.M.C., Cheng, J.C.P., (2016). Comparative environmental evaluation of aggregate production from recycled waste materials and virgin sources by LCA. Resour. Conserv. Recycl. 2016, 109, 67-77. https://doi.org/10.1016/j.resconrec.2016.02.009

[23]. Perkins, L., Royal, A.C.D., Jefferson, I., Hills, C.D., (2021). The Use of Recycled and Secondary Aggregates to Achieve a Circular Economy within Geotechnical Engineering. Geotechnics 2021, 1, 416–438. https://doi.org/10.3390/geotechnics1020020

[24]. Dixit, M.K., Fernández-Solís, J.L., Lavy, S., Culp, C.H., (2010). Identification of parameters for embodied energy measurement: A literature review. Energy Build. 2010, 42, 1238–1247. https://doi.org/10.1016/j.enbuild.2010.02.016

[25]. OECD (2019), Global Material Resources Outlook to 2060: Economic Drivers and Environmental Consequences, OECD Publishing, Paris, https://doi.org/10.1787/9789264307452-en

[26]. Bonifazi, G., Grosso, C., Palmieri, R., Serranti,S., (2025). Current trends and challenges in construction and demolition waste recycling, Curr. Opin. Green Sustain. Chem.,53,101032, https://doi.org/10.1016/j.cogsc.2025.101032

[27]. Lyu, Y., Xiong, N., Liang, Y., Lin, S., Wang, J., (2025). Estimation of construction and demolition waste and assessment of disposal facility location: An integrated Material Flow Analysis and Geographic Information System approach. Resour. Conserv. Recycl., 218, 108226, https://doi.org/10.1016/j.resconrec.2025.108226

[28]. Wang Z, Li H, Zhang X., (2019). Construction waste recycling robot for nails and screws: computer vision technology and neural network approach. Autom ConStruct, 97:220-228. https://doi.org/10.1016/j.autcon.2018.11.009

[29]. Radica F, Iezzi G, Trotta O, Bonifazi G, Serranti S, de Brito J., (2024). Characterization of CDW types by NIR spectroscopy: towards an automatic selection of recycled aggregates. J Build Eng, 88, 109005. https://doi.org/10.1016/j.jobe.2024.109005

[30]. Li, D., Tang, Z., Kang, Q., Zhang, X., & Li, Y. (2023). Machine Learning-Based Method for Predicting Compressive Strength of Concrete. Processes, 11(2), 390. https://doi.org/10.3390/pr11020390

[31]. Feng, D., Ren, X., Li, J., (2016). Stochastic damage hysteretic model for concrete based on micromechanical approach. Int. J. Non-Linear Mech. 2016, 83, 15-25. https://doi.org/10.1016/j.ijnonlinmec.2016.03.012

[32]. Shi, H., Xu, B., Zhou, X, (2009). Influence of mineral admixtures on compressive strength, gas permeability and carbonation of high performance concrete. Constr. Build. Mater. 2009, 23, 1980-1985. https://doi.org/10.1016/j.conbuildmat.2008.08.021

[33]. Bhanja, S., Sengupta, B., (2002). Investigations on the compressive strength of silica fume concrete using statistical methods. Cem. Concr.Res, 32, 1391–1394. https://doi.org/10.1016/S0008-8846(02)00787-1

[34]. Chen, Z., Guo, X., Shao, L., Li, S., Tian, X., (2021). Design of a three-dimensional earth pressure device and its application in a tailings dam construction simulation experiment. Acta Geotech, 16, 2203–2216. https://doi.org/10.1007/s11440-020-01138-w

[35]. Deng, F., He, Y., Zhou, S., Yu, Y., Cheng, H., Wu, X., (2018). Compressive strength prediction of recycled concrete based on deep learning. Constr. Build. Mater, 175, 562-569. https://doi.org/10.1016/j.conbuildmat.2018.04.169

[36]. Chen, Z., Guo, X., Shao, L., Li, S., Gao, L., (2022) Sensitivity analysis of the frozen soil nonlinear latent heat and its precise transformation method. Geophys. J. Int, 228, 240-249. https://doi.org/10.1093/gji/ggab319

[37]. Salehi, H., Burgueño, R., (2018). Emerging artificial intelligence methods in structural engineering. Eng. Struct, 171, 170-189. https://doi.org/10.1016/j.engstruct.2018.05.084

[38]. Taffese, W. Z., & Abegaz, K. A. (2019). Embodied Energy and CO2 Emissions of Widely Used Building Materials: The Ethiopian Context. Buildings, 9(6), 136. https://doi.org/10.3390/buildings9060136

[39]. Mhretu, A., Abadi, H.T., Gebrehiwot, W., Asresie, T., (2025). Challenges and opportunities in construction waste management in Shire Town, Northern Ethiopia. Discov Sustain 6, 599. https://doi.org/10.1007/s43621-025-01226-5

[40]. Dundar, B., Tugluca, M.S., Ilcan, H., Sahin, O., Sahmaran, M., (2025). Valorization of low-quality recycled concrete aggregates in cement-based systems through carbonation: assessment of engineering performance. J Aust Ceram Soc. https://doi.org/10.1007/s41779-025-01208-w

[41]. Nguyen, H.P., Mueller, A., Nguyen, V.T., Nguyen, C.T., (2021). Development and characterization of lightweight aggregate recycled from construction and demolition waste mixed with other industrial by-products. Constr. Build. Mater. 313, 125472. https://doi.org/10.1016/J.CONBUILDMAT.2021.125472

[42]. Rahal, K.N., Hassan, W., (2021). Shear strength of plain concrete made of recycled low-strength concrete aggregates and natural aggregates. Constr. Build. Mater. 311, 125317. https://doi.org/10.1016/j.conbuildmat.2021.125317

[43]. Zou, S., Xiao, J., Duan, Z., Ding, T., Hou, S., (2021). On rheology of mortar with recycled fine aggregate for 3D printing. Constr. Build. Mater. 311, 125312 (2021). https://doi.org/10.1016/J.CONBUILDMAT.2021.125312

[44]. Shi, C., Li, Y., Zhang, J., Li, W., Chong, L., Xie, Z., (2016). Performance enhancement of recycled concrete aggregate – A review. J. Clean. Prod. 112, 466–472. https://doi.org/10.1016/J.JCLEPRO.2015.08.057

[45]. Tam, V.W.Y., Soomro, M., Evangelista, A.C.J., (2018). A review of recycled aggregate in concrete applications (2000–2017). Constr.Build. Mater. 172, 272–292. https://doi.org/10.1016/J.CONBUILDMAT.2018.03.240

[46]. Ai, W., Liu, H., Zhang, J., Lv, S., Xu, Q., Li, H., (2020). Research on crushing and recycling of waste concrete. IOP Conf. Ser. Earth. Environ. Sci. https://doi.org/10.1088/1755-1315/446/3/032069

[47]. Choi, H., Lim, M., Choi, H., Kitagaki, R., Noguchi, T., (2014). Using Microwave Heating to Completely Recycle Concrete, J. Environ. Prot. (Irvine, Calif). 05. https://doi.org/10.4236/jep.2014.57060

[48]. Mistri, A., Bhattacharyya, S.K., Dhami, N., Mukherjee, A., Barai, S.V., (2020). A review on different treatment methods for enhancing the properties of recycled aggregates for sustainable construction materials. Constr. Build. Mater. 233, 117894. https://doi.org/10.1016/J.CONBUILDMAT.2019.117894

[49]. Shmlls, M., Abed, M., Fořt, J., Horvath, T., Bozsaky, D.,(2023). Towards closed-loop concrete recycling: Life cycle assessment and multi-criteria analysis, J. Clean. Prod., 410, 137179, https://doi.org/10.1016/j.jclepro.2023.137179

[50]. Sonmez, M., Ilcan, H., Dundar, B., Yildirim, G., Ersan, Y.C., Sahmaran, M., (2021). The effect of chemical- versus microbial-induced calcium carbonate mineralization on the enhancement of fine recycled concrete aggregate: A comparative study. J. Build. Eng. 44, 103316 (2021). https://doi.org/10.1016/J.JOBE.2021.103316

[51]. Konca, P., Szer, I., Szer, J., Obidowski, D., Gawin, D., Wiśniewski, P., Wiśniewski, B., Jóźwik, K. (2025). Sustainable Infrastructure: Recycled Concrete Aggregates for Cycle Paths. Materials, 18(1), 131. https://doi.org/10.3390/ma18010131

[52]. Zhan, B.J., Xuan, D.X., Poon, C.S., (2018). Enhancement of recycled aggregate properties by accelerated CO2 curing coupled with limewater soaking process. Cem. Concr. Compos. 89, 230–237. https://doi.org/10.1016/J.CEMCONCOMP.2018.03.011

[53]. Dündar, B., SönmezTuğluca, M., İlcan, H., Şahin, O., Şahmaran, M., (2023). The effects of various operational- and materials-oriented parameters on the carbonation performance of low-quality recycled concrete aggregate. J. Build. Eng. 68, 106138. https://doi.org/10.1016/j.jobe.2023.106138

[54]. Manan, A., Pu, Z., Ahmad, J., & Umar, M. (2025). Multi-targeted strength properties of recycled aggregate concrete through a machine learning approach. Eng. Comput., 42(1), 388–430. https://doi.org/10.1108/EC-07-2024-0635

[55]. Patel, S. V., Balakrishna Rao, K., Nayak, G. (2023). Prediction of recycled coarse aggregate concrete mechanical properties using multiple linear regression and artificial neural network. J. Eng. Design Technol., 21(6), 1690–1709. https://doi.org/10.1108/JEDT-07-2021-0373

[56]. Mahmoudian, A., Bypour, M., Kontoni, DP.N., (2024). Tree-based machine learning models for predicting the bond strength in reinforced recycled aggregate concrete. Asian J Civ Eng 25, 5899–5924 (2024). https://doi.org/10.1007/s42107-024-01153-2

[57]. Fanijo, E.O., Kolawole, J.T., Babafemi, A.J., Liu, J., (2023). A comprehensive review on the use of recycled concrete aggregate for pavement construction: Properties, performance, and sustainability, Clean. Mater., 9, 100199, https://doi.org/10.1016/j.clema.2023.100199

[58]. McNeil, K., Kang, T.H-K., (2013). Recycled Concrete Aggregates: A Review. Int J Concr Struct Mater 7, 61–69 (2013). https://doi.org/10.1007/s40069-013-0032-5

[59]. Prasittisopin, L., Tuvayanond, W., Kang, T. H.-K., Kaewunruen, S. (2025). Concrete Mix Design of Recycled Concrete Aggregate (RCA): Analysis of Review Papers, Characteristics, Research Trends, and Underexplored Topics. Resources, 14(2), 21. https://doi.org/10.3390/resources14020021

[60]. Danish, A., & Mosaberpanah, M. A. (2021). A review on recycled concrete aggregates (RCA) characteristics to promote RCA utilization in developing sustainable recycled aggregate concrete (RAC). Eur. J. Environ. Civ. Eng., 26(13), 6505–6539. https://doi.org/10.1080/19648189.2021.1946721

[61]. Mahmoud, A. S., Omar, A. S. (2024). Recycled Concrete Aggregates Utilization in Construction: Publications Trends, Bibliometric Analysis, and Literature Review (2011-2021). J. Scientometric Res., 13(3), 757–772. https://doi.org/10.5530/jscires.20041311

[62]. Feng, R., Xian, X., (2025). A review for accelerated carbonation improvement of recycled concrete coarse aggregates and the meta-analysis of environmental benefit assessment and cost analysis of concrete so produced, J. Build. Eng., 106, 112649, https://doi.org/10.1016/j.jobe.2025.112649.

[63]. Peiris, D., Gunasekara, C., Law, D.W., Patrisia, Y., Tam, VWY., Setunge, S., (2025) . Impact of treatment methods on recycled concrete aggregate performance: a comprehensive review. Environ Sci Pollut Res 32, 14405–14438. https://doi.org/10.1007/s11356-025-36497-y

[64]. Zhong, W., Wang, P., Ye, N., Shu, K., Dai, R., Ba, M., & Fang, X. (2025). Effects of Different Carbonation Treatment Methods for Recycled Concrete Aggregate. Buildings, 15(17), 3054. https://doi.org/10.3390/buildings15173054

[65]. Saavedra, R., Etxeberria, M. (2025). Carbonation Treatments for Durable Low-Carbon Recycled Aggregate Concrete. Materials, 18(17), 4168. https://doi.org/10.3390/ma18174168

[66]. Gebremariam, H.G., Taye, S., Tarekegn, A.G., (2024). Parent Concrete Strength Effects on the Quality of Recycled Aggregate Concrete: A Review, Heliyon, 10(4), e26212, https://doi.org/10.1016/j.heliyon.2024.e26212

[67]. Onyelowe, K.C., Kamchoom, V., Hanandeh, S., Kumar, A., Zabala Vizuete, R., et al.(2025). Physics-informed modeling of splitting tensile strength of recycled aggregate concrete using advanced machine learning. Sci Rep 15, 7135 (2025). https://doi.org/10.1038/s41598-025-91980-3

[68]. Pan, X., Xiao, Y., Suhail, S. A., Ahmad, W., Murali, G., Salmi, A., & Mohamed, A. (2022). Use of Artificial Intelligence Methods for Predicting the Strength of Recycled

Aggregate Concrete and the Influence of Raw Ingredients. Materials, 15(12), 4194. https://doi.org/10.3390/ma15124194

[69]. Zhang, M., Kang, R., (2025). Machine learning methods for predicting the durability of concrete materials: A review. Adv. Cem. Res., 37 (9): 502-517. https://doi.org/10.1680/jadcr.24.00133

[70]. Yuan X, Tian Y, Ahmad W, Ahmad A, Usanova KI, Mohamed AM, Khallaf R. Machine Learning Prediction Models to Evaluate the Strength of Recycled Aggregate Concrete. Materials (Basel). 2022 Apr 12;15(8):2823. https://doi.org/10.3390/ma15082823

[71]. Chen, Y., Chen, C., Cai, Z., Zhu, P., Liu, R., Liu, H., (2025). Effect of strength of parent concrete on utilization of recycled aggregate concrete: A review, J. Build. Eng., 103, 112187, https://doi.org/10.1016/j.jobe.2025.112187

[72]. Han, A.L., Setiawan, H., Hajek, P., (2019). Laboratory Concrete Specimens Waste, a Case Study on Life Cycle Assessment. IOP Conf. Ser.: Earth Environ. Sci. 290, 012015. https://doi.org/10.1088/1755-1315/290/1/012015

7. APPENDICES

Appendix A. RCA preparations and physical property tests

a. Moisture preparation of RCA at 50% water absorption capacity for carbonation test

Parent concrete grade	Mass of sample @SSD (g)	Mass of sample @ oven dry (g)	Water absorption (%)
NRCA25	5510	5184.359	5.91
NRCA67	5503	5260.3177	4.41

Parent concrete grade	Mass of air dry sample (g)	Mass of oven dry sample (g)	Moisture content (air dry (%))	Water absorption @SSD (%)	50% moisture content (w.r to total volume of voids (%))	Required mass of water to be added (%)
NRCA25	1730	1700	1.73	5.91	2.955	1.22
NRCA67	2000	1935	3.25	4.41	2.205	-1.05

Mass of samples (g)	Volume of water to be added in %	Volume of water to be added (ml)
1150	0.14	140.34
1199	-0.13	-125.3

b. Water absorption of NRCA and ARCA.

Sample Name	No. of Trials		Trial 1	Trial 2	Trial 3	Average
N(25)-control	A	Weight of Saturated Surface-Dry sample in air, gm	2000.0 0	2000.00	2000.00	2000.00
	B	Weight of Oven Dry sample in air, gm	1952.5 6	1959.06	1956.18	1955.93
	Test temperature ,ºC		23 ± 2	23 ± 2	23 ± 2	23 ± 2
	Formulation					
	C	Water Absorption = (A-B)/B*100	2.43	2.09	2.24	2.25
NRAC(25)	A	Weight of Saturated Surface-Dry sample in air, gm	2000.0 0	2000.00	2000.00	2000.00
	B	Weight of Oven Dry sample in air, gm	1883.5 9	1891.27	1890.34	1888.41
	Test temperature ,ºC		23 ± 2	23 ± 2	23 ± 2	23 ± 2
	Formulation					
	C	Water Absorption = (A-B)/B*100	6.18	5.75	5.80	5.91
ARAC(25)	A	Weight of Saturated Surface-Dry sample in air, gm	2000.0 0	2000.00	2000.00	2000.00

	B	Weight of Oven Dry sample in air, gm	1903.08	1904.61	1914.32	1907.34
		Test temperature ,ºC	23 ± 2	23 ± 2	23 ± 2	23 ± 2
		Formulation				
	C	Water Absorption = (A-B)/B*100	5.09	5.01	4.48	4.86
N(67)-control	A	Weight of Saturated Surface-Dry sample in air, gm	2000.00	2000.00	2000.00	2000.00
	B	Weight of Oven Dry sample in air, gm	1952.01	1958.72	1957.77	1956.17
		Test temperature ,ºC	23 ± 2	23 ± 2	23 ± 2	23 ± 2
		Formulation				
	C	Water Absorption = (A-B)/B*100	2.46	2.11	2.16	2.24
NRAC(67)	A	Weight of Saturated Surface-Dry sample in air, gm	2000.00	2000.00	2000.00	2000.00
	B	Weight of Oven Dry sample in air, gm	1919.38	1925.08	1927.88	1924.11
		Test temperature ,ºC	23 ± 2	23 ± 2	23 ± 2	23 ± 2
	Formulation					
	C	Water Absorption = (A-B)/B*100	4.20	3.89	3.74	3.94
ARAC(67)	A	Weight of Saturated Surface-Dry sample in air, gm	2000.00	2000.00	2000.00	2000.00
	B	Weight of Oven Dry sample in air, gm	1927.73	1927.61	1921.69	1925.68
		Test temperature ,ºC	23 ± 2	23 ± 2	23 ± 2	23 ± 2
		Formulation				
	C	Water Absorption = (A-B)/B*100	3.75	3.76	4.08	3.86

c. Crushing values of NRCA and ARCA

Sample Name	Total weight of sample (g)				Weight passing 2.36mm sieve(g)				Average Aggregate crushing value (%)
	Trial 1	Trial 2	Trial 3	average	Trial 1	Trial 2	Trial 3	average	
N(25)-control	2000	2000	2000	2000	343.80	347.70	392.00	361.17	18.06
NRAC(25)	2000	2000	2000	2000	591.00	600.80	651.00	614.27	30.71

ARAC(25)	2000	2000	2000	2000	535.00	550.60	631.20	572.27	28.61
N(67)-control	2000	2000	2000	2000	319.20	364.20	397.80	360.40	18.02
NRAC(67)	2000	2000	2000	2000	467.00	470.00	560.80	499.27	24.96
ARAC(67)	2000	2000	2000	2000	405.40	440.00	476.30	440.57	22.03

Appendix B. Microstructural data

The microstructural data used in this study can be found from Zenodo data depository link:

https://doi.org/10.5281/zenodo.17338716

Appendix C. Strength properties

The compressive, split tensile and flexural strength test results used in this study can be found from Zenodo data depository link:

https://doi.org/10.5281/zenodo.17338716

Appendix D. Python script for aggregation, comprehensive ML and SHAP analysis

Optimization of composite indices

```
import pandas as pd
import numpy as np
import random
import statsmodels.api as sm
from statsmodels.stats.outliers_influence import variance_inflation_factor
import seaborn as sns
import matplotlib.pyplot as plt
from sklearn.linear_model import LinearRegression
from sklearn.metrics import r2_score, mean_absolute_error, mean_squared_error
def evaluate_indices(data, exponents):
    a1, a2, a3, a4, a5, a6, a7, a8, a9 = exponents
    X1 = data['Rr'] ** a1
    X2 = data['Dc'] ** a2
    X3 = ((data['C/Ca'] ** a3) * (data['C/Fa'] ** a4)) / (data['W/C'] ** a5)
    X4 = (((data['Pcs'] ** a6) / ((data['Wa'] ** a7) * (data['Cv'] ** a8))) ** a9)
    X = pd.DataFrame({'X1': X1, 'X2': X2, 'X3': X3, 'X4': X4})
    corr = X.corr().abs()
    max_corr = corr.where(np.triu(np.ones(corr.shape), k=1).astype(bool)).max().max()
    X_vif = sm.add_constant(X)
    vif_values = [variance_inflation_factor(X_vif.values, i+1) for i in range(len(X.columns))]
    vif_df = pd.DataFrame({'Feature': ['X1', 'X2', 'X3', 'X4'], 'VIF': vif_values})
    max_vif = vif_df['VIF'].max()
    score = max_corr + 0.1 * max_vif
    return score, max_corr, max_vif, X, vif_df
data = pd.read_csv("individual_data.csv")
best_score = float('inf')
best_exponents = None
best_corr = None
```

```
best_vif = None
best_X = None
best_vif_table = None
ranges = {
    'a1': (0.5, 2.0),
    'a2': (0.1, 1.5),
    'a3': (0.5, 2.0),
    'a4': (0.5, 2.0),
    'a5': (0.5, 2.0),
    'a6': (1.0, 3.0),
    'a7': (0.5, 2.0),
    'a8': (0.5, 2.0),
    'a9': (0.1, 1.0)
}
print("Optimizing exponents... please wait (~1–2 minutes)\n")
for i in range(2000):
    exponents = [random.uniform(*ranges[f'a{j+1}']) for j in range(9)]
    score, corr_val, vif_val, X_tmp, vif_df = evaluate_indices(data, exponents)
    if score < best_score:
        best_score, best_corr, best_vif = score, corr_val, vif_val
        best_exponents = exponents
        best_X = X_tmp
        best_vif_table = vif_df.copy()
print("=== OPTIMIZATION RESULTS ===")
params = [f'a{i+1}' for i in range(9)]
for p, v in zip(params, best_exponents):
    print(f"{p} = {v:.3f}")
print(f"\nBest combined score: {best_score:.4f}")
print(f"Maximum correlation: {best_corr:.3f}")
print(f"Maximum VIF: {best_vif:.3f}\n")
```

```
data[['X1', 'X2', 'X3', 'X4']] = best_X
print("=== VARIANCE INFLATION FACTORS (VIF) ===")
print(best_vif_table.to_string(index=False))
corr_with_target = data[['X1', 'X2', 'X3', 'X4', 'CS']].corr()
plt.figure(figsize=(7, 5))
sns.heatmap(corr_with_target, annot=True, cmap='coolwarm', fmt=".2f")
plt.title("Correlation Matrix (Composite Indices + CS)")
plt.show()
plt.figure(figsize=(6, 4))
sns.barplot(x='Feature', y='VIF', data=best_vif_table)
plt.title("Variance Inflation Factors (Optimized Indices)")
plt.ylabel("VIF Value")
plt.show()
data.to_csv("optimized_composite_indices_with_CS.csv", index=False)
print("\nOptimized dataset saved as 'optimized_composite_indices_with_CS.csv'")
X_final = data[['X1', 'X2', 'X3', 'X4']]
y = data['CS']
model = LinearRegression()
model.fit(X_final, y)
y_pred = model.predict(X_final)
r2 = r2_score(y, y_pred)
mae = mean_absolute_error(y, y_pred)
rmse = np.sqrt(mean_squared_error(y, y_pred))
print("\n=== LINEAR REGRESSION PERFORMANCE ===")
print(f"R²:   {r2:.3f}")
print(f"MAE:  {mae:.3f}")
print(f"RMSE: {rmse:.3f}")
```

full pipeline

Importing necessary libraries

```
import os
```

```
import json
import numpy as np
import pandas as pd
import matplotlib.pyplot as plt
import seaborn as sns
import shap
import joblib
from scipy import stats
from scipy.spatial import distance
from sklearn.model_selection import train_test_split, KFold, RandomizedSearchCV
from sklearn.metrics import mean_squared_error, mean_absolute_error, r2_score
from sklearn.linear_model import LinearRegression, Ridge
from sklearn.preprocessing import PolynomialFeatures
from sklearn.tree import DecisionTreeRegressor, export_text
from sklearn.ensemble import RandomForestRegressor
from lightgbm import LGBMRegressor
```

Dataset loading

```
CSV_PATH = "individual_data.csv"
PREDICTORS = ["C/Ca", "C/Fa", "W/C", "Wa", "Cv", "Rr", "Dc", "Pcs"]
PRED_UNITS = {"C/Ca": "unitless",
"C/Fa": "unitless",
"W/C": "unitless",
"Wa": "%",
"Cv": "%",
"Rr": "%",
"Dc": "%",
"Pcs": "MPa"}
TARGET = "CS"
TARGET_UNIT = "MPa"
TEST_SIZE = 0.20
```

```
RANDOM_SEED_SPLIT = 42
N_FOLDS = 5
KFOLD_RANDOM_STATE = 42
N_SEARCH_ITER = 30
CV_FOR_SEARCH = 5
N_REPEATS = 1
SHAP_BG_SIZE = 200
```

Specifying output directories

```
OUTDIR = "outputs"
PLOTS_DIR = os.path.join(OUTDIR, "plots")
SHAP_DIR = os.path.join(OUTDIR, "shap")
MODELS_DIR = os.path.join(OUTDIR, "models")
os.makedirs(PLOTS_DIR, exist_ok=True)
os.makedirs(SHAP_DIR, exist_ok=True)
os.makedirs(MODELS_DIR, exist_ok=True)
```

CSV loading

```
expected_cols = PREDICTORS + [TARGET]
try:
    df_try = pd.read_csv(CSV_PATH)
    if list(df_try.columns) == expected_cols or TARGET in df_try.columns:
        df = df_try.copy()
    else:
        df = pd.read_csv(CSV_PATH, header=None)
        if df.shape[1] == len(expected_cols):
            df.columns = expected_cols
        else:
            raise ValueError(f"CSV columns do not match expected {expected_cols}")
except Exception as e:
    df = pd.read_csv(CSV_PATH, header=None)
    if df.shape[1] == len(expected_cols):
```

```
        df.columns = expected_cols
    else:
        raise RuntimeError(f"Failed to read CSV: {e}")
df = df.apply(pd.to_numeric, errors="coerce").dropna().reset_index(drop=True)
print(f"Loaded data: {df.shape[0]} rows, {df.shape[1]} columns")
print(f"Target range: min={df[TARGET].min():.3f}, max={df[TARGET].max():.3f} {TARGET_UNIT}")
X_all = df[PREDICTORS].copy()
y_all = df[TARGET].values.reshape(-1, 1)
```

Evaluation function definitions

```
def compute_metrics(y_true, y_pred):
    y_true = np.asarray(y_true).flatten()
    y_pred = np.asarray(y_pred).flatten()
    rmse = np.sqrt(mean_squared_error(y_true, y_pred))
    mae  = mean_absolute_error(y_true, y_pred)
    r2   = r2_score(y_true, y_pred)
    denom = (y_true.max() - y_true.min())
    nrmse = rmse / denom if denom != 0 else np.nan
    return {"MAE": float(mae), "RMSE": float(rmse), "R2": float(r2), "NRMSE": float(nrmse)}
def mean_and_95ci(arr):
    arr = np.asarray(arr)
    mean = float(np.mean(arr))
    lo = float(np.percentile(arr, 2.5))
    hi = float(np.percentile(arr, 97.5))
    return mean, lo, hi
def compute_error_ranges(y_true, y_pred):
    resid = np.asarray(y_true).flatten() - np.asarray(y_pred).flatten()
    abs_resid = np.abs(resid)
    perc_95 = float(np.percentile(abs_resid, 95))
    perc_99 = float(np.percentile(abs_resid, 99))
    max_err = float(np.max(abs_resid))
```

```
    return {"95th_pct_error": perc_95, "99th_pct_error": perc_99, "max_error": max_err}
```

Model definitions & hyperparameter search spaces

```
estimators = {
    "MLR": LinearRegression(),
    "Polynomial MLR (deg=2)": LinearRegression(),
    "Ridge": Ridge(random_state=42),
    "Decision Tree": DecisionTreeRegressor(random_state=42),
    "Random Forest": RandomForestRegressor(random_state=42),
    "LightGBM": LGBMRegressor(random_state=42)
}
search_spaces = {
    "Decision Tree": {
        "max_depth": [None, 3, 5, 10, 20],
        "min_samples_split": [2, 5, 10, 20],
        "min_samples_leaf": [1, 2, 4, 8]
    },
    "Random Forest": {
        "n_estimators": [100, 200, 400],
        "max_depth": [None, 5, 10, 20],
        "min_samples_split": [2, 5, 10],
        "min_samples_leaf": [1, 2, 4]
    },
    "LightGBM": {
        "n_estimators": [100, 200, 400],
        "num_leaves": [15, 31, 63],
        "max_depth": [-1, 5, 10, 20],
        "learning_rate": [0.001, 0.01, 0.05, 0.1],
        "min_child_samples": [5, 10, 20, 50]
    },
    "Ridge": {
```

```
        "alpha": list(np.logspace(-6, 3, 50))
    }
}
with open(os.path.join(OUTDIR, "search_spaces.json"), "w") as f:
    json.dump(search_spaces, f, indent=2, default=lambda x: list(x) if hasattr(x, "__iter__") else
str(x))
```

Data Splitting and locking

```
X_train_full, X_test_locked, y_train_full, y_test_locked = train_test_split(
    X_all, y_all, test_size=TEST_SIZE, random_state=RANDOM_SEED_SPLIT
)
pd.DataFrame({"index": X_test_locked.index}).to_csv(os.path.join(OUTDIR,
"locked_test_indices.csv"), index=False)
cv_fold_metrics = []
locked_test_results = []
hyperparams_records = []
seeds_used = {"split_seed": RANDOM_SEED_SPLIT, "kfold_seed": KFOLD_RANDOM_STATE,
"search_seed": 42}
with open(os.path.join(OUTDIR, "seeds_used.json"), "w") as f:
    json.dump(seeds_used, f, indent=2)
```

Cross-validation setup and looping

```
kf = KFold(n_splits=N_FOLDS, shuffle=True, random_state=KFOLD_RANDOM_STATE)
for fold_id, (train_idx, val_idx) in enumerate(kf.split(X_train_full), start=1):
    print(f"\n=== CV Fold {fold_id}/{N_FOLDS} ===")
    X_tr = X_train_full.iloc[train_idx].reset_index(drop=True)
    X_val = X_train_full.iloc[val_idx].reset_index(drop=True)
    y_tr = y_train_full[train_idx].reshape(-1, 1)
    y_val = y_train_full[val_idx].reshape(-1, 1)
    for name, estimator in estimators.items():
        print(f" Fold {fold_id}: training {name} ...")
        fitted_poly = None
        best_params = {}
```

```
if name in search_spaces:
    base = estimator
    if name == "Decision Tree":
        base = DecisionTreeRegressor(random_state=42)
    elif name == "Random Forest":
        base = RandomForestRegressor(random_state=42)
    elif name == "LightGBM":
        base = LGBMRegressor(random_state=42, verbosity=-1)
    elif name == "Ridge":
        base = Ridge(random_state=42)
    rs = RandomizedSearchCV(
        estimator=base,
        param_distributions=search_spaces[name],
        n_iter=N_SEARCH_ITER,
        scoring="neg_mean_absolute_error",
        cv=CV_FOR_SEARCH,
        random_state=42,
        n_jobs=-1,
        verbose=0,
        refit=True
    )
    try:
        rs.fit(X_tr.values, y_tr.flatten())
        best = rs.best_estimator_
        best_params = rs.best_params_
    except Exception as e:
        print(f"RandomizedSearchCV failed for {name} on fold {fold_id}: {e}")
        base.fit(X_tr.values, y_tr.flatten())
        best = base
        best_params = {"fallback": True}
```

```
        y_val_pred = best.predict(X_val.values).reshape(-1,1)
        y_tr_pred = best.predict(X_tr.values).reshape(-1,1)
    # Polynomial MLR
    elif name == "Polynomial MLR (deg=2)":
        poly = PolynomialFeatures(degree=2, include_bias=False)
        Xtr_poly = poly.fit_transform(X_tr)
        Xval_poly = poly.transform(X_val)
        lr = LinearRegression()
        lr.fit(Xtr_poly, y_tr.flatten())
        y_val_pred = lr.predict(Xval_poly).reshape(-1,1)
        y_tr_pred = lr.predict(Xtr_poly).reshape(-1,1)
        best = lr
        fitted_poly = poly
        best_params = {"poly_degree": 2}
    # Linear MLR
    else:
        est = estimator
        est.fit(X_tr.values, y_tr.flatten())
        y_val_pred = est.predict(X_val.values).reshape(-1,1)
        y_tr_pred = est.predict(X_tr.values).reshape(-1,1)
        best = est
        best_params = {"fitted_default": True}
    # Metrics
    val_metrics = compute_metrics(y_val, y_val_pred)
    tr_metrics = compute_metrics(y_tr, y_tr_pred)
    val_percentiles = compute_error_ranges(y_val, y_val_pred)
    tr_percentiles = compute_error_ranges(y_tr, y_tr_pred)

    cv_fold_metrics.append({
        "Model": name, "Fold": fold_id, "Dataset": "Train",
```

```
        "MAE": tr_metrics["MAE"], "RMSE": tr_metrics["RMSE"], "R2": tr_metrics["R2"],
"NRMSE": tr_metrics["NRMSE"],
        "95th_pct_error": tr_percentiles["95th_pct_error"],
        "99th_pct_error": tr_percentiles["99th_pct_error"],
        "max_error": tr_percentiles["max_error"]
      })
      cv_fold_metrics.append({
        "Model": name, "Fold": fold_id, "Dataset": "Test",
        "MAE": val_metrics["MAE"], "RMSE": val_metrics["RMSE"], "R2": val_metrics["R2"],
"NRMSE": val_metrics["NRMSE"],
        "95th_pct_error": val_percentiles["95th_pct_error"],
        "99th_pct_error": val_percentiles["99th_pct_error"],
        "max_error": val_percentiles["max_error"]
      })
      joblib.dump({"estimator": best, "poly": fitted_poly, "best_params": best_params},
            os.path.join(MODELS_DIR, f"{name}_fold{fold_id}.pkl"))
      hyperparams_records.append({"fold": fold_id, "model": name, "best_params":
best_params})
cv_metrics_df = pd.DataFrame(cv_fold_metrics)
cv_metrics_df.to_csv(os.path.join(OUTDIR, "cv_fold_metrics.csv"), index=False)
print(f"Saved cross-validation metrics (including percentile errors) to {os.path.join(OUTDIR,
'cv_fold_metrics.csv')}")
final_results = []
fitted_final_models = {}
final_hyperparams = []
for name, estimator in estimators.items():
  print(f"\n=== Final training for model: {name} ===")
  fitted_poly = None
  best_params = {}
```

Models with hyperparameter search

```
  if name in search_spaces:
    base = estimator
```

```
  if name == "Decision Tree":
    base = DecisionTreeRegressor(random_state=42)
  elif name == "Random Forest":
    base = RandomForestRegressor(random_state=42)
  elif name == "LightGBM":
    base = LGBMRegressor(random_state=42, verbosity=-1)
  elif name == "Ridge":
    base = Ridge(random_state=42)
  rs = RandomizedSearchCV(
    estimator=base,
    param_distributions=search_spaces[name],
    n_iter=N_SEARCH_ITER,
    scoring="neg_mean_absolute_error",
    cv=CV_FOR_SEARCH,
    random_state=42,
    n_jobs=-1,
    verbose=0,
    refit=True
  )
  rs.fit(X_train_full.values, y_train_full.flatten())
  best = rs.best_estimator_
  fitted_final_models[name] = (best, None)
  final_hyperparams.append({"model": name, "best_params": rs.best_params_})
  preds_test = best.predict(X_test_locked.values).reshape(-1,1)
  preds_train = best.predict(X_train_full.values).reshape(-1,1)
  joblib.dump(best, os.path.join(MODELS_DIR, f"{name}_final_tuned.pkl"))
  best_params = rs.best_params_
elif name == "Polynomial MLR (deg=2)":
  poly = PolynomialFeatures(degree=2, include_bias=False)
  Xtr_poly = poly.fit_transform(X_train_full)
```

```
    lr = LinearRegression().fit(Xtr_poly, y_train_full.flatten())
    fitted_final_models[name] = (lr, poly)
    preds_test = lr.predict(poly.transform(X_test_locked)).reshape(-1,1)
    preds_train = lr.predict(Xtr_poly).reshape(-1,1)
    final_hyperparams.append({"model": name, "best_params": {"poly_degree": 2}})
    fitted_poly = poly
    best = lr
else:
    estimator.fit(X_train_full.values, y_train_full.flatten())
    fitted_final_models[name] = (estimator, None)
    preds_test = estimator.predict(X_test_locked.values).reshape(-1,1)
    preds_train = estimator.predict(X_train_full.values).reshape(-1,1)
    final_hyperparams.append({"model": name, "best_params": "default_fit"})
    best = estimator
train_metrics = compute_metrics(y_train_full, preds_train)
test_metrics = compute_metrics(y_test_locked, preds_test)
train_percentiles = compute_error_ranges(y_train_full, preds_train)
test_percentiles = compute_error_ranges(y_test_locked, preds_test)
final_results.append({
    "Model": name,
    "Train_MAE": train_metrics["MAE"],
    "Train_RMSE": train_metrics["RMSE"],
    "Train_R2": train_metrics["R2"],
    "Train_95th_pct_error": train_percentiles["95th_pct_error"],
    "Train_99th_pct_error": train_percentiles["99th_pct_error"],
    "Train_max_error": train_percentiles["max_error"],
    "Test_MAE": test_metrics["MAE"],
    "Test_RMSE": test_metrics["RMSE"],
    "Test_R2": test_metrics["R2"],
    "Test_95th_pct_error": test_percentiles["95th_pct_error"],
```

```
        "Test_99th_pct_error": test_percentiles["99th_pct_error"],
        "Test_max_error": test_percentiles["max_error"]
    })
    pred_df = pd.DataFrame({
        "Model": name,
        "Actual": y_test_locked.flatten(),
        "Predicted": preds_test.flatten()
    })
    pred_df["Residual"] = pred_df["Actual"] - pred_df["Predicted"]
    pred_df.to_csv(os.path.join(OUTDIR, f"predictions_lockedtest_{name.replace(' ','_')}.csv"),
index=False)
    pd.DataFrame([{"Model": name, **test_metrics,
                "95th_pct_error": test_percentiles["95th_pct_error"],
                "99th_pct_error": test_percentiles["99th_pct_error"],
                "max_error": test_percentiles["max_error"]}]).to_csv(
        os.path.join(OUTDIR, f"metrics_lockedtest_{name.replace(' ','_')}.csv"), index=False
    )
final_results_df = pd.DataFrame(final_results).sort_values("Test_RMSE")
final_results_df.to_csv(os.path.join(OUTDIR, "final_test_results.csv"), index=False)
pd.DataFrame(final_hyperparams).to_csv(os.path.join(OUTDIR, "final_hyperparameters.csv"),
index=False)
print(f"Saved final results and hyperparameters to {OUTDIR}")
```

Regression equations

```
eq_lines = []
for name in ["MLR", "Polynomial MLR (deg=2)", "Ridge"]:
    if name not in fitted_final_models:
        continue
    mdl, poly = fitted_final_models[name]
    try:
        if poly is not None:
            feat_names = poly.get_feature_names_out(PREDICTORS)
```

```
            coefs = mdl.coef_.flatten()
            eq = " + ".join([f"{coef:.6f}*{fn}" for coef, fn in zip(coefs, feat_names)])
            intercept = float(mdl.intercept_)
            eq_lines.append(f"{name} equation: CS (MPa) = {intercept:.6f} + {eq}")
        else:
            coefs = mdl.coef_.flatten() if hasattr(mdl, "coef_") else None
            if coefs is not None:
                eq = " + ".join([f"{coef:.6f}*{f}" for coef, f in zip(coefs, PREDICTORS)])
                intercept = float(mdl.intercept_)
                eq_lines.append(f"{name} equation: CS (MPa) = {intercept:.6f} + {eq}")
    except Exception as e:
        print(f"Could not derive equation for {name}: {e}")
with open(os.path.join(OUTDIR, "Regression_Equations.txt"), "w") as f:
    f.write("\n".join(eq_lines))
print(f"Saved regression equations to {os.path.join(OUTDIR, 'Regression_Equations.txt')}")
```

Parity plots, residual histograms, Q-Q plots

```
for i, row in final_results_df.iterrows():
    name = row["Model"]
    pred_file = os.path.join(OUTDIR, f"predictions_lockedtest_{name.replace(' ', '_')}.csv")
    if not os.path.exists(pred_file):
        continue
    pdf = pd.read_csv(pred_file)
    plt.figure(figsize=(6,6))
    plt.scatter(pdf["Actual"], pdf["Predicted"], alpha=0.8, s=40)
    mn, mx = min(pdf["Actual"].min(), pdf["Predicted"].min()), max(pdf["Actual"].max(),
pdf["Predicted"].max())
    plt.plot([mn, mx], [mn, mx], 'k--', label="y = x")
    plt.xlabel(f"Actual {TARGET} ({TARGET_UNIT})")
    plt.ylabel(f"Predicted {TARGET} ({TARGET_UNIT})")
    plt.title(f"Parity Plot – {name}")
```

```
    m = compute_metrics(pdf["Actual"].values, pdf["Predicted"].values)
    ann = f"R²={m['R2']:.3f}\nMAE={m['MAE']:.3f} {TARGET_UNIT}\nRMSE={m['RMSE']:.3f}
{TARGET_UNIT}"
    plt.annotate(ann, xy=(0.05, 0.95), xycoords='axes fraction', va='top', ha='left',
                 bbox=dict(boxstyle="round", fc="w"))
    plt.grid(True)
    plt.legend()
    plt.tight_layout()
    plt.savefig(os.path.join(PLOTS_DIR, f"Parity_lockedtest_{name.replace(' ', '_')}.png"), dpi=300)
    plt.close()
    resid = pdf["Actual"] - pdf["Predicted"]
    plt.figure(figsize=(6,4))
    sns.histplot(resid, bins=30, kde=True)
    plt.title(f"Residual Histogram - {name}")
    plt.xlabel(f"Residual ({TARGET_UNIT})")
    plt.tight_layout()
    plt.savefig(os.path.join(PLOTS_DIR, f"ResidualHist_lockedtest_{name.replace(' ', '_')}.png"),
dpi=300)
    plt.close()
    plt.figure(figsize=(6,4))
    stats.probplot(resid, dist="norm", plot=plt)
    plt.title(f"Q–Q Plot (Test Residuals) - {name}")
    plt.tight_layout()
    plt.savefig(os.path.join(PLOTS_DIR, f"QQ_lockedtest_{name.replace(' ', '_')}.png"), dpi=300)
    plt.close()
print(f"Saved parity, residual histograms, and Q-Q plots to {PLOTS_DIR}")
```

Feature importance for tree ensembles

```
fi_records = []
for name in ["Random Forest", "LightGBM", "Decision Tree"]:
    if name in fitted_final_models:
        model, _ = fitted_final_models[name]
```

```
        if hasattr(model, "feature_importances_"):
            for feat, imp in zip(PREDICTORS, model.feature_importances_):
                fi_records.append({"Model": name, "Feature": feat, "Importance": float(imp)})
fi_df = pd.DataFrame(fi_records)
if not fi_df.empty:
    fi_df.to_csv(os.path.join(OUTDIR, "feature_importance_final.csv"), index=False)
    print(f"Saved feature importance table to {os.path.join(OUTDIR,
'feature_importance_final.csv')}")
```

Plot feature importance for best model

```
best_model_name = final_results_df.loc[final_results_df["Test_RMSE"].idxmin(), "Model"]
if best_model_name in ["Random Forest", "LightGBM", "Decision Tree"] and not fi_df.empty:
    bm = fi_df[fi_df["Model"] == best_model_name]
    plt.figure(figsize=(8,6))
    sns.barplot(x="Importance", y="Feature", data=bm.sort_values("Importance",
ascending=False))
    plt.title(f"Feature Importance – Best Model ({best_model_name})")
    plt.tight_layout()
    plt.savefig(os.path.join(PLOTS_DIR, f"FeatureImportance_{best_model_name.replace('
','_')}.png"), dpi=300)
    plt.close()
    print(f"Saved feature importance plot for best model to {PLOTS_DIR}")
```

SHAP explainability

```
shap_records = []
dependence_feats = PREDICTORS[:3]
bg_size = min(SHAP_BG_SIZE, len(X_train_full))
X_bg = X_train_full.sample(n=bg_size, random_state=0)
print(f"\nSHAP background sample size: {bg_size}")
for name, (model_obj, poly) in fitted_final_models.items():
    try:
        print(f"Computing SHAP for {name} ...")
        if any(t in name for t in ["Random Forest", "Decision Tree", "LightGBM"]):
```

```
        expl = shap.TreeExplainer(model_obj, data=X_bg if poly is None else
poly.transform(X_bg))
    elif hasattr(model_obj, "coef_"):
        expl = shap.LinearExplainer(model_obj, X_bg if poly is None else poly.transform(X_bg))
    else:
        expl = shap.KernelExplainer(model_obj.predict, X_bg if poly is None else
poly.transform(X_bg))
    # Subsample for speed
    n_eval = min(500, len(X_train_full))
    X_shap_eval = X_train_full.sample(n=n_eval, random_state=1)
    X_shap_for_calc = X_shap_eval if poly is None else poly.transform(X_shap_eval)
    shap_vals = expl(X_shap_for_calc)
    # Summary plot
    plt.figure(figsize=(6,4))
    fnames = list(X_shap_eval.columns) if poly is None else
list(poly.get_feature_names_out(PREDICTORS))
    shap.summary_plot(shap_vals, X_shap_for_calc, feature_names=fnames, show=False)
    plt.title(f"SHAP Summary (mean |SHAP|) - {name}")
    plt.tight_layout()
    plt.savefig(os.path.join(SHAP_DIR, f"{name.replace(' ','_')}_SHAP_summary.png"), dpi=300)
    plt.close()
                              # Global mean |SHAP|
    vals = shap_vals.values if hasattr(shap_vals, "values") else np.array(shap_vals)
    mean_abs = np.mean(np.abs(vals), axis=0)
    for feat, val in zip(fnames, mean_abs):
        shap_records.append({"Model": name, "Feature": feat, "mean_abs_shap": float(val)})
    # Dependence plots
    for feat in dependence_feats:
        if feat in X_shap_eval.columns:
            plt.figure(figsize=(5,4))
            shap.dependence_plot(feat, vals, X_shap_eval, show=False,
feature_names=list(X_shap_eval.columns))
```

```
            unit = PRED_UNITS.get(feat, "")
            plt.xlabel(f"{feat} ({unit})")
            plt.ylabel(f"SHAP value (impact on {TARGET} in {TARGET_UNIT})")
            plt.title(f"SHAP dependence: {feat} - {name}")
            plt.tight_layout()
            plt.savefig(os.path.join(SHAP_DIR, f"{name.replace('
','_')}_dependence_{feat.replace('/','_')}.png"), dpi=300)
            plt.close()
   except Exception as e:
      print(f"SHAP failed for model {name}: {e}")
if shap_records:
   pd.DataFrame(shap_records).to_csv(os.path.join(OUTDIR, "shap_global_mean_abs.csv"),
index=False)
   print(f"Saved global mean |SHAP| to {os.path.join(OUTDIR, 'shap_global_mean_abs.csv')}")
else:
   print("No SHAP records to save.")
```

Appendix E. ML outputs

1. Sample metrics for each fold on composite datasets.

Model	Fold	Dataset	MAE	RMSE	R2	NRMSE	95th % error	99th % error	Max error
MLR	1	Train	3.0519	3.7000	0.9572	0.0714	7.3162	8.1567	8.9808
MLR	1	Test	4.1771	4.7222	0.9201	0.0955	7.0951	7.9756	8.1957
Polynomial MLR (deg=2)	1	Train	0.8752	1.0694	0.9964	0.0206	1.9005	2.5055	2.6471
Polynomial MLR (deg=2)	1	Test	1.7541	2.6310	0.9752	0.0532	6.6331	7.3131	7.4831
Ridge	1	Train	3.0277	3.7158	0.9569	0.0717	7.4134	8.5834	9.0680
Ridge	1	Test	4.2285	4.7935	0.9176	0.0969	7.3928	8.5624	8.8548
Decision Tree	1	Train	0.6964	0.8636	0.9977	0.0167	1.7182	1.8631	1.9050
Decision Tree	1	Test	1.8325	2.9660	0.9685	0.0600	7.8767	8.5567	8.7267
Random Forest	1	Train	0.7145	0.8774	0.9976	0.0169	1.7883	1.8441	1.8492
Random Forest	1	Test	1.5987	2.5271	0.9771	0.0511	6.5266	7.2066	7.3766
LightGBM	1	Train	0.6994	0.8646	0.9977	0.0167	1.7374	1.8556	1.8967
LightGBM	1	Test	1.8290	2.9667	0.9685	0.0600	7.8772	8.5572	8.7272
MLR	2	Train	3.5125	4.0750	0.9497	0.0779	6.9857	7.7213	8.1572
MLR	2	Test	2.8322	3.3439	0.9501	0.0703	5.4699	6.1217	6.2846
Polynomial MLR (deg=2)	2	Train	0.9763	1.2233	0.9955	0.0234	2.4298	2.6534	2.7423
Polynomial MLR (deg=2)	2	Test	1.5124	1.6744	0.9875	0.0352	2.5329	2.6071	2.6257
Ridge	2	Train	3.5125	4.0750	0.9497	0.0779	6.9857	7.7213	8.1572
Ridge	2	Test	2.8322	3.3439	0.9501	0.0703	5.4699	6.1217	6.2846
Decision Tree	2	Train	0.7158	0.8852	0.9976	0.0169	1.8453	2.0381	2.1020
Decision Tree	2	Test	0.8903	1.0917	0.9947	0.0229	1.9875	2.2247	2.2840
Random Forest	2	Train	0.7229	0.9024	0.9975	0.0172	1.8922	2.1423	2.1652
Random Forest	2	Test	1.0345	1.2250	0.9933	0.0257	2.3195	2.3674	2.3794
LightGBM	2	Train	0.7159	0.8852	0.9976	0.0169	1.8456	2.0382	2.1016
LightGBM	2	Test	0.8933	1.0946	0.9947	0.0230	1.9875	2.2239	2.2830
MLR	3	Train	3.2182	3.7958	0.9536	0.0725	6.5135	7.5631	7.8020
MLR	3	Test	3.8168	4.5688	0.9443	0.0882	8.1960	8.3688	8.4120
Polynomial MLR (deg=2)	3	Train	0.9992	1.2591	0.9949	0.0241	2.2727	3.0974	3.1787
Polynomial MLR (deg=2)	3	Test	1.2680	1.4820	0.9941	0.0286	2.6094	2.9102	2.9854
Ridge	3	Train	3.2179	3.7978	0.9535	0.0725	6.6165	7.5537	7.6691
Ridge	3	Test	3.7883	4.5369	0.9450	0.0876	8.0631	8.2359	8.2791
Decision Tree	3	Train	0.7057	0.8859	0.9975	0.0169	1.8201	2.1442	2.2000
Decision Tree	3	Test	0.9375	1.1135	0.9967	0.0215	1.7620	2.0628	2.1380

Model	Fold	Dataset	MAE	RMSE	R2	NRMSE	95th % error	99th % error	Max error
Random Forest	3	Train	0.7104	0.9006	0.9974	0.0172	1.8325	2.2030	2.4820
Random Forest	3	Test	0.9611	1.1359	0.9966	0.0219	1.8317	2.1507	2.2304
LightGBM	3	Train	0.7035	0.8866	0.9975	0.0169	1.8358	2.1412	2.2488
LightGBM	3	Test	0.9617	1.1346	0.9966	0.0219	1.7692	2.0790	2.1564
MLR	4	Train	3.5524	4.0929	0.9496	0.0782	6.7835	7.4320	8.1767
MLR	4	Test	2.6471	3.2121	0.9662	0.0721	5.8926	6.1523	6.2172
Polynomial MLR (deg=2)	4	Train	1.0686	1.3070	0.9949	0.0250	2.4053	2.8059	2.9865
Polynomial MLR (deg=2)	4	Test	0.9468	1.3324	0.9942	0.0299	2.6020	3.2477	3.4091
Ridge	4	Train	3.5395	4.1109	0.9492	0.0785	6.8152	7.6687	8.3476
Ridge	4	Test	2.6582	3.1693	0.9671	0.0712	5.4141	6.3402	6.5717
Decision Tree	4	Train	0.7545	0.9143	0.9975	0.0175	1.7410	2.2146	2.4200
Decision Tree	4	Test	0.7093	0.9366	0.9971	0.0210	1.9393	2.1079	2.1500
Random Forest	4	Train	0.7764	0.9449	0.9973	0.0180	1.8107	2.0267	2.3628
Random Forest	4	Test	0.6323	0.9214	0.9972	0.0207	1.7651	2.4195	2.5831
LightGBM	4	Train	0.7584	0.9164	0.9975	0.0175	1.7254	2.2102	2.4021
LightGBM	4	Test	0.7152	0.9500	0.9970	0.0213	1.9771	2.2373	2.3024
MLR	5	Train	3.0004	3.6231	0.9607	0.0692	6.7253	7.9433	7.9637
MLR	5	Test	4.4039	5.2209	0.9040	0.1010	9.0597	9.8469	10.0437
Polynomial MLR (deg=2)	5	Train	1.0340	1.3319	0.9947	0.0254	2.4405	3.0795	3.6766
Polynomial MLR (deg=2)	5	Test	0.9566	1.2099	0.9948	0.0234	2.3642	2.5457	2.5910
Ridge	5	Train	2.9774	3.6359	0.9604	0.0695	7.1710	8.1027	8.1650
Ridge	5	Test	4.4765	5.3473	0.8993	0.1034	9.1694	9.9566	10.1534
Decision Tree	5	Train	0.6731	0.8589	0.9978	0.0164	1.4524	2.1487	2.6560
Decision Tree	5	Test	0.8607	1.1953	0.9950	0.0231	2.2400	2.7040	2.8200
Random Forest	5	Train	0.7895	0.9657	0.9972	0.0184	1.7270	2.1591	2.4869
Random Forest	5	Test	1.1220	1.4530	0.9926	0.0281	2.6966	3.4838	3.6806
LightGBM	5	Train	0.6927	0.8671	0.9977	0.0166	1.4490	2.1928	2.6503
LightGBM	5	Test	0.8507	1.2297	0.9947	0.0238	2.5590	2.6959	2.7301

2. SHAP analysis outputs

   a. Individual data

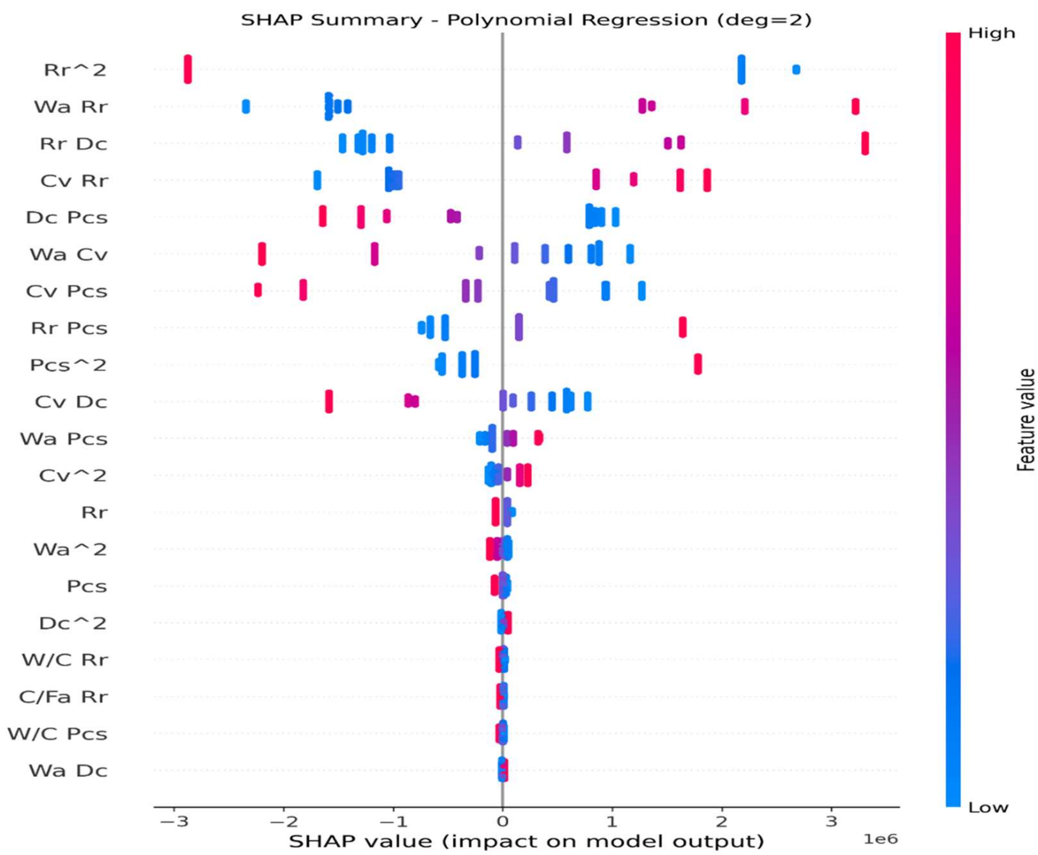

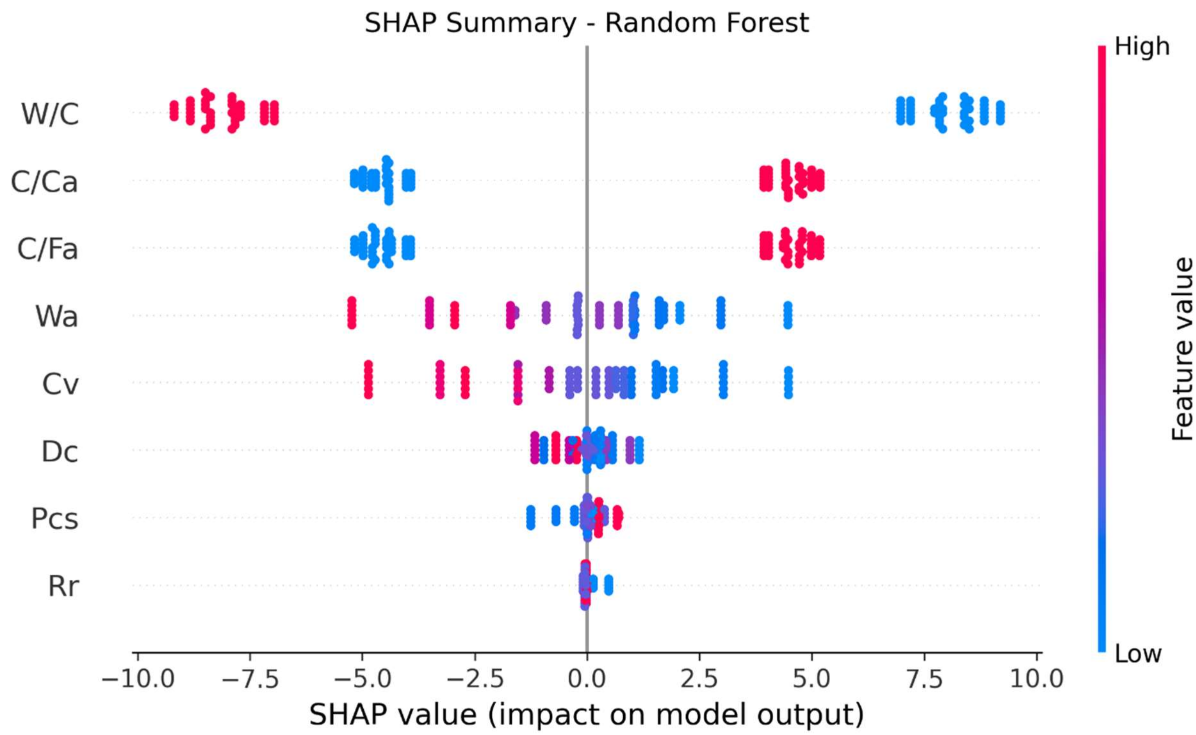

b. Aggregated data

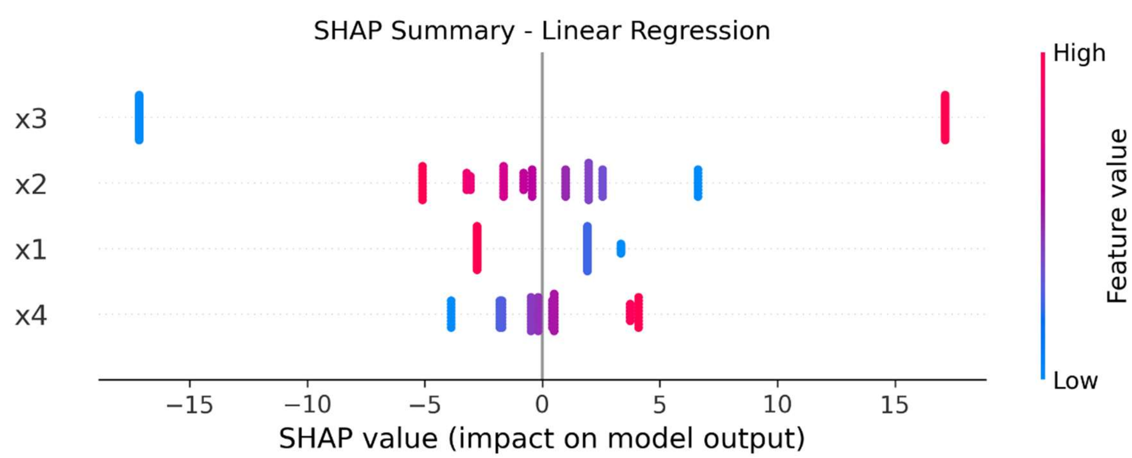

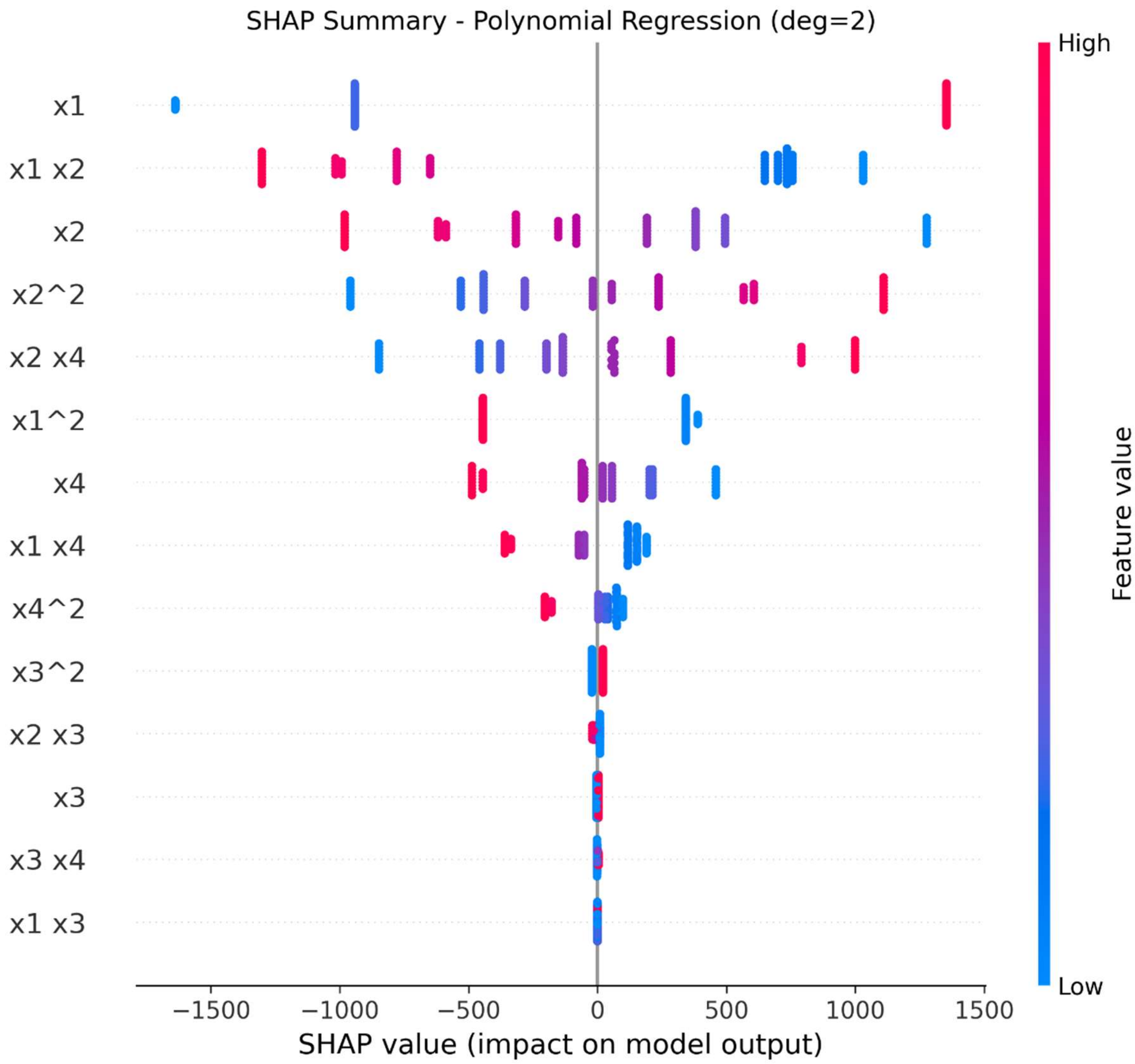
SHAP Summary - Polynomial Regression (deg=2)
x1
x1 x2
x2
x2^2
x2 x4
x1^2
x4
x1 x4
x4^2
x3^2
x2 x3
x3
x3 x4
x1 x3
−1500
−1000
−500
0
500
1000
1500
SHAP value (impact on model output)
High
Low
Feature value

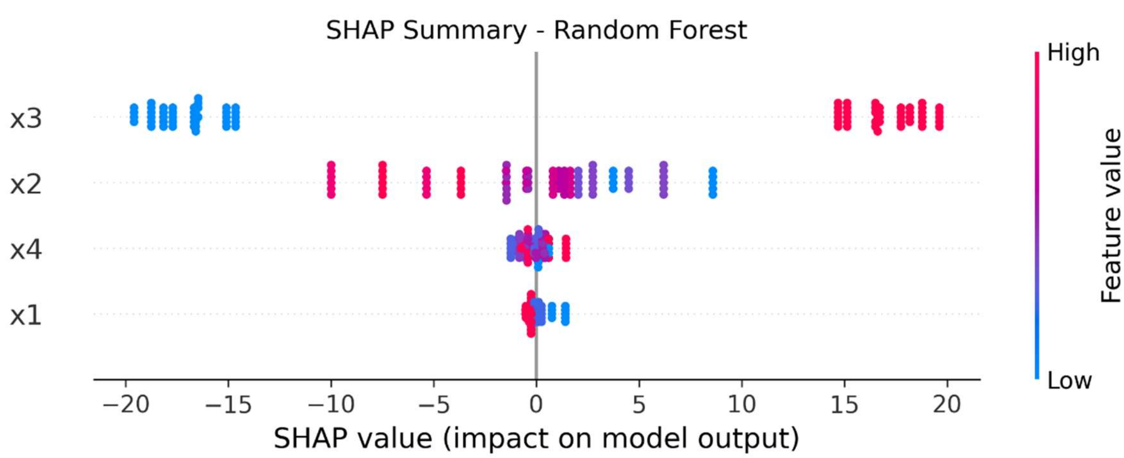
SHAP Summary - Random Forest
x3
x2
x4
x1
−20
−15
−10
−5
0
5
10
15
20
SHAP value (impact on model output)
High
Low
Feature value

Appendix F. Picture gallery

Sample collection cont.

Equipment used

Equipment and instruments cont.

Aggregate test, casting and strength tests

Sum young aggregate crushing plant found in AACRA


Mechanical properties of recycled aggregates:
(a)
(b)
(c)
(a)
(b)
(c)
(d)
(e)
(f)
(d)
(e)
7

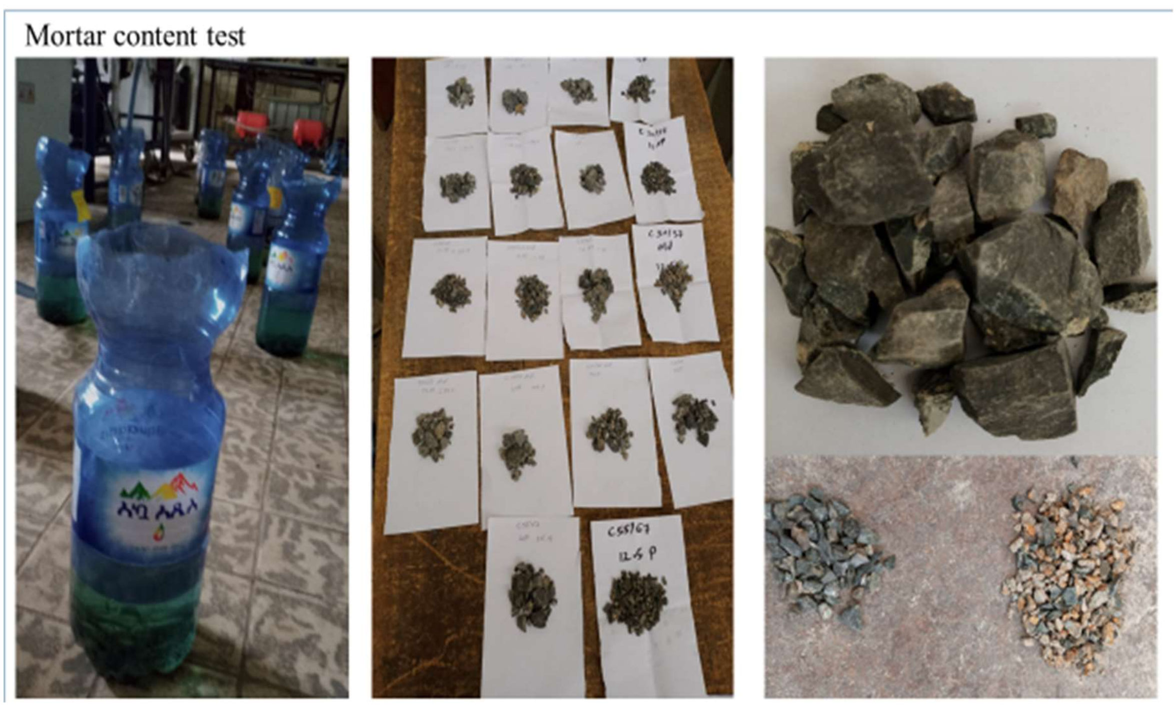
Mortar content test

Chamber construction

Chamber construction and testing cont.

Chamber construction and testing cont.

Chamber construction cont.

Keeping 50 % moisture of its water absorption capacity

Cover plate and loading plate details with pressure gauge reading

Chamber full assembly

Phenolphthalein test

NRCA 25- 25mm size

ARCA 25- 25 mm size, broken into less than 12.5 mm

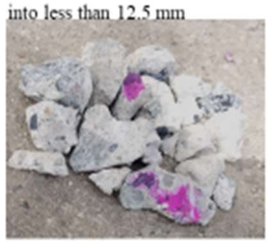

ARCA 25, less than 19 mm size

ARCA 25-12.5 mm size

NRCA 67- 25mm size

ARCA 67- 25 mm size, broken into less than 12.5 mm

ARCA 67, less than 19 mm size

ARCA 67-12.5 mm size

ARCA @SSD, Casting, and cured samples ready for strength test

Strength testing

Strength test

Tested samples